River Water Quality Modelling for River Basin and Water Resources Management

Thesis submitted in partial fulfilment of the requirements for the degree of Doctor of Philosophy in Environmental Engineering, at the Faculty of Engineering, University of Porto

André Ribeiro da Fonseca

Supervisor: Dr. Rui Alfredo Rocha Boaventura

Co-Supervisors: Dr. Cidália Maria de Sousa Botelho

Dr. Vítor Jorge Pais Vilar

Associate Laboratory LSRE-LCM
Department of Chemical Engineering
Faculty of Engineering
University of Porto

October, 2014

Acknowledgments

I am extremely grateful to my supervisors, Dr. Rui Boaventura, Dr. Cidália Botelho and Dr. Vítor Vilar and for their continuous support, ideas and motivation in completing this research.

This research would not have been possible without the support of the Foundation for Science and Technology (FCT) (doctoral grant: SFRH/BD/69654/2010); the Associate Laboratory of Separation and Reaction Engineering (LSRE) and Catalysis and Materials (LCM), Faculty of Engineering of the University of Porto (FEUP) and the Geospatial Software Lab at Idaho State University.

A huge thanks go out to the everyone in BASINS support team, the program difficulties encountered during the model development process were very frustrating and without your expertise this research would not have come close to being completed.

I am very grateful to Dr. Daniel Ames and his family for the research invitation at Idaho State University and extended friendship. To everyone I worked with at Geospatial Software Lab: Tevaganthan Velupillai, Ping Yang, Yan Cao, Jiří Kadlec, Carlos Osorio, Rex Burch, Carol Moore, Tiffany White, Matthew Klein and Robert Beazer who always made me feel very welcome. I particularly thank Ping Yang, his wife Yang Cao and both their kids Christopher and Philip, I hope we get a chance to meet again and maybe cook some dumplings. To Tevaganthan Velupillai: "Hey buddy!" let's grab some coffee and play some disc golf and try not to through it into the river this time around. To Jiří Kadlec and Matthew Klein for the great bicycle ride around the beautiful city and mountains of Idaho Falls.

I would like to thank to all my colleagues at LSRE for putting up with me over the past four years. A special thanks to André Monteiro and Tânia Valente for keeping me sane during this long journey. Those morning coffee chats proved to be a good medicine to survive the PhD.

A special thanks to Ariana Maciel, your friendship means the world to me, and remember: "*Everything will be okay in the end. If it's not okay, it's not the end*".

I would like to express my sincere appreciation to Sandra, for her love, support and encouragement during this journey, and never doubting commitment to my completion of this degree.

A big thank you to my mother, father, brother and sister for raising me to be a man with honesty, persistence, love and creativity.

To my family

Beneath the sun in the summer a sea of flowers

won't bloom without the rain.

Adam Fredric Duritz – High Life, Counting Crows

Abstract

To evaluate the current state and to predict effects of measures taken to improve river water quality, the applicability of a widely accepted hydrodynamic and water quality model was evaluated in two watersheds in Portugal, Lis and Ave River (Ave and Este River segments) basins. The Better Assessment Science Integrating Point and Nonpoint Sources (BASINS) and the Hydrological Simulation Program – FORTRAN (HSPF) were selected as the watershed model. Physical properties of land use, meteorological data and observed flow data were collected for a 4 year period for Lis River, a 6 year period for Este River and a 10 year period for Ave River where complete meteorological and hydrological data time series were available for model calibration and validation. Calibration and validation of all monitoring sites ranged from "good" to "very good" performance based upon a "goodness of fit" statistical guideline. Both River basins are fairly polluted calling for awareness at behavioural change specifically in agriculture practices to prevent the escalation of water quality, with special attention to faecal coliforms.

A methodology for the uncertainty estimation in water quantity and quality modelling was applied to the HSPF model. The Generalized Likelihood Uncertainty Estimation (GLUE) method was used to establish the uncertainty bounds for simulated flow and water quality constituents for a 95% confidence interval. The uncertainty bonds show that the model can predict fairly well all constituents with the exception of low faecal coliform concentrations. Results for model sensitivity parameters showed that the infiltration rate (*INFILT*) and the lower zone nominal soil moisture storage (*LZSN*) are key parameter when modelling streamflow. Both parameters are directly related to precipitation patterns and soil characteristics. Regarding faecal coliforms concentration, first order decay rate (*FSTDEC*) and surface runoff that removes 90% of faecal coliforms from the soil (*WSQOP*) were found to be the most sensitive parameters. Initial evaluation of sensitive parameters for oxygen governing processes (DO, BOD_5, NO_3, PO_4) did not result in an explicit key parameter for calibration of the model. Thus, the statistical significance test (*p*-value) was determined to establish ranking the parameters according their sensitivity. Benthal oxygen demand (*BENOD*), nitrification rate at 20 ºC (*KNO320*) and biochemical oxygen demand decay rate at 20 ºC (*KBOD20*) were found to be the more sensitive parameters.

Land use development scenarios were also addressed. In Lis River basin hypothetical scenarios of land use evolution (deforestation and urban development) were created to assess the impact of nutrient nonpoint pollution sources on water quality. The results showed that nutrient load reductions are observed for all scenarios but further pollution prevention is necessary to achieve a good water quality status. In Ave River basin land use scenarios were based on the evolution of three different land use maps (1990, 2000 and 2006). Land use scenarios evolution (increase of urban areas from forest and agriculture areas) showed inflow reduction for all constituents, since agricultural land showed the highest load of nutrients per area per year followed by forest land. Additionally best management practices (BMPs) (i.e. dry/wet detention basin) were applied to agricultural land to evaluate water quality. While Ave River segment show a good water quality status for all water quality constituents except for faecal coliforms, Este River segment can only achieve a good water quality if BMPs scenarios are considered. The application of best management practices to 3% of agricultural area with a removal capacity of 30% of phosphorus and; to 12% of agricultural area with a removal capacity of 30% of biochemical oxygen demand will result in a good water quality status for these constituents. Further measures need to be considered to reduce nitrogen and faecal coliforms loads to levels where a good water quality status can be achieved.

Climate change scenarios were developed using the Climate Assessment Tool (CAT) within BASINS program. Wet and dry scenarios coupled with temperature increases were set on historical base conditions to evaluate the sensitivity of faecal coliform in response to potential climate changes in Lis River basin. The Lis River model results showed that an increase of 1ºC in air temperature would result in an increase of 1.1ºC in water temperature and 1.5% decrease of faecal coliform concentration in water. The increment of 1% in precipitation will result in a 2% increase of bacteria inflow.

In this study, by applying different methodologies, uncertainty and sensitivity of the HSPF model was assessed and a number of suggestions for river basin management practices were formulated.

Resumo

Para avaliar o estado atual e prever os efeitos das medidas tomadas para melhorar a qualidade da água dos rios, foi avaliada a aplicabilidade de um modelo hidrodinâmico e de qualidade da água, em duas bacias hidrográficas em portuguesas, dos rios Lis e Ave (segmentos Ave e Este). As ferramentas *Better Assessment Science Integrating Point and Nonpoint Sources* (BASINS) e *Hydrological Simulation Program – FORTRAN* (HSPF) foram seleccionadas para avaliação da qualidade da água. As propriedades físicas relativas ao uso do solo, os dados meteorológicos e os dados de caudal observados foram recolhidos para um período de quatro anos no Rio Lis, seis anos no Rio Este e dez anos no Rio Ave, onde existem séries completas de dados meteorológicos e hidrológicos para calibração e validação do modelo. Os resultados da calibração e validação de todos os pontos de monitorização podem ser considerados de "bom" e "muito bom" com base em critérios de ajuste estatístico. Ambas as bacias hidrográficas encontram-se bastante poluídas sendo necessária uma mudança de comportamento no que respeita principalmente a práticas agrícolas (o uso de efluentes do sector pecuário como fertilizante), para evitar a contínua deterioração da qualidade da água, com especial atenção para os níveis de coliformes fecais.

O método *Generalized Likelihood Uncertainty Estimation* (GLUE) foi usado para determinar os limites de incerteza para os parâmetros de qualidade da água e caudal simulado para um intervalo de confiança de 95%. Os limites de incerteza determinados mostram que o modelo pode prever razoavelmente todos os parâmetros, com exceção de concentrações baixas de coliformes fecais. A sensibilidade dos parâmetros do modelo demonstrou que a taxa de infiltração (*INFILT*) e o armazenamento de humidade na zona inferior do solo (*LZSN*) são parâmetros chave na modelação do caudal. Ambos os parâmetros estão diretamente relacionados com os padrões de precipitação e as características do solo. Em relação à concentração de coliformes fecais, a taxa de decaimento de primeira ordem (*FSTDEC*) e o escoamento superficial, que remove 90% de coliformes fecais do solo (*WSQOP*) foram considerados os parâmetros mais sensíveis. Uma avaliação inicial da sensibilidade dos parâmetros para os processos de consumo de oxigénio (oxigénio dissolvido, carência bioquímica de oxigénio, nitratos e fosfatos) não resultou explicitamente num parâmetro chave para a calibração do modelo. Assim, foi realizado o teste de significância estatística

(valor-*p*) para avaliar os parâmetros de classificação de acordo com a sua sensibilidade. A carência bentónica de oxigénio (*BENOD*), a taxa de nitrificação a 20 °C (*KNO320*) e a taxa de redução da carência bioquímica de oxigénio a 20 °C (*KBOD20*) foram classificados como os parâmetros mais sensíveis do modelo.

Para a bacia do Rio Lis foram criados cenários hipotéticos de evolução da ocupação do solo (desflorestação e desenvolvimento urbano) para avaliar o impacto das fontes difusas de poluição de nutrientes na qualidade da água. Os resultados mostraram que são observadas reduções na carga de nutrientes em todos os cenários. No entanto é necessária uma prevenção adicional para atingir um bom nível de qualidade da água. Na bacia do rio Ave os cenários de ocupação do solo foram baseados na evolução de três mapas de diferentes anos (1990, 2000 e 2006). Os cenários da evolução da ocupação do solo (aumento de áreas urbanas com redução de áreas florestais e agrícolas) apresentaram redução de cargas para todos os constituintes, uma vez que as zonas agrícolas apresentam maior carga por unidade de área e por ano, seguidas das zonas florestais. Adicionalmente foram aplicadas melhores práticas de gestão de bacia (BMPs) (ex.: bacias de detenção) em áreas agrícolas com o intuito de melhorar a qualidade da água. Enquanto o segmento do Rio Ave mostra uma boa qualidade de água para todos os constituintes, exceto para os coliformes fecais, o segmento do Rio Este só poderá alcançar o mesmo resultado com a aplicação de BMPs. A aplicação de BMPs em 3% da área agrícola com capacidade de remoção de 30% de fósforo e, em 12% da área agrícola, com uma capacidade de remoção de 30% da carência bioquímica de oxigénio resultará numa boa qualidade da água para estes constituintes. Deverão ser consideradas medidas adicionais para reduzir as cargas de azoto e coliformes fecais para níveis que permitam alcançar uma boa qualidade da água.

Foram desenvolvidos cenários de alterações climáticas utilizando a ferramenta *Climate Assessment Tool* (CAT) dentro do programa BASINS. Foram criados cenários de aumento de precipitação, com aumento da temperatura baseados em dados históricos, para avaliar o comportamento dos coliformes fecais. Com base nos resultados obtidos no modelo para a bacia do Rio Lis verifica-se que o aumento de 1 °C na temperatura do ar reflectir-se-ia num aumento de 1.1 °C na temperatura da água e uma redução de 1.5% na concentração de coliformes fecais. O incremento de 1% na precipitação resulta num aumento de 2% na carga de coliformes fecais para a linha de água.

Neste estudo, foi avaliada a incerteza e a sensibilidade do modelo HSPF aplicando diferentes metodologias e foram formuladas sugestões para boas práticas de gestão de bacias hidrográficas.

Table of Contents

Table of Figures

Table of Tables

Notation

Model Parameters

ACQOP	Accumulation rate of quality constituent
AGWETP	Fraction of remaining evapotranspiration from active groundwater
AGWRC	Base groundwater recession
ALR20	Phytoplankton unit respiration rate at 20ºC
ANAER	Concentration of dissolved oxygen below which anaerobic condition exist
BASETP	Fraction of remaining evapotranspiration from baseflow
BASINS	Better Science Integrating point and Nonpoint Sources
BENOD	Benthal oxygen demand at 20ºC
BRBOD1	Benthal release of BOD at high oxygen concentration
BRBOD2	Incremental to benthal release of BOD under anaerobic conditions
BRNIT1	Benthal release rate of inorganic nitrogen under aerobic conditions
BRNIT2	Benthal release rate of inorganic nitrogen under anaerobic conditions
BRPO41	Benthal release rate of ortho-phosphate under aerobic conditions
BRPO42	Benthal release rate of ortho-phosphate under anaerobic conditions
CEPSC	Interception storage capacity
CFSAEX	Correction factor for solar radiation
DEEPFR	Fraction of groundwater inflow to deep groundwater
DENOXT	Dissolved oxygen concentration threshold above which denitrification ceases
ELEV	Mean reach elevation
EXPOD	Exponential factor in the dissolved oxygen term of the benthal oxygen demand equation
EXPRED	Exponent to depth used in the calculation of the reaeration coefficient
EXPREL	Exponential factor in the dissolved oxygen term of the benthal BOD release equation
EXPREV	Exponent to velocity used in the calculation of the reaeration coefficient
EXPSND	Exponent of sandload input power function formula
INFEXP	Exponent in infiltration equation
INFILD	Ratio between maximum and mean infiltration capacities
INFILT	Index to infiltration capacity of the soil
INTFW	Interflow inflow parameter
IOAD	Index of Agreement
IRC	Interflow recession parameter
KATRAD	Longwave radiation coefficient
KBOD20	BOD decay rate at 20ºC
KCOND	Conduction-convection heat transport coefficient
KEVAP	Evaporation coefficient

KGRND	Heat conductance coefficient between the ground and the mud layer
KMUD	Heat conductance coefficient between water and the ground
KNO220	Unit oxidation rate of nitrite at 20ºC
KNO320	Unit denitrification rate of nitrate at 20ºC
KODSET	Rate of BOD settling
KSAND	Coefficient of sandload input power function formula
KTAM20	Unit oxidation rate of total ammonia at 20ºC
KVARY	Variable groundwater recession
LSUR	Lenght of overland flow plane
LZETP	Lower zone evaportranspiration parameter
LZSN	Lower zone soil nominal storage
M	Erodibility coefficient of the sediment
MALGR	Maximal unit algal growth rate for phytoplankton
MUDDEP	Depth of mud layer
NSUR	Manning's n (roughness) for overland flow plane
PETMAX	Temperature below which evapotranspiration is reduced
PETMIN	Temperature below which evapotranspiration is zero
PHYSET	Rate of phytoplankton settling
REAK	Empirical constant for equation used to calculate the reaeration coefficient
SLSUR	Slope of overland flow plane
SQOLIM	Limiting storage of quality constituent
SUPSAT	Allowable dissolved oxygen supersaturation
TAUCD	Critical bed shear stress for deposition
TAUCS	Critical bed shear stress for scour
TCBEN	Temperature correction coefficient for benthal oxygen
TCBOD	Temperature correction coefficient for BOD decay
TCDEN	Temperature correction coefficient for the denitrification rate
TCGINV	Temperature correction coefficient for surface gas invasion
TCNIT	Temperature correction coefficient for the nitrogen oxidation rates
TGRND	Ground temperature
UZSN	Upper zone nominal soil moisture storage
WSQOP	Rate of surface runoff which will remove 90% of stored quality constituent

General Notations

BIT	Bacteria Indicator Tool
BMPs	Best Management Practices
BOD	Biochemical oxygen demand
CAT	Climate Assessment Tool
CBOD	Carbonaceous Biochemical Oxygen Demand
CFU	Coliform Forming Units

DO	Dissolved oxygen
D_v	Deviation of Volumes
E	Nash-Sutcliffe Coefficient of Efficiency
EEC	European Economic Community
FC	Faecal coliform
GIS	Geographical Information System
GLUE	Generalized Likelihood Uncertainty Estimation
HRU	Hydrologic Response Unit
HSPF	Hydrological Simulation Program FORTRAN
MCS	Monte Carlo Simulations
MSE	Mean Square Error
NPS	Nonpoint Pollution Sources
NO_3	Nitrates
PCP	Precipitation
R^2	Coefficient of Determination
PO_4	Orthophosphates
R4MS4E	Fourth Root Mean Quadruple Error
RMSE	Root Mean Square Error
RSR	Standard Deviation Ratio
RVE	Relative Volume Error
TIC	Total Inorganic Carbon
TMDLs	Total Maximum Daily Loads
UCI	User Control Input
TN	Total Nitrogen
TP	Total Phosphorus
USEPA	United States Environmental Protection Agency
WDMutil	Weather Data Management Utility
WFD	Water Framework Directive

Equation Parameters

A	Frequency factor
a	Emissivity of water surface
A_S	Algal settling rate to sediment
b	Empirical coefficients
B	Rate of oxygen uptake by benthal processes
Br	Bowen ratio
C	Mean concentration of constituent
c	Empirical coefficients
C_{BOD}	First stage BOD
$C_{BOD}a$	Rate of BOD discharged;

C_{CBOD}	Carbonaceous BOD concentration
C_{DO}	DO concentration
$C_{DO\,S}$	DO saturation concentration
C_{DOW}	Oxygen concentration in the overlying water
C_{FC}	Coliform concentration
C_{FC0}	Initial coliform concentration
C_{FCt}	Coliform concentration at time t
D	Dissolved oxygen deficit
d	Water depth
D_0	Initial dissolved oxygen deficit
E	Activation energy
e_a	Vapour pressure of the overlying atmosphere
e_p	Particulate excretion rate of nutrient by all animals
Er	Evaporation rate
e_S	Soluble excretion rate of nutrient by all organisms
e_{sat}	Saturation vapour pressure at the surface water temperature
f_1	Fraction of soluble excretions which are inorganic
f_2	Fraction of detritus decomposition products which are immediately available for algal uptake
f_3	Fraction of sediment decomposition products which are immediately available for algal uptake
F_{CDO}	Flux of dissolved oxygen across the water surface
G_z	Detritus grazing rate by zooplankton
H	Net surface heat flux
k'	Light dependent coliform disappearance rate
k_1	BOD decay rate
k_2	Reaeration rate
k_{20}	Rate constant at 20ºC
kd	Deoxygenation rate
k_{det}	Decomposition rate of particulate organic nutrient
k_{FC}	Disappearance rate constant
k_i	Transformation rate of S' into S
k_{ii}	Transformation rate of S into some other dissolved inorganic form of the nutrient
k_L	Surface transfer coefficient
k_l	Proportionality constant for the specific organism
k_{n1}	Ammonia to nitrite oxidation rate
k_{n2}	Nitrite to nitrate oxidation rate
k_o	First order oxidation rate
k_{org}	Hydrolysis rate of dissolved organic nutrient
K_R	Ressuspension coefficient

k_S	Settling rate of particulate organic nutrient
k_{sed}	Decomposition rate of organic sediment nutrient
k_T	Rate coefficient at temperature T
k_{Tr}	Reference temperature rate constant
K_x, K_y, K_z	Eddy dispersion coefficients
l_a	Light attenuation at coefficient
LE	Coefficient of longitudinal dispersion
L_w	Latent heat of vaporization
M_p	Total rate of plankton mortality
N_1	Ammonia-nitrogen concentration
N_2	Nitrite-nitrogen concentration
Ø	Temperature adjustment coefficient
p	Atmospheric pressure
P	Barometric pressure
Q_a	Incoming long wave radiation from atmosphere
Q_{an}	Net long wave atmospheric radiation
Q_{ar}	Reflected long wave radiation
Q_{br}	Long wave back radiation
Q_c	Rnergy converted to or from the water body at the surface
Q_e	Heat loss due to evaporation
Q_S	Shortwave radiation incident to water surface
Q_{sc}	Clear sky solar radiation
Q_{sr}	Reflected shortwave radiation
R	Gas constant
S	Sum of source and sink rates and nutrient interactions
S_I	Dissolved inorganic nutrient concentration
S'	Another inorganic form of the nutrient which decays to the form S
S_{det}	Suspended particulate organic nutrient concentration
SK	Fraction of sky covered by clouds
SOD	Sediment oxygen demand
S_{org}	Dissolved organic nutrient concentration
S_{sed}	Organic sediment nutrient concentration
t	Time
T	Temperature
T_a	Absolute temperature
T_d	Dry bulb air temperature
t_e	Exposure time
T_r	Reference temperature
Ts	Surface water temperature

T_w	Water temperature
u	Mean velocity in x-direction
v	Mean velocity in y-direction
V_S	Photosynthetic uptake rate for nutrient S
w	Mean velocity in z-direction
W	Wind speed at a specific elevation above water surface
x	Distance downstream
z	Depth
a_1	Empirical constant
a_2	Empirical constant
ϱ	Fluid density
σ	Stefan-Boltzman constant

1 Introduction

1.1 Relevance and Motivation

With the advancement in technology, water resource engineers have the opportunity to use cutting edge tools to fulfil their interests in a more efficient frame time and effort. In the absence of computing technologies, water resource management practices are fragmented. Data monitoring is limited by manpower and short term sampling studies and intermittent monitoring programs are commonly observed. Application of technological innovations provides some enhancement to these practices. New technologies give modelling programs speed and flexibility to manage large quantities of dynamic data input, transferring data from similar gaged environment or by extrapolating the available data to ungagged environments. However, due to spatial and temporal variability of watershed properties (i.e. topography, geologic, climate, etc.) these methods face significant uncertainties.

This thesis focused on the applicability of a water quality model (Hydrological Simulation Program – FORTRAN, HSPF) for water quality management in river basins. It is widely used to simulate basin hydrology and water quality on the land surface and in stream channel. The model contains hydrological tools to simulate the impact of land use and climate change on basin hydrology. It is used for continuous watershed simulation.

The work presents the application of HSPF model to two Portuguese river basins (Lis and Ave River), and it was evaluated current and future land use and climate change effects on water quality. It also addresses the uncertainty in model predictions in gaged and ungagged environments. Former studies normally consider the uncertainty and sensitivity of model parameter on their own and have, overall, insufficiently addressed the combined effects of several model parameters within the distributed model.

1.2 Thesis Objective and Layout

This thesis presents a calibration and validation of a water quantity and quality model to background conditions. The validated model was then applied to determine the relationships between land use, climate change, and water quality in Lis and Ave River basins through different scenarios to aid the implementation of best management practices (BMPs). The objectives of this research were to evaluate the accuracy of the model results; streamflow and water quality in a temporal (daily and monthly) and spatial scale (different watershed sizes). Evaluate the uncertainty and sensitivity of model parameters to determine the most important parameters when addressing model calibration. Promote good modelling practices and provide, in a systematic way, methods that help managers to minimize the uncertainty on the model results. The developed methods and tools were applied and tested in real scenarios, either in Lis River or Ave River, both in Portugal. The methods and conclusions of these case studies are kept general and described in such a way that they form guidelines for further modelling work, applicable to other basins. To accomplish this, the US EPA's Better Assessment Science Integrating Point and Nonpoint Source (BASINS) model coupled with the Hydrological Simulation Program – FORTRAN (HSPF) was used to simulate hydrologic and water quality processes in Lis and Ave River basins.

This thesis consists of 9 main chapters, including this introduction, Chapter 1, which provides a description of the research scope and objectives. In Chapter 2, a literature review on water distribution and regulation status is presented as well as an overview on water quality modelling. Detailed research on the methodology adopted for this study is presented in Chapter 3. This chapter also highlights methods for data collection including physical characteristics, meteorological conditions, population and administration information, land use cover and water quality conditions. In Chapter 4 and 5 HSPF model uncertainty and model parameter is addressed when calibrating the model for streamflow and water quality constituents. The evaluation of uncertainty propagation into river water quantity and quality predictions provide guidance on future monitoring campaigns. Sensitivity analysis defines the most sensitive parameter subset for calibration of HSPF river water quality model. Also, common hydrology statistical criteria are also determined to validate model results. Chapter 6 presents a study in Lena River (Lis River tributary) to assess the impact of point and nonpoint sources in water quality. Maximum daily loads of nutrients were calculated to determine the reduction need to achieve a good water quality status. In Chapter 7, the impact of land use development on water quality is addressed for both river basins and several scenarios of best management practices applications are presented. Chapter 8 addresses the impact of climate change on faecal coliforms bacteria watershed impairments on Lis River basin. Finally, Chapter 9 provides a brief conclusion, summarizing the model's applications and outcomes. In addition implications of the findings and potential future investigations that can be conducted to assist in a better basin management are also described.

2 Literature Review

This chapter presents a general overview of water quality regulation and its current state. A brief introduction to water quality modelling and its origin is presented. A review of some of the most common models and a description of the procedures and mathematical methodology used in hydrology is included.

2.1 Fundamentals of Hydrology

Hydrology deals with the scientific study of water; it describes and predicts the occurrence, circulation and distribution of water through the Earth atmosphere system (air, land and ocean). It studies the global water cycle and the physical, chemical and biological processes involved in all fluxes within the water cycle. Water is essential, not only to people but to all forms of life on Earth. The significance of water for the improvement of life quality, food production and industry support is vital in the rapidly developing world of today. Over the past 50 years the world population has increased from 3 billion to 6.5 billion and it is likely to rise by another 3 billion by 2050 and expected to reach 10 billion in 2100 (Nations, 2011). This reflects in a higher demand of food and water, which will imply a great pressure on agriculture and a rapid urbanization, resulting in an accelerating land use change, increasing stress on local, regional and global water quantity and quality (Collins et al., 2000; Duh et al., 2008; Groffman et al., 2004; Mills, 2007; Pickett et al., 2001). In addition to this, there is the specter of climate change. During the last one hundred years, the temperature has arisen nearly 0.6 °C and it is expected to raise at least 4 degree Celsius by 2100 and twice that by 2200 due to carbon dioxide emissions (Sherwood et al., 2014). Also according to Wentz et al. (2007) precipitation is increasing at a rate of 7% per degree Celsius of surface temperature as a response to global warming. This would result in an intensification of the hydrologic cycle; more frequently floods and droughts, deterioration of water quality, migration of species and changes in plant growth (Allen and Ingram, 2002; Delpla et al., 2009; Held and Soden, 2006). Current uses of water resources are resulting in a reduced volume of fresh water in rivers and change in the balance between fresh and salt water (Figure 2.1).

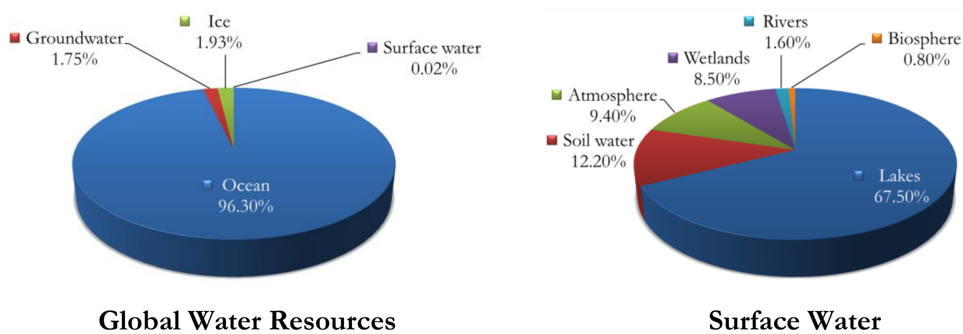

Figure 2.1 The global water inventory (Marshall, 2013).

2.2 Hydrologic Cycle and Climate Change

The hydrologic cycle describes the continuous movement of water above, on and below the surface of the Earth (Figure 2.2), changing its form: in the atmosphere as water vapour; in oceans, lakes and rivers as liquid water; and in polar ice caps and mountain glaciers as ice.

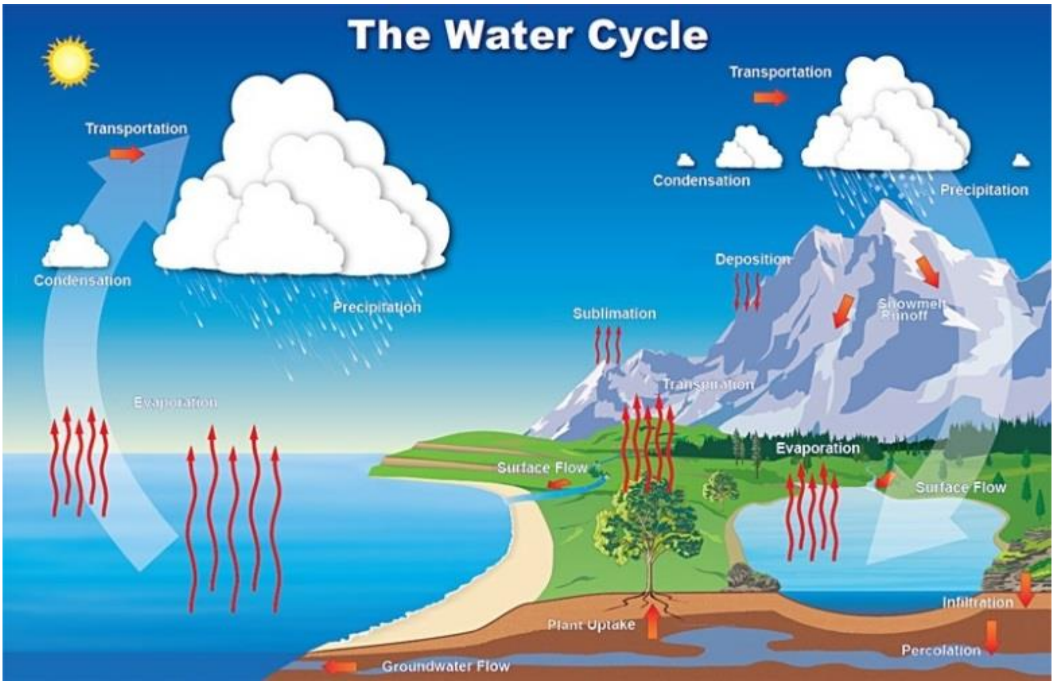

Figure 2.2 The global water cycle (NWS, 2010).

The hydrologic cycle on Earth is considered a closed system (Gupta, 2011), meaning it neither loses nor gains significant amounts of water, in what is called the hydrosphere. The hydrological process has no end or beginning and occurs continuously. Water evaporates from water bodies and land surface into the atmosphere, where it condensates and precipitates back on the land surface or water bodies moving through the surface and subsurface reservoirs until it reaches the ocean or returns to the atmosphere by evaporation. The cycle begins again and the water remains in continuous movement because of solar energy (Chow and Maidment, 1988). Thus, any changes in the climatic system or the energy balance in the atmosphere may alter the water balance of the hydrologic cycle. An estimate of global water distribution is given in Table 2.1.

Table 2.1 An estimate of volume of water distribution on Earth (Chilton et al., 2006; Gleick, 1996; Gupta, 2011).

Water in	Volume (1000 km³)	% Total Water	% Fresh Water	Residence Time
Oceans, seas and bays	1338000	96.5	---	4000 yr
Ice caps, glaciers and permanent snow	24064	1.74	68.7	10-100000 yr
Groundwater	23400	1.69	---	Weeks-100000 yr
Fresh	(10530)	0.760	30.1	
Saline	(12870)	0.929	---	
Soil moisture	16.5	0.001	0.05	Weeks-several yr
Ground ice and permafrost	300	0.022	0.86	
Lakes	176.4	0.013	---	10 yr
Fresh	(91.0)	0.007	0.26	
Saline	(85.4)	0.006	---	
Atmosphere	12.9	0.001	0.04	10 days
Wetlands	11.47	0.001	0.03	1-10 yr
Rivers	3.24	0.0003	0.009	2 weeks
Total	1385985	100	100	

The flow of a river represents the integrated basin response to various inputs: land cover, human activities and climatic inputs (Sharma et al., 2000), with precipitation and temperature playing the higher role. In the international arena, research projects and observation studies are tackling with complex questions about the important factors that regulate the global climate (solar irradiance, surface energy fluxes, surface albedo, surface temperatures, greenhouse gas concentrations, among others) (Loaiciga et al., 1996) and its impact in the Earth's hydrological cycle.

Higher temperatures increase the ratio of rain to snow, accelerate glacier melt and shorten the snowfall season (Frederick and Gleick, 2001), with consequences to seasons with high water demand being impacted by a reduced availability of fresh water. Since the end of the Little Ice Age (Matthes, 1939) temperatures have been generally increasing (Oliver, 1993) and the majority of the world's glaciers are retreating. Warmer temperatures will also increase the water holding capacity of the atmosphere (Cline, 1992) which generally results in an increased potential evaporation. However the actual rate of evaporation is constrained by water availability. A consequence of higher vapour concentrations is the increase of intense precipitations events.

With a perceptible trend towards more frequent extreme weather conditions, it is likely that the frequency of occurrence of floods and droughts will increase. Stream flows in low flow periods may well decrease and water quality is likely to deteriorate, because of higher pollution loads and concentrations and higher water temperatures (UNESCO, 2003).

2.3 Global Water Crisis

In the last century the population of the world has tripled, but the use of water has grown six-fold (Cosgrove and Rijsberman, 2014). This along with water availability, spatial and temporal variations, means that the water needed for industrial processes, food production and all other uses is becoming increasingly scarce. Demand for fresh water has driven determined endeavours to model global water resources for a better understanding of water resources infrastructure and management strategies (Alcamo et al., 2003; Davies and Simonovic, 2011). Water deficits are already driving heavy grain imports in some countries, such as China and India (Magdoff, 2008). Other countries such as United States, Mexico, Pakistan, Algeria, Egypt and Iran are also suffering from water shortages special in the arid and semi-arid regions due to continuous over pumping of groundwater to satisfy their water needs. The Himalayan glaciers, sources of Asia's largest rivers, could disappear by 2035 as global temperature rises (Khadka, 2004)

Clean, safe drinking water is scarce. Nearly 1 billion people in the developing world do not have access to clean drinking water (Jury and Vaux Jr, 2007). As the demand for fresh water increases so does the cost to build or maintain access to it. More than 3 million people die every year from water and sanitation related causes (Prüss-Üstün et al., 2008), it claims more lives through disease than any war claims through guns (Watkins, 2006). Water should be recognized as a great priority, and it should be protected both in terms of quantity and quality.

2.4 European Union Water Framework Directive

Perceptions of the global water crisis and the need to preserve it have progressively developed since the latter part of the 20th century. It is far more effective and economic to deal with water problems through advance preparedness and forewarning than after a disaster has actually struck. Thus, it is the obligation of engineers, scientists and other experts to provide the best possible solutions and disseminate information to local and national authorities.

The historical development of the European Union (EU) water legislation is presented elsewhere (Blöch, 2001; Kallis and Butler, 2001; Tyson et al., 1993; Zabel et al., 2001) and can be summarized in three stages. The first stage addressed the waters such as rivers and lakes for drinking water abstraction. The water use directives include drinking water directives (CEC, 1975, 1980b), the bathing waters directive (CEC, 1976b), fish and shellfish harvesting directives (CEC, 1978, 1979), and water pollutant directives for dangerous substances for surface waters (CEC, 1976a) and groundwater (CEC, 1980a). The ecological problem was later addressed and resulted in the second stage of EU water legislation: the Urban Wastewater Directive (CEC, 1991b), which addresses the water pollution from all settlements and the Nitrates Directive (CEC, 1991a), which addresses the water pollution by nitrates from agriculture. With the nitrates directive proven unsatisfactory, new framework legislation was proposed to involve a range of instruments, scientific and technical cooperation at regional and European level. This brings about the third stage or the so called Water Framework Directive (WFD).

On October 2000 the European Union (EU) approved a new Water Framework Directive (WFD) (CEC, 2000) that lays down a strategy against pollution of all EU waters. Surface water, coastal water and groundwater are affected by this regulation becoming imperative the management of river basins and their catchment areas. In the light of the WFD, member states must develop River Basin Management Plans (RBMPs) that assess current conditions and define actions to be taken to achieve the targets established in the Directive. This new directive is established with the following key objectives (Blöch, 2001; Kallis and Butler, 2001):

- Protection of all water bodies (surface water and groundwater);
- Achieve a "good" ecological and chemical status for all water by a set deadline of 15 years;
- Water management based on a river basin approach;
- Emissions and discharges control by a "combined approach" of emission limit values and quality standards;
- Mandatory pricing for water, contributing to the wise use of water and thus to resource protection, and;
- Strengthen public participation.

In Portugal, the Water Law (DR, 2005) established five River Basin Districts Administrations (ARH-APA) (Figure 2.3) as basic water resources planning and management units and institutions, which are responsible for the elaboration and execution of the RBMPs. A framework of plan implementation in Portugal is very well described in Vieira (2011), where it specifies the current problems, needs and methodology to follow, implementation and self-assessment of the plans and their supporting activities at a national level.

The European Directive 75/440/EEC (CEC, 1975) establishes the quality requirements which surface fresh intended for use in the abstraction of drinking water must meet after application of appropriate treatments. A complete list of parameters and concentration ranges are listed in this Directive. Table 2.2 presents quality parameters that are commonly used when modelling water quality in a river network.

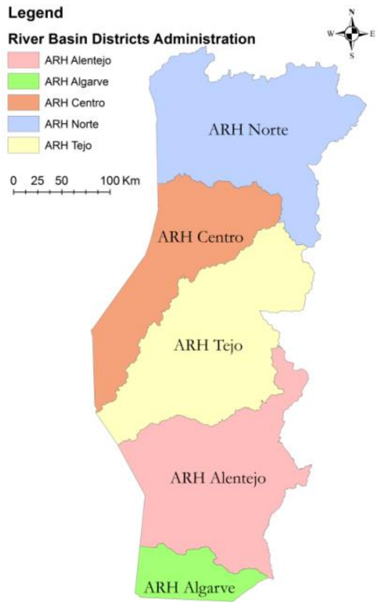

Figure 2.3 River basin districts administration limits.

Table 2.2 Characteristics of surface water intended for the abstraction of drinking water.

Parameters	Units	A1	A2	A3
pH		6.5 - 8.5	5.5 - 9.0	5.5 - 9.0
Total Suspended solids	mg L^{-1} SS	25	25	25
Temperature	º C	22	22	22
Conductivity	µs cm^{-1} at 20 ºC	1000	1000	1000
Nitrates	mg L^{-1} NO_3	25	50	50
Sulfates	mg L^{-1} SO_4	150 -250	150 -250	150 -250
Chlorides	mg L^{-1} Cl	200	200	200
Phosphates	mg L^{-1} P_2O_5	0.4	0.7	0.7
Chemical oxygen demand	mg L^{-1} O_2	30	30	30
Biochemical oxygen demand	mg L^{-1} O_2 at 20 ºC	<3	<5	<7
Ammonia	mg L^{-1} NH_4	0.05	1 - 1.5	2 - 4
Total coliforms	CFU/100 mL	50	5000	50000
Faecal coliforms	CFU 100/mL	20	2000	20000

A1 – Simple physical treatment and disinfection (e.g. rapid filtration and disinfection);

A2- Normal physical treatment, chemical treatment and disinfection (e.g. pre-chlorination, coagulation, flocculation, decantation, filtration, final chlorination);

A3 – Intensive physical and chemical treatment, extended treatment and disinfection (e.g. chlorination to break-point, coagulation, flocculation, decantation, filtration, adsorption (activated carbon), ozonation, final chlorination).

2.5 Water System Modelling

During the past few decades, increased demands on water for various applications have stimulated many unsustainable practices of exploitation but, on the other hand, numerous responses have been put forward to meet the ever increasing demand for water (Gupta, 2011).

2.5.1 The Beginning of Modelling

Aroused by the need to control pollution of the major sources of freshwater supply and to ensure protection of public health, studies to examine the physical, chemical and biological responses of streams to loading nutrients, either natural or man induced were developed. In the 1920s, from an intensive study of sources of pollution and their impacts on domestic water supply emerged one of the first if not the first mathematical models of an aquatic environment, the *Streeter-Phelps* equation, describing the balance of dissolved oxygen in a stream (Streets and Phelps, 1925). Development of the computer and the mathematical techniques that followed, especially numerical methods, had a huge impact in water resource technology. In the late 1950s methods were developed for solving large sets of simultaneous algebraic equations and finite difference representations of more complex and linear and nonlinear differential equations (Orlob, 1983). Among the first models of this new era in water management, an extension to the Streeter-Phelps model was developed (Thomann, 1963) where multiple waste loads were distributed along a river stretch of non-uniform cross section and where the rates of biodegradation and reaeration could be expected to vary spatially and temporally with hydrological conditions. In the late 1960s simple Streeter-Phelps model appeared in a variety of computerized forms: the DOSAG (Board, 1970) solved steady state problem for a multi-segment river system; QUAL I (Masch, 1970) simulated stream temperature as well as DO and BOD, allowing temperature adjustments in rate coefficients; QUAL II (WRE, 1973) included the capability to simulate more complex stream systems for both steady and unsteady flow and to evaluate impacts of nutrient loading on the stream. Further models were developed for lakes and reservoirs (WRE, 1968) to include quality constituents: DO and BOD (Markofsky and Harleman, 1973); nutrients and biota (Chen and Orlob, 1972); improvements on heat exchange of air water interface (TVA, 1972) and cause effect relationships between carbon, nitrogen and phosphorus (Imboden, 1974; O'Melia, 1974; Vollenweider, 1975). A brief summary of modelling chronology is presented in Figure 2.4.

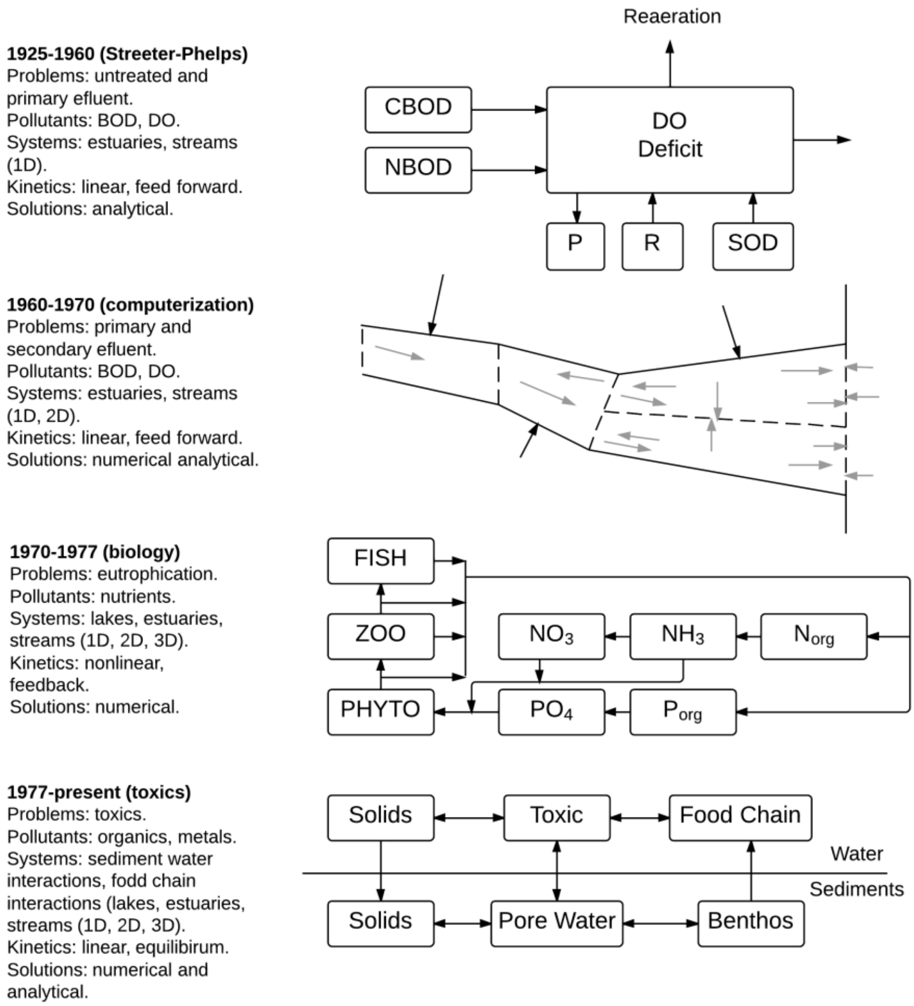

Figure 2.4 Development of water quality models (Chapra, 1997).

Several other models were also developed: Stanford Watershed Model IV (Crawford and Linsley, 1966); Hydrocomp Simulation Programming (Hydrocomp, 1976); NonPoint Source Model (Donigian and Crawford, 1976); the Agricultural Runoff Management Model (Donigian, 1977); and the Sediment and Radionuclides Transport (Onishi and Wise, 1982). The previous models eventually led to the development of the most commonly used models today: the Enhanced Stream Water Quality Model – Qual2E and Qual2K (Brown and Barnwell, 1987); the Hydrologic Simulation Program – FORTRAN (HSPF) (Bicknell et al., 2001); and the Soil and Water Assessment Tool (SWAT) (Arnold and Fohrer, 2005; Arnold et al., 1998).

2.5.2 Watershed Concept

A watershed also called a drainage basin or catchment area is a natural hydrologic entity that covers a specific area of land surface in which all water flowing into it goes to a common outlet, where all activities, human and wildlife are an integral part of it and affect their productivity. Not only is an hydrological unit but also a social-political-ecological entity which plays a crucial role in providing food, social and economic security and life support services to rural people (Wani et al., 2008).

When rain falls on the landscape it is subjected to infiltration, evaporation and evapotranspiration or it ends up in a river system, which is the lowest point in the surrounding landscape. Rivers begin as small tributaries that flows from hillsides, wetlands, lakes and as melt water from glaciers and snowpack. Some are temporary, flowing only during a heavy rain event or spring snow melt; others are fed by springs and groundwater as well as by surface runoff. Small tributaries streams will join others to form larger creeks and rivers that flow into another river, lake or ocean like the overall shape of the veins of a leaf or the branches of a tree.

While it is important to know how much water is stored in groundwater, lakes and wetlands (Döll et al., 2012), understanding the movement of water within and from individual watersheds is far more important. Viewing the land surface as a series of watersheds it promotes organization patterns to accurately manage them appropriately.

2.5.3 Commonly Used Models

Mathematical models are valuable tools that allow one to make decisions, investigate alternative scenarios and assist in developing effective management strategies. When looking at modelling, there is no one model to rule them all. They can be classified according their process characteristics; on the environment modelled, the purpose of the model, the number of dimensions considered, the process described and whether temporal variability is considered (Figure 2.5).

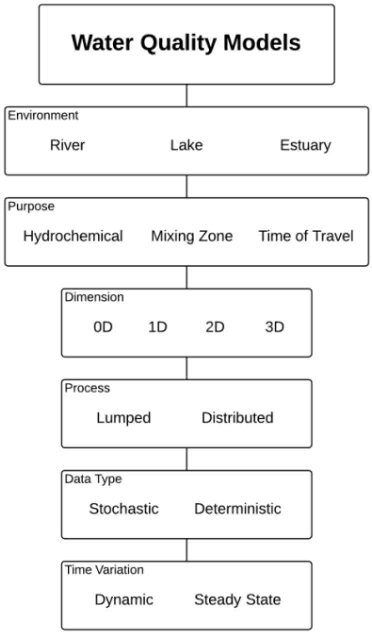

Figure 2.5 Different categories of water quality models (adapted from Vandenberghe, 2008).

Zero dimensional models, applied only to lakes (similar to continuously stirred tank reactor), does not represent the processes of dispersion of contaminants in any direction. It is often sufficient for problem applications where hydrodynamics are not required, no transport direction can be specified and the water volume changes are accounted only by the water entering and leaving the system (Anderson et al., 1976). One dimensional models are most commonly used in rivers, but can also be used in special cases in estuaries and lakes with long residence times and stratification in the vertical direction (Imberger and Hamblin, 1982; Smith, 1978a; Wlosinski et al., 1995). The process of advection is assumed to transport a constituent horizontally by movement of the water, requiring that variables like depth and velocity change predominantly along the channel. The stream is assumed to be completely and instantaneously mixed across its width and depth (Brocard and Harleman, 1976; Cox, 2003; Peterson et al., 1973). Two and three dimensional models are used in rivers, reservoirs, lakes and estuaries. Two dimensional models (Blumberg, 1977; Najarian et al., 1982; Simons, 1976; Taylor and Pagenkopf, 1981; Wang and Connor, 1975) will either simulate dispersion across the width or depth of the stream but not both, while three dimensional models (Blumberg and Mellor, 1980; Huyakorn et al., 1987; Walters, 1992) account for water flows and dispersion of solutes in all directions. The application of these models are complex and in many cases not justifiable in terms of effort and cost running (Cox, 2003). However they start playing an important role in large scale hydrodynamic regimes in water quality simulations with the continue decrease of computational cost and increased sophistication of numerical techniques.

Lumped models usually use average values to characterize several processes over an entire watershed in order to achieve an overall output at the basin outlet (Rosso, 1994). A lumped model does not consider spatial variability of model parameters and hydrologic processes within a watershed and is a function of time alone (Clarke, 1973; Singh, 1988, 1995; Woolhiser and Brakensiek, 1982). In general, this will mean solving a set of ordinary differential equations. Distributed models are mathematical equations that are function of time and one or more spatial variables of the modelled watershed (Clarke, 1973; Rosso, 1994; Singh, 1995; Woolhiser and Brakensiek, 1982). In general, distributed models will require more information and watershed parameterization than do lumped models (Singh, 1995). However, data limitations often avert the realization of fully distributed models, as some system characteristics may have to be lumped within the distributed models. Thus, some distributed models are more appropriately classified as semi or quasi-distributed in cases where the lumping of certain watershed characteristics exists (Singh, 1995).

Hydrologic models can also be classified as either deterministic or stochastic. A deterministic model is one whose variables are generally free from random variation (Clarke, 1973; Woolhiser and Brakensiek, 1982) and the output of the model is fully determined by the parameter values and their initial conditions. In a deterministic model for a given input there is only one output. A stochastic model, however, has one or more variables that are randomly distributed in probability (Clarke, 1973; Woolhiser and Brakensiek, 1982). The same set of parameter values and initial conditions will lead to a myriad of different outputs.

Models may also be classified according to their temporal variability output: as either single event or continuous based according to the number of hydrologic events simulated. An event based model only simulates a single hydrologic event (hours to days) without considering the period between events (Bowie and Tech, 1985). A continuous model calculates flow rates and watershed conditions continuously over longer periods of time covering a variety of hydrometeorological events.

As discussed previously, there is a general common structure to most of the models, falling to the modeller to choose which one is more suitable to the situation at hand. Table 2.3 shows the properties of some commonly used models. It is not mandatory that all these process be included in a model for a particular application; nevertheless the model user should know what processes have been omitted in the model and the reason for not considering them (Palmer, 2001). Some of the reasons for omitting processes may be the lack of site specific data and the reluctance to use literature or default values instead of site specific data.

Water quality models attempt to support the decision making process in a scientific and technical approach. They make it possible to quickly and methodically run simulations over large periods of time and draw results and conclusions based on those assumptions. With the aid of models, effects of point and nonpoint pollution, best management practices and water transfers can be assessed a priori before large investments take place that may or may not result in the desired effect.

2.5.4 Point and nonpoint pollution sources

Water pollution is a combination of adverse effects upon water bodies mainly caused by human activities. There are two main types of water source pollution: point and nonpoint source pollution. Other natural causes of pollution that affect water quality exist, such as: volcanoes, algae blooms, storms and earthquakes (Devane et al., 2014; Hochmuth et al., 2014; Jennerjahn et al., 2013) which are not discussed herein. Point source pollution is characterized by discharge at a fixed location that can be easily identified. The main point pollution sources are from industrial plants and those from wastewater treatment plants discharges. The emissions from smaller industries and unconnected households are often estimated on average values of water discharge per sector and per capita respectively (Gupta, 2011). Nonpoint source pollution also referred as diffuse pollution results from the release of a variety of substances in many different situations: fertilizers and manures; irrigation; pathogens from livestock; soil particles from arable and livestock farming, forestry, upland erosion; pesticides; acidifying pollutants and chemicals from atmospheric deposition; etc. (Vandenberghe, 2008).

Table 2.3 Properties of some commonly used models.

Management Analysis	**QUAL2E-UNCAS**[1]	**WASP4**[2]	**HSPF**[3]	**SWAT**[4]	**SWMM**[5]	**WQRRS**[6]	**CE-QUAL-W2**[7]	**MIKE**[8]	**TRISULA-DELWAQ**[9]	**DIVAST**[10]
Receiving Water										
River	X	X	X	X	X	X		X	X	
Reservoirs & Lakes		X	X	X		X	X	X	X	X
Estuaries, Coastal Areas		X					X	X	X	X
Attributes										
Dynamic		X	X	X	X	X	X	X	X	X
Stochastic	X									
Stormwater Flow			X	X	X			X		
Sewer System					X					
Water Quality										
Dissolved Oxygen	X	X	X	X		X	X	X	X	
Nitrogen	X	X	X	X		X	X	X	X	
Phosphorus	X	X	X	X		X	X	X	X	
Indicator Bacteria	X	X	X	X		X	X	X	X	X
Suspended Solids		X	X	X		X	X	X	X	
Heavy Metals		X	X	X				X		
Dissolved Substances	X	X	X	X		X	X	X	X	X
Temperature	X	X	X	X		X	X	X	X	
Oils, Grease, PAHs								X		

[1] (Brown and Barnwell, 1987); [2] (Ambrose et al., 1988); [3] (Bicknell et al., 2001); [4] (Neitsch et al., 2005); [5] (Rossman, 2010); [6] (Smith, 1978b); [7] (Cole and Buchak, 1995); [8] (Warren and Bach, 1992); [9] (van der Kuur et al., 1989); [10] (Falconer et al., 1998).

2.5.5 Advective and Disperse Transport

The transport and fate of a substance at a particular site within a system is continually governed by physical processes of advection and dispersion which transport fluid constituents through water bodies. The three dimensional advection-dispersion(Fick, 1855) mass balance equation can be written as:

$$\frac{\partial C}{\partial t}+\frac{u\partial C}{\partial x}+\frac{v\partial C}{\partial y}+\frac{w\partial C}{\partial z}-\frac{\partial}{\partial x}\left(K_x\frac{\partial C}{\partial x}\right)-\frac{\partial}{\partial y}\left(K_y\frac{\partial C}{\partial y}\right)-\frac{\partial}{\partial z}\left(K_z\frac{\partial C}{\partial z}\right)=\sum S \qquad (2.1)$$

Where:

C = mean concentration of constituent (mass volume^{-1});

u = mean velocity in x-direction (length time^{-1});

v = mean velocity in y-direction (length time^{-1});

w = mean velocity in z-direction (length time^{-1});

K_x, K_y, K_z = eddy dispersion coefficients (lenght^2 time^{-1});

$\sum S$ = sum of source and sink rates and nutrient interactions (mass volume^{-1} time^{-1});

t = time.

It is not always easy to quantify all the terms in equation (2.1), especially the velocity terms (u, v, w). The complete evaluation involves the simultaneous solution of the momentum, continuity, hydrostatic, and state equations in three dimensions (Hinwood and Wallis, 1975; Leendertse and Liu, 1975). Even though sophisticated hydrodynamic models exist it is not always feasible or justifiable (expensive and extensive data inputs) to apply such models for water quality computations, especially for long term and steady state simulations.

The dispersive transport is incorporated in equations of motion and continuity by temporal and spatial averaging.

Spatial averaging is usually used to simplify three dimensional models to two or one dimensions.

Dispersive transport in river is usually modelled in one dimensional equation such as:

$$\frac{\partial C}{\partial t}+\frac{u\partial C}{\partial x}=\frac{\partial}{\partial x}\left(K_x\frac{\partial C}{\partial x}\right)+\sum S \qquad (2.2)$$

Where:

C = mean concentration of constituent (mass volume^{-1});

(length);

t = time.

Specific governing equations can be derived for vertical and horizontal dispersion for lakes and estuaries. A detailed discussion of this subject can be found elsewhere (Fischer, 1979). These formulations tend to be model dependent and are all based to some extent on general lack of a complete understanding of the highly complex turbulence induced mixing processes which exists in natural water bodies (Zison, 1978).

2.5.6 Common Modelled Water Quality Parameters

Quality of water is of concern, essentially in relation to its intended use. For example, water that is good for irrigation may not be good enough for washing or drinking water production or may not even support aquatic life. The term water quality is used to describe physical, chemical, and biological characteristics of water, usually with reference to its suitability for a particular use. Standards and guidelines have been established to classify water for designated uses such as drinking, recreation, agricultural irrigation, or protection and maintenance of aquatic life.

2.5.6.1 Water Temperature

The rates of most reactions in natural waters increase with temperature, approximately double for a temperature rise of 10 ºC (Chapra, 1997). A rigorous quantification of the temperature dependence is provided by the *Arrhenius* equation:

$$k(T_a)=Ae^{\frac{-E}{RT_a}} \tag{2.3}$$

Where:

A = frequency factor;

E= activation energy (J mole^{-1});

R = the gas constant (8.314 J mole^{-1} K^{-1});

T_a = absolute temperature (K).

Temperature in a water body includes the effects of inflows (tributaries, discharges), outflows, heat generated by chemical biological reactions, heat exchange with the stream bed, and atmospheric heat exchange at the water surface. The dominant process controlling the heat budget is determined by the amount of solar energy absorbed by water as well as the surrounding soil and air. The net external heat flux (kcal m^{-2} hr^{-1}), is most often formulated as an algebraic sum of several component energy fluxes (Baca and Arnett, 1976; Edinger and Buchak, 1979; Ryan and Harleman, 1973; Thomann, 1975; TVA, 1972):

$$H = Q_s - Q_{sr} + Q_a - Q_{ar} - Q_{br} - Q_e + Q_c \tag{2.4}$$

Where:

H = net surface heat flux;

Q_S = shortwave radiation incident to water surface;

Q_{sr} = reflected shortwave radiation;

Q_a = incoming long wave radiation from atmosphere;

Q_{ar} = reflected long wave radiation

Q_{br} = back radiation emitted by the water body;

Q_e = energy utilized by evaporation;

Q_c = energy converted to or from the water body at the surface.

In order to calculate these fluxes, all or some of the following meteorological data may be required: atmospheric pressure; cloud cover; wind speed and direction; wet and dry bulb air temperatures; dew point temperatures; short wave solar radiation; relative humidity; water temperature; latitude; and longitude (Shanahan, 1984).

Net short wave solar radiation (Q_{sn})

Net short wave radiation is the difference between the incident and reflected solar radiations (Q_s-Q_{sr}). The most common formulation (Ryan and Harleman, 1973) is expressed as:

$$Q_{sn} = Q_s - Q_{sr} \approx 0.94 Q_{sc}\left(1 - 0.65 SK^2\right) \tag{2.5}$$

Where:

Q_{sc} = clear sky solar radiation (kW m^{-2});

SK = fraction of sky covered by clouds.

A number of methods are available for estimating the clear sky solar radiation as a function of: geographical location, time of the year and hour and day (TVA, 1972); latitude, longitude, month and sky cover (Thackston, 1974; Thompson, 1976); daily average insolation as a function of latitude (Hamon et al., 1954); reflectivity of water and sun's altitude in degrees (Lombardo, 1972) and; shading (Jobson and Keefer, 1979).

Net atmospheric radiation (Q_{an})

The net atmospheric radiation is calculated based on the empirical determination of an overall atmospheric emissivity. Many water quality models adopted the following equation (Swinbank, 1963):

$$Q_{an}= Q_a-Q_{ar} =1.16\times10^{-13} \left(1+0.17SK^2\right)(T_d-460)^6 \qquad (2.6)$$

Where:

Q_{an} = net long wave atmospheric radiation (kW m^{-2});

SK = cloud cover fraction;

T_d = dry bulb air temperature (ºC).

Other formulations are available in literature for specific latitude and altitude ranges (Hatfield et al., 1983).

Long wave back radiation (Q_{br})

The long wave back radiation is determined as a function of the emissivity of water surface and temperature:

$$Q_{br}=a\,\sigma\,T_s^4 \qquad (2.7)$$

Where:

Q_{br} = long wave back radiation (kW m^{-2});

a = emissivity of water surface (0.97)

Ts = surface water temperature (K);

σ = Stefan-Boltzman constant (5.670x10^{-12} kW m^{-2} K^{-4})

Evaporative Heat Flux (Q_e)

Evaporative heat loss occurs when water changes from liquid to vapour state, by absorbing latent heat of vaporization. The common formulation used by many models is:

$$Q_e = \varrho L_w E_r \tag{2.8}$$

$$L_w = 597 - 0.57\, T_s \tag{2.9}$$

$$E_r = (b + cW)(e_{sat} - e_a) \tag{2.10}$$

Where:

Q_e = heat loss due to evaporation (kW m^{-2});

ϱ = fluid density (kg m^{-3});

L_w = latent heat of vaporization (kW kg^{-1});

E_r = evaporation rate (m s^{-1});

T_s = surface water temperature (ºC);

b, c = empirical coefficients (temperature dependant; a usually zero; b varies between 1x10^{-9} to 5x10^{-9});

W = wind speed at a specific elevation above water surface (m s^{-1});

e_{sat} = saturation vapour pressure at the surface water temperature (mbar);

e_a = vapour pressure of the overlying atmosphere (mbar).

There are a large number of formulae available in literature to calculate the evaporation rate for a natural water surface, nevertheless studies showed that no significant discrepancies between the formulae where found (Ryan and Harleman, 1973).

<u>Convective heat flux (Q_c)</u>

The convective heat flux corresponds to the heat transfer by conduction between water and air and transported away from the interface air-water by convection with the moving air mass. It is calculated using the Bowen ratio (Bowen, 1926) and it is related to the evaporative heat flux (Q_e):

$$B_r = \frac{Q_c}{Q_e} = \left(6.19\times10^{-4}\right) p \left|\frac{T_s - T_d}{e_s - e_a}\right| \tag{2.11}$$

Where:

B_r = Bowen ratio;

p = atmospheric pressure (Lombardo);

T_d = dry bulb air temperature (ºC);

T_s = surface water temperature (ºC);

e_s = saturation vapour pressure at the surface water temperature (mbar);

e_a = vapour pressure of the overlying atmosphere (mbar).

The Bowen ratio is used in the surface heat transfer budget of several models (Brocard and Harleman, 1976).

A more detailed explanation on the estimation of the various fluxes components is discussed elsewhere (Edinger et al., 1974; Paily et al., 1974; Ryan and Harleman, 1973; TVA, 1972).

2.5.6.2 Dissolved Oxygen

Dissolved oxygen (DO) is essential for most aquatic life and is one of the most important quality parameters. Figure 2.6 shows the dissolved oxygen sources (external supply, photosynthesis, surface reaeration, and denitrification) and sinks (BOD, sediment oxygen demand, respiration and nitrification).

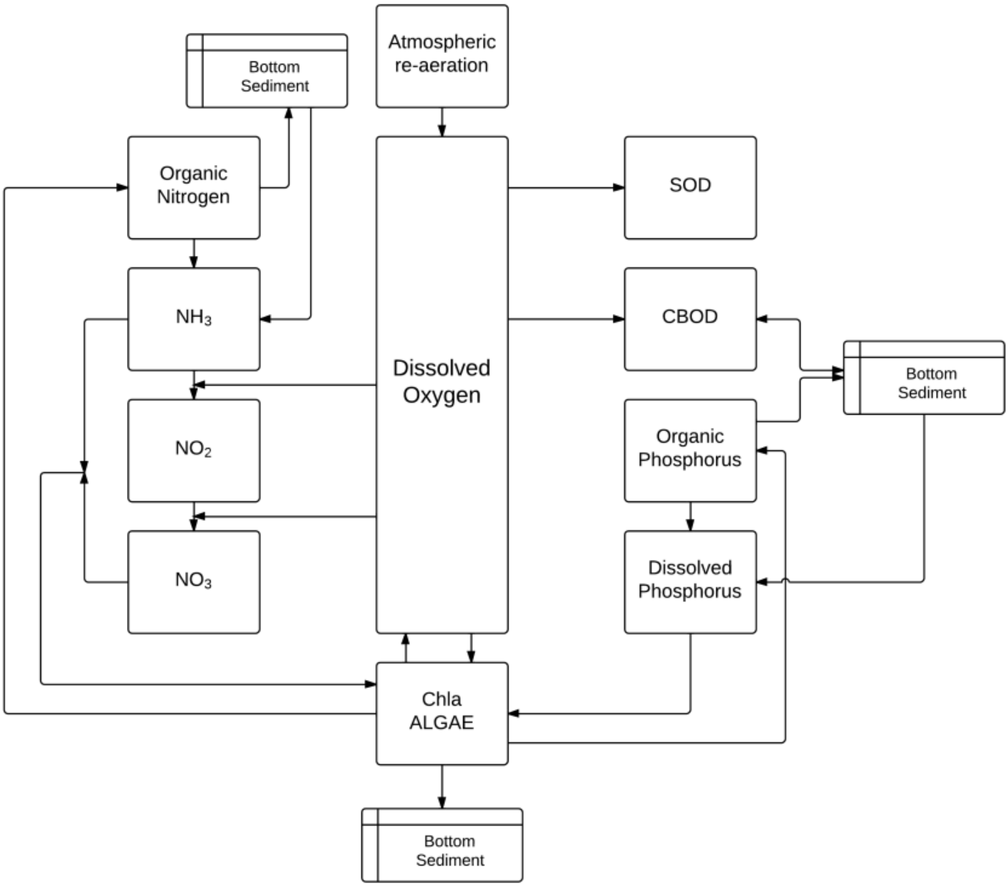

Figure 2.6 Dissolved oxygen process (adapted from Palmer, 2001).

DO is modelled as oxygen deficit, or the difference between the DO concentration and the concentration of the DO when the water is saturated with DO (Bowie and Tech, 1985). The saturation concentration is a function of temperature, atmospheric pressure and salinity. The DO concentration is a function of several physical and biochemical processes. Many of these processes are difficult to measure and consequently are imprecise. Simplifying the model by omitting processes that are known to be very imprecise can improve the precision of the model predictions.

Earlier attempts at DO/BOD model involved the concept of oxygen sag, where DO concentration was represented by two competing processes: deoxygenation (2.12) and reaeration (2.13). In its simplest form the oxygen sag model does not directly represent either advection or dispersion. However, more sophisticated versions have been formulated:

$$\frac{dC_{BOD}}{dt} = -k_1[BOD] \tag{2.12}$$

$$\frac{dC_{DO}}{dt} = k_2[C_S - C] \tag{2.13}$$

$$\frac{\partial C_{BOD}}{\partial t} = -u\frac{\partial C_{BOD}}{\partial x} + K_x\frac{\partial^2 C_{BOD}}{\partial x^2} - (K_1 + K_R)C_{BOD} + C_{BOD_a} \tag{2.14}$$

$$\frac{\partial C_{DO}}{\partial t} = -u\frac{\partial C_{DO}}{\partial x} + K_x\frac{\partial^2 C_{DO}}{\partial x^2} - K_1 C_{BOD} + K_2(C_{DO_S} - C_{DO}) - B \tag{2.15}$$

Where:

C_{BOD} = first stage BOD;

C_{BODa}= rate of BOD discharged;

C_{DO} = DO concentration (mg L^{-1});

C_{DOS} = DO saturation concentration (mg L^{-1});

x = distance downstream (m);

t = time (hr);

u = average velocity (m s^{-1})

k_1 = BOD decay rate (hr^{-1});

k_2 = reaeration rate (hr^{-1});

K_R = ressuspension coefficient (hr^{-1});

B = rate of oxygen uptake by benthal processes (hr^{-1}).

Advection is only used in the sense of the relationship between time and distance travelled, where dispersion is included within K_1 and K_2.

Because the temperature of a stream can vary daily and even hourly, it is important to consider the effect of temperature when analysing the DO levels in the water. This is achieved by looking at the saturation value, which is the maximum level of DO that would be present in a specific water body at a specific temperature.

Dissolved oxygen saturation

Dissolved oxygen saturation in pure water, commonly symbolized as C_S expressed as a function of site pressure to sea level and as temperature (Johanson et al., 1981):

$$C_{DOS}=\left(14.652 - 0.41002T + 0.007910T^2 - 7.7774\times10^{-5}T^3\right)\times\left(\frac{P}{29.92}\right) \tag{2.16}$$

Where:

T = Temperature (ºC);

P = Barometric pressure (in Hg).

<u>Reaeration</u>

Reaeration is the process of oxygen exchange between the atmosphere and a water body in contact with the atmosphere. The exchange is typically from the atmosphere to the water, since dissolved oxygen levels in most natural waters are below saturation (Chapman et al., 1996). However, transfer from the water to the atmosphere may happen when photosynthesis leads to dissolved oxygen supersaturated water (Bowie and Tech, 1985). The reaeration process is modelled as the product of a mass transfer coefficient multiplied by the difference between the dissolved oxygen saturation and the actual dissolved oxygen concentration:

$$F_{C_{DO}}=k_L(C_{DOS}-C_{DO}) \tag{2.17}$$

Where:

F_{CDO} = flux of dissolved oxygen across the water surface (mass per area and time);

C_{DO} = dissolved oxygen concentration (mass per volume);

C_{DOS} = saturation dissolved oxygen concentration (mass per volume);

k_L = surface transfer coefficient (length per time).

In river modelling and for vertically mixed estuaries a depth average flux (F_C'), is used:

$$F'_{CDO}=\frac{F_{CDO}}{d}=\frac{k_L}{d}(C_{DOS}-C_{DO}) \tag{2.18}$$

Where:

d = water depth (length).

The reaeration rate coefficient commonly expressed as k_2, can be calculated as:

$$k_2 = \frac{k_L}{H} \tag{2.19}$$

The reaeration coefficient can also be influenced by certain special factors that rarely are included in water quality models such as: surfactants, suspended/floating particles, wind and hydraulic structures. More information about the influence of these factors is discussed elsewhere (Alonso et al., 1975; Eloubaidy and Plate, 1972; Frexes et al., 1984; Gameson et al., 1958; Gulliver and Stefan, 1981; Holley, 1977; Jarvis, 1970; Nakasone, 1975; Poon and Campbell, 1967; Tsivoglou and Wallace, 1972; Zison, 1978).

Carbonaceous Deoxygenation

Biochemical oxygen demand (BOD) corresponds to the utilization of dissolved oxygen by aquatic microbes to metabolize organic matter, oxidize reduced nitrogen and mineral species. BOD is commonly divided in two fractions: carbonaceous (CBOD) and nitrogenous matter (NBOD). CBOD decay commonly follows first order kinetics represented by:

$$\frac{\partial C_{CBOD}}{\partial t} = -\, k_0 C_{CBOD} \tag{2.20}$$

Where:

C_{CBOD} = carbonaceous BOD concentration (mg L^{-1});

k_0 = first order oxidation rate (day^{-1});

t = time (day).

This equation when coupled with stream dissolved oxygen kinetics becomes the classic *Streeter-Phelps* equation, which is similar in nearly all state of the art water quality models:

$$D = \frac{k_d C_{DO}}{k_2 - k_d}\left[e^{-k_d t} - e^{k_2 t}\right] + D_0 \times e^{-k_2 t} \tag{2.21}$$

Where:

D = dissolved oxygen deficit (mg L^{-1});

k_2 = stream reaeration rate (day^{-1});

k_d = deoxygenation rate (day^{-1});

D_0 = initial dissolved oxygen deficit (mg L^{-1}).

Nitrogenous biochemical oxygen demand

The transformation of reduced forms of nitrogen to more oxidized ones consumes oxygen. Nitrification is a two stage process, the oxidation of ammonia to nitrite and nitrite to nitrate.

$$NH_4^+ + 1.5O_2 \rightarrow NO_2^- + H_2O + 2H^+ \tag{2.22}$$

$$NO_2^- + \frac{1}{2}O_2 \rightarrow NO_3^- \tag{2.23}$$

The complete oxidation of ammonia can be represented by combining equations (2.22)and (2.23):

$$NH_4^+ + 2O_2 \rightarrow NO_3^- + H_2O + 2H^+ \tag{2.24}$$

First order kinetics is the predominant method used to simulate nitrogenous biochemical oxygen demand decay:

$$\frac{\partial C_{DO}}{\partial t} = -\alpha_1 k_{n_1} N_1 - \alpha_2 k_{n_2} N_2 \tag{2.25}$$

Where:

k_{n1} = ammonia to nitrite oxidation rate (time^{-1});

k_{n2} = nitrite to nitrate oxidation rate (time^{-1});

a_1 = 3.43, typically;

a_2 = 1.14, typically;

N_1 = ammonia-nitrogen concentration (mass volume^{-1});

N_2 =nitrite-nitrogen concentration (mass volume^{-1}).

Sediment Oxygen Demand (SOD)

A large fraction of oxygen consumption in surface waters is due to oxygen demand by sediments and organisms (Held and Soden, 2006). The major factors affecting SOD are: temperature, oxygen concentration at the sediment water interface, makeup of the biological community, organic and physical characteristics of the sediment, current velocity over the sediments, and chemical of the interstitial water (Di Toro et al., 1971). The generalized equation for sediment oxygen demand is:

$$\frac{\partial C_{DOW}}{\partial t} = - \frac{SOD}{H} \tag{2.26}$$

Where:

H = water depth (m);

SOD = sediment oxygen demand ($gO_2\ m^{-2}$ day);

t = time (day);

C_{DOW} = oxygen concentration in the overlying water (mg L^{-1}).

Temperature and oxygen are usually modelled explicitly, and can be used as input variables to the SOD process equations, while the remaining factors are usually neglected. Dissolved oxygen concentration affects the rate of sediment oxygen utilization exponentially (2.27) and temperature effects on SOD are most commonly modelled using the *van't Hoff* equation from of the *Arrhenius* relationship (Atkins and de Paula, 2014; Connors, 1990) (2.28) or a linear function (2.29):

$$\frac{\partial C_{DO}}{\partial t} = \frac{-k_T^{\left(1-e^{-1.22 C_{DO}}\right)}}{H} \tag{2.27}$$

$$k_T = k_{T_r} \emptyset^{(T_W - T_r)} \tag{2.28}$$

$$k_T = 0.05\, T_W\, k_{20} \tag{2.29}$$

Where

k_T = temperature adjusted rate constant (mg m^{-2} day);

k_{Tr} = reference temperature rate constant (usually 20ºC);

$\emptyset$ = temperature coefficient for SOD rate;

k_{20} = rate constant at 20ºC;

T_w = water temperature (ºC);

T_r = reference temperature (ºC).

2.5.6.3 Nutrients

Nutrients are essential to the life processes of aquatic organisms. The major nutrients of concern are carbon, nitrogen, phosphorus and silicon. However in water quality studies, only nitrogen and phosphorus are considered because of their high concentration in water when compared to the remaining ones that are usually present in quantities adequate to meet the biochemical requirements of microorganisms (Palmer, 2001). Nutrients are present in several different forms in aquatic systems: dissolved inorganic nutrients, dissolved organic nutrients, particulate organic nutrients, sediment nutrients, and biotic nutrients (fish, algae, zooplankton, etc.). Each nutrient undergoes continuous recycling between their major forms. Figure 2.7 shows their interaction in the aquatic system (Tech, 1979). Aquatic organisms can only exist in the presence of nutrients, however high concentration of nutrients, particularly nitrogen can result in inconvenient growth of aquatic plants and species. In particularly ammonia, the preferred nutrient for microorganisms can be toxic to fish (Palmer, 2001). Phosphorus is often the nutrient that limits excessive aquatic plant growth. For this reason excessive phosphorus can also lead to water quality degradation.

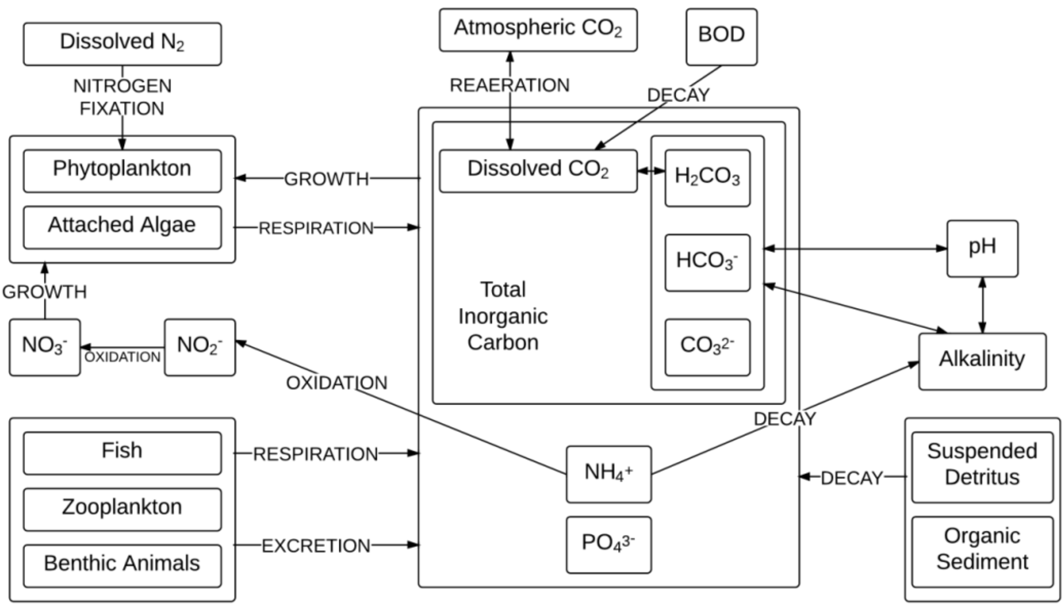

Figure 2.7 Nutrient interactions for carbon, nitrogen and phosphorus (adapted from Tetra Tech, 1979).

Predicting the nutrient concentrations in water bodies using water quality models requires that the phytoplankton biomass and species as well as the macrophyte biomass be known (Denman et al., 1977; Harris, 1980; Palmer, 1981).

Nutrients are modelled by using a system of coupled mass balance equations describing each nutrient stage and each of the following different forms: dissolved inorganic (2.30) and organic nutrients (2.31), particulate organic nutrients (2.32), and sediment nutrients (2.33). The equations for each nutrient are expressed as follows:

$$\frac{\partial S_i}{\partial t} = -V_S + k_i S' - k_{ii} S_i + f_1 k_{det} S_{det} + f_2 k_{sed} S_{sed} \tag{2.30}$$

$$\frac{\partial S_{org}}{\partial t} = (1-f_1)e_S - k_{org} S_{org} + (1-f_2)k_{det} S_{det} + (1-f_3)k_{sed} S_{sed} \tag{2.31}$$

$$\frac{\partial S_{det}}{\partial t} = e_p + M_p - k_{det} S_{det} - k_s S_{det} - G_z \tag{2.32}$$

$$\frac{\partial S_{sed}}{\partial t} = k_s S_{det} + A_S - k_{sed} S_{sed} \tag{2.33}$$

Where:

S_i = dissolved inorganic nutrient concentration, (mass volume^{-1});

S' = another inorganic form of the nutrient which decays to the form S (e.g., NH_3, NO_3), (mass volume^{-1});

S_{org} = dissolved organic nutrient concentration, (mass volume^{-1});

S_{det} = suspended particulate organic nutrient concentration, (mass volume^{-1});

S_{sed} = organic sediment nutrient concentration, (mass volume^{-1});

k_i = transformation rate of S' into S, (time^{-1});

k_{ii} = transformation rate of S into some other dissolved inorganic form of the nutrient, (time^{-1});

k_{org} = hydrolysis rate of dissolved organic nutrient (time^{-1})

k_{det} = decomposition rate of particulate organic nutrient, (time^{-1});

k_{sed} = decomposition rate of organic sediment nutrient, (time^{-1});

k_S = settling rate of particulate organic nutrient, (time^{-1});

V_S = photosynthetic uptake rate for nutrient S, (mass volume^{-1} time^{-1});

e_S = soluble excretion rate of nutrient by all organisms, (mass volume^{-1} time^{-1});

f_1 = fraction of soluble excretions which are inorganic;

f_2 = fraction of detritus decomposition products which are immediately available for algal uptake;

f_3 = fraction of sediment decomposition products which are immediately available for algal uptake;

e_p = particulate excretion rate of nutrient by all animals, (mass volume^{-1} time^{-1});

M_p = total rate of plankton mortality, (mass volume^{-1} time^{-1});

G_z = detritus grazing rate by zooplankton, (mass volume^{-1} time^{-1});

A_S = algal settling rate to sediment, (mass volume^{-1} time^{-1}).

The approach used by almost all water quality models is described by first order kinetics for all transformations between the various abiotic nutrient stages. The nutrient cycles are often simplified by combining or omitting some of the equations above. Many models do not simulate sediment nutrients instead they include sediment fluxes in the dissolved inorganic and organic nutrients balance. Some models do not simulate dissolved organic nutrients as well; instead all products go directly to the dissolved inorganic nutrient stage. Also, instead of the full oxidation sequence of ammonia to nitrite and to nitrate, some models only include ammonia to nitrate, and only a few include denitrification.

Temperature influences the first order rate coefficients of all of the nutrient transformation processes in equations (2.30) through (2.33). Just like the influence of temperature in DO concentrations, for nutrients almost all models use the exponential *Arrhenius* relationship to describe the effect of temperature on the kinetics.

$$k_T = k_{20}{}^{\varnothing\,(T-20)} \tag{2.34}$$

Where:

k_T = rate coefficient at temperature T (time^{-1});

T = temperature (ºC);

k_{20} = rate coefficient at 20ºC (time^{-1});

$\varnothing$ = temperature adjustment coefficient.

Carbon process characterization is usually neglected in models since the relationship between carbon dynamics and water quality modelling is not considered essential (Di Toro and Connolly, 1980), and whenever it is considered it is computed as first order kinetics.

Silica is only simulated when diatoms are modelled as a separate group, because they are the only freshwater organisms that utilize silica in significant amounts. They have an important role in phytoplankton succession, aquatic food chain, and a potential effect on water treatment plants (Knappe, 2004). In comparison to the other nutrients, particulate and sediment silicon decay straight to dissolved inorganic silicon rather than passing through a dissolved organic phase (Figure 2.8) (Tech, 1979).

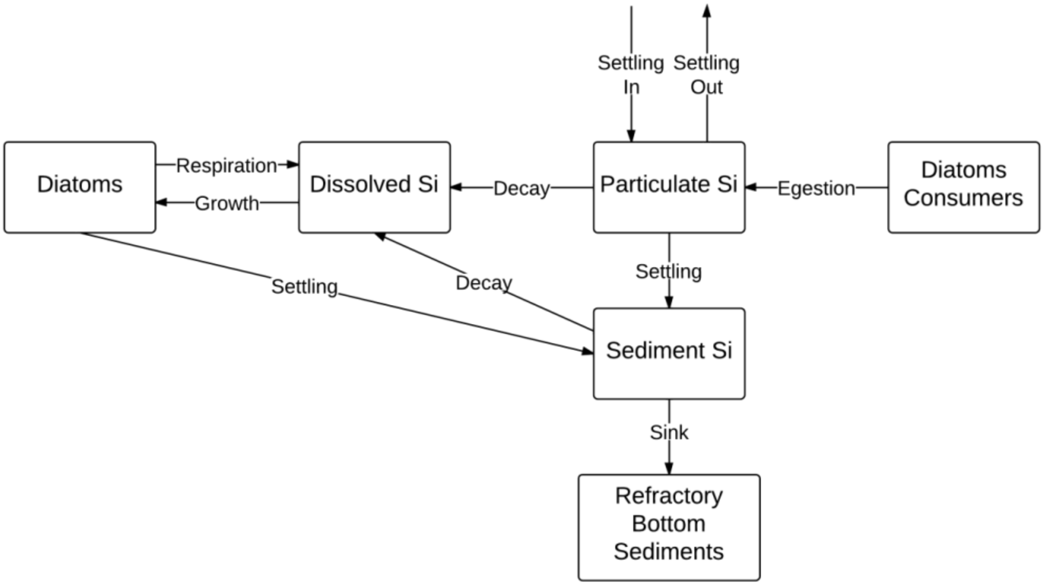

Figure 2.8 Nutrient interactions for silica (adapted from Tetra Tech, 1979).

Nitrogen dynamics play an important role in water quality modelling due to biogeochemical and oxidation-reduction reactions, which normally include: ammonification; nitrification; denitrification; uptake; and nitrogen fixation. Figure 2.9 (adapted from Baca and Arnett (1976)) describes the nitrogen process in a receiving water environment. Ammonification or hydrolyses is the release of ammonia due to decay processes, which includes the breakdown of organic compounds and sediment nitrogen to ammonia and the oxidation of ammonia to nitrate. Both denitrification and nitrogen fixation represent the nitrogen transport to and from the atmosphere respectively. Nitrogen fixation is the reduction of N_2 to ammoniated compounds. It is modelled by assuming that growth is not limited by nitrogen and that it makes up for all nitrogen requirements that cannot be satisfied by ammonia and nitrate (Tech, 1979). The uptake is the accumulation of inorganic nitrogen (ammonia and nitrate) by plants during photosynthetic growth.

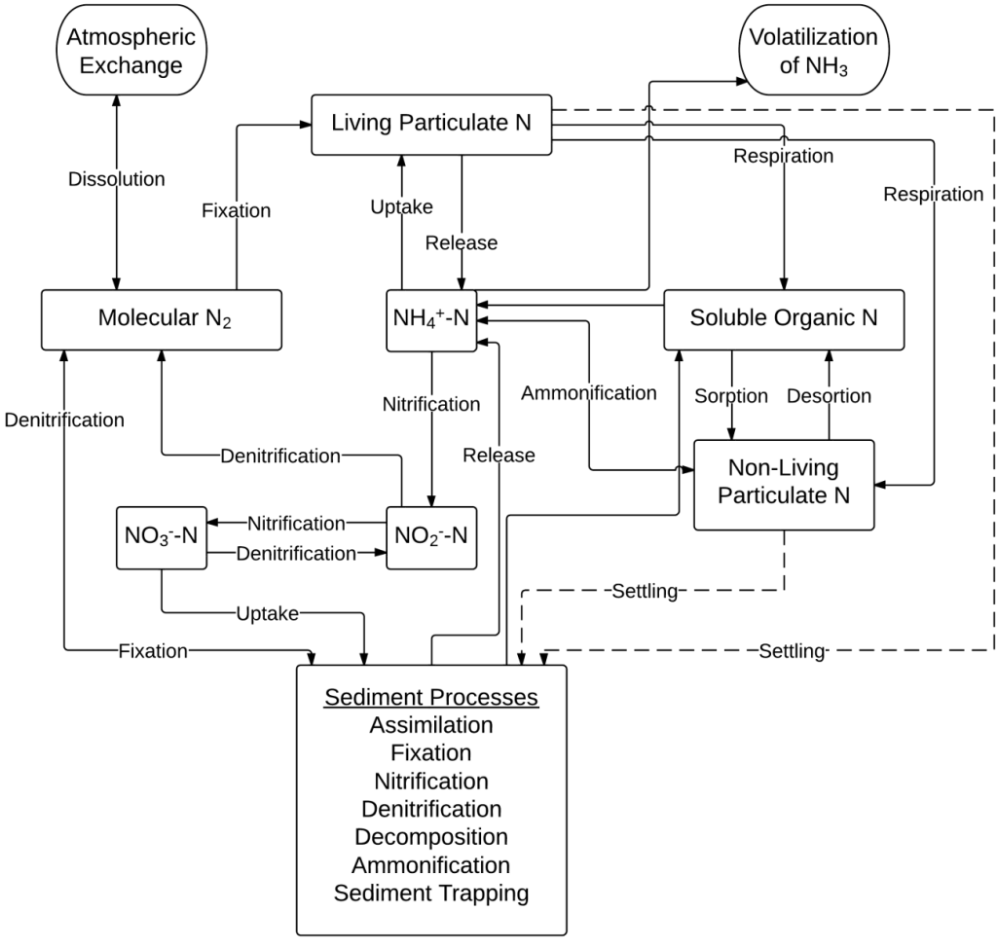

Figure 2.9 Nutrient interactions for nitrogen (adapted from Baca and Arnett, 1976).

Phosphorus transformation in a water receiving environment (Figure 2.10) (Baca and Arnett, 1976) include: the decay of particulate organic phosphorus; sediment phosphorus; and settled algae. Organic phosphorus is released by degradation of organic matter (BOD) resulting in dissolved phosphate. Just like nitrogen, uptake of phosphorus is also part of the photosynthesis and respiration process. The transformations include the decay of particulate organic phosphorus, sediment phosphorus, and settled algae to dissolved organic phosphorus or directly to orthophosphate.

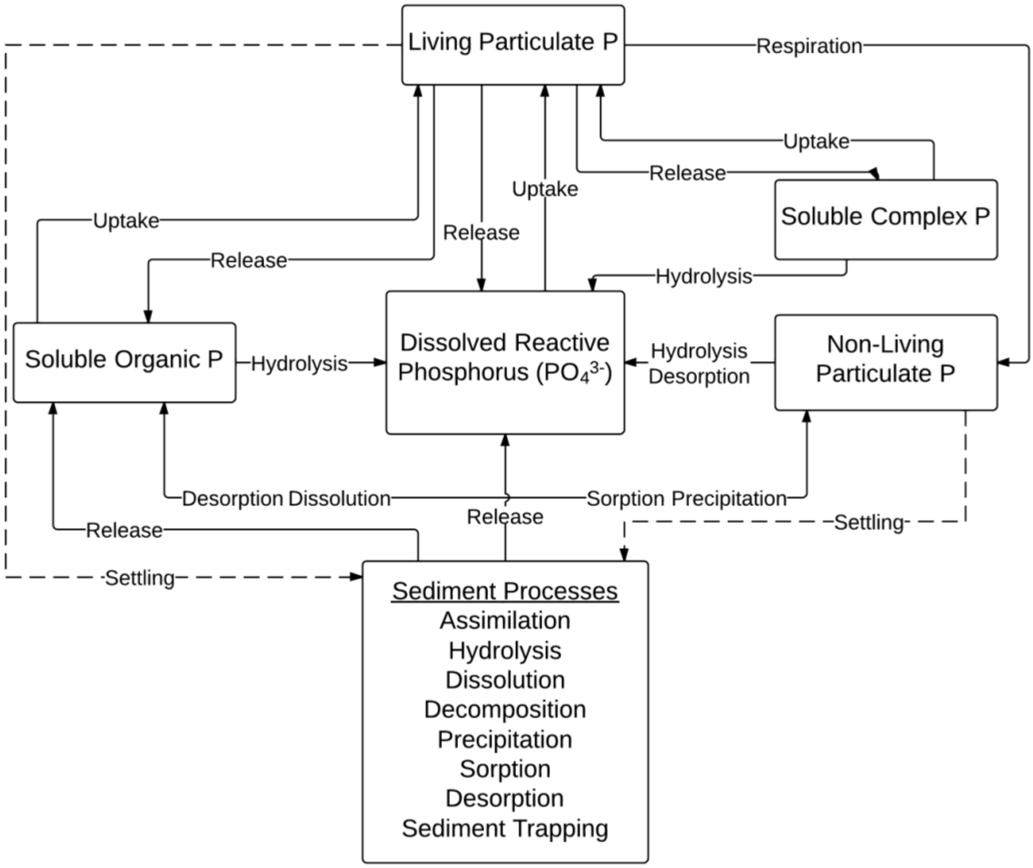

Figure 2.10 Nutrient interactions for phosphorus (adapted from Baca and Arnett, 1976).

All nutrients recycle continuously in the water column between particulate and sediment forms, dissolved organic forms, and biotic forms. The main processes are decomposition of organic particulates and sediments, decay of dissolved organic to inorganic forms and nitrification. Denitrification and nitrogen fixation are also important but neglected in most models. Table 2.4 presents a comparison of the various nutrient forms included in several models (adapted from Bowie and Tech (1985)).

Table 2.4 Comparison of various nutrients forms in several models.

Model	Nutrients Modelled				Nutrient Forms							Inorganic Nutrient Forms			References
	C	N	P	Si	Dissolved Inorganic	Dissolved Organic	Particulate Organic	Seds	Algae	Zooplk	Other Organisms	NH_3	NO_2	NO_3	
CE-QUAL-W1	X	X	X		X		X	X	X	X	X	X	X	X	(Wlosinski et al., 1995)
MS.CLEANER	X	X	X	X	X	X	X	X	X	X	X				(Park et al., 1980)
DOSAG		X	X		X			X	X			X	X	X	(Duke and Marsh, 1973)
EAM	X	X	X	X	X		X	X	X	X	X	X	X	X	(Tech, 1979)
HSPF	X	X	X		X		X	X	X	X		X	X	X	(Johanson et al., 1981)
SWAT	X	X	X		X		X	X	X	X		X	X	X	(Arnold and Fohrer, 2005)
QUAL-II		X	X		X			X	X			X	X	X	(Roesner et al., 1981)
WASP	X	X	X	X	X	X	X	X	X	X		X		X	(Park et al., 1980)
WQRSS	X	X	X		X		X	X	X	X	X	X	X	X	(Smith, 1978b)
BIERMAN		X	X	X	X		X		X	X					(Bierman et al., 1980)
CANALE		X	X	X	X	X	X		X	X		X		X	(Canale et al., 1976)

2.5.6.4 Indicator Bacteria

The primary agents of many contagious diseases in contaminated water are pathogens (Chapra, 1997). Due to the cost and difficulty in measuring individual pathogens (bacteria, viruses, protozoa, helminths, etc.), water quality management and models have focus on the levels of indicator bacteria.

The three major types of indicator bacteria are: total coliform, faecal coliform and faecal streptococci. Coliform concentrations in natural waters have been used as an indicator of potential pathogen contamination since at least 1890's (Whipple, 1917), because they were believed to be more persistent in natural waters and therefore a conservative index of potential pathogens levels. Traditionally total coliforms were the most widely used indicator of contamination and subsequently switched to faecal coliforms and faecal streptococci (Chapra, 1997) due to the presence of non-faecal coliform bacteria and more recently (Odonkor and Ampofo, 2013) to *Escherichia coli*. Beyond the selection of the indicator or set of indicators many models only simulate faecal coliforms, which allows establishing the level of faecal and/or soiling pollution and potential pathogen contamination. Figure 2.11 presents the sources and transport of faecal coliform in the environment.

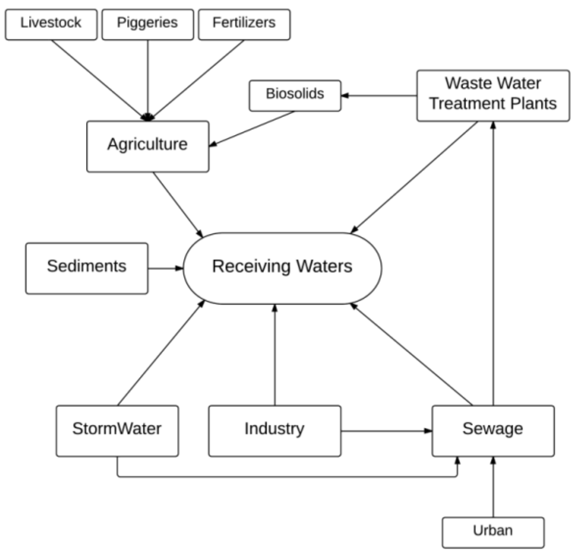

Figure 2.11 Faecal coliform transport and sources (adapted from Moyer and Hyer, 2003).

The conventional approach of coliforms modelling is to estimate coliform levels as a function of initial loading and disappearance rate which is function of time or distance travel and temperature, salinity and light intensity. Simple first order kinetics is used:

$$\frac{\mathrm{d}C_{FC}}{\mathrm{dt}} = -k_{FC}C_{FC} \tag{2.35}$$

Or

$$\mathrm{C_{FCt}} = \mathrm{C_{FC0}}\mathrm{e}^{-k_{FC}t_e} \tag{2.36}$$

Where:

C_{FC} = coliform concentration (count 100 mL^{-1});

C_{FC0} = initial coliform concentration (count 100 mL^{-1});

C_{FCt} = coliform concentration at time t (count 100 mL^{-1});

k_{FC} = disappearance rate constant (time^{-1});

t_e = exposure time (time^{-1}).

Although first order kinetics is commonly used, it gives only an approximation of the actual disappearance rate value (Velz, 1970), because the decay rate is nonlinear with time, which will result in an overestimate or underestimate of the concentration over time.

Chamberlin and Mitchell (1978) suggested that incident light levels affect coliform decay rates and defined a light level dependent disappearance rate coefficient as:

$$\mathrm{k}' = \mathrm{k_l}\,\mathrm{l_0}\,\mathrm{e}^{-\mathrm{la}\,\mathrm{z}} \tag{2.37}$$

Where:

k' = light dependent coliform disappearance rate (hr^{-1});

k_l = proportionality constant for the specific organism (cm^2 J^{-1});

l_0 = incident light energy at the surface (J cm^{-2} hr^{-1});

l_a = light attenuation at coefficient (per unit depth);

z = depth (in units consistent with a).

When incorporation vertical distribution of bacterial cells and assuming that decay rate is a function of only light intensity and the vertical distribution of coliforms is non-uniform over depth (Chamberlin, 1977), the coliform concentration can be calculate as:

$$\frac{\partial C_{FC}}{\partial \mathrm{t}} - \mathrm{w}\frac{\partial C_{FC}}{\partial \mathrm{z}} = \mathrm{K_Z}\frac{\partial^2 C_{FC}}{\partial z^2} - \mathrm{k}'C_{FC} \tag{2.38}$$

Where:

K_Z = vertical dispersion coefficient ($cm^2\ hr^{-1}$);

w = vertical settling velocity ($cm\ hr^{-1}$).

Indicator bacteria is of interest as an index of potential pathogen contamination of surface water, more specifically faecal coliforms and more recently *Escherichia coli*. Regrowth is generally neglected and thus is not considered by models.

2.5.6.5 Other Quality Constituents

There are other common quality parameters that are usually part of monitoring programs but not always are considered for modeling purposes. A summary of these parameters and their description is presented in Table 2.5.

Table 2.5 Common water quality monitoring parameters.

Parameter	Description
Alkalinity	It measures the amount of alkaline compounds in water (mainly carbonates, bicarbonates and hydroxides),and is related to the resistance of water to a change in pH. It affects corrosion or scale deposition.
Conductivity	It is an indirect measure of the presence of ionic species in water (chloride, nitrate, sulfate, phosphate, sodium, magnesium, calcium, iron and aluminum). Conductivity tests are often used to assess water suitability for irrigation.
pH	It is an important limiting chemical factor for aquatic life, if water is too acidic or too basic ion activity may disrupt aquatic organism. Streams usually have pH values ranging between 6 and 9.
Sulphate	High concentration in water can be a laxative effect to humans and livestock, and cause brain disorders in cattle and pigs.
Metals	The effect of metals in water ranges from beneficial to toxic. The most toxic heavy metals include: copper, iron, cadmium, zinc, chromium, mercury and lead.
Total Solids	It is a measure of suspended and dissolved solids in a body of water. It is related to both conductivity and turbidity.
Turbidity	It is associated with fine particles naturally suspended in water, such as: clay, silt or plankton. They block light needed by submerged aquatic vegetation.

2.6 Statistical Analysis in Hydrology

Hydrologic phenomena such as precipitation, floods and droughts are inherently random by nature (Pizarro et al., 2012). The complexity of the hydrologic system (i.e. physical processes) is not fully understood and reliable deterministic mathematical models have yet to be developed (Grimaldi et al., 2011).

A myriad of hydrology models are available, each with their own range of characteristics to measure and represent natural water body behaviour. Establishing confidence in the outputs of such models is crucial in justifying their continuing use while also recognizing limitations (Bennett et al., 2013). Many different approaches and debates on the identification of a most appropriate technique to evaluate a model's performance are discussed in literature (Alexandrov et al., 2011; McIntosh et al., 2011). This is why statistical approaches have been commonly adopted (Grimaldi et al., 2011) to provide useful analysis for the hydrological phenomena in the environment. Methods for measuring quantitative performance (Table 2.6) include: direct model comparison, comparison of real and modelled values concurrently, key residual criteria, residual methods using data transformations and, correlation and model efficiency performance measures.

A complete review of qualitative and quantitative methods of characterising performance of environmental models is presented by Bennett et al. (2013). Independently of the purpose why the model is used, it is always good to know how it behaves when compared to the data available. Many criteria are available but there is not an evaluation standard when characterising the model performance, and it will ultimately depends on the goal of the model (Alexandrov et al., 2011).

Table 2.6 Overview of methods for characterizing performance of environmental models.

Name	Formula	Range	Ideal Value	Description
Key Residual Criteria				
Percent Bias	$D_v[\%]\ \frac{\sum_i^n(O_i-S_i)}{\sum_i^n O_i}\times 100$	(-∞, +∞)	0	Calculates the mean error. A value of zero does not necessarily indicate low error due to cancelation.
Mean Square Error	$MSE=\frac{1}{n}\sum_{i=1}^{n}(S_i-O_i)$	(0, +∞)	0	Same as percent bias, but it is not affect by cancelation. May cause bias towards large events.
Root Mean Square Error	$RMSE=\sqrt{\frac{1}{n}\sum_{i=1}^{n}(S_i-O_i)^2}$	(0, +∞)	0	Standard deviation of the differences between predicted and observed values.
Residual Methods that use Data Transformation				
Fourth Root Mean Quadrupled (Fourth Power) Error	$R4MS4E=\sqrt[4]{\frac{1}{n}\sum_{i=1}^{n}(S_i-O_i)^4}$	(0, +∞)	0	Similar to root mean square error but with more emphasis to larger events.
Correlation and model efficiency performance measures				
Nash-Sutcliffe Model Efficiency	$NSE=1-\frac{\sum_{i=1}^{n}(S_i-O_i)^2}{\sum_{i=1}^{n}(O_i-\emptyset_i)^2}$	(-∞, 1)	1	Indicates the percentage of the observed variance that is explained by the model.
Coefficient of Determination	$R^2=\left[\frac{\sum_{i=1}^{n}[(O_i-\bar{O})(S_i-\bar{S})]}{[\sum_{i=1}^{n}(O_i-\bar{O})^2]^{1/2}[\sum_{i=1}^{n}(S_i-\bar{S})^2]^{1/2}}\right]^2$	(0, 1)	1	Determines how much the variance between two variables is described by a linear fit.
Index of Agreement	$IoAd=1-\frac{\sum_{1=1}^{n}(S_i-O_i)^2}{\sum_{1=1}^{n}(\lvert O_i-\emptyset\rvert-\lvert S_i-\emptyset\rvert)^2}$	(0, 1)	1	Similar to R^2 but designed to be better at handling differences in modelled and observed means and variances.
Standard Deviation Ratio	$RSR=\frac{\sqrt{\sum_{i=1}^{n}(S_i-O_i)^2}}{\sqrt{\sum_{i=1}^{n}(O_i-\emptyset)^2}}$	(0, +∞)	0	Similar to RMSE but weighted by the standard deviation of the observed values.

2.7 Uncertainty and Sensitivity Analysis

"All models are wrong, but some are useful" (Box and Draper, 1987). Every model is wrong because they are a simplification of reality, but they are useful because they can help us to explain, predict and understand all Nature phenomena. Simplification leads to uncertainty in model output. Meticulous uncertainty analysis in water quality modelling is rare (Stow et al., 2007). Uncertainty in water simulation models is expected due to the difficulty of accurately represent water quantity and quality against a real environment (Beck, 1987; van Straten, 1998). The existence of too many methods to perform uncertainty analysis for water quality results interpretation is considered an hindrance (Pappenberger and Beven, 2006). To understand the general behaviour of a water quality model it is advisable to perform an uncertainty and sensitivity analysis. Two of the most common methodologies are simple parameter perturbation and Monte Carlo technique (which provides a more general approach). Parameter perturbation consists of varying each of the model parameters while holding all other terms constant. The corresponding variations of the state variables reflect the sensitivity of the solution to the varied parameter. By using constant perturbations the uncertainty ascribed to each parameter will be the same. Rather than prescribing a range for the parameters, random numbers are used to generate a series of parameter estimates that follow a distribution (Monte Carlo approach). Monte Carlo based methodologies of uncertainty and sensitivity analysis such as those implemented by Hornberger and Spear (1981), Beven and Binley (1992) and Kuczera and Parent (1998) have found myriad applications in environmental modelling, including surface water quality modelling. Figure 2.12 shows probability distributions that are commonly used to describe parameter variability in water quality modelling.

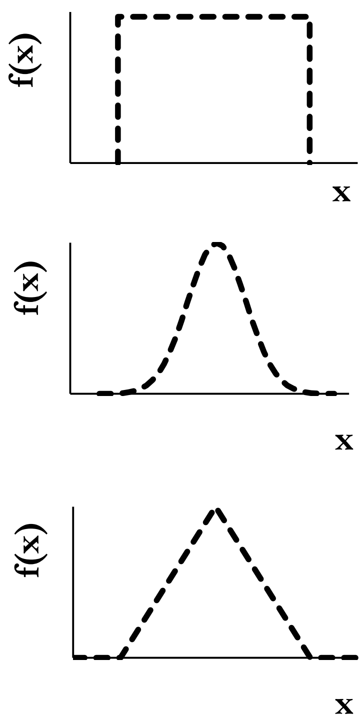

a) The normal distribution assumes that there is an equal likelihood of occurrence between two bounds. It is often used when only the range of the parameter is known.

b) The normal distribution assumes that the parameter follows a symmetrical bell shaped curve, having more occurrences at a most likely value in the center and fewer occurrences at the extremes.

c) The triangular distribution provides a simplistic representation of the probability distribution when limited sample data is available. It is defined by a minimum, a most likely value and a maximum.

Figure 2.12 Probability density distributions commonly used to characterize uncertainty in water quality modelling parameters: a) uniform; b) normal and c) triangular.

The predefined parameter probability distribution is usually estimated from: a review of relevant literature; historical data; or other uncertainty techniques like Generalized Likelihood Uncertainty Estimation (GLUE); Bayesian Monte Carlo (BMC); and Markov Chain Monte Carlo (MCMC) (Mishra, 2011).

2.7.1 Generalized Likelihood Uncertainty Estimation (GLUE)

In GLUE (Beven and Binley, 1992) there is not a single optimum set of parameters for a hydrologic model. Instead, there are multiple sets of parameters that acceptably represent a hydrologic model, adopting the concept of equifinality of models, parameters and variables. Monte Carlo simulation is performed by generating different sets of parameters from prior distributions and a likelihood weight is applied to each parameter set depending on its model output result. Likelihood is a measure of how well a given combination of parameter sets fits the available set of observations (Blasone et al., 2008). The likelihood is normally evaluated by a goodness-of-fit criterion (Stow et al., 2007) like those discussed in section 2.6, and assigned to each parameter set as an acceptable or non-acceptable solution for model output. Following the GLUE approach a validation of all observation points should be performed. Normally a confidence interval of 95% is defined and the majority of the observations should be within this interval. GLUE has been widely used to conduct uncertainty analysis using different hydrologic modelling software (Balin, 2004; Beven and Binley, 1992; Freer et al., 1996).

2.8 Better Assessment Science Integrating point and Nonpoint Sources

Better Assessment Science Integrating Point and Nonpoint Sources (BASINS) is a multipurpose environmental analysis system designed to help regional and local agencies by providing a framework for integrating spatial data (land use, vegetation, climate and elevation) to perform watershed and water quality based studies (Lahlou et al., 1998). Developed and distributed by the United States Environmental Protection Agency (USEPA), BASINS is built on the open source geographic information system (GIS) MapWindow (Ames et al., 2008) and addresses three objectives: 1) to facilitate examination of environmental information; 2) provide an integrated watershed and modelling framework; and 3) support analysis of point and nonpoint source management alternatives.

Aside from the open source geographic information system it also includes several other *add ins* such as the water quantity and quality model Hydrological Simulation Program – FORTRAN (HSPF), the utility program to manage weather data time series, WDMutil, and, the climate assessment tool , CAT, which allows to create hypothetical weather scenarios. Thus, for the reasons mentioned above BASINS was the chosen software addressed in this study.

2.8.1 Hydrologic Simulation Program – FORTRAN

Use of the Hydrological Simulation Program – FORTRAN (HSPF) watershed model (Bicknell et al., 2001) traditionally involved a text editor to build an input sequence to describe the watershed's physical and water management characteristics (Duda et al., 2001). HSPF is a comprehensive, conceptual, continuous watershed simulation model designed to simulate all water quantity and quality processes that occur in a watershed and in stream, including sediment transport and movement of contaminants for extended periods of time. For large or complex river basins it would become unfeasible, when applied to both hydrology and quality simulation, becoming difficult to understand the behaviour of the model inputs and their relation to the watershed. The development of WinHSPF came as a response to the need to make HSPF input sequences easier to build and modify (Duda et al., 2001). WinHSPF was created by the US Environmental Protection Agency's BASINS system. A graphical user interface for HSPF is included in the free software, BASINS, developed and distributed by the United States Environmental Protection Agency. HSPF is based on the original Stanford Watershed Model IV and is a consolidation of three previously developed models: Agricultural Runoff Management Model (Donigian, 1977), Nonpoint Source Runoff Model (NPS) (Donigian and Crawford, 1976) and Hydrological Simulation Program (HSP) including HSP Quality (Donigian et al., 1991; Donigian Jr et al., 1995). HSPF is a semi distributed model that simulates water and contaminant transport through spatially distributed, physically homogenous areas within a watershed called Hydrologic Response Units (HRUs). HRUs are presumed to hydrologically respond similarly to given meteorological inputs (precipitation, potential evapotranspiration and temperature). In this way, HSPF can simulate the hydrological, hydraulic and water quality processes on pervious and impervious land surfaces, in soil profiles and in streams and well mixed impoundments on a continuous basis (Bicknell et al., 2001). The use of BASINS to develop HSPF models has been reported in several studies (Bergman et al., 2002; Carrubba, 2000; Lian et al., 2007; Lowe and Doscher, 2003; Zhang et al., 2009). However there are limitations to HSPF, such as limited spatial definition (finite element analysis model), limited to non-tidal freshwater systems and extensive data requirements (i.e. meteorological and most important gauging stations of interest in the watershed) (Figure 2.13).

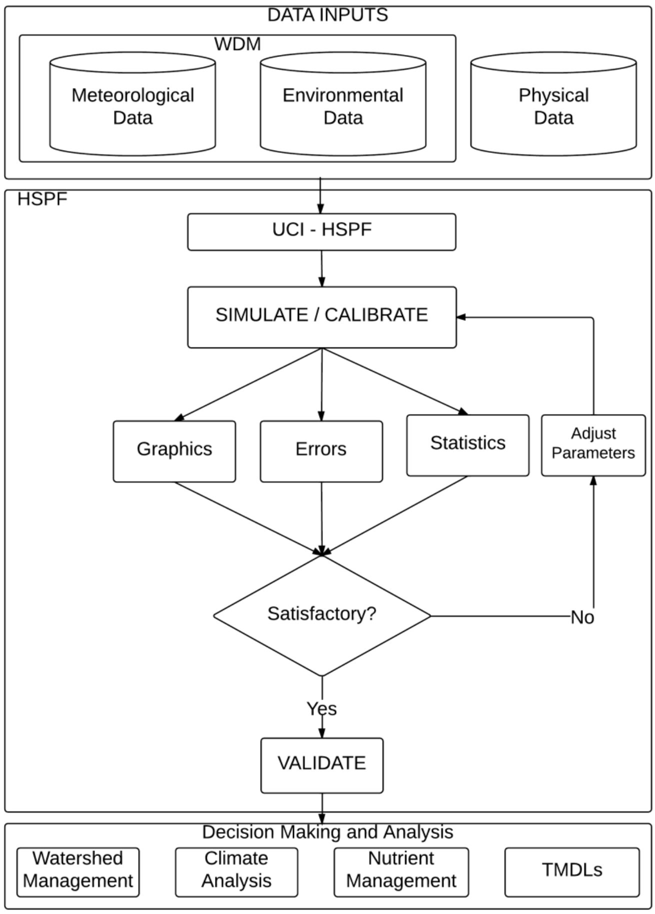

Figure 2.13 HSPF model calibration steps.

An effective simulation of the model depends on the development of accurate and representative time series inputs. Time series data include precipitation, maximum and minimum air temperature, dew point temperature, wind movement, solar radiation, evaporation and evapotranspiration, and inflow accounts from tributaries. Based on a continuous record data, it can compute a continuous hydrograph of stream flow at the chosen outlet and provide a time history of the runoff, sediment load and nutrient and pesticide concentrations (Donigian et al., 1991). Additionally, to perform a calibration, gauge station with discharge and water quality information must be available. HSPF also contains tabular input parameter, such as monthly varying inputs, program control flags, constants for model algorithms and state variables.

2.8.1.1 Streamflow model

In HSPF, the mechanisms by which precipitation is routed from the land surface, through the various soil layers and to the stream channel is represented by the pervious land segments (PERLND), impervious land segments (IMPLND) and the stream channel (RCHRES) modules. The PERLND module simulates storage and transport of precipitation through three flow pathways: overland flow, interflow, and baseflow. The simulated hydrologic cycle is presented in Figure 2.14, the acronyms in brackets are HSPF modelling parameters.

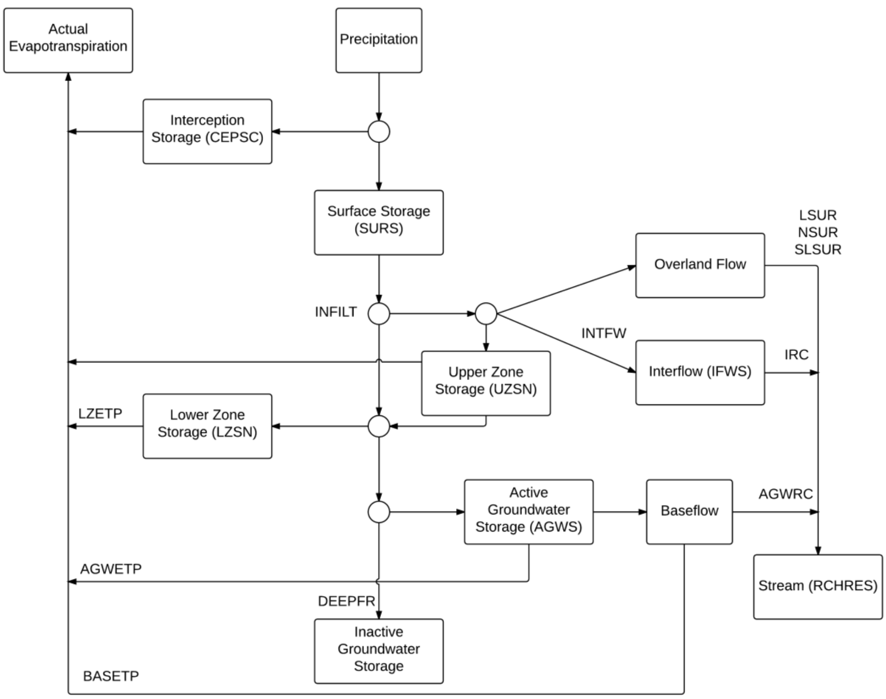

Figure 2.14 Rainfall routing processes associated with pervious land segments, represented by HSPF (Moyer and Hyer, 2003).

Precipitation is intercepted (CEPSC) by vegetation and routed to the land surface. The amount that is intercepted is eventually lost through evaporation. The water is then temporarily stored (SURS) before infiltration (INFILT) occurs. The infiltrated water is distributed to: active ground water (AGWS), lower zone storage (LZSN) and upper zone storage (UZSN). Water that is not infiltrated is routed to interflow storage (IFWS) (just beneath the land surface), which will eventually be released to the stream based on residence time recession constant (IRC). Stored water is also routed directly to the stream through overland flow; it is governed by length (LSUR), slope (SLSUR), and roughness (NSUR) of the overland flow. This happens when all other subsurface storages are full. Water in the upper zone (UZSN) is eventually lost to the atmosphere through evapotranspiration and to the deeper subsurface through infiltration. Deep subsurface water is divided to the lower zone storage (LZSN); and active (AGWS) and inactive ground water; which will eventually be lost to the atmosphere through evapotranspiration (LZETP and AGWETP respectively). The residence time for water in baseflow is controlled by the active groundwater recession constant (AGWRC) and a portion is also lost through evapotranspiration (BASETP) before entering the channel. Finally, a portion of the infiltrated water is allocated to inactive groundwater storage (DEEPFR) that will never reach the stream channel.

The IMPLND module is similar to the PERLND module but less complex since there is no infiltration or subsurface processes. Precipitation is first intercepted by impervious surfaces (roads, roof tops; urban vegetation; etc.) and lost to the atmosphere through evaporation. Water that is routed to the land surface is transported to the stream reach as surface runoff. An impervious coefficient is assigned to each impervious segment which determines the fraction of impervious area within urban and residential land types.

The RCHRES module is used to simulate water routing and associated water quality constituents through the stream channel, which may consist of a series of connected stream reaches. The channel properties (width, depth, cross sectional area and slope) for each segment are usually retrieved from the watershed delineation based on the digital elevation model.

2.8.1.2 Water Quality Parameters

The water quality balances used in HSPF model, which includes inorganic carbon, BOD, DO, phytoplankton, zooplankton and benthic algae mass balances, inorganic nitrogen or phosphorus sources, sinks and transformations, heat exchange mass balance and refractory organic (N, P, C) mass balance are shown in Figure 2.15.

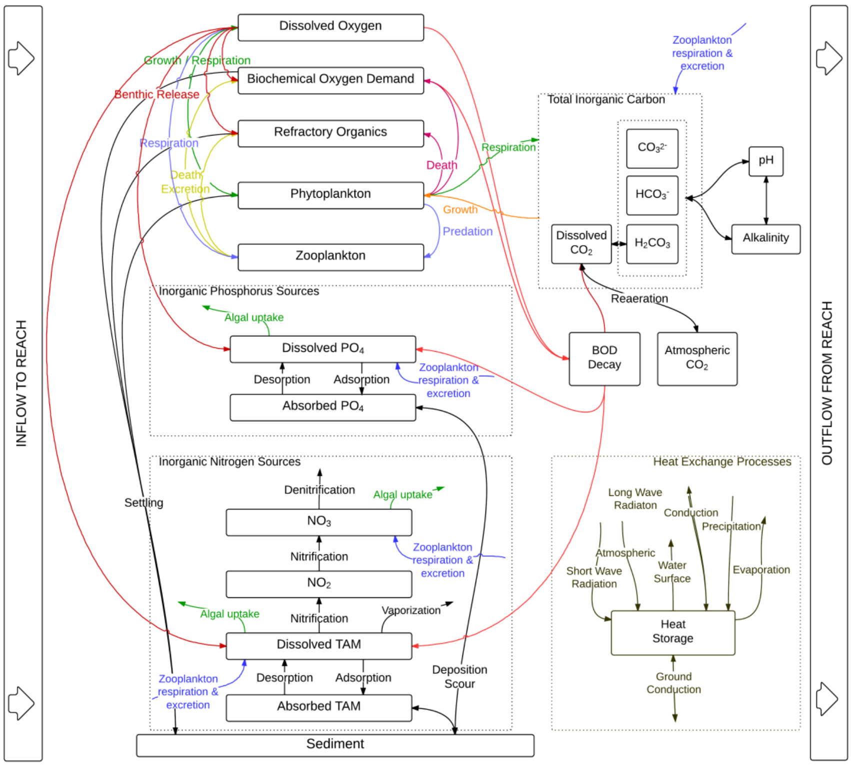

Figure 2.15 Instream water quality constituents' balance.

The water quality parameters addressed in this study and their governing equations where previously discussed on section 2.5.6. A summary of the water quality parameters is briefly described in Table 2.7. A detailed description of HSPF parameters governing equations is available on appendix A.

Table 2.7 Water quality parameters addressed for model calibration.

Parameter	Modelling Considerations	Environmental Properties
Temperature	Heat flux balances	Bacteria activity; Fish habitat; Solubility of oxygen
Suspended Solids	Currents and bottom shears; Partitioning coefficients	Aquatic plants; Dissolved oxygen sink
Faecal Coliform	Temperature; Suspended solids, Sunlight	Animal intestinal bacteria
Dissolved Oxygen	BOD; SOD; Nitrogen; Photosynthesis and respiration; Temperature; Suspended solids	Required for aquatic life
Nitrogen	DO processes; Aquatic plant demand; Temperature; Bacterial biomass	Required for aquatic plants; Ammonia toxic to fish but preferred nutrient for most bacteria; Dissolved oxygen sink and source
Phosphorus	Aquatic plant demand	Required for aquatic plants

2.8.2 Weather Data Management Utility

The Weather Data Management Utility, WDMutil, (Hummel et al., 2001) is a tool which allows users to import available meteorological data into *WDM* files format and perform needed operations such as editing, aggregation/disaggregation, filling missing data, etc. to create the necessary input time series data to run the HSPF model. The WDMutil user interface has a main form that displays lists of scenarios that have been collected (observed data) or developed (computed data) and, locations and constituents for which data are available. The user may analyse results by selecting desired scenarios, locations and, constituents for any specific span of time and generate time series or graphical plots.

2.8.3 Climate Assessment Tool

The Climate Assessment Tool, CAT (Imhoff et al., 2007), provides a flexible set of capabilities for users to create watershed based assessments of the potential implications of climate variability to run with the HSPF model. The user can create any climate change scenario assumed to be of interest in a specific watershed (what if scenarios) and general worldwide trends (global warming).

2.9 References

Alcamo, J., DÖLL, P., Henrichs, T., Kaspar, F., Lehner, B., RÖSCH, T., Siebert, S., 2003. Development and testing of the WaterGAP 2 global model of water use and availability. Hydrological Sciences Journal 48, 317-337.

Alexandrov, G.A., Ames, D., Bellocchi, G., Bruen, M., Crout, N., Erechtchoukova, M., Hildebrandt, A., Hoffman, F., Jackisch, C., Khaiter, P., Mannina, G., Matsunaga, T., Purucker, S.T., Rivington, M., Samaniego, L., 2011. Technical assessment and evaluation of environmental models and software: Letter to the Editor. Environmental Modelling & Software 26, 328-336.

Allen, M.R., Ingram, W.J., 2002. Constraints on future changes in climate and the hydrologic cycle. Nature 419, 224-232.

Alonso, C., McHenry, J., Hong, J., 1975. The influence of suspended sediment on the reaeration of uniform streams. Water Research 9, 695-700.

Ambrose, R.B., Wood, T.A., Connolly, J.P., Schanz, R.W., 1988. WASP4, a hydrodynamic and water quality model: model theory, user's manual and programmer's guide, WASP4, a hydrodynamic and water quality model: model theory, user's manual and programmer's guide. EPA.

Ames, D.P., Michaelis, C., Anselmo, A., Chen, L., Dunsford, H., 2008. MapWindow GIS, in: Springer (Ed.), Encyclopedia of GIS, New York, pp. 633-634.

Anderson, D.R., Dracup, J.A., Fogarty, T.J., Willis, R., 1976. Water quality modeling of deep reservoirs. Journal (Water Pollution Control Federation) 48, 134-146.

Arnold, J., Fohrer, N., 2005. SWAT2000: current capabilities and research opportunities in applied watershed modelling. Hydrological processes 19, 563-572.

Arnold, J.G., Srinivasan, R., Muttiah, R.S., Williams, J.R., 1998. Large area hydrologic modeling and assessment part I: Model development1. Wiley Online Library.

Atkins, P., de Paula, J., 2014. Physical chemistry. Oxford University Press.

Baca, R.G., Arnett, R.C., 1976. A limnological model for eutrophic lakes and impoundments. Battelle, Pacific Northwest Laboratories, forU. SEPA, Office of Research and Development.

Balin, D., 2004. Hydrological behaviour through experimental and modelling approaches. Application to the Haute-Mentue catchment, School of Agriculture, Civil and Environmental Engineering. Ecole Polythechnique Fédérale de Lausanne, Lausanne, Switzerland.

Beck, M.B., 1987. Water quality modeling: a review of the analysis of uncertainty. Water Resources Research 23, 1393-1442.

Bennett, N.D., Croke, B.F.W., Guariso, G., Guillaume, J.H.A., Hamilton, S.H., Jakeman, A.J., Marsili-Libelli, S., Newham, L.T.H., Norton, J.P., Perrin, C., Pierce, S.A., Robson, B., Seppelt, R., Voinov, A.A., Fath, B.D., Andreassian, V., 2013. Characterising performance of environmental models. Environmental Modelling & Software 40, 1-20.

Bergman, M.J., Green, W., Donnangelo, L.J., 2002. Calibration of Storm Loads in the South Prong Watershed, Florida, Using BASINS/HSPF. JAWRA Journal of the American Water Resources Association 38, 1423-1436.

Beven, K., Binley, A., 1992. The future of distributed models: model calibration and uncertainty prediction. Hydrological processes 6, 279-298.

Bicknell, B., Imhoff, J., Kittle Jr, J., Jobes, T., Donigian Jr, A., Johanson, R., 2001. Hydrological Simulation Program–FORTRAN: HSPF Version 12 User's Manual. AQUA TERRA Consultants, Mountain View, California.

Bierman, V., Dolan, D., Stoermer, E., Gannon, J., Smith, V., Commision, G.L.B., 1980. Development and calibration of a spatially simplified multi-class phytoplankton model for Saginaw Bay, Lake Huron, Development and calibration of a spatially simplified multi-class phytoplankton model for Saginaw Bay, Lake Huron. GLEPS.

Blasone, R.-S., Vrugt, J.A., Madsen, H., Rosbjerg, D., Robinson, B.A., Zyvoloski, G.A., 2008. Generalized likelihood uncertainty estimation (GLUE) using adaptive Markov Chain Monte Carlo sampling. Advances in Water Resources 31, 630-648.

Blöch, H., 2001. EU policy on nutrients emissions: legislation and implementation. Water Science & Technology 44, 1-6.

Blumberg, A.F., 1977. Numerical model of estuarine circulation. Journal of Hydraulic Engineering 103, 295-310.

Blumberg, A.F., Mellor, G.L., 1980. A coastal ocean numerical model, Mathematical Modelling of Estuarine Physics. Springer, pp. 203-219.

Board, T.W.D., 1970. DOSAG-I Simulation of Water Quality in Streams and Canals Program Documentation and Users Manual. Systems Engineering Division of the Texas Water Development Board.

Bowen, I.S., 1926. The ratio of heat losses by conduction and by evaporation from any water surface. Physical review 27, 779.

Bowie, G.L., Tech, T., 1985. Rates, constants, and kinetics formulations in surface water quality modeling.

Box, G.E., Draper, N.R., 1987. Empirical model-building and response surfaces. John Wiley & Sons.

Brocard, D.N., Harleman, D.R., 1976. One-dimensional temperature predictions in unsteady flows. Journal of the Hydraulics Division 102, 227-240.

Brown, L.C., Barnwell, T.O., 1987. The enhanced stream water quality models QUAL2E and QUAL2E-UNCAS: documentation and user manual. US Environmental Protection Agency. Office of Research and Development. Environmental Research Laboratory.

Canale, R.P., DePalma, L.M., Vogel, A., 1976. A plankton-based food web model for Lake Michigan. Modeling biochemical processes in aquatic ecosystems, 33-74.

Carrubba, L., 2000. Hydrologic Modeling at the Watershed Scale Using NPSM. JAWRA Journal of the American Water Resources Association 36, 1237-1246.

CEC, C.o.t.E.C., 1975. Directive concerning the quality of surface waters intended for the abstraction of drinking water (75/440/EEC). Official Journal of the European Communities, 26.

CEC, C.o.t.E.C., 1976a. Directive concerning pollution caused by dangerous substances discharged into the aquatic environment (76/464/ECC). Official Journal of the European Communities, 32.

CEC, C.o.t.E.C., 1976b. Directive concerning the quality of bathing waters (76/160/EEC). Official Journal of the European Communities, 1.

CEC, C.o.t.E.C., 1978. Directive concerning the quality of fish waters (78/659/EEC). Official Journal of the European Communities, 1.

CEC, C.o.t.E.C., 1979. Directive concerning the quality of shellfish waters (79/923/EEC). Official Journal of the European Communities, 47.

CEC, C.o.t.E.C., 1980a. Directive concerning the protection of groundwater against pollution caused by certain dangerous substances (80/68/EEC). Official Journal of the European Communities, 43.

CEC, C.o.t.E.C., 1980b. Directive concerning the quality of water for human consumption (80/778/EEC). Official Journal of the European Communities, 11.

CEC, C.o.t.E.C., 1991a. Directive concerning protection of water against pollution by nitrates from agriculture (97/676/EEC). Official Journal of the European Communities, 1.

CEC, C.o.t.E.C., 1991b. Directive concerning urban waste water treatment (91/271/EEC). Official Journal of the European Communities, 12.

CEC, C.o.t.E.C., 2000. Directive 2000/60/EC of the European Parliament and the Council of 23 October 2000, establishing a framework for Community action in the field of water policy. Official Journal of the European Communities.

Chamberlin, C.E., 1977. A Model of Coliform Bacteria Survival in Seawater. Harvard University, Cambridge, Massachusetts.

Chamberlin, C.E., Mitchell, R., 1978. A decay model for enteric bacteria in natural waters. Water pollution microbiology 2, 325-348.

Chapman, D.V., Organization, W.H., Press, C., 1996. Water quality assessments: a guide to the use of biota, sediments and water in environmental monitoring.

Chapra, S., 1997. Surface water-quality modeling. WCB McGraw-Hill, Boston.

Chen, C.W., Orlob, G.T., 1972. Ecologic simulation for aquatic environments, Systems Analysis and Simulation in Ecology, pp. 475-528.

Chilton, J., Seiler, K., Schmoll, O., Howard, G., Chorus, I., 2006. Groundwater occurrence and hydrogeological environments. Protecting groundwater for health: managing the quality of drinking-water sources, 21-47.

Chow, V.T., Maidment, D.R., 1988. Applied hydrology. McGraw-Hill series in water resources and enviromental engineerin.

Clarke, R., 1973. A review of some mathematical models used in hydrology, with observations on their calibration and use. Journal of Hydrology 19, 1-20.

Cline, W.R., 1992. Economics of Global Warming, The. Peterson Institute Press: All Books.

Cole, T.M., Buchak, E.M., 1995. CE-QUAL-W2: A Two-Dimensional, Laterally Averaged, Hydrodynamic and Water Quality Model, Version 2.0. User Manual. DTIC Document.

Collins, J.P., Kinzig, A., Grimm, N.B., Fagan, W.F., Hope, D., Wu, J., Borer, E.T., 2000. A new urban ecology. American Scientist 88, 416-425.

Connors, K.A., 1990. Chemical kinetics: the study of reaction rates in solution. John Wiley & Sons.

Cosgrove, W.J., Rijsberman, F.R., 2014. World water vision: making water everybody's business. Routledge.

Cox, B., 2003. A review of currently available in-stream water-quality models and their applicability for simulating dissolved oxygen in lowland rivers. Science of The Total Environment 314, 335-377.

Crawford, N.H., Linsley, R.K., 1966. Digital Simulation in Hydrology'Stanford Watershed Model IV. Report No. 39, Department of Civil Engineering Stanford University, CA, 210.

Davies, E.G.R., Simonovic, S.P., 2011. Global water resources modeling with an integrated model of the social–economic–environmental system. Advances in Water Resources 34, 684-700.

Delpla, I., Jung, A.-V., Baures, E., Clement, M., Thomas, O., 2009. Impacts of climate change on surface water quality in relation to drinking water production. Environment International 35, 1225-1233.

Denman, K., Okubo, A., Platt, T., 1977. The chlorophyll fluctuation spectrum in the sea. Limnology and Oceanography 22, l033-l038.

Devane, M.L., Moriarty, E.M., Wood, D., Webster-Brown, J., Gilpin, B.J., 2014. The impact of major earthquakes and subsequent sewage discharges on the microbial quality of water and sediments in an urban river. Science of The Total Environment 485–486, 666-680.

Di Toro, D.M., Connolly, J.P., 1980. Mathematical Models of Water Quality in Large Lakes Part 2: Lake Erie. U.S. Environmental Protection Agency Ecological Research Series EPA-600/3-3-80-065.

Di Toro, D.M., O'Connor, D.J., Thomann, R.V., 1971. A dynamic model of the phytoplankton population in the Sacramento San Joaquin Delta. Adv. Chem. Ser 106, 131-180.

Döll, P., Hoffmann-Dobrev, H., Portmann, F.T., Siebert, S., Eicker, A., Rodell, M., Strassberg, G., Scanlon, B.R., 2012. Impact of water withdrawals from groundwater and surface water on continental water storage variations. Journal of Geodynamics 59–60, 143-156.

Donigian, A.S., 1977. Agricultural runoff management (ARM) model version II: refinement and testing. Environmental Protection Agency, Office of Research and Development, Environmental Research Laboratory.

Donigian, A.S., Crawford, N.H., 1976. Modeling nonpoint pollution from the land surface. US Environmental Protection Agency, Office of Research and Development, Environmental Research Laboratory.

Donigian, A.S., Huber, W.C., Consultants, A.T., 1991. Modeling of nonpoint source water quality in urban and non-urban areas.

Donigian Jr, A., Bicknell, B., Imhoff, J., Singh, V., 1995. Hydrological Simulation Program-Fortran (HSPF). Computer models of watershed hydrology., 395-442.

DR, 2005. Lei n.º 58/2005 de 29 de Dezembro, Diário da República - I Série A Portugal.

Duda, P., Kittle Jr, J., Gray, M., Hummel, P., Dusenbury, R., Consultants, A.T., Decatur, G., No, W.A., Kinerson, R., 2001. An Interactive Windows Interface to HSPF (WinHSPF). Users Manual for Version 2.

Duh, J.-D., Shandas, V., Chang, H., George, L.A., 2008. Rates of urbanisation and the resiliency of air and water quality. Science of The Total Environment 400, 238-256.

Duke, J., Marsh, F., 1973. Computer program documentation for the stream quality model DOSA G3. Prepared for the Systems Development Branch, US Environmental Protection Agency, Washington, DC.(Available from: US Environmental Protection Agency, Ariel Rios Building, 1200 Pennsylvania Avenue NW, Washington, DC 20460 USA.).

Edinger, J., Buchak, E., 1979. A hydrodynamic two-dimensional reservoir model: development and test application to Sutton Reservoir, Elk River, West Virginia. Prepared for US Army Engineering Division, Ohio River, Cincinnati, Ohio.

Edinger, J.E., Brady, D.K., Geyer, J.C., 1974. Heat exchange and transport in the environment, Heat exchange and transport in the environment. Johns Hopkins University.

Eloubaidy, A.F., Plate, E.J., 1972. Wind shear-turbulence and reaeration coefficient. Journal of the Hydraulics Division 98, 153-170.

Falconer, R., Lin, B., Wu, Y., Harris, E., 1998. DIVAST User Manual. Environmental Water Management Research Centre, Cardiff University, UK.

Fick, A., 1855. Ueber Diffusion. Annalen der Physik 170, 59-86.

Fischer, H.B., 1979. Mixing in inland and coastal waters. Academic press.

Frederick, K.D., Gleick, P., 2001. Water resources and climate change. Climate change economics and policy: an RFF anthology, 67.

Freer, J., Beven, K., Ambroise, B., 1996. Bayesian estimation of uncertainty in runoff prediction and the value of data: An application of the GLUE approach. Water Resources Research 32, 2161-2173.

Frexes, P., Jirka, G.H., Brutsaert, W., 1984. Examination of recent field data on stream reaeration. Journal of Environmental Engineering 110, 1179-1183.

Gameson, A., Vandyke, K., Ogden, C., 1958. The effect of temperature on aeration at weirs. Water and Water Engineering (British) v 753, 489.

Gleick, P.H., 1996. Water resources. Oxford University Press, New York.

Grimaldi, S., Kao, S.C., Castellarin, A., Papalexiou, S.M., Viglione, A., Laio, F., Aksoy, H., Gedikli, A., 2011. Statistical Hydrology, in: Wilderer, P. (Ed.), Treatise on Water Science. Elsevier, Oxford, pp. 479-517.

Groffman, P.M., Law, N.L., Belt, K.T., Band, L.E., Fisher, G.T., 2004. Nitrogen fluxes and retention in urban watershed ecosystems. Ecosystems 7, 393-403.

Gulliver, J., Stefan, H., 1981. Air-water surface exchange of oxygen: theory and application to the USEPA Monticello Experimental Field Channels. St. Anthony Falls Hydraulic Laboratory External Memorandum.

Gupta, S.K., 2011. Modern hydrology and sustainable water development. John Wiley & Sons.

Hamon, R.W., Weiss, L.L., Wilson, W.T., 1954. Insulation as an empirical function of daily sunshine duration. Monthly Weather Review 82, 141-146.

Harris, G.P., 1980. Temporal and spatial scales in phytoplankton ecology. Mechanisms, methods, models, and management. Canadian Journal of Fisheries and Aquatic Sciences 37, 877-900.

Hatfield, J., Reginato, R.J., Idso, S., 1983. Comparison of long-wave radiation calculation methods over the United States. Water Resources Research 19, 285-288.

Held, I.M., Soden, B.J., 2006. Robust responses of the hydrological cycle to global warming. Journal of Climate 19, 5686-5699.

Hinwood, J.B., Wallis, I.G., 1975. Review of models of tidal waters. Journal of the Hydraulics Division 101, 1405-1421.

Hochmuth, J.D., Asselman, J., De Schamphelaere, K.A.C., 2014. Are interactive effects of harmful algal blooms and copper pollution a concern for water quality management? Water Research 60, 41-53.

Holley, E., 1977. Oxygen transfer at the air-water interface, Transport processes in lakes and oceans. Springer, pp. 117-150.

Hornberger, G.M., Spear, R., 1981. Approach to the preliminary analysis of environmental systems. J. Environ. Manage.;(United States) 12.

Hummel, P., Kittle Jr, J., Gray, M., 2001. WDMUtil Version 2.0, A tool for managing watershed modeling time-series data: user's manual. Health Protection and Modeling Branch, Standards and Health Protection Division, Office of Science and Technology, Office of Water, United States Environmental Protection Agency 1200.

Huyakorn, P.S., Andersen, P.F., Mercer, J.W., White, H.O., 1987. Saltwater intrusion in aquifers: Development and testing of a three-dimensional finite element model. Water Resources Research 23, 293-312.

Hydrocomp, 1976. Hydrocomp Simulation Programming: Operations Manual, 2nd Edition ed, Palo Alto CA.

Imberger, J., Hamblin, P., 1982. Dynamics of lakes, reservoirs, and cooling ponds. Annual Review of Fluid Mechanics 14, 153-187.

Imboden, D.M., 1974. Phosphorus model of lake eutrophication. Limnol. Oceanogr 19, 297-304.

Imhoff, J., Kittle Jr, J., Gray, M., Johnson, T., 2007. Using the climate assessment tool (CAT) in US EPA BASINS integrated modeling system to assess watershed vulnerability to climate change. Water science and technology 56, 49-56.

Jarvis, P., 1970. A Study in the Mechanics of Aeration at Weirs. University of Newcastle upon Tyne. 1970.

Jennerjahn, T.C., Jänen, I., Propp, C., Adi, S., Nugroho, S.P., 2013. Environmental impact of mud volcano inputs on the anthropogenically altered Porong River and Madura Strait coastal waters, Java, Indonesia. Estuarine, Coastal and Shelf Science 130, 152-160.

Jobson, H.E., Keefer, T.N., 1979. Modeling highly transient flow, mass, and heat transport in the Chattahoochee River near Atlanta, Georgia.

Johanson, R., Imhoff, J., Davis, H., Kittle, J., Donigian, A., 1981. User's Manual for the Hydrologic Simulation Program—FORTRAN (HSPF): Release 7.0. US EPA Environmental Research Laboratory, Athens, GA.

Jury, W.A., Vaux Jr, H.J., 2007. The Emerging Global Water Crisis: Managing Scarcity and Conflict Between Water Users, in: Donald, L.S. (Ed.), Advances in Agronomy. Academic Press, pp. 1-76.

Kallis, G., Butler, D., 2001. The EU water framework directive: measures and implications. Water policy 3, 125-142.

Khadka, N.S., 2004. Himalaya glaciers melt unnoticed. Science/Nature.

Knappe, D.R., 2004. Algae detection and removal strategies for drinking water treatment plants. American Water Works Association.

Kuczera, G., Parent, E., 1998. Monte Carlo assessment of parameter uncertainty in conceptual catchment models: the Metropolis algorithm. Journal of Hydrology 211, 69-85.

Lahlou, M., Shoemaker, L., Choudhury, S., Elmer, R., Hu, A., 1998. Better assessment science integrating point and nonpoint sources (BASINS), version 2.0. Users manual. Tetra Tech, Inc., Fairfax, VA (United States); EarthInfo, Inc., Boulder, CO (United States); Environmental Protection Agency, Standards and Applied Science Div., Washington, DC (United States).

Leendertse, J.J., Liu, S.-K., 1975. A Three-dimensionl Model for Estuaries and Coastal Seas: Volume II, Aspects of Computation. Rand.

Lian, Y., Chan, I.C., Singh, J., Demissie, M., Knapp, V., Xie, H., 2007. Coupling of hydrologic and hydraulic models for the Illinois River Basin. Journal of Hydrology 344, 210-222.

Loaiciga, H.A., Valdes, J.B., Vogel, R., Garvey, J., Schwarz, H., 1996. Global warming and the hydrologic cycle. Journal of Hydrology 174, 83-127.

Lombardo, P.S., 1972. Mathematical Model of Water Quality Indices in Rivers and Impoundments. Hydrocomp, Incorporated.

Lowe, S., Doscher, R., 2003. Modeling of urban watersheds using basins and HSPF. Journal of Environmental Hydrology 11.

Magdoff, F., 2008. The world food crisis: sources and solutions. Monthly review - New York 60, 1.

Markofsky, M., Harleman, D.R., 1973. Prediction of water quality in stratified reservoirs. Journal of the Hydraulics Division 99, 729-745.

Marshall, S.J., 2013. Hydrology, Reference Module in Earth Systems and Environmental Sciences. Elsevier.

Masch, F., 1970. QUAL-1 simulation of water quality in-stream and canals. Program Documentation and User's Manual, Texas Water Development Board.

Matthes, F.E., 1939. Report of committee on glaciers, April 1939. Transactions, American Geophysical Union 20, 518-523.

McIntosh, B.S., Alexandrov, G., Matthews, K., Mysiak, J., van Ittersum, M., 2011. Preface: Thematic issue on the assessment and evaluation of environmental models and software. Environmental Modelling & Software 26, 245-246.

Mills, G., 2007. Cities as agents of global change. International Journal of Climatology 27, 1849-1857.

Mishra, A., 2011. Estimating uncertainty in HSPF based water quality model: application of Monte-Carlo based techniques, Biological Systems Engineering. Virginia Polytechnic Institute, Blacksburg, p. 112.

Moyer, D.L., Hyer, K.E., 2003. Use of the hydrological simulation program-FORTRAN and bacterial source tracking for development of the fecal coliform total maximum daily load (TMDL) for Christians Creek, Augusta County, Virginia. US Department of the Interior, US Geological Survey.

Najarian, T.O., Wang, D.-P., Huang, P.-S., 1982. Lagrangian transport in estuaries and sea-level canals. NASA STI/Recon Technical Report N 83, 16580.

Nakasone, H., 1975. Study on the aeration at falls and spillways, 1: Derivation of aeration equation and its verification. Transactions of the Japanese Society of Irrigation, Drainage and Reclamation Engineering, 42-48.

Nations, D.o.E.a.S.A.U., 2011. World Population Prospects: The 2010 Revision. United Nations Publications, New York.

Neitsch, S., Arnold, J., Kiniry, J., Williams, J., King, K., 2005. Soil and water assessment tool: theoretical documentation, version 2005. Texas, USA.

NWS, N.W.S., 2010. Learning Lesson: The hydrologic cycle. National Weather Service JetStream Online School for Weather.

O'Melia, C.R., 1974. Phosphorus cycling in lakes. Water Resources Research Institute of the University of North Carolina.

Odonkor, S.T., Ampofo, J.K., 2013. Escherichia coli as an indicator of bacteriological quality of water: an overview. Microbiology Research 4, e2.

Oliver, J.E., 1993. Climatology: An Atmospheric Science, 2/e. Pearson Education India.

Onishi, Y., Wise, S.E., 1982. Mathematical model, SERATRA, for sediment-contaminant transport in river and its application to pesticide transport in Four Mile and Wolf Creeks in Iowa. BPNL, RICHLAND, WA(USA). 1982.

Orlob, G.T., 1983. Mathematical modeling of water quality: streams, lakes, and reservoirs. John Wiley.

Paily, P.P., Macagno, E.O., Kennedy, J.F., 1974. Winter-regime thermal response of heated streams. Journal of the Hydraulics Division 100, 531-551.

Palmer, M., 1981. Some measurements of near surface turbulence in the depth direction and some phytoplankton distribution implications. Journal of Great Lakes Research 7, 171-181.

Palmer, M.D., 2001. Water quality modeling: a guide to effective practice. World bank publications.

Pappenberger, F., Beven, K.J., 2006. Ignorance is bliss: Or seven reasons not to use uncertainty analysis. Water Resources Research 42.

Park, R., Collins, C., Connolly, C., Albanese, J., MacLeod, B., 1980. Documentation of the Aquatic Ecosystem Model MS CLEANER, Rensselaer Polytechnic Institute. Center for Ecological Modeling. For US Environmental Protection Agency, Environmental Research Laboratory, Troy, New York.

Peterson, D., Sonnichsen, J.C., Engstrom, S., Schrotke, P., 1973. Thermal Capacity of Our Nation's Waterways. Journal of the Power Division 99, 193-204.

Pickett, S.T.A., Cadenasso, M.L., Grove, J.M., Nilon, C.H., Pouyat, R.V., Zipperer, W.C., Costanza, R., 2001. Urban ecological systems: Linking terrestrial ecological, physical, and socioeconomic components of metropolitan areas. Annual Review of Ecology and Systematics 32, 127-157.

Pizarro, R., Valdés, R., García-Chevesich, P., Vallejos, C., Sangüesa, C., Morales, C., Balocchi, F., Abarza, A., Fuentes, R., 2012. Latitudinal analysis of rainfall intensity and mean annual precipitation in Chile. Chilean Journal of Agricultural Research 72, 252-261.

Poon, C., Campbell, H., 1967. Diffused aeration in polluted water. Water Sew. Works 114, 461-463.

Prüss-Üstün, A., Bos, R., Gore, F., Bartram, J., 2008. Safer water, better health: costs, benefits and sustainability of interventions to protect and promote health. World Health Organization.

Roesner, L.A., Giguere, P.R., Evenson, D.E., 1981. Computer program documentation for the Stream quality model QUAL-II. US Environmental Protection Agency, Office of Research and Development, Environmental Research Laboratory.

Rossman, L.A., 2010. Storm water management model user's manual, version 5.0. National Risk Management Research Laboratory, Office of Research and Development, US Environmental Protection Agency.

Rosso, R., 1994. An introduction to spatially distributed modelling of basin response. Advances in distributed hydrology 3, 30.

Ryan, P.J., Harleman, D.R., 1973. An analytical and experimental study of transient cooling pond behavior. Dept. of Civil Engineering, Massachusetts Institute of Technology.

Shanahan, P., 1984. Water temperature modeling: a practical guide, Proceedings of stormwater and water quality model users group meeting.

Sharma, K.P., Moore Iii, B., Vorosmarty, C.J., 2000. Anthropogenic, climatic, and hydrologic trends in the Kosi Basin, Himalaya. Climatic Change 47, 141-165.

Sherwood, S.C., Bony, S., Dufresne, J.-L., 2014. Spread in model climate sensitivity traced to atmospheric convective mixing. Nature 505, 37-42.

Simons, T.J., 1976. Verification of numerical models of Lake Ontario: Part III. Long term heat transports. Journal of Physical Oceanography 6, 372-378.

Singh, V.P., 1988. Hydrologic systems. Volume I: Rainfall-runoff modeling. Prentice Hall, Englewood Cliffs New Jersey. 1988. 480.

Singh, V.P., 1995. Computer models of watershed hydrology. Water Resources Publications.

Smith, D., 1978a. Water quality for river-reservoir systems. Resource Management Associates, Inc., Lafayette, CA. For US. Army Corps of Engineers, Hydrologic Engineering Center (HEC), Davis, CA.

Smith, D., 1978b. WQRRS, Generalized computer program for River-Reservoir systems. USACE Hydrol. Engr. Center, Davis, CA.

Stow, C.A., Reckhow, K.H., Qian, S.S., Lamon, E.C., Arhonditsis, G.B., Borsuk, M.E., Seo, D., 2007. Approaches to Evaluate Water Quality Model Parameter Uncertainty for Adaptive TMDL Implementation1. Wiley Online Library.

Streets, H., Phelps, E., 1925. Study of the pollution and natural purification of the Ohio river. III. Factors concerned in the phenomena of oxidation and reaeration. Rapport technique.

Swinbank, W.C., 1963. Long-wave radiation from clear skies. Quarterly Journal of the Royal Meteorological Society 89, 339-348.

Taylor, G., Pagenkopf, J., 1981. TRANQUAL-Two-dimensional modelling of transport water quality processes, Proceedings, EPA storm water and water quality management modelling group meeting, Niagara Falls, Canada.

Tech, T., 1979. Methodology for evaluation of multiple power plant cooling system effects, Volume II. Technical Basis for Computations. Tetra Tech, Inc., Lafayette, California. For Electric Power Research institute. Report EPRI EA-IIII.

Tetra Tech, I., 1979. Methodology for Evalutation of Multiple Power Plant Cooling System Effects, Volume II: Techincal Basis for Computations. Electric Power Research Institute, Report EPRI EA-1111.

Thackston, E.L., 1974. Effect of geographical variation on performance of recirculating cooling ponds. National Environmental Research Center, Office of Research and Development, US Environmental Protection Agency; for sale by the Supt. of Docs., US Govt. Print. Off., Washington.

Thomann, R.V., 1963. Mathematical model for dissolved oxygen. Proceedings of American Society of Civil Engineers, Journal of Sanitary Engineering Division, 1-30.

Thomann, R.V., 1975. Mathematical modeling of phytoplankton in Lake Ontario. National Environmental Research Center.

Thompson, E.S., 1976. Computation of solar radiation from sky cover. Water Resources Research 12, 859-865.

Tsivoglou, E.C., Wallace, J.R., 1972. Characterization of stream reaeration capacity. Office of Research and Monitoring, US Environmental Protection Agency; For sale by the Supt. of Docs., US Govt. Print. Off.

TVA, T.V.A., 1972. Heat and mass transfer between a water surface and the atmosphere. Tennessee Valley Authority, Division of Water Control Planning, Engineering Laboratory.

Tyson, J., Guarino, C., Best, H., Tanaka, K., 1993. Management and institutional aspects. Water Science & Technology 27, 159-172.

UNESCO, W., 2003. Water for People Water for Life: UN World Water Development Report. Paris: UN.

van der Kuur, P., Roelfzema, A., Verboom, G., 1989. The threedimensional program TRISULA with curvilinear orthogonal coordinates. Advances in Water Modelling and Measurement, MH Palmer (Ed.), BHRA (Information Servies), Cranfield, UK, 135-147.

van Straten, G., 1998. Models for water quality management: the problem of structural change. Water Science and Technology 37, 103-111.

Vandenberghe, I.V., 2008. Methodologies for reduction of output uncertainty of river water quality models, Applied Mathematics, Biometrics and Process Control. Ghent University, p. 254.

Velz, C.J., 1970. Applied stream sanitation, John Willey & Sons. New York, USA, 242-246.

Vieira, J. 2011. A strategic approach for Water Safety Plans implementation in Portugal. Journal of water and health,*9*(1), 107-116.

Vollenweider, R.A., 1975. Input-output models. Schweizerische Zeitschrift für Hydrologie 37, 53-84.

Walters, R.A., 1992. A three-dimensional, finite element model for coastal and estuarine circulation. Continental Shelf Research 12, 83-102.

Wang, J.D., Connor, J.J., 1975. Mathematical modeling of near coastal circulation. Massachusetts Institute of Technology Cambridge.

Wani, S., Sreedevi, T., Reddy, T.V., Venkateswarlu, B., Prasad, C.S., 2008. Community watersheds for improved livelihoods through consortium approach in drought prone rainfed areas. Journal of Hydrological Research and Development 23, 55-77.

Warren, I., Bach, H.K., 1992. MIKE 21: a modelling system for estuaries, coastal waters and seas. Environmental Software 7, 229-240.

Watkins, K., 2006. Human Development Report 2006-Beyond scarcity: Power, poverty and the global water crisis. UNDP Human Development Reports (2006).

Wentz, F.J., Ricciardulli, L., Hilburn, K., Mears, C., 2007. How much more rain will global warming bring? Science 317, 233-235.

Whipple, G.C., 1917. State sanitation: a review of the work of the Massachusetts State Board of Health. Harvard University Press, Massachusetts.

Wlosinski, J.H., Lessem, A.S., Dortch, M.S., Schneider, M., Martin, J.L., 1995. CE-QUAL-R1: A Numerical One-Dimensional Model of Reservoir Water Quality; User's Manual. DTIC Document.

Woolhiser, D., Brakensiek, D., 1982. Hydrologic system synthesis. Hydrologic Modeling of Small Watersheds, 3-16.

WRE, 1968. Prediction of thermal energy distribution in streams and reservoirs. Report to California Department of Fish and Game, 90.

WRE, 1973. Computer Program Documentation for the Stream Quality Model QUAL-II. Water Resources Engineers.

Zabel, T., Milne, I., Mckay, G., 2001. Approaches adopted by the European Union and selected Member States for the control of urban pollution. Urban Water 3, 25-32.

Zhang, J., Ross, M., Trout, K., Zhou, D., 2009. Calibration of the HSPF model with a new coupled FTABLE generation method. Progress in Natural Science 19, 1747-1755.

Zison, S.W., 1978. Rates, constants, and kinetics formulations in surface water quality modeling. Environmental Protection Agency, Office of Research and Development, Environmental Research Laboratory.

3 Materials and Methods

This chapter contains an overview of the tools used and data collected for Lis and Ave River basins. The methodology used are also herein described.

3.1 HSPF model

The hydrological model, Hydrologic Simulation Program FORTRAN (HSPF) is a comprehensive river basin model that provides an integrated framework for modeling various hydrological and quality processes. Developed by the United States Environmental Protection Agency (USEPA), it is used worldwide and its applications have been reported in the literature (Albek et al., 2004; Binkley and Brown, 1993; Bouraoui and Wolfe, 1990; Jacomino and Fields, 1997; Liao and Tim, 1997; Razavian, 1990; Zhang et al., 2009). HSPF is a semi-distributed, conceptual model that combines spatially distributed physical attributes into hydrologic response unites (HRUs), which is considered to behave in uniform manner in response to meteorological inputs and storage capacity factors. In this way, HSPF can simulate, on a continuous basis, the hydrological, hydraulic and water quality processes on pervious and impervious land surfaces, in soil profiles and in streams and well-mixed impoundments (Bicknell et al., 2005). Hydrology simulation is based in the kinematic wave model. HSPF uses a one dimensional model representation, and this means the system geometry is formulated conceptually as a linear network. In this case, longitudinally as the water is transported out from one segment into the next one. Nutrients are modeled by using a system of coupled mass balance equations describing each nutrient compartment: dissolved inorganic and organic nutrients, particulate organic nutrients and sediment nutrients. HSPF does not simulate dissolved organic nutrient forms. Fecal coliforms model is based on a first order kinetics approach, taking into account the decay rate. It requires extensive data (hourly meteorological data), follows a lumped parameter approach, and hydraulics are limited to non-tidal freshwater systems and unidirectional flow. A more detailed description of the parameters and governing equations used in this study and their linkage to HSPF can be found in the Appendix A.

Using HSPF to simulate water quality requires information about several hydrologic and water quality parameters. Data required by the model included meteorological data, fecal coliform and nutrients loadings from cattle, hogs, wildlife and industry and inflow discharges as time series. Prior to assess the uncertainty and sensitivity of the model, calibration and validation of flow and water quality parameters was performed. The model was calibrated manually following a list of hydrology, hydraulic and quality parameters and corresponding to recommended value ranges that can be found in BASINS Technical Note 6 (USEPA, 2000).

To calculate the bacteria contribution in the basin, HSPF uses a spreadsheet (Bacterial Indicator Tool, BIT) that estimates loads from multiple sources, by populating the spreadsheet with the number of animals present on each sub basin (Beef Cattle, Swine, Dairy Cattle, Chickens, Horses and Sheep). Output from the tool is used as input to HSPF model. The tool estimates the monthly accumulation rate of fecal coliform bacteria on different land uses as well as the asymptotic limit for the accumulation if no wash off occur. BIT also estimates the direct input of fecal coliform bacteria to streams from grazing agricultural animals and failing septic systems.

3.1.1 Delineation

The BASINS watershed delineation tool allows defining multiple hydrologically connected subwatersheds within a given study area. This is useful in watershed characterization and modeling providing the flexibility in editing shapes and attributes of delineated watersheds and outlets, and in generating stream networks. Delineated watersheds are required for HSPF modeling and for BASINS characterization reports. The delineation process creates GIS layers required for setting up an HSPF model (streams; sub-basins and outlets) from the Digital Elevation Model. It is part of the process known as watershed segmentation, dividing the watershed into discrete land and channel segments to analyze watershed behavior.

3.1.2 Segmentation

Model segments are sub areas of a watershed comprised of one or more sub basins with uniform data inputs that are connected by a reach network (meteorological data; soil type; land use conditions; reach characteristics). Dividing a watershed into two or more model segments has several advantages, especially in large sub basins where more than one representative meteorological station may be required to adequately represent climate variations. On the other hand too many model segmentations will imply greater level of detail to parameterize the model, increasing the opportunity for errors when modifying parameter values.

3.2 Study Area

This study covers two watersheds in Portugal; Lis watershed (Lena and Lis River) and Ave watershed (Ave and Este River).

3.2.1 Lis River Basin

Lis River basin (Figure 3.1) covers an area of approximately 850 km², including its main tributary Lena River. Located in the central region of Portugal, this costal basin crosses Leiria city and flows into the sought-after Vieira beach. The Lis River basin is one of the most important natural resources of the Leiria region, rich in fish species and sought for sport fishing events. It has been subjected to continuous discharges of industrial, livestock, piggeries and domestic wastewaters without adequate treatment (Vieira et al., 2013; Vieira et al., 2012).

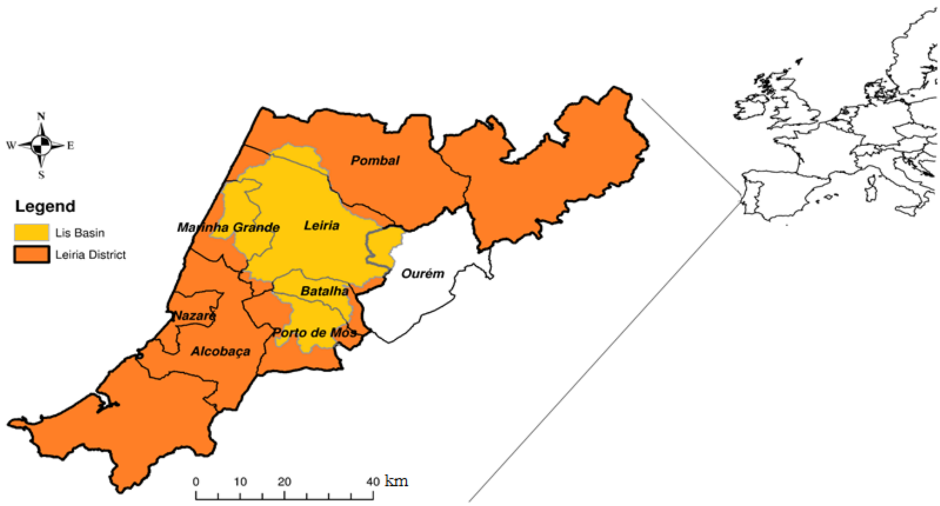

Figure 3.1 Lis River basin; Leiria, Portugal.

Meteorological, discharge and water quality data for the Lis River basin was retrieved from SNIRH – Sistema Nacional de Informação de Recursos Hídricos (National Information System for Water Resources). A high resolution Digital Elevation Model (DEM, 25m) was provided by ARH-Centro, Administração de Recursos Hídricos (Water Resources Administration – Center Portugal) and the Land Use and Soil Data from Agência Portuguesa do Ambiente- Atlas do Ambiente (Ministry of Agriculture, Sea, Environment and Spatial

Planning). The annual average precipitation in Lis basin is 855 mm, most of which occurs (63%) from September to December. The average annual daily temperature of 14.8ºC ranges from -1ºC in January to 40ºC in June and snow is not a factor to be considered in the simulation. According to hydrologic soil groups classification (Donigihan and Davis, 1978), Lis basin is considered to have a moderate and moderate to high runoff potential (Group B and C). Land use categories were condensed into 5 main categories (Mapoteca, 2008) to simplify the modeling process (Urban or Built-up Area, Forest Land, Agricultural Land, Barren Land and Wetlands) (Table 3.1). The land use is mainly forest land (45%), agricultural land covers 39% and urban land accounts for 10%. The remainder of the watershed area is divided between barren land (5%) and wetland (<1%) Figure 3.2.

Table 3.1 Rearranged land use.

New Land Use	Before	Impervious Coefficient
Urban or Built-up Area	Airports; continuous and discontinuous urban fabric; roads, port areas; quarrying; mining extraction zones and construction sites.	0.7
Forest Land	Forest cover of: cork, holm oak, chestnut, oak, eucalyptus and pine	0.3
Agricultural Land	Arable land; permanent crops; orchards; meadows	0.4
Barren Land	Bare rock, beaches, dunes, sands and soils without vegetation	0.1
Wetlands	Watercourses, pounds and reservoirs.	1.0

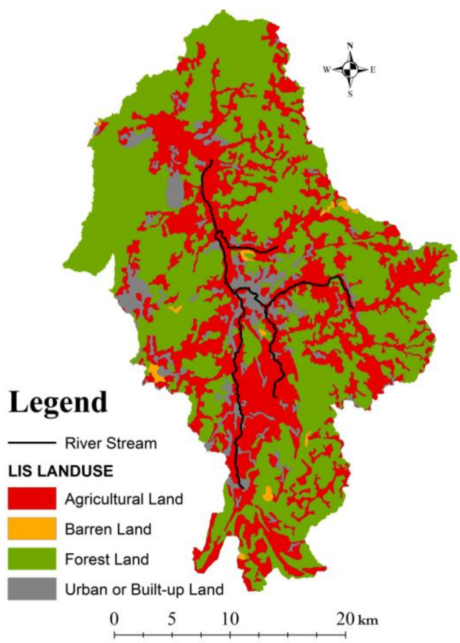

Figure 3.2 Lis watershed land use.

HSPF coupled with BASINS data management and graphical user interface tools, was used to model the hydrology of the Lena River watershed Figure 3.3 in Leiria (Portugal) for the years 1985-1989 and, validated for a 4 year period (2003-2006) at station 15E03. Since there was no observed flow data for the other stations addressed in this study, the same hydrology behaviour was assumed for the entire basin in order to perform water quality assessment. The model domain is not extended further downstream, because beyond station 14D03 there was no other station with water quality data available and Lis River is subject to tides and HSPF is only applicable to non-tidal watershed simulations. The calibrated hydrologic parameter values were added to the watershed model prior to calibrating water quality constituents.

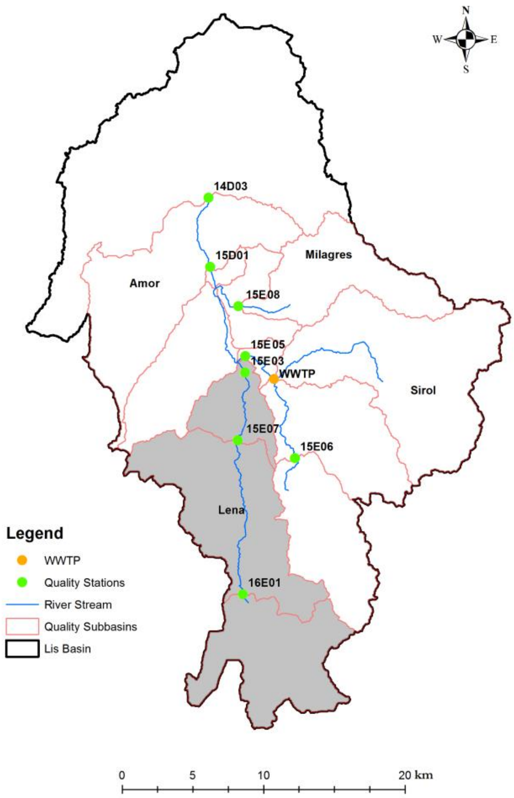

Figure 3.3 Lis River basin.

Lis river water quality was modeled from its source until station 14D03 (636 km² watershed area), for the year period 2003-2004 and validated for 2005-2006 period. Lis River has been subjected to continuous discharges of effluents especially in the brook of Milagres (station 15E08) due to the high concentration of piggeries in this water course (Figure 3.4), (Vieira et al., 2013; Vieira et al., 2012). Water quality was calibrated and validated for 8 stations: 14D03;

15D01; 15E08; 15E05; 16E06; 15E03; 15E06 and; 16E01. Values of the analytical parameters were collected for all stations.

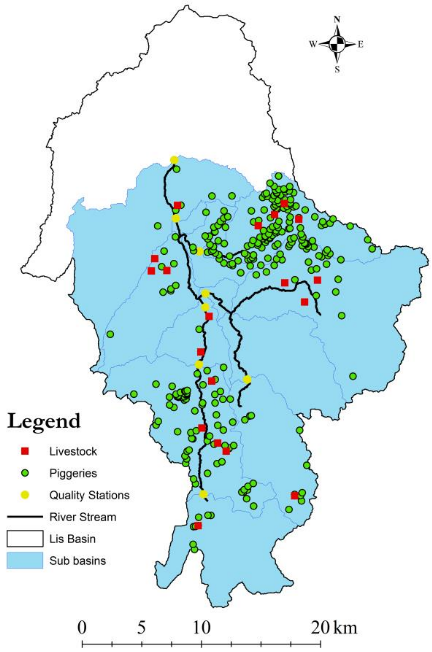

Figure 3.4 Lis watershed: piggeries and livestock location.

The point and nonpoint pollution sources were retrieved from Lis Watershed Plan (ARH-Centro, 2012). The main nonpoint pollution sources are due to agriculture, piggeries and livestock activities as specified in Lis Watershed Plan. Table 3.2 shows the yearly loads of nitrogen and phosphorus per county. Through the use of GIS, the sub basins loads were calculated on a weighted percentage area (clipped with the county shape file) and assuming afterwards that the load was evenly distributed through the sub basin, obtaining in this way the loads associated with each land use (

Table 3.3).

Table 3.2 County nonpoint water pollution source loads.

(kg yr^{-1})	Agriculture		Piggeries		Livestock	
County	**Nitrogen**	**Phosphorus**	**Nitrogen**	**Phosphorus**	**Nitrogen**	**Phosphorus**
Batalha	5263	979	160935	48884	11094	3750
Leiria	96773	8941	3784889	1198674	274576	96715
Marinha Grande	1772	135	24519	8173	1591	548
Ourém	11471	3410	1769	573	7527	2506

Pombal	75095	10201	486133	159270	138141	48446
Porto de Mós	13605	4506	667227	219509	84166	29943

Table 3.3 Distribution loads of nitrogen and phosphorus per sub basin and land use.

(kg yr^{-1})	**For-N**	**Agr-N**	**Urb-N**	**Bar-N**	**For-P**	**Agr-P**	**Urb-P**	**Bar-P**
15E06	2930	2680	288	753	869	637	52	211
15E05	87	360	1122	0	9	33	117	0
15D01	396	695	0	0	42	67	0	0
14D03	16315	9650	3548	191	3021	2023	730	36
15E03	2435	6213	2016	0	441	1125	365	0
15E07	27867	53271	12946	4092	8548	16341	3971	1255
16E01	1806	2804	293	4198	602	934	97	1398
15E08	53999	39149	6233	0	16019	10818	1899	0

For – Forest Land; Agr – Agricultural Land; Urb – Urban Land; Bar – Barren Land.

Table 3.4 and Table 3.5 shows the different sources associated with nitrogen and phosphorus and BOD_5 in Lis basin, respectively. The same criteria, as nonpoint pollution, were applied to obtain the loads for each individual sub basin. The pollutant loads per capita after the wastewater treatment plant discharge in Lis basin regarding nitrogen, phosphorus and BOD_5 are 2, 0.2 and 0.7 (kg cap^{-1} yr^{-1}) respectively and the average flow associated is 250 L cap^{-1} day^{-1}. The population of each sub basin was retrieved from the Portuguese Geographic Information Reference Base (BGRI, 2001) and the point source loads associated with the number of people per sub basin was calculated. Table 3.6 shows the point source pollution loads for each sub basin.

Table 3.4 County point source of nitrogen and phosphorus pollution loads.

(kg yr^{-1})	**Wineries**		**Dairy**		**Olive Oil Cellars**		**Agrifood Industry**		**Manufacturing Industry**		**Piggeries**	
County	**N**	**P**	**N**	**P**	**N**	**P**	**N**	**P**	**N**	**P**	**N**	**P**
Batalha	720	234	---	---	300	104	---	---	---	---	---	---
Leiria	29	19	---	---	25	21	273	91	53	---	3264	1250
Marinha Grande	---	---	---	---	---	---	---	---	---	---	---	---
Ourém	4	3	13	4	13	4	---	---	---	---	---	---
Pombal	---	---	955	287	59	50	---	---	1	---	3574	2383
Porto de Mós	41	13	---	---	55	47	19	6	---	---	713	475

N – Nitrogen; P - Phosphorus

Table 3.5 County point source of biochemical oxygen demand pollution loads.

BOD_5 (kg yr^{-1}) **County**	**Wineries**	**Dairy**	**Agrifood Ind.**	**Manufacturing Ind.**	**Piggeries**
Batalha	7020	---	319	2086	---
Leiria	78	---	---	32993	8077
Marinha Grande	---	---	---	19723	---
Ourém	10	14	---	377	---
Pombal	---	1011	22	12281	9528
Porto de Mós	400	---	---	1872	---

Table 3.6 Sub basin point source loads.

(kg yr^{-1})	**N**	**P**	**BOD_5**	**Flow (m^3 s^{-1})**
15E06	15509	1599	6765	0.022
15E05	44372	4455	16234	0.064
15D01	1957	208	1176	0.003
15E03	25839	2655	11854	0.037
15E07	49452	5075	20677	0.071
16E01	10132	1126	4040	0.014
14D03	70042	7156	33937	0.101
15E08	21668	2226	9919	0.031

The model was calibrated for the following water quality parameters: temperature, orthophosphates (PO_4), dissolved oxygen (DO), chlorophyll-a (Cl-a), nitrates (NO_3), fecal coliforms (FC), biochemical oxygen demand (BOD_5), total suspended solids (TSS) and pH. The water quality calibration was performed considering the following steps: a) estimate model parameters, including land use, specific accumulation and depletion/removal rates and subsurface concentrations; b) analyze and compare simulated nonpoint source loadings with literature values for each land use and adjust them when necessary; c) calibrate in stream water temperature; d) compare observed and simulated in stream concentrations (FC; TSS; DO; NO_3; PO_4; BOD_5 and; Cl-a). There was no observed data available for chlorophyll-a to perform model validation in Lis River Basin.

3.2.2 Ave River Basin

Ave River Basin (Figure 3.5) covers an area of approximately 1388 km^2 located in northern region of Portugal. With a stream line of 90.9 km and two main tributaries, Este River (247 km^2) and Vizela River (342 km^2), it has an annual average precipitation of 1522 mm, an average temperature of 13.9ºC and an average annual flow rate of 30.6 $m^3\ s^{-1}$. The land use occupation of the basin comprises 46.6% of forest land, 42.6% of agricultural land, 10.7% of urban land and 0.2% of wetland. Meteorological, discharge and water quality data for Ave River basin was retrieved from SNIRH – Sistema Nacional de Informação de Recursos Hídricos (National Information System for Water Resources) for the years 1990-2000. A Digital Elevation Model (DEM, 80 m) was provided by ARH-Norte, Administração de Recursos Hídricos (Water Resources Administration – North Portugal) and the Land use and Soil Data from Agência Portuguesa do Ambiente- Atlas do Ambiente (Ministry of Environment, Spatial Planning and Energy). Land use (Figure 3.6) categories were aggregated into 5 main categories.

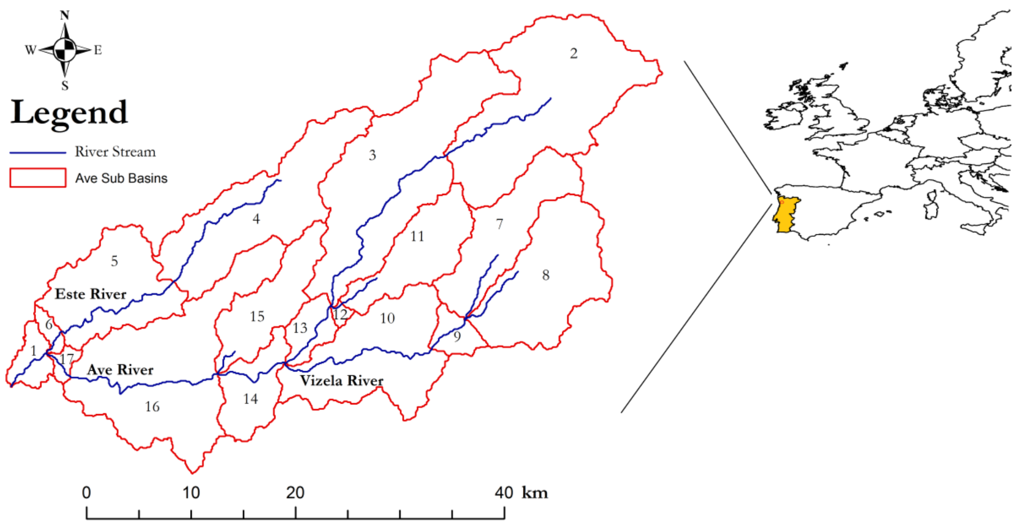

Figure 3.5 Ave River sub basins; Portugal.

The measurement network consists of five meteorological stations, spread over the catchment and two gauges, 15E03 (Ave River) and 15E01 (Este River), located 5.3 km upstream the river mouth. Due to the meteorological data available in Ave watershed it was possible to segment the watershed according to the meteorological stations. Once segmented, it is possible to assign a separate meteorological station to each model segment, improving accuracy of the model (Figure 3.7). The watershed was delineated to characterize the stations where observed data was available, station 15E03 (Ave River) and station 15E01 (Este River). The river basin receives a number of point discharges from industries and wastewater treatment plants (Figure 3.8); the corresponding loads are presented in Table 3.7 and Table 3.8 as given by the ARH-Norte, Administração de Recursos Hídricos (Water Resources Administration – North Portugal)

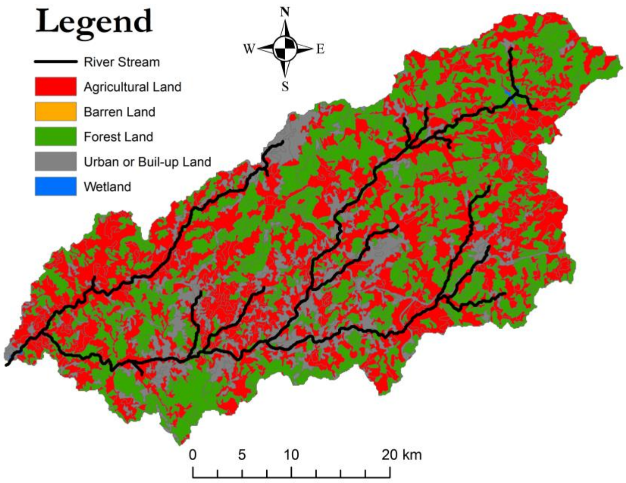

Figure 3.6 Ave watershed land use.

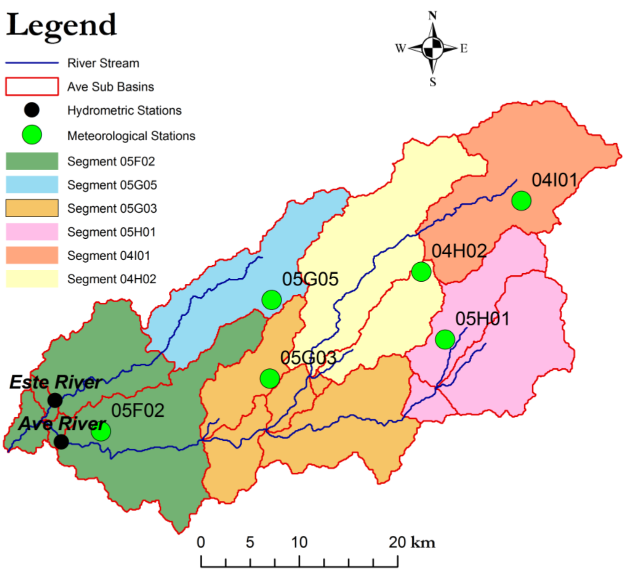

Figure 3.7 Ave watershed segmentation.

Table 3.7 Point and nonpoint pollution sources per sub basin in Ave watershed (1/2).

	1	**2**	**3**	**4**	**5**	**6**	**7**	**8**	**9**
Nonpoint ($kg\ yr^{-1}$)									
Industry									
BOD	3838	6913	16364	25345	18881	2731	12201	14996	1174
TN	6380	731060	53680	8360	69520	3520	12100	16940	2200
TP	25380	3600	2520	4320	63900	1800	6660	9360	1080
Agriculture									
BOD	346422	50386	177380	495825	1326404	87171	22581	42406	22676
TN	152382	53995	123727	205316	544301	28019	30641	36699	8350
TP	49891	9995	29713	63675	179174	9768	4760	6145	2466
Forest									
BOD	335511	48799	171793	480208	1284627	84425	21870	41071	21962
TN	128443	15662	61696	142063	445812	21737	7495	9047	5081
TP	46080	5862	22529	55447	164234	8860	2760	3782	2090
Point ($kg\ hr^{-1}$)									
BOD	0.06	0.409	0.649	1.044	0.632	0.087	0.914	1.184	0.026
NO_3	0.014	0.068	0.066	0.213	0.276	0.017	0.149	0.19	0.003
PO_4	0.003	0.01	0.009	0.036	0.048	0.003	0.023	0.03	0

Table 3.8 Point and nonpoint pollution sources per sub basin in Ave watershed (2/2).

	10	11	12	13	14	15	16	17
Nonpoint ($kg\ yr^{-1}$)								
Industry								
BOD	18085	7482	369	8203	9261	23100	70644	1449
TN	26620	1320	0	3300	19360	6600	55220	0
TP	14400	720	0	1800	10440	3600	77580	9180
Agriculture								
BOD	274388	58245	2961	191095	249889	521312	1930563	118991
TN	133867	41564	2096	60822	102365	164561	747174	54399
TP	39341	10384	527	20938	32921	56634	246873	17635
Forest								
BOD	265746	56411	2868	185076	242018	504893	1869758	115244
TN	94950	23489	1196	44537	79993	119010	585347	45648
TP	34610	8275	421	18707	29909	50419	223553	16254
Point ($kg\ hr^{-1}$)								
BOD	0.459	0.351	0.017	0.281	0.335	0.796	3.512	0.025
NO_3	0.131	0.035	0.002	0.059	0.125	0.153	2.344	0.006
PO_4	0.029	0.004	0	0.012	0.031	0.03	0.175	0.001

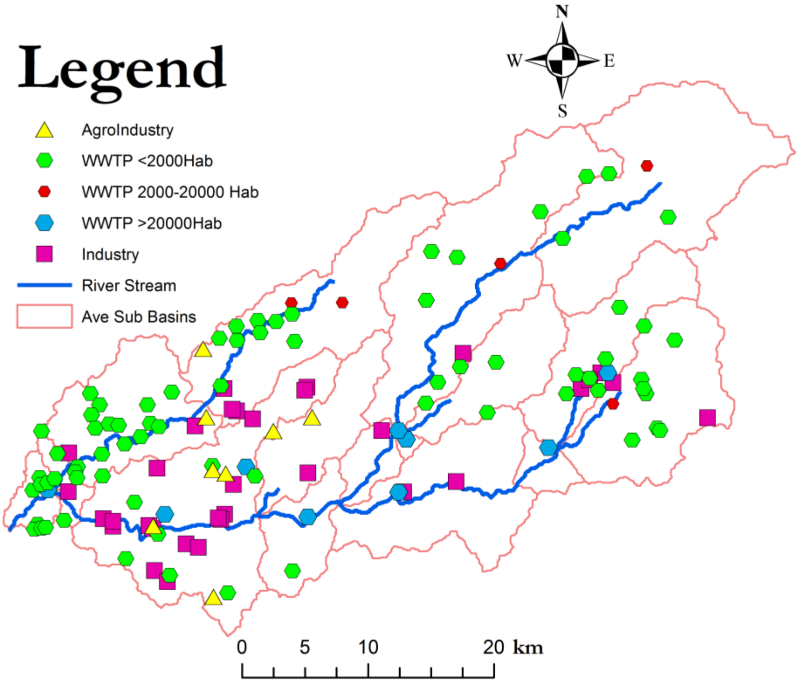

Figure 3.8 Point source locations in Ave watershed.

Water quantity and quality of Ave River was calibrated for the period of 1990-1994 and validated for 1995-2000, while Este River was calibrated for the period of 1994-1997 and validated for 1998-2000 (where complete series of observed data was available). For each station concerning quality data, the following parameters were assessed: water temperature, dissolved oxygen (DO), biochemical oxygen demand (BOD_5), nitrate (NO_3), orthophosphate (PO_4) and fecal coliforms (FC).

3.3 Calibration and Statistical Criteria

The water quality calibration was performed considering the following steps: a) estimate model parameters, including land use, specific accumulation and depletion/removal rates and subsurface concentrations; b) analyze and compare simulated nonpoint source loadings with literature values for each land use and adjust them when necessary; c) calibrate in stream water temperature; d) compare observed and simulated in stream concentrations (Fecal coliforms, TSS, DO, NO_3, PO_4, BOD_5, pH and Cl-a) and e) statistically and graphically evaluate model results.

To quantify model performance, several statistical measures were calculated for both calibration and validation simulations. Bennett et al. (2013) presents several methods for measuring quantitative performance including: direct model comparison, comparison of real and modeled values concurrently, key residual criteria, residual methods using data transformations and, correlation and model efficiency performance measures. A brief description of the statistical criteria used in this study is shown in Table 2.6. Water quality model performance was normally evaluated (statistically and graphically) by monthly time step outputs.

The deviation of runoff volumes *Dv*, also known as the percentage bias, is the simplest goodness-of-fit criterion (Legates and McCabe, 1999). The model simulation performance rating for the deviation of volumes (Donigian Jr., 2002) is considered very good for values inferior to 15%, good between 15 and 25% and satisfactory for values between 25 and 35%. According to Santhi et al. (2001) and Singh et al. (2005) satisfactory model performance is achieved when the coefficient of determination is above 0.6 for monthly simulated constituents, but a value of 0.5 is still acceptable.

3.4 Scenarios Assessment

Once calibrated and validated, HSPF allows the prediction of water quality under different scenarios such as: impact of point and nonpoint pollution sources; maximum daily loads to comply with water quality standards; land use development and; climate change.

3.4.1 Maximum Daily Loads

The calculation of maximum daily loads includes pollutant loads from point sources, such as identified discharge points (WLA – point source waste load allocation) and nonpoint source loads, such as diffuse sources (LA – nonpoint load allocation), as well as a margin of safety (MOS) (Mostaghimi et al.) to account for uncertainty (generally 10%). This criterion deriving from the U.S. Clean Water Act (CWA, 1972), Total Maximum Daily Load (TMDL), was used in the same way to calculate the maximum amount of pollutant loading to the basin that would achieve the quality standards specified in 75/440/EEC (1975) for surface water intended for the abstraction of drinking water, including the margin of safety. TMDL is calculated as the sum of these parameters:

$$\text{TMDL}= \sum \text{WLA}+ \sum \text{LA} +\text{MOS} \tag{3.1}$$

Best Management Practices (BMPs) such as: filter strips; retention pounds; stream buffers; etc.; can be applied to various land segments until the highest daily simulated concentration is just below the quality standards. Maximum daily loads were computed in Lis watershed for nitrates, orthophosphates and faecal coliforms using the HSPF model. The TMDLs values were achieved by reducing both point and nonpoint sources loads to the Lis River watershed until the maximum concentration of the quality constituents was below the quality standards specified in the Directive 75/440/EEC (1975) including the margin of safety.

Hypothetical BMPs were applied to Ave River basin in agricultural areas with three to fifteen percent area application. The quality of constituents removal capability was based on the literature values presented in Table 3.9. In HSPF, the removal capability is a user defined step and it is chosen independently of the BMP considered. The removal capability used in the model was: faecal coliform 50%; nitrogen 30%; phosphorus 40% and; BOD 30%.

Table 3.9 Removal capability of BMPs (DiToro et al., 1970; Donigian and Crawford, 1976; International et al., 2004).

BMP	FC	BOD	N	P
Dry detention basin	50%-90%	20%-30%	10%-20%	20%-30%
Wet detention basin	50%-90%	20%-40%	30%-40%	50%-70%
Filter strip	76%	70%	20%-30%	30%-40%
Infiltration drain fields	90%	20%-30%	30%-40%	40%-50%

3.4.2 Land Use Change Scenarios

To sustain water use, water resource managers should take into account long term perspective approaches when planning and managing activities in watersheds. The HSPF model can be used to predict the behavior of water quality on different scenarios of land use by modifying the areas of different land types in the basin.

In this study, the calibrated model was used as a baseline for predicting the consequences of various scenarios associated with potential future land use changes in Lis River basin. Since there is no historical data of land use evolution in Lis Basin and there is no predominant land use, alternative scenarios simulated included: conversion of land use from forest to urban (scenario 1), forest to agriculture (scenario 2) and, agriculture to urban (scenario 3), with area conversions of 25%, 50% and 75% and high (50%) and low (-30%) precipitation events. These values were obtained through the difference between a high and low precipitation year and the annual average over all time. This means that a wet year will have 50% more rain than the annual average in Lis basin where in a dry year 30% less rain is observed. The land use scenarios presented here, even though hypothetical can indicate the trend towards the assessment of water quality based on land use development.

Ave River basin land use scenarios were based on the evolution of land use from 1990, 2000 and 2006. Table 3.10 shows the average evolution per year of the land use in Ave River basin. The HSPF model land use areas were changed to reflect these changes for the years 2050, 2100 and 2150 starting at the year 2006. Additionally three more scenarios were considered where the impervious coefficient of urban areas also increased with the increase of urban areas (Table 3.11).

Table 3.10 Ave River basin land use evolution per year.

Type of Land Use	Change
Agricultural land	-0.21%
Barren land	0%
Forest land	-0.15%
Urban or build-up areas	0.36%
Wetland	0%

Table 3.11 Ave River basin scenarios summary.

Scenario	Description
BMP3	Applied to 3% of agriculture areas.
BMP6	Applied to 6% of agriculture areas.
BMP9	Applied to 9% of agriculture areas.
BMP12	Applied to 12% of agriculture areas.
BMP15	Applied to 15% of agriculture areas.
LU2050	44*x* Change
LU2100	94*x* Change
LU2150	144*x* Change
LU2050I	44*x* Change; +10% impervious
LU2100I	94*x* Change; +15% impervious
LU2150I	144*x* Change; +20% impervious

3.4.3 Climate Change Scenarios

In Lis River basin the model was used to predict fecal coliform bacteria impairments resulting from climate change factors. The following scenarios were considered: (Scenario 1) + 2ºC air temperature increase; (Scenario 2) + 4ºC air temperature increase; (Scenario 3) + 2ºC air temperature increase with 14% precipitation increase and (Scenario 4)+ 4ºC air temperature increase with 28% precipitation increase. Scenarios 1 and 2 were chosen due to global warming projections across the globe as explained by Sherwood et al. (2014) while scenario 3 and 4 also consider the precipitation effects resulting from the projected temperature increase specified by Wentz et al. (2007). Although literature (Alexander et al., 2006, Bauer et al., 2003, Beltrami et al., 2002, Crowley 2000) states that changes in daily climate extremes of temperature and precipitation are being observed, scenarios of decreased temperature and precipitation where not addressed herein.

3.5 Uncertainty and Sensitivity Analysis

3.5.1 Lena River Basin

Uncertainty analysis was conducted using a Monte Carlo approach. Multiple model simulation runs were performed using the 5 years period, with values for selected model parameters randomly chosen from assigned probability distributions. Table 3.12 shows the parameters used in the uncertainty analysis, their units and distribution. Minimum and maximum values were obtained from BASINS Technical Note 6. The parameter, IRC, follows a triangular distribution since it has a most common value of 0.7, while all other parameters follow a uniform distribution.

Table 3.12 Range and parameter distribution of uncertainty for water balance parameters.

Name	Units	Range	Designation	Type
LZSN[a]	mm	(76.2,203.2)	Lower zone storage nominal	Soil Climate
AGWRC[a]	day^{-1}	(0.92,0.99)	Basic groundwater recession rate	Baseflow recession
DEEPFR	---	(0.0,0.2)	Fraction of groundwater inflow which will enter deep groundwater and be lost	Geology, GroundWater recharge
BASETP	---	(0.0,0.05)	Fraction of potential evapotranspiration, which is fulfilled only as outflow exists	Riparian Vegetation
AGWETP	---	(0.0,0.05)	Fraction of remaining potential evapotranspiration	Marsh/Wetlands
INTFW[a]	---	(1,3)	Interflow inflow parameter	Soils, Topography, Land Use
UZSN[a]	mm	(2.54,25.4)	Upper zone storage nominal	Surface soil conditions, Land Use
LZETPA[a]	---	(0.5,0.7)	Lower zone evapotranspiration parameter for agricultural land.	Vegetation type/density, Root depth
LZETPU[a]	---	(0.2,0.7)	Lower zone evapotranspiration parameter for urban or build-up areas.	Vegetation type/density, Root depth
LZETPF[a]	---	(0.6,0.8)	Lower zone evapotranspiration parameter for forest land.	Vegetation type/density, Root depth
LZETPB[a]	---	(0.1,0.4)	Lower zone evapotranspiration parameter for barren land.	Vegetation type/density, Root depth
IRC[a]	day^{-1}	(0.5,0.7,0.7)	Interflow recession parameter	Soils, Topography, Land Use
INFILT[a]	mm h^{-1}	(0.254,25.4)	Index to the infiltration capacity of the soil	Soils, Land Use

To explore the uncertainty in this parameter space (Refsgaard et al., 2007), the GLUE method was implemented with repeated model simulations using HSPF hydrologic parameter values that were randomly selected from a predetermined probability distribution (Monte Carlo simulations) (Beven and Binley, 1992; Beven, 2001). This method was used to derive the 97.5% and 2.5% uncertainty bounds (95% confidence interval) for HSPF predictions of monthly discharge and evaluate the relationship between model uncertainty bounds and the threshold chosen for the likelihood measure.

To ensure that the Monte Carlo Simulations (MCS) adequately approximate model output uncertainty, 1000 model runs were performed. To calculate the model uncertainty, quantiles of time series weighted by the Nash-Sutcliffe coefficient (E) (2.5% and 97.5%), for a 95% confidence interval of discharge, were derived (where E was above or equal to 0.5). If x is period in months (January through December) and there are m samples (m=1 to 1000) and n are data months (n=1 to 60) we will get:

x(1,1) x(1,2) x(1,3) … x(1,n);

x(2,1) x(2,2) x(23) … x(2,n);

…

x(m,1) x(m,2) x(m,3) … x(m,n);

Sort ascending by the Nash-Sutcliffe Efficiency coefficient (for behavioral samples only):

x(5,1) x(5,2) x(5,3) … x(5,n);

x(2,1) x(2,2) x(2,3) … x(2,n);

…

x(9,1) x(9,2) x(9,3) … x(9,n)

x(m-3,1) x(m-3,2) x(m-3,3) … x(m-3,n);

where: x(5,1) < x(2,1) < … < x(9,1) < x(m-3,1), this means that trial *5* has the lower *E* value (0.5) and trial *m-3* has the higher *E* value of all trials.

The percentiles of all samples for the first month are:

x(5,1) x(5,2) x(5,3) … x(5,n) according with percentile : Per(1) = E(1) / E(all);

x(2,1) x(2,2) x(2,3) … x(2,n) according with percentile : Per(2) = Per(1) + E(2) / E(all);

…

x(9,1) x(9,2) x(9,3) … x(9,n);

x(m-3,1) x(m-3,2) x(m-3,3) … x(m-3,n) according with percentile:

Per(m-3) = Per(9) + E(m-3)/E(all);

where: E(all) = $\sum^{m}_{i=1} E_i$.

The next step was to find the discharge values for each month whose percentiles are 2.5% and 97.5%.

To identify parameter sets as acceptable (behavioral) or unacceptable (non-behavioral) the user must specify a threshold for the likelihood measure. In this study we considered behavioral parameter sets when the Nash-Sutcliffe coefficient was equal or above 0.5, and the relationship between model uncertainty bounds and the threshold chosen for the likelihood measure was evaluated.

A sensitivity analysis was performed to study the responses of the HSPF hydrological parameters for our study area. To perform a multi-parameter sensitivity analysis, GLUEWIN software from Joint Research Centre, JRC, (Ratto et al., 2001) developed in Matlab™ environment was used. This software provides visual sensitivity analysis through scatter plots and cumulative distributions proposed by Spear and Hornberger (1980). The outputs (objective function values, Nash-Sutcliffe coefficient) are classified into two groups: the 50% smallest values and the 50% highest values; by plotting the cumulative distributions for the two classes (high and low values) it is possible to perform a sensitivity analysis for a given parameter. The further apart the cumulative distributions are, the more important the parameter is to that specific model and therefore more sensitive. Alternatively, if the parameter values do not split, then the parameter is unimportant and less sensitive.

Assessment of HSPF water balance parameter sensitivity was performed to evaluate the impact of specific parameters (Table 3.12) on the output variables of interest. Since the sensitivity of model results to parameters in a specific watershed depends on the combined impacts of climate and watershed conditions (AquaTerra, 2004), the studies reported in the literature used for comparison have an average annual precipitation range from 800 to 3837 mm and catchment areas of 16 to 6965 km^2.

3.5.2 Ave River Basin

Uncertainty analysis was conducted using a Monte Carlo (MC) approach. Multiple model simulation runs were performed using the 10 year period, with values for the selected model parameters randomly chosen from assigned probability distributions. The water quality parameters that were considered knowledge uncertain (parameters which there is insufficient field data available) are listed in Table 3.13 with their respective distributions. The range represents the lower and upper limits for the distributions which correspond to the typical minimum and maximum limits for these parameters from HSPF user's manual. Since some parameter values can vary up to infinite, the maximum value used for the distributions was based on those reported in literature (Mishra, 2011; Paul et al., 2004) or the calibrated value if it was above the latter. A uniform distribution was assigned to parameters for which no additional information is available in the manual, while accumulation and storage parameters were assigned a triangular distribution where the most probable value is the mode of the parameter value of the calibrated model.

The accumulation rate of the quality constituent (ACQOP) and the asymptotic limit storage of the quality constituent on the surface (SQOLIM) values for the remaining months were calculated by multiplying the January distribution with a monthly adjustment factor from the calibrated model. This resulted in 85 parameters analyzed.

To ensure that the MC simulations satisfactorily approximate model output uncertainty, *1000* model runs were performed. To calculate the model uncertainty, quantile regression of time series were weighted by the Nash-Sutcliffe coefficient (E), deviation of volumes (D_v) and the coefficient of determination (R^2), for a 95% confidence interval. This procedure was applied for all quality parameters described where satisfactory model performance was achieved for all criteria concurrently.

Table 3.13 Range and distribution of uncertainty for water quality parameters.

Parameter	Description	Range	Distribution
FSTDEC	First order decay rate of bacteria (day^{-1})	(0.1;5)	Uniform
WSQOP	Rate of surface runoff that will remove 90% of stored fecal coliform from pervious land use	(0.5;1.0)	Uniform
WSQOP*	Rate of surface runoff that will remove 90% of stored quality constituent from pervious land use	(0.5;2.4)	Uniform
KBOD20	BOD decay rate at 20ºC (hr^{-1})	(0.0001;1)	Uniform
KODSET	Rate of BOD settling ($m\ hr^{-1}$)	(0;0.3)	Uniform
BENOD	Benthal oxygen demand at 20ºC ($mg\ m^{-2}\ hr^{-1}$)	(0;500)	Uniform
REAK	Empirical constant to calculate the reaeration coefficient (hr^{-1})	(0.01;2)	Uniform
KTAM20	Nitrification rate of ammonia at 20ºC (hr^{-1})	(0.001;1)	Uniform
KNO220	Nitrification rate of nitrites at 20ºC (hr^{-1})	(0.001;1)	Uniform
KNO320	Nitrate denitrification rate at 20ºC (hr^{-1})	(0.001;1)	Uniform
ACQOP**	Accumulation of fecal coliform on pervious land per day (CFU day^{-1})	($2x10^8$;$2x10^{10}$;$2x10^{12}$)	Triangular
SQOLIM Factor	Factor which is multiplied to ACQOP to obtain maximum accumulation of fecal coliform on pervious	(2;10)	Triangular
$ACQOPNO_3$**	Accumulation of nitrates on pervious land per day ($lb\ ac^{-1}\ day^{-1}$)	(0.05;30)	Triangular
$ACQOPPO_4$**	Accumulation of nitrates on pervious land per day ($lb\ ac^{-1}day^{-1}$)	(0.001;1)	Triangular

* Constituents: nitrates, orthophosphates and biochemical oxygen demand;
** For the months of January.

The MC simulations that were used to generate data for the model comparison were executed using an *R* script (Team, 2008) written specifically for this study. The *R* script populated all the parameters subroutine tables in the HSPF user control input (UCI) file, resulting in *1000* UCI files representing the parameter sets from the distributions. *R* was also used to perform all statistical criteria presented in Table 2.6.

A multi parametric sensitivity analysis (MPSA) was applied to the parameters referred in Table 3.13 in an attempt to recognize the significance of each parameter involved in the model. The MPSA followed the procedure proposed by Chang and Delleur (1992) and Choi et al. (1998) and consists on implementing a generalized sensitivity analysis (Hornberger and Spear, 1981); select the parameters to analyze; assign distribution to the selected parameters;

run the model and determine whether the *1000* parameter sets are “behaviour” or “non-behaviour” by evaluating the statistical errors mentioned previously; compare the cumulative frequency distributions for each parameter associated with the acceptable and unacceptable results. If the two distributions are not statistically different, the parameter is classified as insensitive, otherwise the parameter is sensitive.

Although statistics can be displayed to help the modeller compare various modelling runs, there is always the uncertainty associated with the observed data. In general, water quality data collected at each site complies with guideline standards, but water quality degradation is always expected between the sample site and the laboratory. Also different entities may use different methods of analysis which may result in different outcomes. It is recommended that monitoring programs should always maintain the same schedule at each sampling site.

3.6 References

75/440/EEC, 1975. Council Directive 75/440/EEC of 16 June 1975 concerning the quality required of surface water intended for the abstraction of drinking water in the Member States. Volume 1.

2000/60/EC, 2000. Directive 2000/60/EC of the European Parliament and of the Council of 23 October 2000 establishing a framework of Community action in the field of water policy.

Albek, M., Bakır Öğütveren, Ü., Albek, E., 2004. Hydrological modeling of Seydi Suyu watershed (Turkey) with HSPF. Journal of Hydrology 285, 260-271.

Alexander, L. V., et al. "Global observed changes in daily climate extremes of temperature and precipitation. 2006. "Journal of Geophysical Research: Atmospheres (1984–2012) 111.D5.

AquaTerra, 2004. BASIN/HSPF Training Handbook. US EPA.

ARH-Centro, 2012. Plano de Gestão das Bacias Hidrográficas dos rios Vouga, Mondego e Lis Integrados na Região Hidrográfica 4.

Bauer, E., Claussen, M., Brovkin, V., & Huenerbein, A. (2003). Assessing climate forcings of the Earth system for the past millennium. *Geophysical Research Letters*, *30*(6).

Beltrami, H., Smerdon, J. E., Pollack, H. N., & Huang, S. (2002). Continental heat gain in the global climate system. *Geophysical research letters*, *29*(8), 8-1.

Bennett, N.D., Croke, B.F., Guariso, G., Guillaume, J.H., Hamilton, S.H., Jakeman, A.J., Marsili-Libelli, S., Newham, L.T., Norton, J.P., Perrin, C., 2013. Characterising performance of environmental models. Environmental Modelling & Software 40, 1-20.

Beven, K., Binley, A., 1992. The future of distributed models: model calibration and uncertainty prediction. Hydrological processes 6, 279-298.

Beven, K.J., 2001. Rainfall-runoff modelling. Wiley Online Library.

BGRI, 2001. Base Geográfica de Referenciação da Informação 2001, http://mapas.ine.pt, 2001-06-22 ed.

Bicknell, B., Imhoff, J., Kittle, J., Jobes, T., Donigian, A., 2005. Hydrological Simulation Program - FORTRAN: HSPF Version 12.2 User's Manual, Athens, GA.

Binkley, D., Brown, T.C., 1993. Forest Practices as Nonpoint Sources of Pollution in North America. JAWRA Journal of the American Water Resources Association 29, 729-740.

Bouraoui, F., Wolfe, M.L., 1990. Application of hydrologic models to rangelands. Journal of Hydrology 121, 173-191.

Chang, F.J., Delleur, J., 1992. Systematic parameter estimation of watershed acidification model. Hydrological processes 6, 29-44.

Choi, J., Hulseapple, S., Conklin, M., Harvey, J., 1998. Modeling CO< sub> 2</sub> degassing and pH in a stream–aquifer system. Journal of Hydrology 209, 297-310.

Crowley, T. J. (2000). Causes of climate change over the past 1000 years.*Science*, *289*(5477), 270-277.

CS/AR-17, 2000. Surface Water Quality Assessment of River Kali, U.P., with Special Emphasis to Non-Point Source Pollution. National Institute of Hydrology Jalvigyan Bgawan.

CWA, 1972. Clean Water Act §§101-607; United Staates Code 33: §§1251 et seq.

DiToro, D.M., O'Connor, D.J., Thomann, R.V., 1970. A dynamic model of phytoplankton populations in natural waters.

Donigian, A.S., Crawford, N.H., 1976. Modeling nonpoint pollution from the land surface. US Environmental Protection Agency, Office of Research and Development, Environmental Research Laboratory.

Donigian Jr., A.S., 2002. Watershed Model Calibration and Validation: The HSPF Experience. AquaTerra Consultants, Mountain View, California.

Donigihan, A.S., Davis, H.H., 1978. User's manual for agricultural runoff management (ARM) model. Environmental Protection Agency, Office of Research and Development, Environmental Research, Technology Development and Applications Branch ; for sale by the National Information Service, Athens, Ga. : Springfield, Va.

Hornberger, G.M., Spear, R., 1981. Approach to the preliminary analysis of environmental systems. J. Environ. Manage.;(United States) 12.

International, A., Testing, A.S.f., Materials, 2004. Annual book of ASTM standards. American Society for Testing & Materials.

Jacomino, V.M.F., Fields, D.E., 1997. A Critical Approach to the Calibration of a Watershed Model. Journal of the American Water Resources Association 33, 143-154.

Legates, D.R., McCabe, G.J., 1999. Evaluating the use of “goodness-of-fit” measures in hydrologic and hydroclimatic model validation. Water Resources Research 35, 233-241.

Liao, H.-H., Tim, U.S., 1997. An Interactive Modeling Environment for Non-Point Source Pollution Control. JAWRA Journal of the American Water Resources Association 33, 591-603.

Mapoteca, 2008. http://web.letras.up.pt/mapoteca.

Mishra, A., 2011. Estimating Uncertainty in HSPF Based Water Quality Model: Application of Monte-Carlo Based Techniques, Biological Systems Engineering. Faculty of Virginia Polytecnic Institute and State University, Blacksburg, Virginia, p. 103.

Mostaghimi, S., Park, S.W., Cooke, R.A., Wang, S.Y., 1997. Assessment of management alternatives on a small agricultural watershed. Water Research 31, 1867-1878.

Paul, S., Haan, P., Matlock, M., Mukhtar, S., Pillai, S., 2004. Analysis of the HSPF water quality parameter uncertainty in predicting peak in: Stream fecal coliform concentrations. Transactions of the ASAE 47, 69-78.

Ratto, M., Tarantola, S., Saltelli, A., 2001. Sensitivity analysis in model calibration: GSA-GLUE approach. Computer Physics Communications 136, 212-224.

Razavian, D., 1990. Hydrologic Responses of an Agricultural Watershed to Various Hydorlogic and Management Conditions. JAWRA Journal of the American Water Resources Association 26, 777-785.

Refsgaard, J.C., van der Sluijs, J.P., Højberg, A.L., Vanrolleghem, P.A., 2007. Uncertainty in the environmental modelling process – A framework and guidance. Environmental Modelling & Software 22, 1543-1556.

Santhi, C., Arnold, J.G., Williams, J.R., Dugas, W.A., Srinivasan, R., Hauck, L.M., 2001. Validation of the SWAT Model on a Large River Basins with Point and Nonpoint Sources. JAWRA Journal of the American Water Resources Association 37, 1169-1188.

Sherwood, S.C., Bony, S., Dufresne, J.-L., 2014. Spread in model climate sensitivity traced to atmospheric convective mixing. Nature 505, 37-42.

Singh, J., Knapp, H.V., Arnold, J., Demissie, M., 2005. Hydrological modeling of the iroquois river watershed using HSPF and SWAT. JAWRA Journal of the American Water Resources Association 41, 343-360.

Spear, R., Hornberger, G., 1980. Eutrophication in peel inlet--II. Identification of critical uncertainties via generalized sensitivity analysis. Water Research 14, 43-49.

Team, R.C., 2008. R: A language and environment for statistical computing, Vienna, Austria.

USEPA, 2000. BASINS Technical Note 6: Estimating Hydrology and Hydraulic Parameters for HSPF. Office of Water EPA-823-R00-012.

Vieira, J., Fonseca, A., Vilar, V., Boaventura, R., Botelho, C., 2013. Water Quality Modelling of Lis River, Portugal. Environ Sci Pollut Res 20, 508-524.

Vieira, J., Fonseca, A., Vilar, V.P., Boaventura, R.R., Botelho, C.S., 2012. Water quality in Lis river, Portugal. Environmental Monitoring and Assessment 184, 7125-7140.

Wentz, F.J., Ricciardulli, L., Hilburn, K., Mears, C., 2007. How much more rain will global warming bring? Science 317, 233-235.

Zhang, J., Ross, M., Trout, K., Zhou, D., 2009. Calibration of the HSPF model with a new coupled FTABLE generation method. Progress in Natural Science 19, 1747-1755.

4 Watershed Model Parameter Estimation and Uncertainty in Data-Limited Environments[1]

Parameter uncertainty and sensitivity for a watershed-scale simulation model in Portugal were explored to identify the most critical model parameters in terms of model calibration and prediction. The research is intended to provide guidance regarding allocation of limited data collection and model parameterization resources for modellers working in any data and resource limited environment. The watershed-scale hydrology and water quality simulation model, Hydrologic Simulation Program – FORTRAN (HSPF), was used to predict the hydrology of Lena River basin in Portugal. The model was calibrated for a 5-year period 1985-1989 and validated for a 4-year period 2003-2006. Agreement between simulated and observed stream flow data was satisfactory considering the performance measures such as Nash-Sutcliffe efficiency (E), deviation volumes (Dv) and coefficient of determination (R^2). The Generalized Likelihood Uncertainty Estimation (GLUE) method was used to establish uncertainty bounds for the simulated flow using the Nash-Sutcliffe coefficient as a performance likelihood measure. Sensitivity analysis results indicate that runoff estimations are most sensitive to parameters related to climate conditions, soil and land use. These results state that even though climate conditions are generally most significant in water balance modelling, attention should also focus on land use characteristics as well. Specifically with respect to HSPF, the two most sensitive parameters, INFILT and LZSN, are both directly dependent on soil and land use characteristics.

[1] Fonseca A, Ames DP, Yang P, Botelho C, Boaventura R, Vilar V. Watershed model parameter estimation and uncertainty in data-limited environments. Environmental Modelling & Software 2014; 51: 84-93.

4.1 Introduction

Like many similar government initiatives throughout the world, the European Union Water Framework Directive (WFD) was established to restore and protect both surface and ground water with ambitious goals to be met by a target date of 2015 (2000/60/EC, 2000). Watershed modelling software can be used to help scientists and watershed managers to meet these goals by simulating the effect on water quality and quantity considering different water management strategies, types of land use and climate change.

Many commercial and open source watershed simulation models are available and much care and consideration needs to be employed when choosing a model for application in a particular watershed (Borah and Bera, 2004). Regardless of the chosen model, even greater attention must be given to the task of "populating" the selected model with appropriate and physically meaningful model parameters that accurately characterize the surficial landscape, subsurface geology, atmospheric conditions, and other constraints affecting the storage and flux of water and contaminants through the environment (Doherty and Johnston, 2003; Donigian, 2002).

Because many watershed model parameters are difficult or impossible to measure in the natural world, parameters must often be estimated or otherwise evaluated from secondary information sources and hence are typically laden with notable degrees of uncertainty (Gallagher and Doherty, 2007). This chapter presents a watershed modelling study in the Lis River basin (Portugal) with the express purpose of identifying those parameters, whose accurate characterization is most critical for the success of the modelling effort. This study includes a complete model parameterization and calibration effort combined with parameter uncertainty estimation techniques. The results provided here can be used to inform other modelers in data and resource limited situations as to which parameters warrant the greatest resource-allocation and technical attention – allowing for the more efficient use of limited resources.

The hydrological model, Hydrologic Simulation Program FORTRAN (HSPF) was used in this study. HSPF is based on the original Stanford Watershed Model IV (Crawford and Linsley, 1966) and is a consolidation of three previously developed models: Agricultural

Runoff Management Model (Moriasi et al., 2007) (Donigian and Davis, 1978), Non-point Source Runoff Model (NPS) (Donigian and Crawford, 1976) and Hydrological Simulation Program (HSP) including HSP Quality (Donigian et al., 1991; Donigian Jr et al., 1995; Hydrocomp, 1977).

HSPF is a semi-distributed model that simulates water and contaminant transport through spatially distributed, physically homogenous areas within a watershed called Hydrologic Response Units (HRUs). HRUs are presumed to hydrologically respond similarly to given meteorological inputs (precipitation, potential evapotranspiration and temperature). In this way, HSPF can simulate the hydrological, hydraulic and water quality processes on pervious and impervious land surfaces, in soil profiles and in streams and well-mixed impoundments on a continuous basis (Bicknell et al., 2001).

A graphical user interface for HSPF is included in the free software, BASINS, developed and distributed by the United States Environmental Protection Agency. BASINS is built on the open source geographic information system (GIS) MapWindow GIS (Ames et al., 2008). The use of BASINS to develop HSPF models has been reported in several studies (Bergman et al., 2002; Carrubba, 2000; Lian et al., 2007; Lowe and Doscher, 2003; Zhang et al., 2009).

Calibration of HSPF is an iterative procedure of parameter evaluation, as a result of comparing simulated against observed values of interest. Since HSPF uses a large number of parameters that can be adjusted to represent the physical environment, an expert system, HSPExp is available to assist modelers with hydrology calibration. Typically a dozen or less parameters are used in most studies. HSPExp advises the user on which parameters can be meaningfully adjusted to reduce simulation error while providing explanations regarding the modifications (Lumb et al., 1994). However, there are limitations to HSPF, such as limited spatial definition (finite element analysis model), limited to non-tidal freshwater systems and extensive data requirements (i.e. meteorological and most important gauging stations of interest in the watershed).

Model validation is necessary in any model application and is an extension of the calibration process. Its purpose is to assure that the calibrated model properly assesses all the variables and conditions which can affect model results and, the ability to predict the behaviour of the system for periods separated from the calibration. Model credibility is based on the ability of a single set of parameters to represent the entire range of observed data. If a single parameter set can reasonably represent wide range of events, then this is a form of validation (Donigian Jr., 2002).

Sensitivity and uncertainty analysis of model parameters is conventionally considered to be one of the primary steps in the development and evaluation of models (Jakeman et al., 2006; Sudheer et al., 2011). Over the past decade it has become widely accepted that hydrological models with numerous parameters are likely to produce equally acceptable predictions for multiple different parameter sets (Hope et al., 2004) and a unique "best" parameter set cannot necessarily be found in the parameter space (Christiaens and Feyen, 2001). A structured method to quantify model uncertainty, Generalized Likelihood Uncertainty Estimation (GLUE), proposed by Beven and Binley (1992) establishes uncertainty bounds for the simulated value using parameter sets that are determined to be acceptable based on a performance likelihood measure. The implementation of this method requires the user to make a number of subjective decisions such as the threshold value of the likelihood measure to classify the model as acceptable or unacceptable (Beven and Binley, 1992; Beven, 2001). With GLUE, model parameters are sampled from distributions, typically with independent uniform or normal distributions for each parameter. The model is then run with each parameter set, generating multiple sets of model output, which are used to generate uncertainty intervals for model predictions. The generated model parameters are grouped in two categories: behavioural, sets of model parameters that produce results consistent with the observations and non-behavioural, results that contradict the observations (Hornberger and Spear, 1980).

As discussed previously the model HSPF, requires extensive parameterization to simulate hydrology fluxes due to both uncertainty in modeled processes and observation errors (Ratto et al., 2001).

The remainder of this study includes a discussion of the methods employed, and results related to the hydrology calibration parameters with focus on assessing the sensitivity of the model to selected parameters and determination of parameter priority in the model.

4.2 Results and Discussion

The hydrologic parameter set values for the expert system calibration discussed in chapter 3 are within the range of those presented in literature (USEPA, 2000). Table 4.1 shows the HSPExp criteria achieved in the calibration process. All criteria parameters were met except for evapotranspiration with 36.4% error. The total runoff was overestimated by 4.8%. As stated, this is a data limited watershed and evaporation was not available at any of the meteorological stations for Lis watershed. The evapotranspiration error presented here is associated with the difference between simulated evaporation and derived evaporation (from observed maximum and minimum temperature).

Table 4.1 Output error percentage for the Lena River watershed model calibration.

Flow component (units)	Simulated	Observed	% Error	Criteria
Total Runoff (mm)	1770.1	1689.6	4.8%	10%
Total of highest 10% flows (mm)	848.6	881.9	-3.8%	15%
Total of lowest 50% flows (mm)	99.3	109.9	-9.6%	10%
Evapotranspiration (mm)	2367.8	3723.64	**-36.4%**	10%
Total storm volume (mm)	312.9	288.4	8.4%	10%
Average of storm peaks ($m^3 s^{-1}$)	11.8.	11.7	0.8%	15%
Summer flow volume (mm)	79.6	78.1	1.9%	10%
Winter flow volume (mm)	985.8	1047.5	-5.9%	10%
Baseflow recession rate	23.6	23.4	1.1%	1%

Daily (Figure 4.1) and monthly (Figure 4.2) hydrographs from the HSPExp model were plotted with the respective observed discharge from the Lis gaging station to determine the relative errors and to compare the timings of the flood peaks. The peaks correlate very well for most of the entire period.

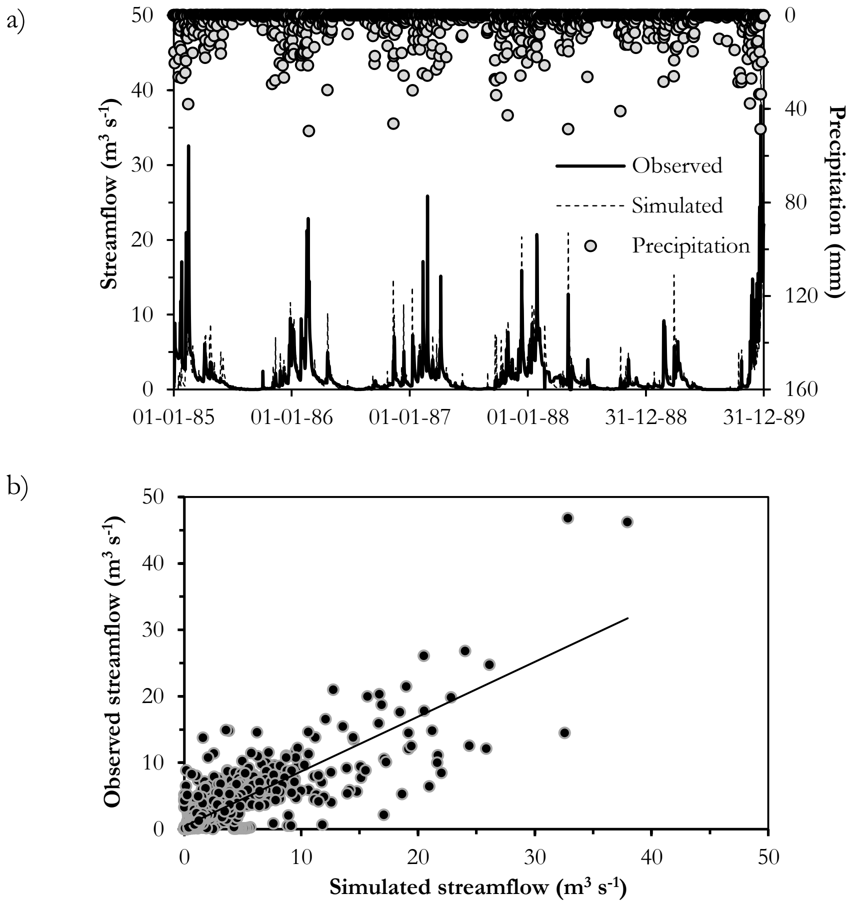

Figure 4.1 Daily observed and simulated streamflows for station 15E03: a) time series with precipitation and b) scatter plot (R^2 = 0.716).

According to the literature, the mathematical statistical criteria show good results for the daily and monthly simulation according to the coefficient of determination criteria and the Nash-Sutcliffe coefficient of efficiency. Table 4.2 shows the results achieved for the statistical methods previously discussed for both the calibrated and validated model.

For validation purposes, the calibrated model was run for 2003-2006 without changing any parameter values. Simulated daily and average monthly were compared with respective observed data values, as it can be seen in Figure 4.3 and Figure 4.4 respectively.

Even though the Nash-Sutcliffe coefficient of efficiency and the coefficient of determination increased, showing a very good approach, the simulated flow is overestimated by approximately 13%. An increase of almost 10% due to calibrated model, still according to literature for monthly simulation (15 per cent variation), shows good results.

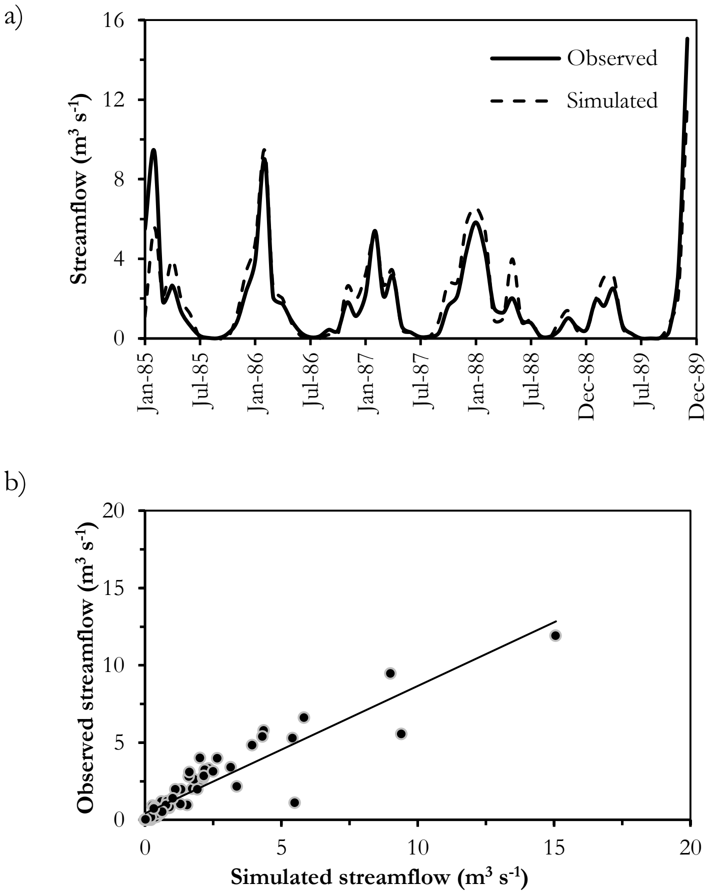

Figure 4.2 Monthly observed and simulated streamflows for station 15E03: a) time series and b) scatter plot (R^2 = 0.842).

Table 4.2 Model criteria statistical values.

	E	***R²***	***Dv* (%)**
Model Calibration (1985-1989)			
Daily	0.70	0.72	4.8
Average monthly	0.84	0.84	4.5
Model validation (2003-2006)			
Daily	0.84	0.86	12.9
Average monthly	0.86	0.96	12.8

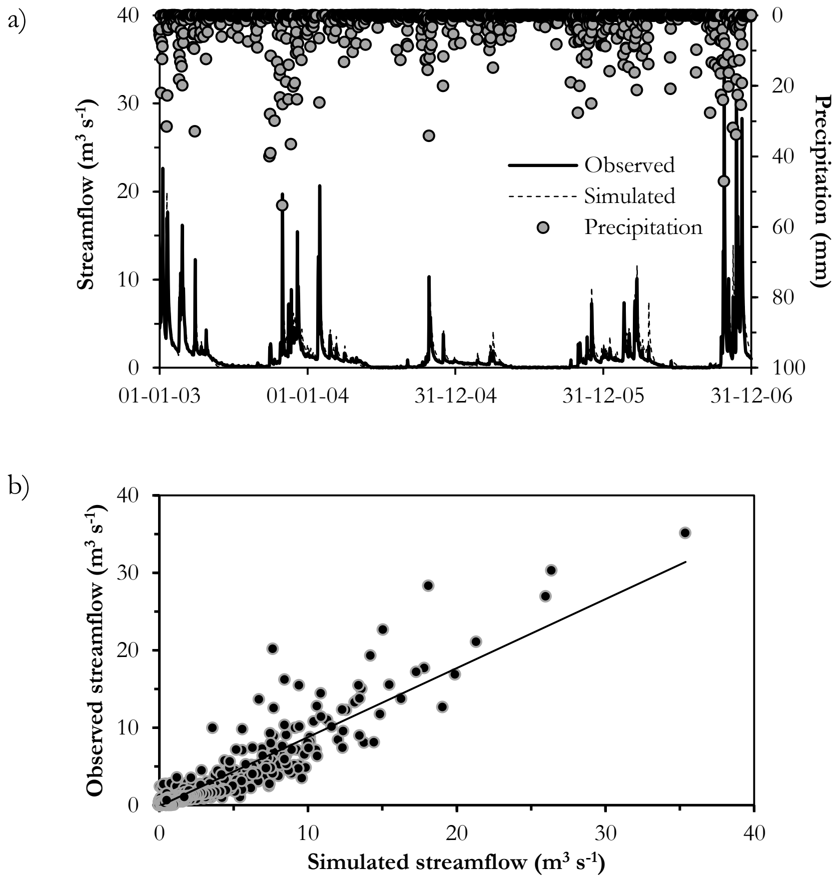

Figure 4.3 Daily observed and simulated streamflows for validated model at station 15E03: a) time series with precipitation and b) scatter plot (R^2 = 0.860).

One thousand parameter sets were included in the Monte Carlo parameter simulations. Table 4.3 shows the statistical distribution of these parameters. More than 90 percent of the 1000 MCS model runs produced values of E greater than 0.5, 49.8% percent had an E greater than 0.7 and 125 parameter sets were associated with an E equal or greater than 0.8.

The results indicate that the HSPF platform is well suited for the simulation of river discharge in the Lis River watershed, achieving a 0.70 and 0.84 Nash-Sutcliffe efficiency coefficient for daily and monthly calibration respectively. The threshold value for the likelihood measure to classify the model parameter sets as behavioural was determined as equal or greater than 0.5.

a)

b)

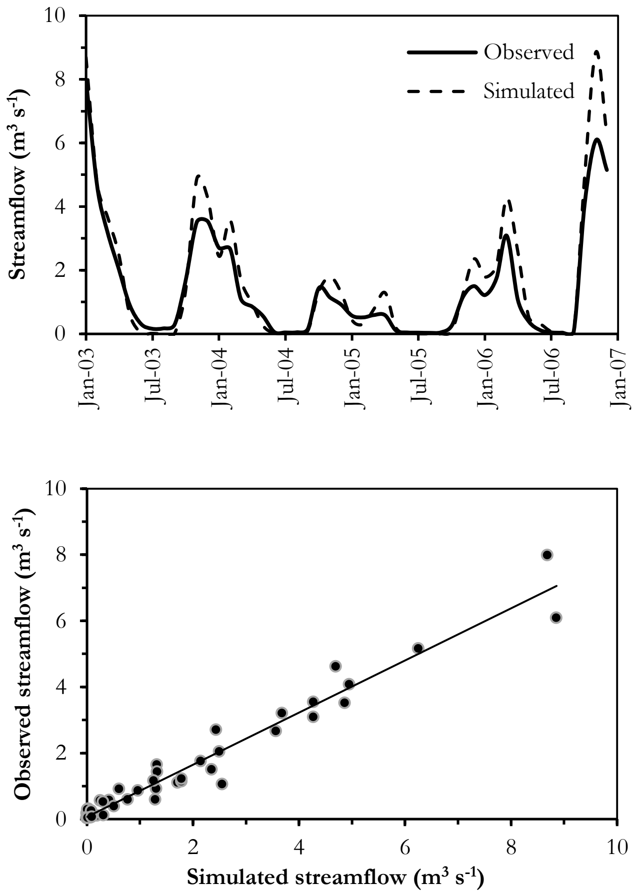

Figure 4.4 Monthly observed and simulated streamflows for the validated model at station 15E03: a) time series with precipitation and b) scatter plot (R^2 = 0.956).

To illustrate how sensitive the simulation of monthly discharge in the Lis watershed is related to the choice of the threshold value, when using GLUE method with *E* as an efficiency of the likelihood measure, the model uncertainty bounds for thresholds of 0.5 and 0.8 were calculated. The 95% confidence intervals of model uncertainty due to parameter uncertainty with thresholds of 0.5 and 0.8 are compared in Figure 4.5. The confidence interval of the simulated discharge changes significantly depending on the chosen threshold value. The lower the threshold value the wider the confidence interval of model uncertainty. The percentage of monthly average flows that fall outside the 95% confidence interval associated for a threshold of 0.5 and 0.8 is 4.8 % and 6.0% respectively. Although a 5 year calibration and 4 year validation might be considered a short duration to ensure a wide range of wet and dry periods as well as storm events of varying intensity and duration, the results give an indication how the model might perform for an independent period having similar conditions.

Table 4.3 Statistical parameter distribution.

	Minimum Calibrated Value	Maximum Calibrated Value	Mean	Standard Deviation
LZSN	76.285	203.074	137.964	36.313
AGWRC	0.920	0.990	0.956	0.020
DEEPFR	0.000	0.200	0.101	0.057
BASETP	0.000	0.050	0.025	0.014
AGWETP	0.000	0.050	0.025	0.015
INTFW	1.003	2.999	1.999	0.590
UZSN	2.548	25.391	14.111	6.389
LZETPA	0.501	0.700	0.601	0.057
LZETPU	0.200	0.699	0.451	0.145
LZETPF	0.600	0.800	0.700	0.057
LZETPB	0.100	0.399	0.245	0.085
IRC	0.507	0.699	0.631	0.047
INFILT	0.481	24.849	13.054	5.330

Sensitivity analysis (Figure 4.6) clearly indicate that changes in five specific parameters (*LZSN*, *AGWRC*, *UZSN*, *DEEPFR* and *INFILT*) result in significant changes in the hydrology output (i.e. the model is most sensitive to these parameters), since the 50% high values are set apart from the 50% low values for the output (Nash-Sutcliffe weight). This means that by changing those parameters within the acceptable boundaries, model performance changes significantly. Conversely, the five parameters, *BASETP*, *AGWETP*, *INTFW*, *IRC* and, *LZETP* for all land uses have little effect on the output of the hydrology simulation in the Lis River watershed.

The sensitivity analysis results reported in the literature show similar frequency occurrences on ranking HSPF water balance parameters the most sensitive in HSPF modelling.

a)

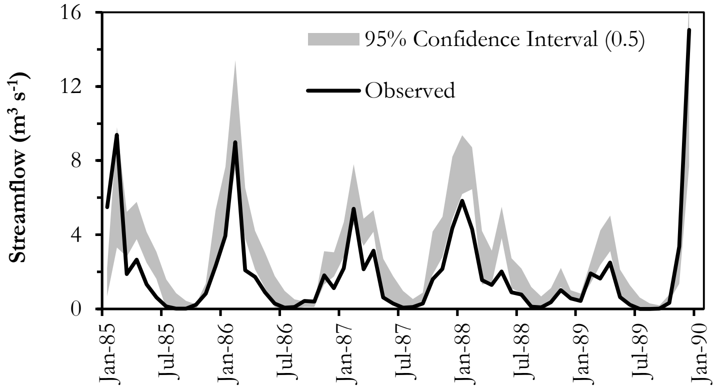

b)

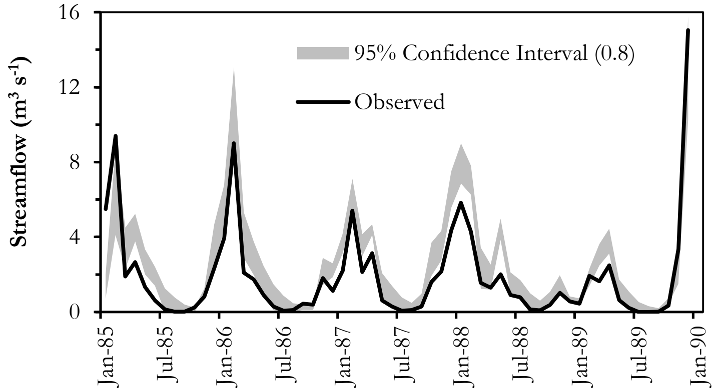

Figure 4.5 Comparison of 95% confidence interval of monthly stream flow due to parameter uncertainty with different thresholds: a) 0.5 and b) 0.8.

Table 4.4 shows the most sensitive parameters for different studies including this work. By adding the parameters according to the frequency observed in the hydrology calibration process, we established a ranking system to classify the most important parameters to calibrate water balance in HSPF.

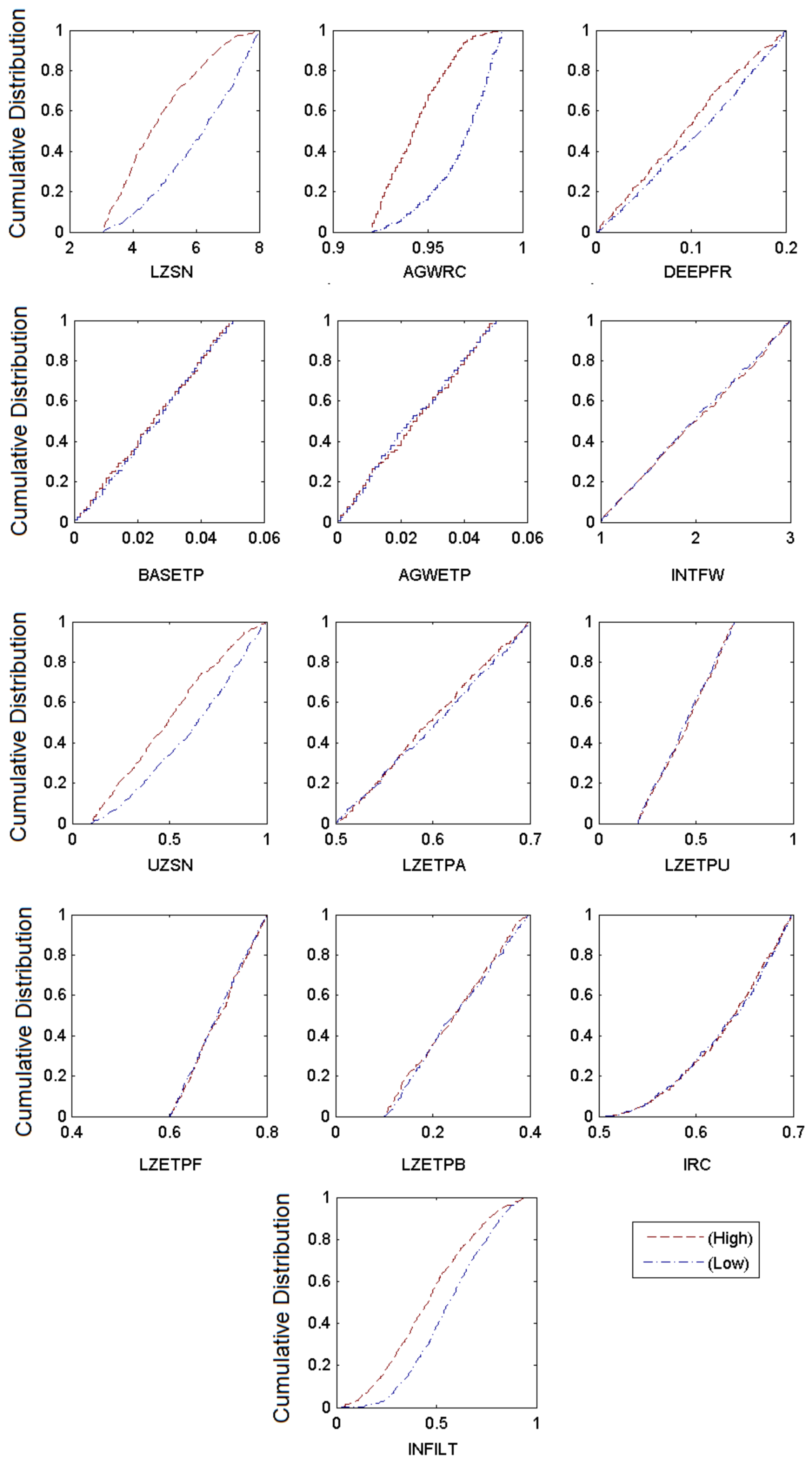

Figure 4.6 HSPF parameters sensitivity analysis in the Lis River watershed.

Table 4.4 Most sensitive HSPF water balance parameters reported in literature.

	AGWETP	AGWRC	BASETP	DEEPFR	INFILT	INTFW	IRC	LZETP	LZSN	UZSN
Fontaine and Jacomino (1997) (Normal Flow)		X			X					
Fontaine and Jacomino (1997) (Flood Flow)		X			X				X	X
AlAbed and Whiteley (2002)				X	X	X			X	
Chung and Lee (2009)		X			X	X	X		X	X
Chou et al. (2007)					X	X		X	X	
(Abdulla et al., 2009)	X	X		X	X				X	
Donigian Jr and Love (2007)				X				X	X	X
Kourgialas et al. (2008)					X				X	X
This Study		X		X	X				X	X

According to Table 4.5, *INFILT* and *LZSN* are the most sensitive parameters followed by *AGWRC* and *UZSN* which shows that HSPF calibration for water balance is most sensitive to soil and land use parameters. This clearly indicates that HSPF hydrology modelling is most sensitive to precipitation patterns, soil characteristics (*LZSN*, *INFILT* and *UZSN*) and land use characteristics (*INFILT* and *UZSN*).

Table 4.5 Number of occurrences and parameter ranking.

Parameters	Occurrences	Ranking
INFILT	8	A
LZSN	8	A
AGWRC	5	B
UZSN	5	B
DEEPFR	4	C
INTFW	3	D
LZETP	2	E
AGWETP	1	F
IRC	1	F
BASETP	0	G

Table 4.6 summarizes climate and geographic information, about the studies presented in Table 4.4, which can be helpful to explain the relationship between parameter(s) sensitivity and climate and geographic conditions. These studies range from high to low catchment areas and average annual precipitation as well as different soil and land use composition. From the relationship analysis one concludes that *LZSN* and *INFILT* parameters are generally sensitive as they appear in eight out of nine of the research papers presented. Although more information is required regarding soil composition it seems *INFILT* is considered a sensitive parameter in soils rich with loam rather than only one type of soil (sand, clay or silt).

Table 4.6 Watershed characteristics for the studies related to the parameter sensitivity analysis.

Study	Catchment Area (km²)	Average Annual PCP (mm)	Soil	Land Use
Fontaine and Jacomino (1997)	16	1372	Silty; very fine loam	80% Forest 10% Grass 10% Urban
AlAbed and Whiteley (2002)	6965	800-950	Predominant loam and sand	78% Agriculture 19% Forest 3% Urban
Chung and Lee (2009)	287	1325	---	43% Urban 40% Forest 13% Agriculture
Chou et al. (2007)	303	3495-3837	---	88% Forest 4% Tea Garden
Abdulla et al. (2009)	4000	150-400	Clay and clay loams Silty loam	---
Donigian Jr and Love (2007)	5058	1092	Sandy till, Clay and Silt	67% Forest 12% Agriculture 10% Urban 9% Wetland 2% Barren
Kourgialas et al. (2008)	130	500-2000	Clay loam	58% Pasture 29.4% Crops 8.5% Forest 2.8% Urban
This Study	176	855	Silt loam or loam (46%), sandy clay loam (40%) and sand, loamy sand or sandy loam (14%)	46% Agriculture 24% Forest 20% Barren 10% Urban

4.3 Conclusions

The hydrological behaviour of Lis River watershed was modeled. The model prediction compared reasonably well to the observed data on daily and monthly flow rates and flow duration, resulting in a Nash-Sutcliffe efficiency coefficient of 0.70 and 0.84 respectively. Model validation demonstrates a good representation of the observed data. This is the outcome of graphical and statistical comparisons and measures of the model performance for daily and monthly streamflow.

Modelling uncertainty and parameter sensitivity for the HSPF model using the GLUE method was evaluated in the Lis River watershed, with the aim to identify parameters that demand the greatest attention in light of limited data and where limited financial resources are often more intensive. The application of GLUE based on the Nash-Sutcliffe coefficient led to a good prediction uncertainty regarding the coverage of measurements by the uncertainty bands.

The results provided in this study show that even though monitoring climate conditions and stream flow are important in model performance, attention should be devoted to soil and land use data collection (*LZSN* and *INFILT*) since these data have been demonstrated herein as one important factor when characterizing river hydrology. Decisions may be taken directly from primary data measurements, derived statistics or the results of many steps of modelling, but it is the collected data that build the support for these decisions. A data set is clearly of great value as it is inevitably collected through a huge commitment of time and money. Developing a hydrologic foundation based on this data for river segments throughout a region, for a selected time period long enough to represent climate variability, will provide water managers more time allocation on other water management decisions.

4.4 References

2000/60/EC, C.D., 2000. Directive 2000/60/EC of the European Parliament and of the Council of 23 October 2000 establishing a framework of Community action in the field of water policy.

Abdulla, F., Eshtawi, T., Assaf, H., 2009. Assessment of the impact of potential climate change on the water balance of a semi-arid watershed. Water resources management 23, 2051-2068.

AlAbed, N., Whiteley, H., 2002. Calibration of the Hydrological Simulation Program Fortran (HSPF) model using automatic calibration and geographical information systems. Hydrological processes 16, 3169-3188.

Ames, D.P., Michaelis, C., Anselmo, A., Chen, L., Dunsford, H., 2008. MapWindow GIS, in: Shekhar, S., Xiong, H. (Eds.), Encyclopedia of GIS. Springer US, pp. 633-634.

Bergman, M., Green, W., Donnangelo, L., 2002. Calibration of Storm Loads in the South Prong Watershed, Florida, Using BASINS/HSPF1. JAWRA Journal of the American Water Resources Association 38, 1423-1436.

Beven, K., Binley, A., 1992. The future of distributed models: model calibration and uncertainty prediction. Hydrological processes 6, 279-298.

Beven, K.J., 2001. Rainfall-runoff modelling. Wiley Online Library.

Bicknell, B., Imhoff, J., Kittle Jr, J., Jobes, T., Donigian Jr, A., Johanson, R., 2001. Hydrological Simulation Program–FORTRAN: HSPF Version 12 User's Manual. AQUA TERRA Consultants, Mountain View, California.

Borah, D.K., Bera, M., 2004. Watershed-scale hydrologic and nonpoint-source pollution models: Review of applications. Transactions of the ASAE 47, 789-803.

Carrubba, L., 2000. Hydrologic Modeling at the Watershed Scale Using NPSM1. JAWRA Journal of the American Water Resources Association 36, 1237-1246.

Chou, W.S., Lee, T.C., Lin, J.Y., Yu, S.L., 2007. Phosphorus load reduction goals for Feitsui Reservoir watershed, Taiwan. Environmental monitoring and assessment 131, 395-408.

Christiaens, K., Feyen, J., 2001. Analysis of uncertainties associated with different methods to determine soil hydraulic properties and their propagation in the distributed hydrological MIKE SHE model. Journal of Hydrology 246, 63-81.

Chung, E.S., Lee, K.S., 2009. Prioritization of water management for sustainability using hydrologic simulation model and multicriteria decision making techniques. Journal of Environmental Management 90, 1502-1511.

Crawford, N.H., Linsley, R.K., 1966. Digital Simulation in Hydrology 'Stanford Watershed Model 4.

Doherty, J., Johnston, J.M., 2003. Methodologies for Calibration and Predictive Analysis of a Watershed Model. JAWRA Journal of the American Water Resources Association 39, 251-265.

Donigian, A., 2002. Watershed model calibration and validation: The HSPF experience. Proceedings of the Water Environment Federation 2002, 44-73.

Donigian, A.S., Crawford, N.H., 1976. Modeling nonpoint pollution from the land surface. US Environmental Protection Agency, Office of Research and Development, Environmental Research Laboratory.

Donigian, A.S., Davis, H.H., 1978. User's Manual for Agricultural Runoff Management(ARM) Model. Available from the National Technical Information Service, Springfield VA 22161 as PB-286 366, Price codes: A 08 in paper copy, A 01 in microfiche. Report.

Donigian, A.S., Huber, W.C., Laboratory, E.R., Consultants, A.T., 1991. Modeling of nonpoint source water quality in urban and non-urban areas. Environmental Research Laboratory, Office of Research and Development, US Environmental Protection Agency.

Donigian Jr, A., Bicknell, B., Imhoff, J., Singh, V., 1995. Hydrological Simulation Program-Fortran (HSPF). Computer models of watershed hydrology., 395-442.

Donigian Jr, A., Love, J., 2007. The Housatonic River Watershed Model: Model Application and Sensitivity/Uncertainty Analysis.

Donigian Jr., A.S., 2002. Watershed Model Calibration and Validation: The HSPF Experience. AquaTerra Consultants, Mountain View, California.

Fontaine, T.A., Jacomino, V.M.F., 1997. Sensitivity Aanalysis of Simulated Contaminated Sediment Transport. JAWRA Journal of the American Water Resources Association 33, 313-326.

Gallagher, M., Doherty, J., 2007. Parameter estimation and uncertainty analysis for a watershed model. Environmental Modelling & Software 22, 1000-1020.

Hope, A., Stein, A., McMichael, C., 2004. Uncertainty in monthly river discharge predictions in a semi-arid shrubland catchment. British Hydrological Society, pp. 284-290.

Hornberger, G., Spear, R., 1980. Eutrophication in Peel Inlet—I. The problem-defining behavior and a mathematical model for the phosphorus scenario. Water Research 14, 29-42.

Hydrocomp, I., 1977. Hydrocomp Water Quality Operations Manual, Hydrocomp Inc, Palo Alto, CA.

Jakeman, A.J., Letcher, R.A., Norton, J.P., 2006. Ten iterative steps in development and evaluation of environmental models. Environmental Modelling & Software 21, 602-614.

Kourgialas, N., Karatzas, G., Nikolaidis, P., 2008. Simulation of the flow in the Koiliaris River basin (Greece) using a combination of GIS, the HSPF model and a karstic–snow melt model, pp. 512-520.

Lian, Y., Chan, I., Singh, J., Demissie, M., Knapp, V., Xie, H., 2007. Coupling of hydrologic and hydraulic models for the Illinois River Basin. Journal of Hydrology 344, 210-222.

Lowe, S., Doscher, R., 2003. Modeling of urban watersheds using basins and HSPF. Journal of Environmental Hydrology 11.

Lumb, A.M., McCammon, R.B., Kittle, J.L., Division, G.S.W.R., 1994. Users Manual for an Expert System (HSPEXP) for Calibration of the Hydrological Simulation Program--Fortran. US Geological Survey Reston, VA.

Moriasi, D., Arnold, J., Van Liew, M., Bingner, R., Harmel, R., Veith, T., 2007. Model evaluation guidelines for systematic quantification of accuracy in watershed simulations. Transactions of the ASABE 50, 885-900.

Ratto, M., Tarantola, S., Saltelli, A., 2001. Sensitivity analysis in model calibration: GSA-GLUE approach. Computer Physics Communications 136, 212-224.

Sudheer, K.P., Lakshmi, G., Chaubey, I., 2011. Application of a pseudo simulator to evaluate the sensitivity of parameters in complex watershed models. Environmental Modelling & Software 26, 135-143.

USEPA, 2000. BASINS technical note 6. Estimating hydrology and hydraulic parameters for HSPF.

Zhang, J., Ross, M., Trout, K., Zhou, D., 2009. Calibration of the HSPF model with a new coupled FTABLE generation method. Progress in Natural Science 19, 1747-1755.

5 Analysis of Uncertainty in Ave and Este River Water Quality Modelling[2]

This study concerns the statistical evaluation of the water quality modelling system Hydrologic Simulation Program FORTRAN as a tool to improve monitoring planning and mitigate uncertainty in water quality predictions. A two-step statistical evaluation framework is presented based on the most common hydrology criteria for model calibration and validation and, a Monte Carlo methodology for uncertainty evaluation approach, coupled with multi parametric sensitivity analyses, to assess model uncertainty and parameter sensitivity. 85 water quality model parameters are used as input factors for the Monte Carlo simulation, considering normal or triangular probability distributions. In stream faecal coliform concentration was found to be more sensitive to first order decay rate (FSTDEC) and surface runoff that removes 90 percent of fecal coliforms (WSQOP) parameters. Regarding oxygen governing process (DO, BOD_5, NO_3, PO_4), benthal oxygen demand (BENOD) and nitrification rate (KNO320) were the most sensitive parameters.

[2] Fonseca A, Botelho C, Boaventura R, Vilar VJ.P. Analysis of uncertainty in river water quality modelling. Submitted to Environmental Modelling & Software.

5.1 Introduction

Uncertainty in water simulation models is expected due to the difficulty of accurately represent water quantity and quality against a real environment (Beck, 1987; van Straten, 1998). Extrapolation of water process has proven to be challenging even though there is a thorough knowledge about water process from laboratory experiments. Regardless of the model chosen, great attention must be given when assigning parameters with appropriate and physically meaningful values that accurately describe the watershed in terms of water process through the environment (Doherty and Johnston, 2003; Donigian, 2002; Fonseca et al., 2014). Because the modelling scale is different from a real environment to the laboratory, many model parameters are difficult or impossible to measure and must often be estimated or evaluated from secondary information sources and hence are typically laden with notable degrees of uncertainty (Gallagher and Doherty, 2007). Evaluating a model performance with respect to observed water quality data is not an easy task due to data scarcity, accuracy and frequency, since data can be expensive to collect and analyse. Also, water quality data are susceptible to noise and bias due to sampling, handling and measurement procedures (Keith, 1990) and often come from sampling programs which are fixed in frequency and location (Brown and Mac Berthouex, 2002). Pollution sources data presents the same limitations especially those which are difficult to measure such as nonpoint pollution sources. Compendiously, lack of good quality data to support model performance is a major cause of model uncertainty.

Sensitivity and uncertainty analysis of model parameters is usually considered to be one of the primary steps in the development and evaluation of models (Jakeman et al., 2006; Sudheer et al., 2011). Over the past decade has become widely accepted that hydrological models with numerous parameters are likely to produce equally acceptable predictions for multiple parameter sets (Hope et al., 2004) and a unique "best" parameter set cannot necessarily be found in the parameter space (Christiaens and Feyen, 2001). Monte Carlo based methodologies of uncertainty and sensitivity analysis such as those implemented by Hornberger and Spear (1980), Beven and Binley (1992) and Kuczera and Parent (1998) have found a myriad applications in environmental modelling, including surface water quality modelling. Uncertainty analysis in environmental modelling can provide information on the "goodness" of a result and enables us to understand the sources of error in the modelling process (Freni and Mannina, 2010; Willems, 2008). Assessment of the range of uncertainty in model prediction allows decision makers to evaluate the risk when model results are used on the basis of decisions (Novotny and Witte, 1997; Reda and Beck, 1997), since model outputs from predicting future conditions are somewhat uncertain. An uncertainty analyses attempts to evaluate all possible model outcomes together with their associated probabilities of occurrence, while a sensitivity analyses determines the change in model outputs derived from different model input values.

This study presents an analysis of uncertainty in river water quality modelling, considering the Ave River basin situated in the north of Portugal, in order to assess the risk to water quality status in the context of typical scarcity, accuracy and frequency of experimental data. This study takes into account all parameters involved in the calibration of water quality constituents; (i.e. nitrates are not calibrated in a watershed without looking at dissolved oxygen, biochemical oxygen demand, etc). The model also provides insight of the water quality model parameters sensitivity by applying different probability distribution assumptions.

5.2 Results and Discussion

5.2.1 Model Calibration and Validation

Key calibration parameters for nutrients, dissolved oxygen and algae modelling are specified in the HSPF manual (Bicknell et al., 2005). Nutrient loadings are governed by the potency factors (*POTFW*), rate of accumulation (*ACQOP*), maximum storage (*SQOLIM*) and sub-surface concentrations (*IOCQ* and *AOQC*). Instream nitrification and denitrification are governed by the respective reaction rates (*KTAM20* and *KNO320*). The channel reaeration contribution to the dissolved oxygen modelling was calculated as a power function of velocity and depth coefficients. Input parameters like the escape coefficient in the reaeration equation (*REAK*), the exponent to velocity and depth (*EXPREV* and *EXPRED*) and the temperature correction coefficient for reaeration (*TCGINV*) are key calibration parameters for in stream DO concentration. The values of *TCGINV*, *EXPREV* and *EXPRED* were the default values of HSPF (1.024, -1.673 and 0.969 respectively). *REAK* was adjusted accordingly to match the observed DO for all stations (0.2 – 2.0 hr^{-1}). Other parameters that affect DO concentration are: biochemical oxygen demand settling rate (*KBOD20*); benthal oxygen demand (*BENOD* and *EXPOD*) and the dissolved oxygen super saturation factor (*SUPSAT*). Key parameters in calibrating phytoplankton and benthic algae are: algal growth rate (*MALGR*); algal respiration rate (*ALR20*) and phytoplankton settling rate (*PHYSET*).

Point sources in a watershed are represented using a constant or time-variable discharge directly to the receiving water. The point sources addressed in chapter 3 were added to the model and model outputs were analysed. In stream HSPF water quality calibration procedures are highly dependent on constituents and processes that are represented. For example, the increase of algal respiration rate to reduce simulated plankton will result in increased values for nutrients and a decrease value for dissolved oxygen. The calibration is complete for any one water constituent when all adjustments have been made to the associated constituents by achieving the best overall fit against observed values (Duda P.B. et al., 2012).

Simulated and observed daily and monthly flow (Figure 5.1 and Figure 5.2) and in stream constituents concentrations (Figure 5.3 through Figure 5.6) for calibration and validation at Ave and Este River monitoring stations were visually compared and evaluated by statistical criteria (Table 5.1 and Table 5.2).

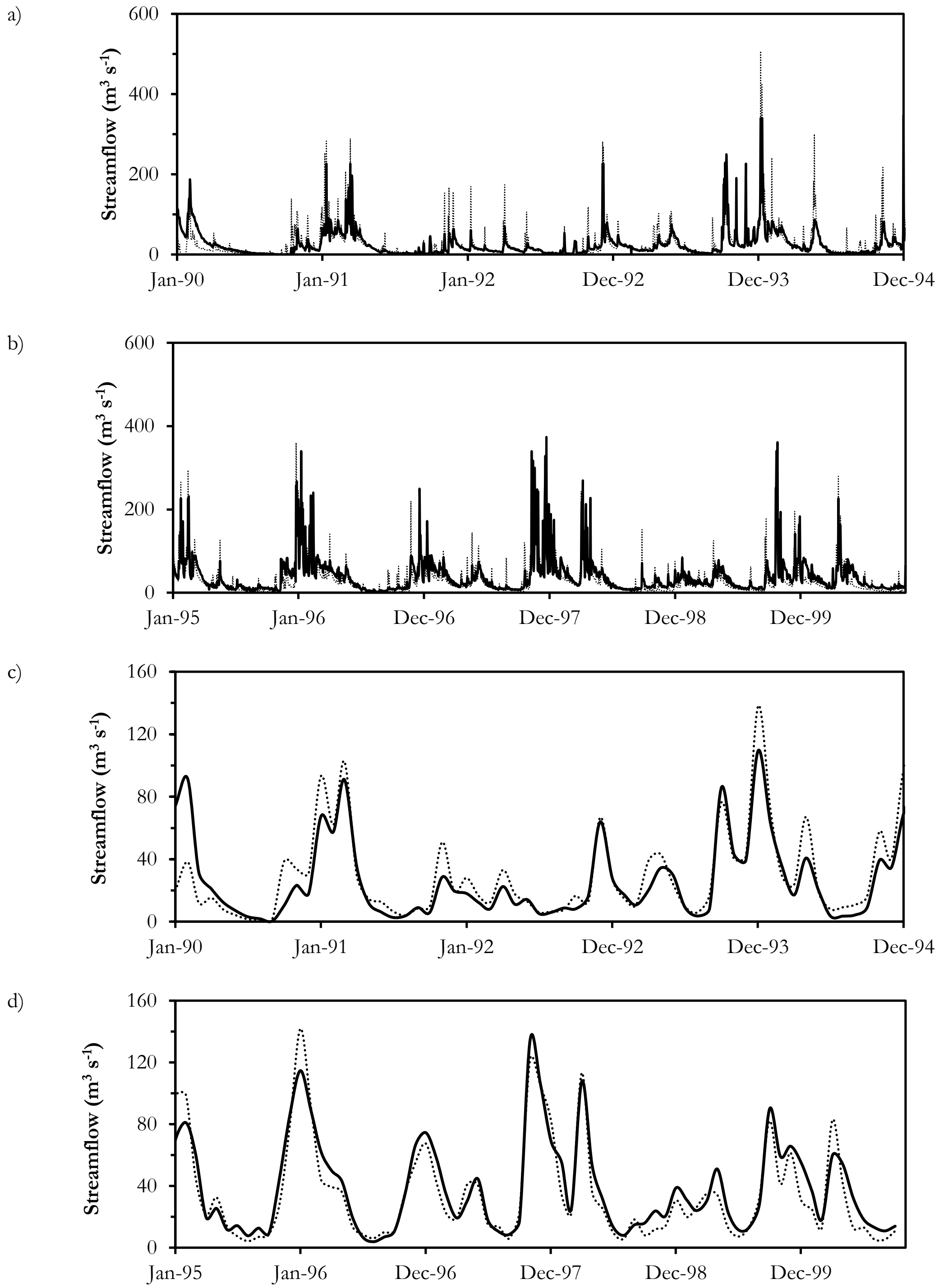

Figure 5.1 Streamflow plots at Ave River station; a) daily calibration; b) daily validation; c) monthly calibration; d) monthly validation; **–** observed values; -- simulated values.

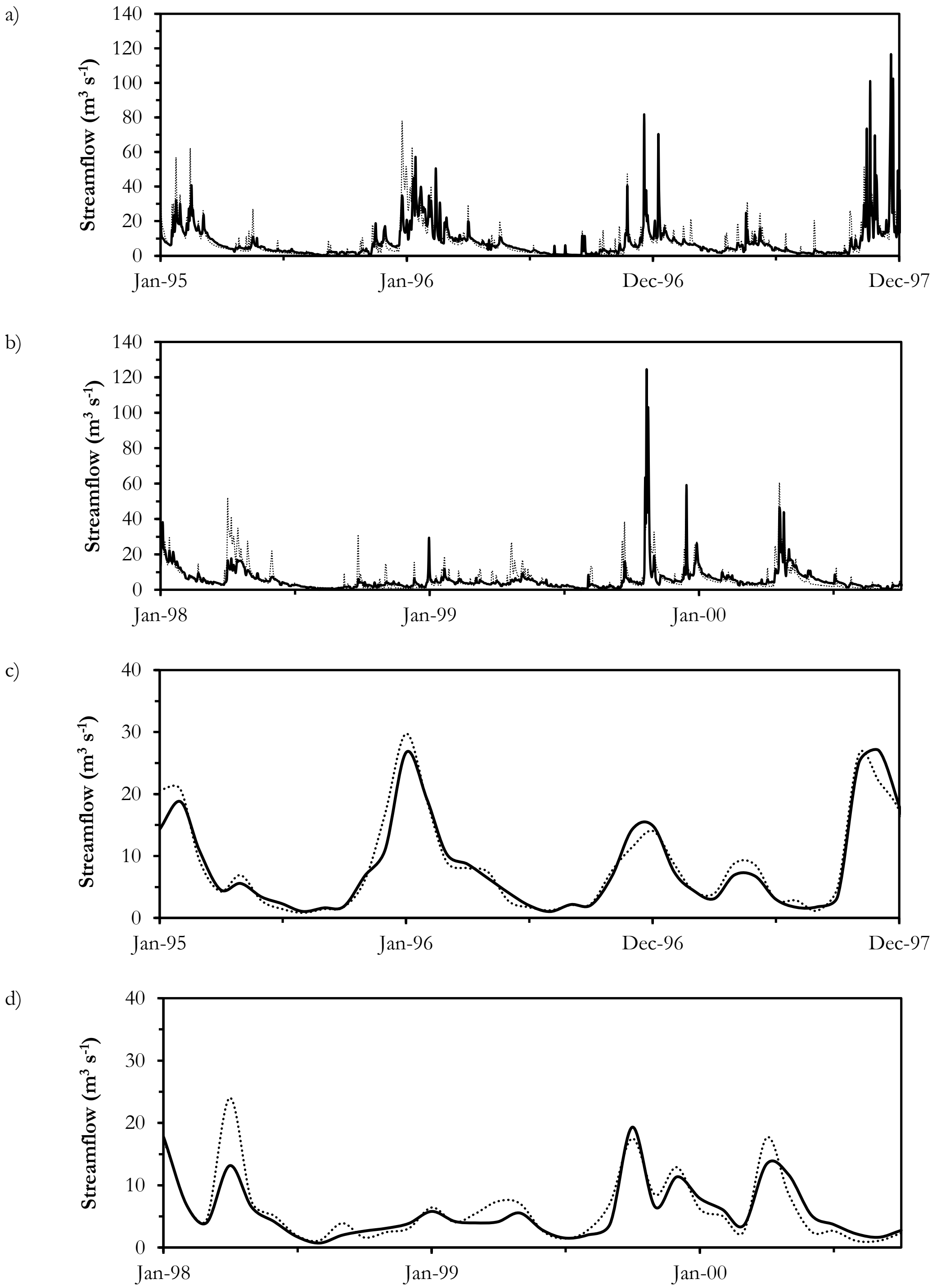

Figure 5.2 Stream flow plots at Este River station; a) daily calibration; b) daily validation; c) monthly calibration; d) monthly validation; – observed values; -- simulated values.

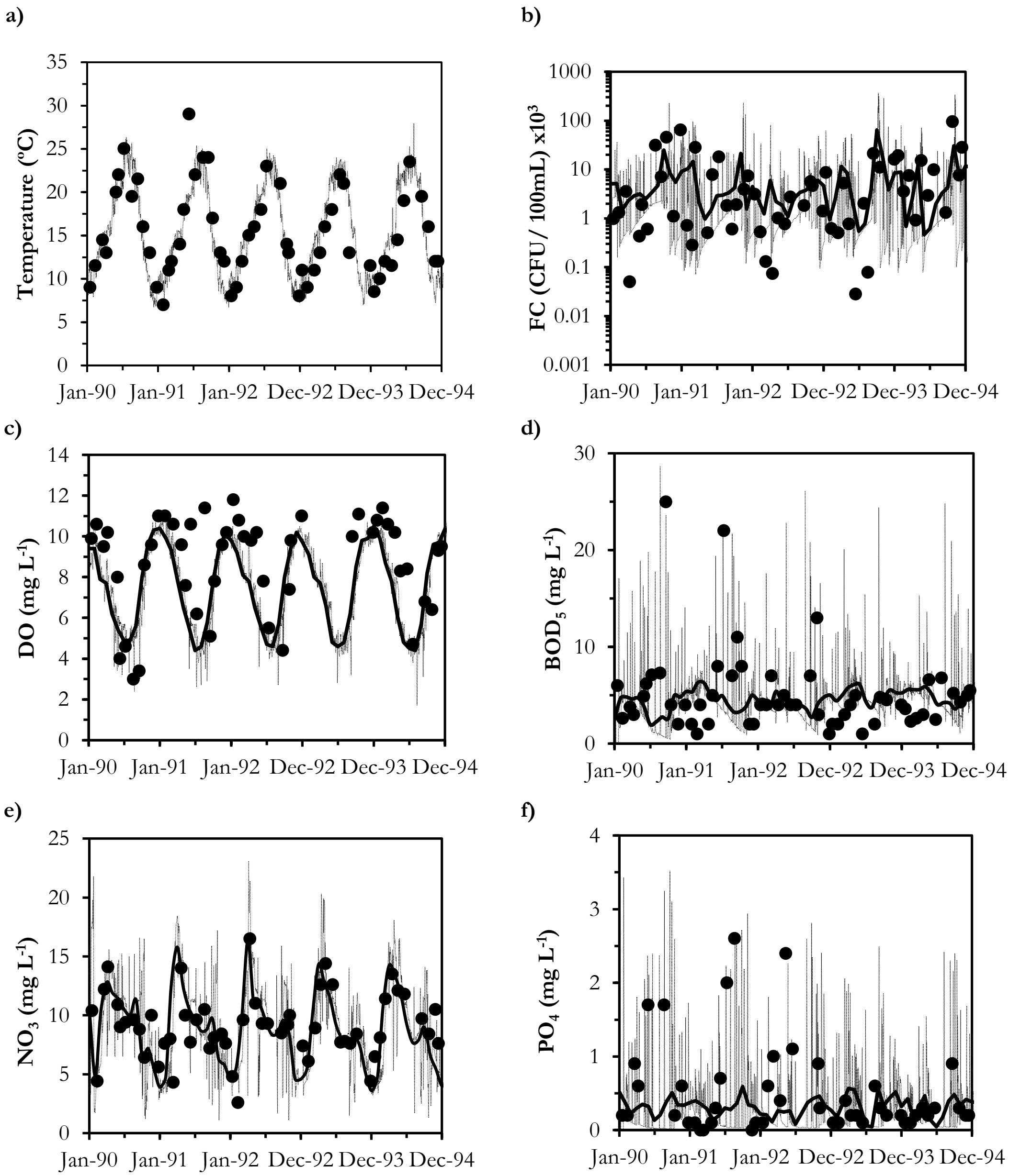

Figure 5.3 Calibration plots at Ave River Station; a) temperature; b) fecal coliforms; c) dissolved oxygen; d) biochemical oxygen demand; e) nitrates and f) orthophosphates; – monthly average; -- daily simulation; • observed values.

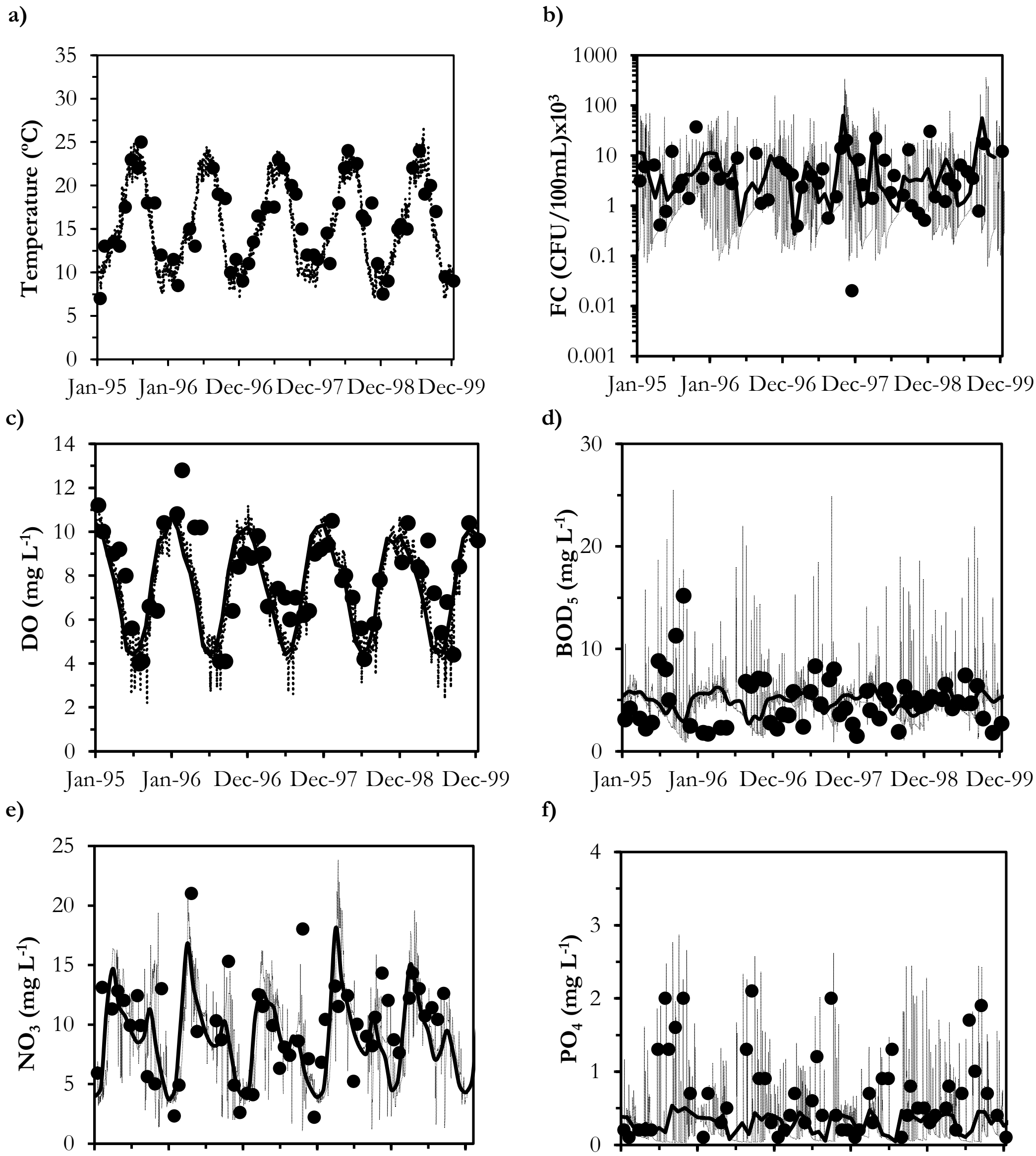

Figure 5.4 Validation plots at Ave River Station; a) temperature; b) fecal coliforms; c) dissolved oxygen; d) biochemical oxygen demand; e) nitrates and f) orthophosphates; – monthly average; -- daily simulation; • observed values.

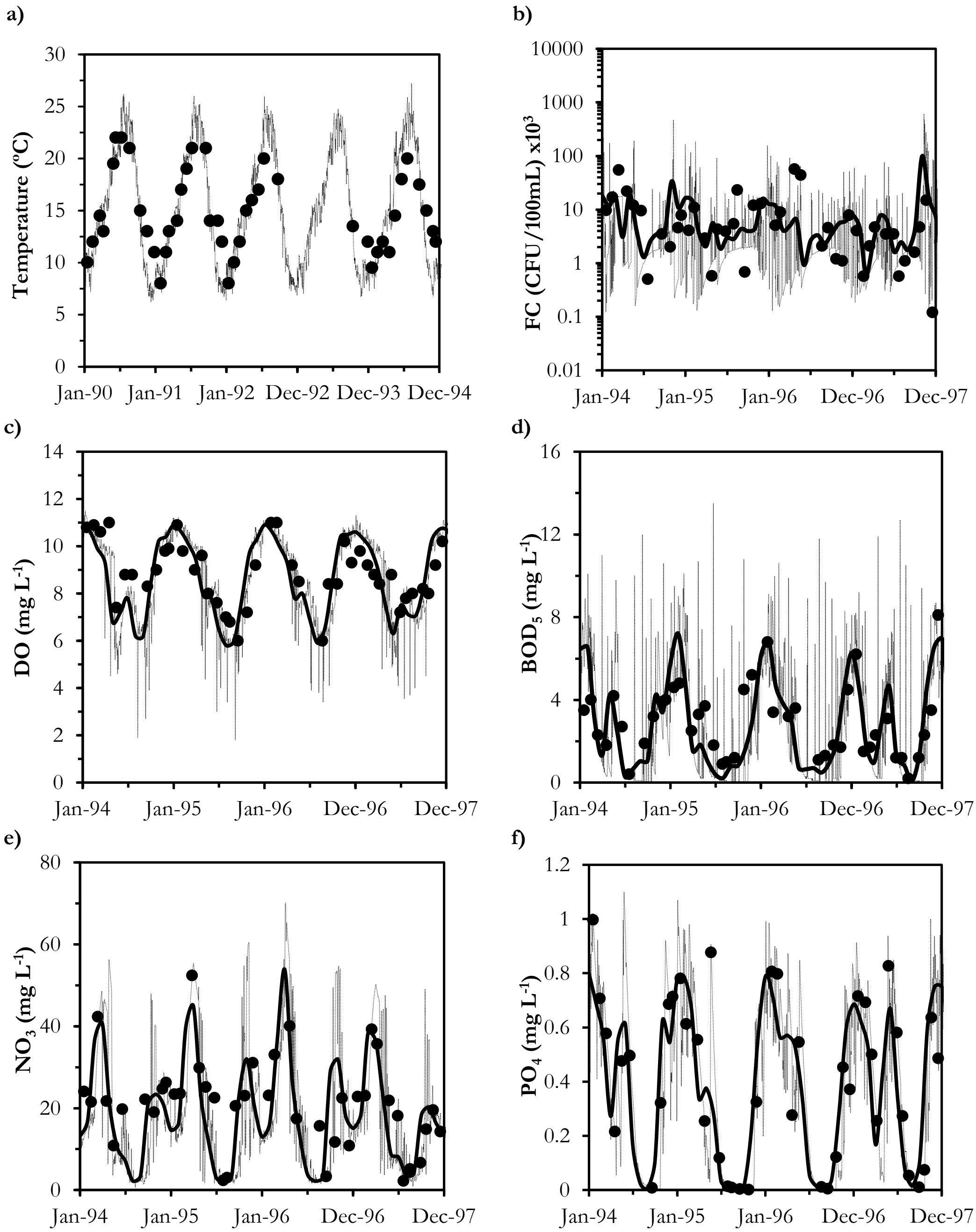

Figure 5.5 Calibration plots at Este River Station; a) temperature; b) fecal coliforms; c) dissolved oxygen; d) biochemical oxygen demand; e) nitrates and f) orthophosphates; – monthly average; -- daily simulation; • observed values.

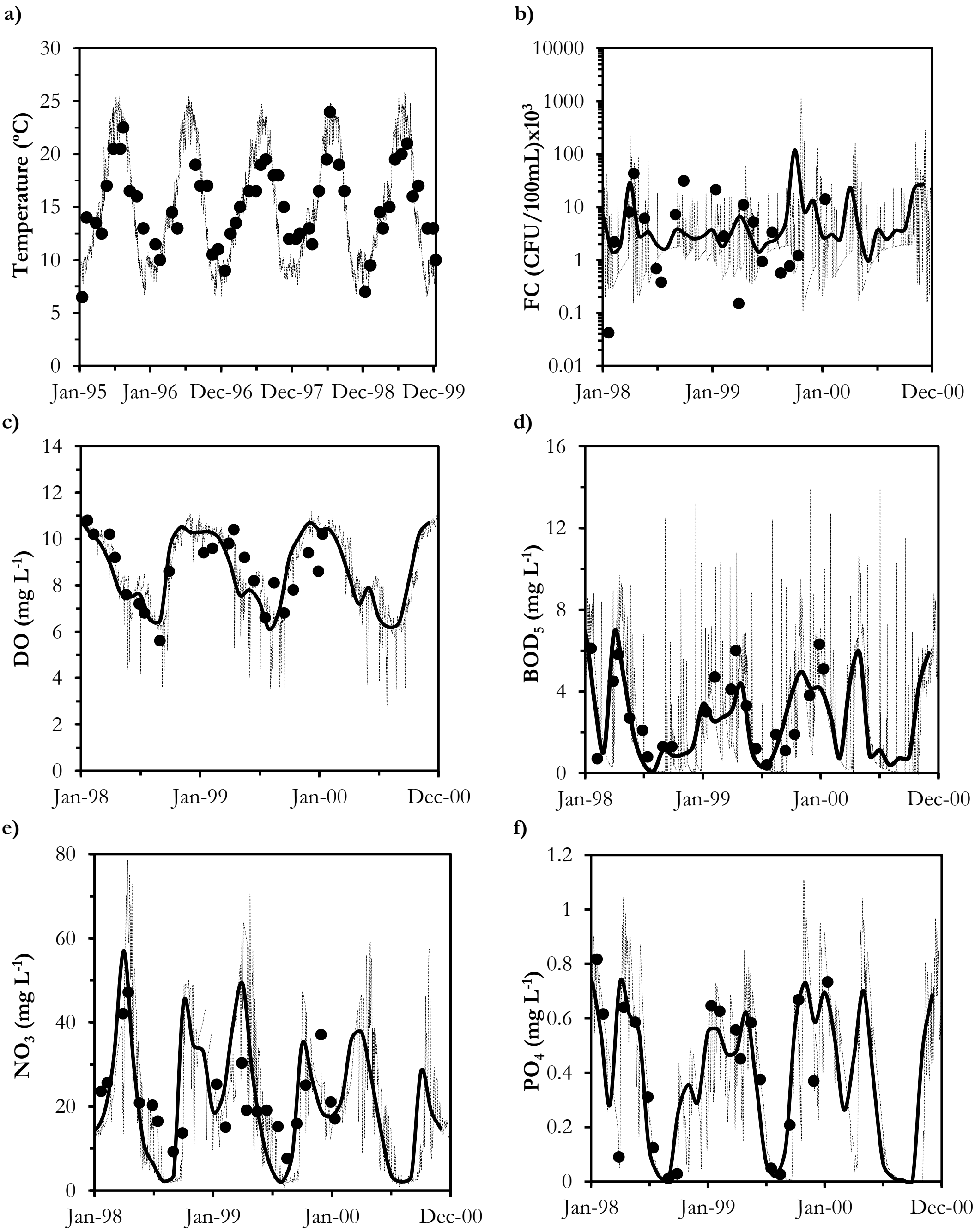

Figure 5.6 Validation plots at Este River Station; a) temperature; b) fecal coliforms; c) dissolved oxygen; d) biochemical oxygen demand; e) nitrates and f) orthophosphates; – monthly average; -- daily simulation; • observed values.

Table 5.1 Statistical criteria results at Ave River station.

Parameters	*Dv*	*E*	*R^2*	*MSE*	*RMSE*	*R4MS4E*	*IOAD*	*RSR*
Calibration								
Q (daily)	0.10	0.54	0.67	1.31	0.66	1.36	0.90	0.68
Q(monthly)	0.10	0.69	0.74	0.80	0.40	0.68	0.92	0.55
T	0.00	0.70	0.72	7.99	2.83	4.05	0.92	0.55
FC	-0.13	0.71	0.72	$8x10^7$	8966	13327	0.90	0.54
DO	-0.10	0.38	0.53	3.47	1.86	2.61	0.82	0.79
BOD_5	0.07	0.63	0.64	6.76	2.60	3.22	0.89	0.61
NO_3	-0.01	0.60	0.68	3.02	1.74	2.16	0.90	0.63
PO_4	0.09	0.72	0.75	0.11	0.32	0.42	0.93	0.53
Validation								
Q (daily)	-0.09	0.72	0.75	1.28	0.64	1.16	0.93	0.53
Q(monthly)	-0.09	0.87	0.90	0.62	0.31	0.41	0.97	0.37
T	-0.03	0.69	0.73	7.08	2.66	3.78	0.92	0.56
FC	-0.12	0.33	0.34	$3x10^7$	6031	9839	0.73	0.82
DO	-0.01	0.56	0.58	1.92	1.39	1.76	0.87	0.66
BOD_5	0.08	0.28	0.21	5.79	2.41	2.80	0.69	0.96
NO_3	-0.08	0.37	0.46	9.34	3.06	3.96	0.81	0.79
PO_4	-0.13	0.63	0.70	0.12	0.35	0.46	0.91	0.61

The statistical criteria were used as a guide in estimating satisfactory model performance. The deviation of volumes values for all constituents produced good results, with faecal coliforms showing the highest deviation at both stations. Nash-Sutcliffe values produced very good results for calibration and validation purposes; however nitrates and biochemical oxygen demand validation at both stations resulted only in a satisfactory approach (<0.50). Regarding the coefficient of determination, the constituents that resulted in values inferior to 0.50 (unsatisfactory) were FC, BOD and NO_3 for validation purposes at Ave River station.

Table 5.2 Statistical criteria results at Este River station.

Parameters	***Dv***	***E***	***R^2***	***MSE***	***RMSE***	***R4MS4E***	***IOAD***	***RSR***
Calibration								
Q (daily)	0.04	0.60	0.64	0.38	0.19	0.45	0.89	0.63
Q (monthly)	0.04	0.92	0.93	0.11	0.06	0.09	0.98	0.28
T	0.02	0.50	0.77	7.50	2.74	3.54	0.91	0.71
FC	-0.13	0.43	0.46	9.6×10^7	9815	16489	0.81	0.75
DO	-0.01	0.42	0.67	1.02	1.01	1.18	0.88	0.76
BOD_5	0.00	0.43	0.62	1.68	1.30	1.72	0.88	0.75
NO_3	-0.02	0.42	0.61	69.51	8.34	10.78	0.87	0.76
PO_4	-0.02	0.55	0.56	0.04	0.19	0.29	0.86	0.67
Validation								
Q (daily)	0.08	0.58	0.64	0.28	0.14	0.34	0.89	0.65
Q (monthly)	0.08	0.70	0.81	0.01	0.01	0.01	0.94	0.54
T	0.00	0.41	0.68	8.70	2.95	3.57	0.89	0.77
FC	-0.31	0.64	0.77	4.5×10^7	6690	9671	0.86	0.60
DO	0.02	0.49	0.56	1.02	1.01	1.31	0.86	0.72
BOD_5	0.01	0.45	0.54	2.04	1.43	1.75	0.85	0.74
NO_3	-0.11	0.27	0.66	67.28	8.20	8.68	0.86	0.86
PO_4	-0.13	0.63	0.70	0.12	0.35	0.46	0.91	0.61

To prevent the effect of the deviation volume, where positive and negative errors cancel each other, the *MSE*, *RMSE* and *R4MS4E* criteria were calculated. Both criteria show good results with values close to zero. Although *RMSE* and *R4MS4E* are more useful for interpretation since the results returned are in the same units as model and indicates an overall agreement between predicted and observed data, the bigger the mean square (two to four) the higher the emphasis on larger events. The results indicate that HSPF model is well suited for the simulation of river discharge and in stream water quality in Ave Watershed.

5.2.2 Uncertainty Analysis

The uncertainty analysis was performed for the entire calibration and validation period: 10 years for Ave River station and 6 year for Este River station. The threshold established for the likelihood measure to classify the model parameter sets as behaviour was determined based on the model output for each quality parameter that resulted in positive *E* values, *Dv* between -30 and 30%, and R^2 above 0.50 concurrently. After filtering the model output results based on these criteria, behavioural parameter sets showed *E* values above 0.40. Figure 5.7 and Figure 5.8 show the uncertainty band for the water quality constituents addressed in this study with a 95% confidence interval for Ave and Este River respectively. The 95% confidence interval was determined based on the 2.5% and 97.5% quantiles of behavioural parameter sets.

This approach resulted in the number of acceptable parameter sets shown in Table 5.3. Este River station resulted in lesser acceptable parameter sets due to an inferior time period of analysis. Nitrates and orthophosphates uncertainty analysis resulted in the lowest acceptable parameter sets observed. Table 5.3 also reports the percentage of occurrences in which observed data is within the 95% confidence interval. This shows that the threshold defined as acceptable affects the confidence interval size, also the size of the sample will affect the confidence interval; Ave River station shows a higher percentage of data within the confidence interval than Este River station, since higher available observed data results in a better calibrated model. When calibrating oxygen governing reactions, the calibrated model will depend on all parameters that will affect nutrients, biochemical oxygen demand and dissolved oxygen. For instance, a good calibration and validation for nitrates does not mean that the model describes the watershed perfectly since all other oxygen demanding processes must be analysed concurrently.

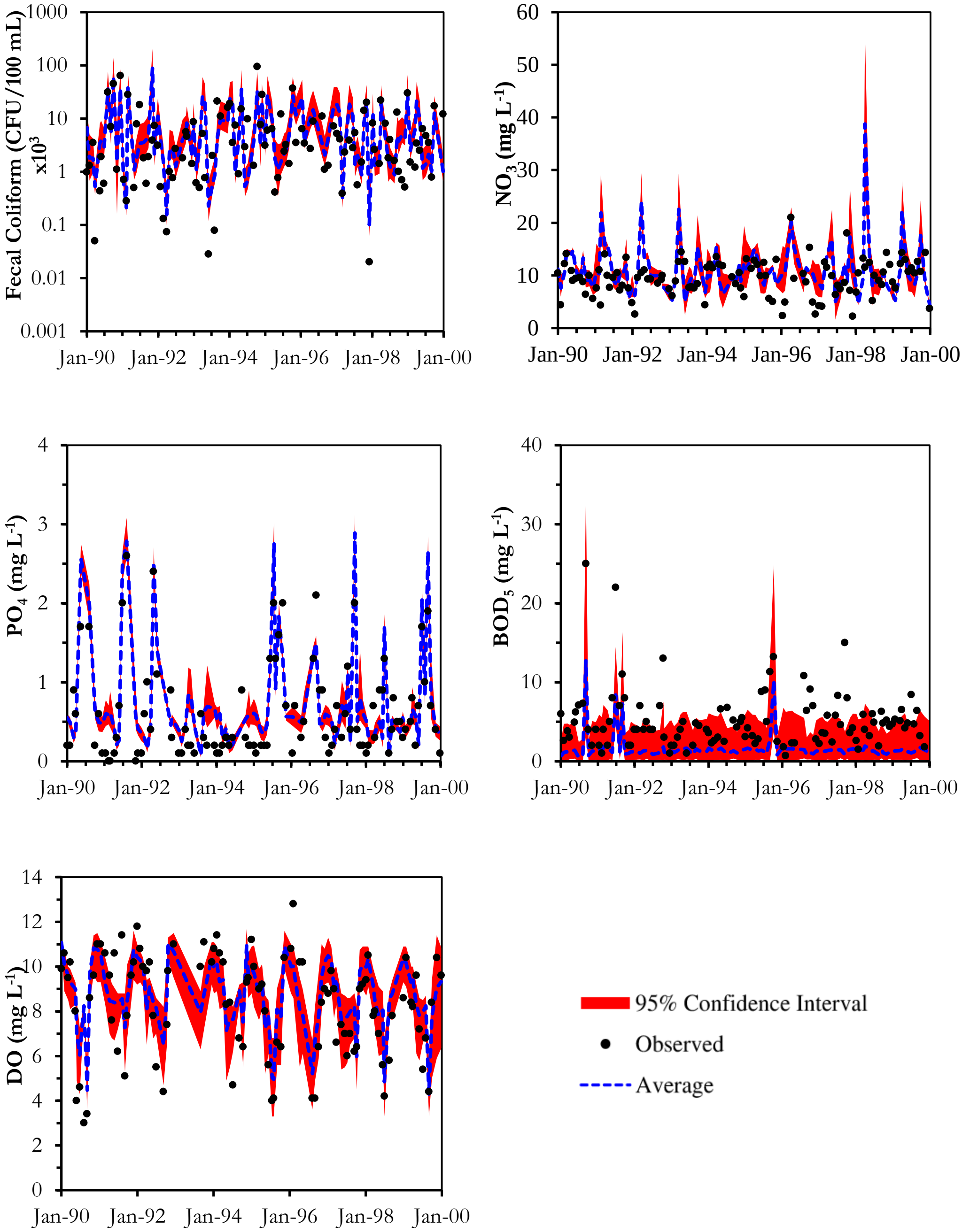

Figure 5.7 Uncertainty band for water quality constituents at Ave River station.

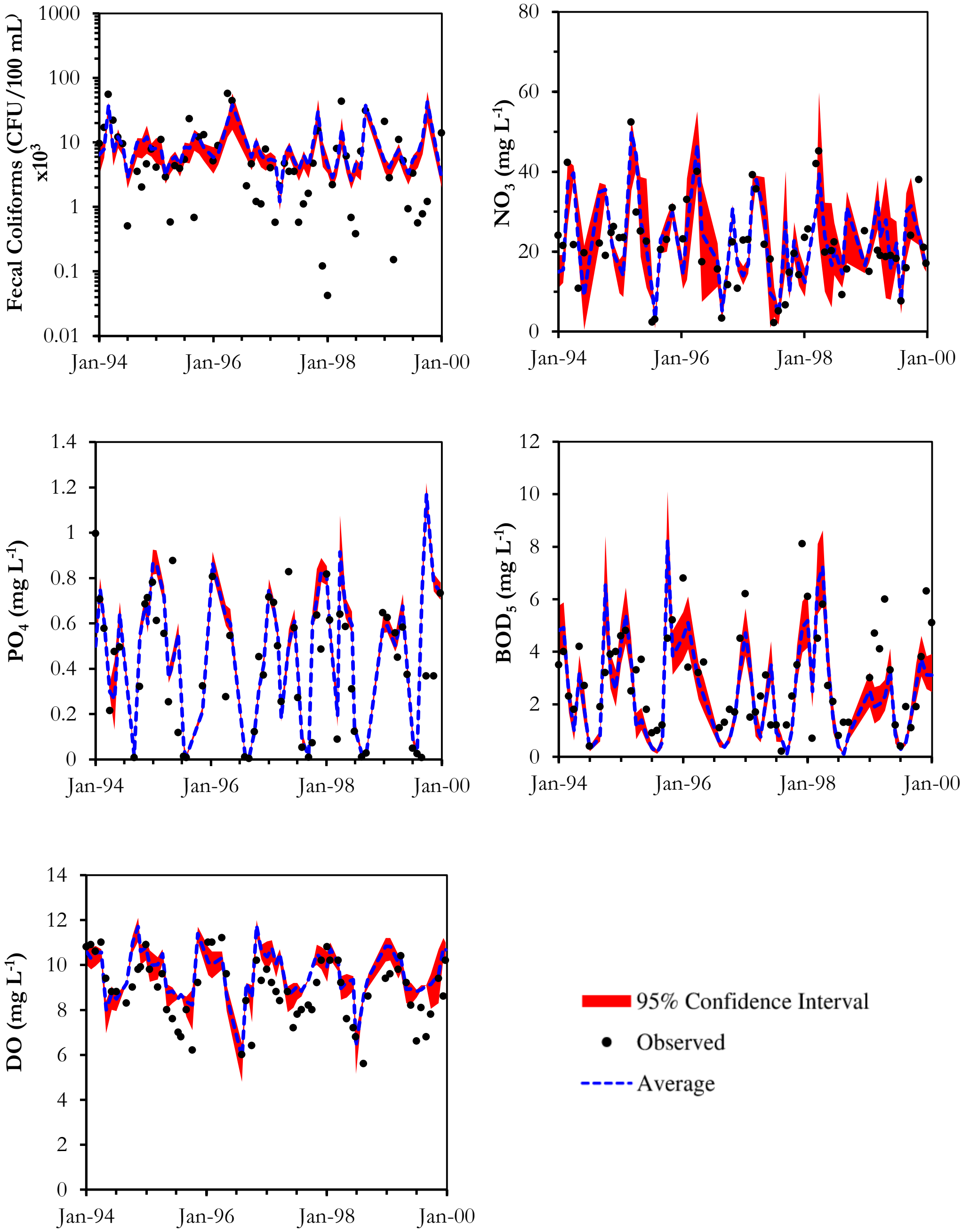

Figure 5.8 Uncertainty band for water quality constituents at Este River station.

Table 5.3 Behavioural parameter sets from the uncertainty analysis.

	FC	NO_3	PO_4	BOD_5	DO
Parameter Sets					
Ave	309	66	85	276	623
Este	112	63	104	38	62
Contingency					
Ave	29%	36%	48%	61%	58%
Este	27%	48%	27%	26%	28%

From all the behavioural parameter sets, only 32 for Ave River station and 17 for Este River station resulted in behavioural for all oxygen involving processes concurrently for the threshold defined. Changing the criterion of R^2 to 0.40 and D_v limits between -35% and 35% results in 373 and 284 behavioural parameter sets for Ave River and Este River station respectively, with the lowest observed E value of 0.12. This illustrates that the effect of criteria chosen will greatly affect the number of behaviour parameter sets and that more than one criteria should be used when weighting the quantile regression of the time series. Uncertainty analysis of HSPF revealed that the model is unable to capture low values of FC at both stations. Due to the significant effect of knowledge uncertainty in model output, future efforts in collecting more information to reduce model uncertainty is advised.

5.2.3 Sensitivity Analysis

The sensitivity analysis for FC output revealed that the model is most sensible to first order decay rate (*FSTDEC*) and the rate of surface runoff that will remove 90% of the stored FC (*WSQOP*). The results also show that maximum storage rate (*SQOLIM*) is more sensible than the monthly accumulation storage (*ACQOP*) (Figure 5.9). Extent of separation between both lines represents the degree of sensitivity of each parameter. Figure 5.9 also shows that the sensitivity is decreased with the increase of observed data and therefore a better model fit is obtained (Ave versus Este), but both sensitivity analysis confirmed the same parameters as the most sensitive in the model. To further complement these results the statistical significance test was determined for each parameter (Table 5.4). The statistical significance test (p-value) helps ranking the parameters according to their sensitivity. The higher the values, the less important (or sensitive) the parameter is.

Table 5.4 Statistical significance test of model parameters.

Parameter	Este	Ave
FSTDEC	<0.01	<0.01
KBOD20	0.22	0.08
KODSET	0.39	0.25
BENOD	0.73	0.79
REAK	0.83	0.97
KTAM20	0.51	0.33
KNO220	0.51	0.98
KNO320	0.27	0.78
WSQOP FC	<0.01	<0.01
WSQOP NO_3	0.38	0.24
WSQOP PO_4	0.45	0.79
WSQOP BOD	0.94	0.31
ACQOP FC	0.32	0.97
ACQOP NO_3	0.86	0.81
ACQOP PO_4	0.86	0.83
ACQOP BOD	0.78	0.69
SQOLIM FC	<0.01	0.08
SQOLIM NO_3	0.88	0.86
SQOLIM PO_4	0.88	0.82
SQOLIM BOD	0.66	0.61

Dissolved oxygen concentration was more sensitive to benthal oxygen demand (*BENOD*) and nitrate denitrification rate (*KNO320*); nitrates were more sensitive to the rate of removal of nitrogen storage (*WSQOP*), nitrification rates (*KNO320* and *KNO220*) and the biochemical oxygen demand rate (*KBOD20*) at both stations. Regarding orthophosphates all parameters analysed showed similar cumulative frequencies, though the surface runoff rate of phosphorus (*WSQOP*) and benthal oxygen demand (*BENOD*) were the most sensitive parameters for calibration of orthophosphates at both stations.

Biochemical oxygen demand sensitivity was governed by almost all parameters analysed but the more significant ones were the decay rate (*KBOD20*) and the settling rate (*KODSET*) at Este River station, where at Ave River station no parameter showed a significant degree of sensitivity. This means that all parameters are to be considered important when calibrating biochemical oxygen demand concentration. Figure 5.10 shows the frequency distributions of the most sensitive parameters addressed here.

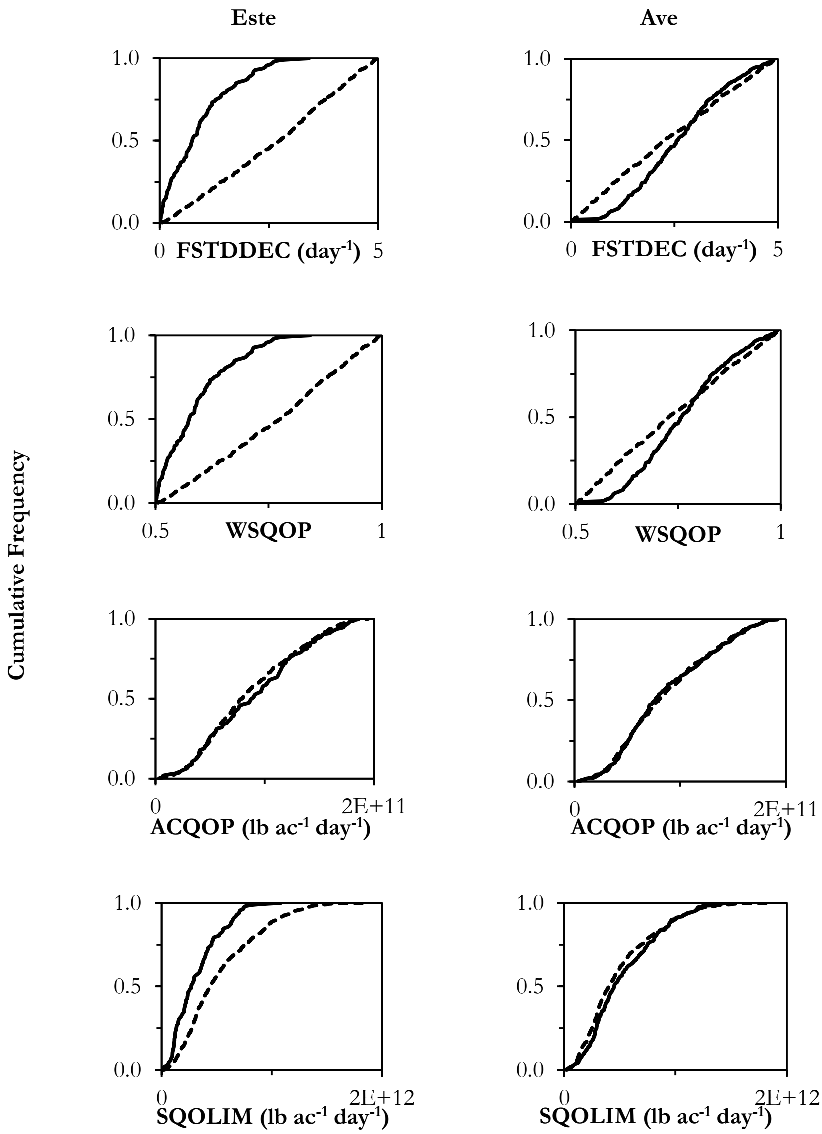

Figure 5.9 Results of MPSA for faecal coliform concentration; behavioural (black line); non-behavioural (dashed line).

Oxygen governing process involves many parameters to perform a proper calibration of the model. While MPSA does not show a top sensitive parameter some could be considered of great importance. The results show that biochemical oxygen demand decay rate (*KBOD20*), nitrification rates (*KNO320* and *KNO220*) and benthal oxygen demand (*BENOD*) are key parameters for a good model calibration. Accumulation rates (*ACQOP*) and maximum storage (*SQOLIM*) of nutrients did not result in high output variation, though the results may be masked by the rate of removal of nutrients (*WSQOP*) that simulates the washoff of nutrients from the land. Also algae simulation parameters, such as phytoplankton growth and settling rates should be considered, however no observed data was available at any of the stations, which made it impossible to perform a calibration and statistically classify it as acceptable or unacceptable.

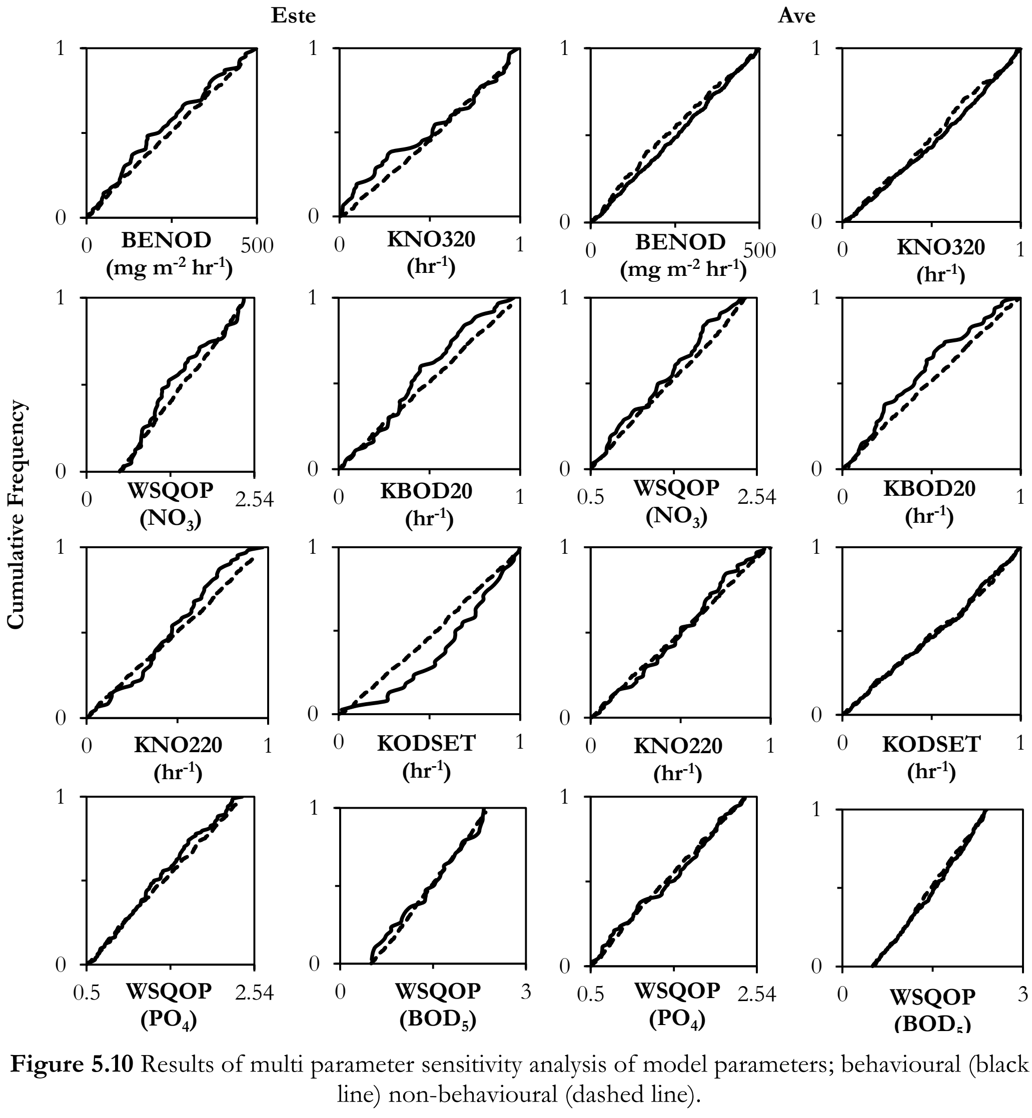

Figure 5.10 Results of multi parameter sensitivity analysis of model parameters; behavioural (black line) non-behavioural (dashed line).

5.3 Conclusions

Simulated temperature, faecal coliforms, dissolved oxygen, biochemical oxygen demand, nitrates and orthophosphates were calibrated and validated visually and statistically comparing with the observed values. The HSPF model proved to be a good tool to predict water quantity and quality in Ave River basin.

Uncertainty in water quality modelling is usually high due to data scarcity, namely the identification and quantification of nonpoint pollution sources. The complexity of the model approach (high parameterization) and likelihood established greatly modify the propagation of uncertainties, especially with the uncertainty associated with limited quality data. Ave River basin results showed that taking into account the interaction between quality constituents is crucial to assess uncertainty and parameters sensitivity, as it will greatly influence the outcome of behavioural parameter sets. Without good calibration data (or scarce) it is especially hard to carry out a validation of a model in particularly with such a small time period (four to five years). The work carried out by (Demissie et al., 2007) shows that for a twenty to thirty year period optimum calibration and validation statistical results can be achieved.

Despite this, water quality models are an important tool to assist managers in modelling a complex system. An uncertainty and sensitive analysis can lead to additional resources to establish an adequate monitoring program, providing vital information that would improve budget allocation for both target assessment (more accurate quality data) and eventually reduce uncertainty in model results. A modeller can use this information to focus future efforts in collecting more information that would help to characterize the most sensitive parameters and those subject to most uncertainty.

The results of this study can provide references for parameter calibration of water quality prediction using HSPF. The main findings are summarized below:

- High sampling is needed to get representative samples for a specific site; Este River station parameters uncertainty resulted in narrower confidence intervals than Ave River station due to data scarcity which lead to inferior acceptable parameter sets;

- Two parameters, *FSTDEC* followed by *WSQOP*, have great influence on FC concentration model output;

- Accumulation and maximum storages of nutrients are less important than kinetic governing equations for nutrient calibration;

- At the same time the high parameterization of the integrated model does not allow for clearly identifying relevant parameters, especially to oxygen governing processes where several parameters show similar behaviours on modelling outputs;

- Estimating uncertainty could also help in prioritizing implementation of control measures (pollution sources of greater uncertainty).

Of course these results are partly subjective and will depend on the specific details of particular watersheds, but the intension is to provide a general guide to reduce uncertainty when modelling water quality constituents.

5.4 References

Beck, M.B., 1987. Water quality modeling: a review of the analysis of uncertainty. Water Resources Research 23, 1393-1442.

Beven, K., Binley, A., 1992. The future of distributed models: model calibration and uncertainty prediction. Hydrological processes 6, 279-298.

Bicknell, B., Imhoff, J., Kittle, J., Jobes, T., Donigian, A., 2005. Hydrological Simulation Program - FORTRAN: HSPF Version 12.2 User's Manual, Athens, GA.

Brown, L.C., Mac Berthouex, P., 2002. Statistics for environmental engineers. CRC Press.

Christiaens, K., Feyen, J., 2001. Analysis of uncertainties associated with different methods to determine soil hydraulic properties and their propagation in the distributed hydrological MIKE SHE model. Journal of Hydrology 246, 63-81.

Demissie, Misganaw, Jaswinder Singh, H. Vernon Knapp, Patricia Saco, and Yanqing Lian. "Hydrologic Model Development for the Illinois River Basin Using BASINS 3.0." (2007).

Doherty, J., Johnston, J.M., 2003. Methodologies for Calibration and Predictive Analysis of a Watershed Model. JAWRA Journal of the American Water Resources Association 39, 251-265.

Donigian, A., 2002. Watershed model calibration and validation: The HSPF experience. Proceedings of the Water Environment Federation 2002, 44-73.

Duda P.B., Hummel P.R., Donigian Jr. A.S., J.C., I., 2012. BASINS/HSPF: Model Use, Calibration and Validation. American Society of Agricultural and Biological Engineers 55, 1523-1547.

Fonseca, A., Ames, D.P., Yang, P., Botelho, C., Boaventura, R., Vilar, V., 2014. Watershed model parameter estimation and uncertainty in data-limited environments. Environmental Modelling & Software 51, 84-93.

Freni, G., Mannina, G., 2010. Bayesian approach for uncertainty quantification in water quality modelling: The influence of prior distribution. Journal of Hydrology 392, 31-39.

Gallagher, M., Doherty, J., 2007. Parameter estimation and uncertainty analysis for a watershed model. Environmental Modelling & Software 22, 1000-1020.

Hope, A., Stein, A., McMichael, C., Webb, B., Arnell, N., Onof, C., MacIntyre, N., Gurney, R., Kirby, C., 2004. Uncertainty in monthly river discharge predictions in a semi-arid shrubland catchment, Hydrology: science and practice for the 21st century. Proceedings of the British Hydrological Society International Conference, Imperial College, London, July 2004. British Hydrological Society, pp. 284-290.

Hornberger, G., Spear, R., 1980. Eutrophication in Peel Inlet—I. The problem-defining behavior and a mathematical model for the phosphorus scenario. Water Research 14, 29-42.

Jakeman, A.J., Letcher, R.A., Norton, J.P., 2006. Ten iterative steps in development and evaluation of environmental models. Environmental Modelling & Software 21, 602-614.

Keith, L.H., 1990. Environmental sampling: a summary. Environmental Science & Technology 24, 610-617.

Kuczera, G., Parent, E., 1998. Monte Carlo assessment of parameter uncertainty in conceptual catchment models: the Metropolis algorithm. Journal of Hydrology 211, 69-85.

Novotny, V., Witte, J.W., 1997. Ascertaining aquatic ecological risks of urban stormwater discharges. Water Research 31, 2573-2585.

Reda, A.L.L., Beck, M.B., 1997. Ranking strategies for stormwater management under uncertainty: Sensitivity analysis. Water Science and Technology 36, 357-371.

Sudheer, K.P., Lakshmi, G., Chaubey, I., 2011. Application of a pseudo simulator to evaluate the sensitivity of parameters in complex watershed models. Environmental Modelling & Software 26, 135-143.

van Straten, G., 1998. Models for water quality management: the problem of structural change. Water Science and Technology 37, 103-111.

Willems, P., 2008. Quantification and relative comparison of different types of uncertainties in sewer water quality modeling. Water Research 42, 3539-3551.

6 Integrated Water Quality Modelling for River Management: A Lena River Case Study[3]

The HSPF model was used to assess the impact of wastewater discharges on the water quality of a Lis River tributary (Lena River), a 176 km² watershed in Leiria region, Portugal. The model parameters obtained in this study, could potentially serve as reference values for the calibration of other watersheds in the area or with similar climatic characteristics, which don't have enough data for calibration. Water quality constituents modeled in this study included temperature, fecal coliforms, dissolved oxygen, biochemical oxygen demand, total suspended solids, nitrates, orthophosphates and pH. The results were found to be close to average observed values for all parameters studied for both calibration and validation periods with percent bias values between -10% and 33% for calibration and -14% and 40% for validation for all parameters, with fecal coliforms showing the highest deviation. The model revealed a poor water quality in Lena River for the entire simulation period, according to Council Directive concerning the quality required of surface water intended for the abstraction of drinking water in the Member States (75/440/EEC). Fecal coliforms, orthophosphates and nitrates where found to be 99, 82 and 46% above the limit established in the Directive. HSPF was used to predict the impact of point and nonpoint pollution sources on the water quality of Lena River. Winter and summer scenarios were also addressed to evaluate water quality in high and low flow conditions. A maximum daily load was calculated to determine the reduction needed to comply with the Council Directive 755/440/EEC. The study showed that Lena River is fairly polluted calling for awareness at behavioral change of waste management in order to prevent the escalation of these effects with especially attention to fecal coliforms.

[3] Fonseca, A., Botelho, C., Boaventura, R.A.R., & Vilar, V.J.P. (2014). Integrated hydrological and water quality model for river management: A case study on Lena River. Science of The Total Environment, 485-486(0), 474-489.

6.1 Introduction

The Water Framework Directive set ambitious environmental objectives to EU Member States, who are required to achieve and maintain a good status of all their waters by 2015, as well as to prevent any further deterioration of that status (2000/60/EC, 2000). To attain this objective, the ecological and chemical status of surface water bodies needs to be assessed and the quality conditions must be reported using a classification diagram. Public awareness of environmental issues has increased and the impact of wastewater discharges in water bodies has begun receiving increased attention (Liu et al., 2014; Mannina and Viviani, 2010; Refsgaard et al., 2007; Voyslavov et al., 2013).

Water quality assessment became an extremely important issue mainly due to Man activities leading to the emission of different pollutants to the aquatic system. Swine and livestock wastewaters constitute nowadays one of the principal sources of diffuse pollution (Bouraoui and Grizzetti, 2014; Godos et al., 2010; Zhang et al., 2012). An integrated environmental modeling approach accounting for various sources of pollution and impacts (social and economic) on receiving water bodies is required due to the awareness that optimal management of the individual components of urban wastewater systems does not conduct to optimum performance of the entire system (Freni et al., 2011; Rauch et al., 2002; ReuBner et al., 2008).

The meteorological input data needed to perform quality assessment in a river stream includes: precipitation, temperature, wind speed, dew point temperature, cloud cover and solar radiation. Environmental data include all data of interest available for the basin (point and diffuse sources) and physical data are a set of GIS maps such as: digital elevation model, land use and soil properties. After organizing all inputs, a User Control Input (UCI) file is created and a series of simulations are performed until all user criteria are met.

Degradation of water quality can result from multiple land use activities, including both point sources that receive a single waste load allocation and nonpoint sources that receive diffuse pollution loads. While point source pollution can be easily identified, nonpoint source pollution from land uses is often difficult to attribute to a single location (Lee et al., 2010; León et al., 2001; McElroy et al., 1975; Wang et al., 2012).

The calculation of the pollutant load that a water body can receive and still meet water quality standards is the sum of point sources, nonpoint sources (background loadings included) and a margin of safety. The implementation of a watershed quality management plan is of vital importance in order to evaluate the effects of daily loads on the water system (Alameddine et al., 2011; Chen et al., 2012; He et al., 2007).

The watershed water quality calibration goal is to obtain an acceptable agreement between observed and simulated concentrations, while maintaining the in stream water quality parameters within physically realistic bounds, and the nonpoint loading rates within the expected ranges from the literature (Donigian Jr., 2002).

This study assesses the water quality along a catchment of Lis River (Lena River) taking into account diffuse and topic sources of pollution, which has been subject to constant ecological disasters due to discharges without adequate treatment (Vieira et al., 2013). The main objective of this work is the water quality calibration and validation in Lena tributary from Lis River, allowing the prediction of water quality under different scenarios (impact of point and nonpoint sources; seasonal and maximum daily loads assessment), getting the necessary information to promote a proper management of water resources in the basin. The assessment of water quality in the basin and sources of contamination that underlie it, are extremely important, since the basin is one of the most important natural resources of the region and has serious problems of contamination. The study consist in four task: 1) evaluate water quality at 3 cross sections along Lena River; 2) identify point and nonpoint sources of nutrients and fecal coliform in Lena basin; 3) determine maximum daily loads to achieve the desired water quality status established in 75/440/EEC (1975) concerning the quality required of surface water intended for the abstraction of drinking water; 4) investigate seasonal variations of nutrients and fecal coliforms concentrations. The Lena River hydrologic model used in this study is the result of the model previously reported in chapter 3 where flow was calibrated and validated for station 15E03.

6.2 Results and Discussion

6.2.1 Nitrogen (N) and Phosphorus (P) Loadings Calibration

For nutrient loading as diffuse source, key HSPF calibration parameters are related to rate of accumulation, storage and wash-off parameters. The approach followed in this study was to vary these parameters in a monthly time step base. The calibration was considered acceptable when the difference between simulated and observed loads of nitrogen and phosphorus was inferior to 10%. The simulated loadings used for comparison with observed values were those of the year 2004 because it is the period during which the annual rainfall was closest to the average annual rainfall of the basin. The total nitrogen and phosphorus observed loadings were 117940 and 35079 kg yr^{-1} respectively versus 120963 and 36351 kg yr^{-1} simulated loadings (Table 6.1). The distribution loading in the watershed is illustrated on Figure 6.1. The high loading values of nutrients are due primarily to the high concentration of piggeries located in each sub basin.

Table 6.2 shows the average simulated loading coefficients for the Lis River basin land use against the loading coefficients found in the literature (Loehr et al., 1989). Every coefficient falls within the interval found in the literature except for the Total-P associated with barren and forest land use. This may be due to the consideration reported previously where the loadings were considered evenly distributed in the sub basin according to the land use composition, which is reflected in an overestimation of the coefficients when populating the accumulation rates and storage tables in HSPF.

Table 6.1 Land use nutrient loadings and simulation results (kg yr^{-1}).

Land Use	Nitrogen Loadings		Phosphorus Loadings	
	Observed	Simulated	Observed	Simulated
Agricultural15E03	6213	5993	1125	1229
Urban15E03	2016	1881	365	337
Forest15E03	2435	2456	441	413
Agricultural15E07	53271	57454	16341	17335
Forest15E07	27866	27214	8548	8958
Urban15E07	12946	12278	3971	3784
Barren15E07	4092	4080	1255	1212
Forest16E01	1806	1932	601	661
Barren16E01	4198	4278	1398	1320
Agricultural16E01	2804	3069	934	997
Urban16E01	293	328	98	104

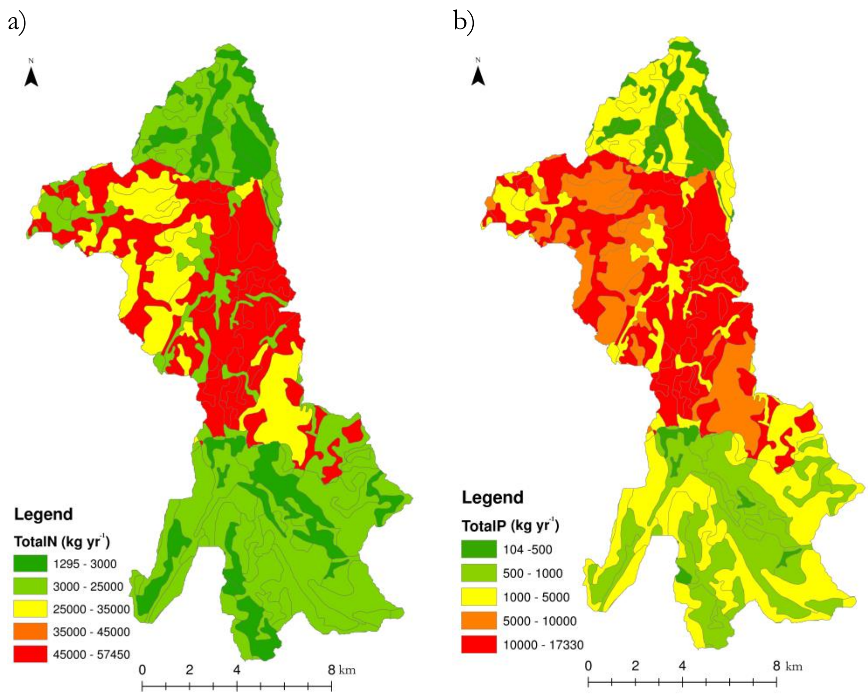

Figure 6.1 Nutrient loads distribution in Lena River; a) Nitrogen loads; b) Phosphorus loads.

Table 6.2 Land use loading coefficients.

(kg $ha^{-1}yr^{-1}$)	Simulated		Literature	
	TN	**TP**	**TN**	**TP**
Agricultural	6.39	1.50	4.0-13.0	0.80-2.90
Barren	3.97	1.00	0.5-6.0	0.05-0.25
Forest	6.18	1.59	1.0-6.3	0.01-0.88
Urban	6.06	1.65	4.7-25.0	0.30-3.70

TN – Total Nitrogen; TP- Total Phosphorus.

6.2.2 In stream Calibration

Water quality constituents' calibration (Figure 6.2 through Figure 6.4) was based on field measurements in the stream at the sampling stations mentioned in the Materials and Methods Chapter. For water temperature, the model was calibrated by adjusting coefficients of equations that relate: air to water temperature, heat transfer in surface water bodies and interflow and groundwater contributions to stream flow. Stream temperature was found to be more sensitive to solar radiation and to bed heat conduction (interflow and groundwater contributions) than to stream heat transport by conduction-convection. The modeling process for fecal coliform bacteria was achieved through the adjustment of three parameters: the first order decay rate coefficient, the amount of rainfall necessary to remove 90% of accumulated load and the mean monthly water temperature. The calibration approach was based on the monthly average values derived from daily simulation against observed values. Dissolved oxygen (DO) level in streams is a function of flow rate, air and water temperature, biochemical oxygen demand (BOD), nitrification and denitrification rates, and algae growth in the water. During stream calibration of nitrate concentration, special attention was also focused on BOD and DO as well as phytoplankton growth and decay because these constituents' concentrations are interdependent. The same procedure must be applied to total ammonia but in this case no observed values were available to perform a calibration. Observed BOD concentrations were often below detection limit of the analytical method, which made point to point comparison of model data difficult. The calibration was achieved when the predicted in stream concentrations were close to the observed values, using acceptable parameter range values (Imhoff et al., 1981). If the simulated concentrations were still too high or too low, iterations were performed by changing watershed loadings and parameter values within reasonable limits found in literature (Loehr et al., 1989).

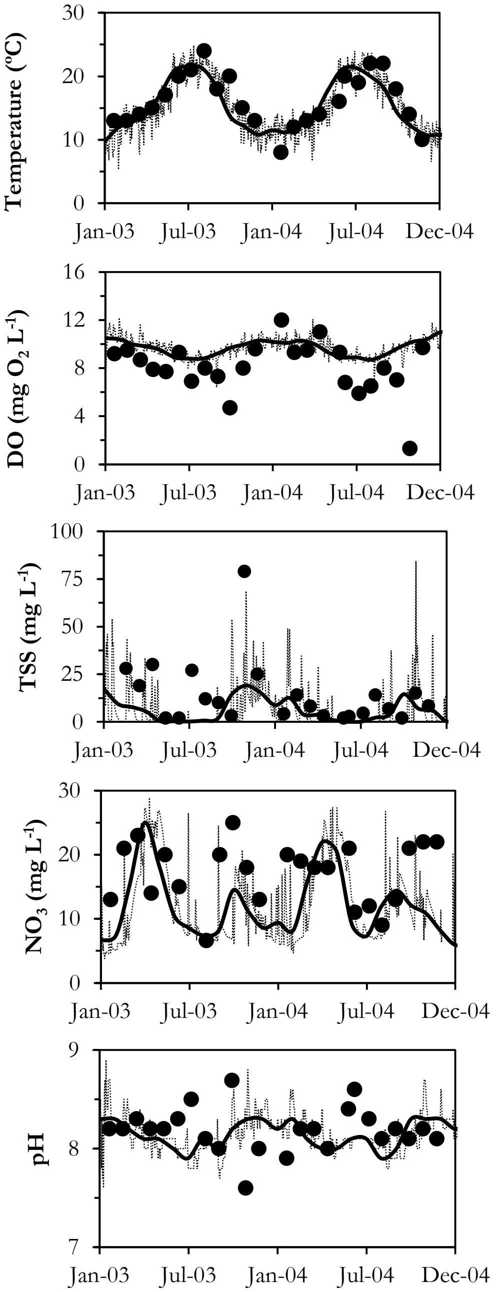

Figure 6.2 Calibration results for 15E03 station; – monthly average; -- daily simulation; • observed values.

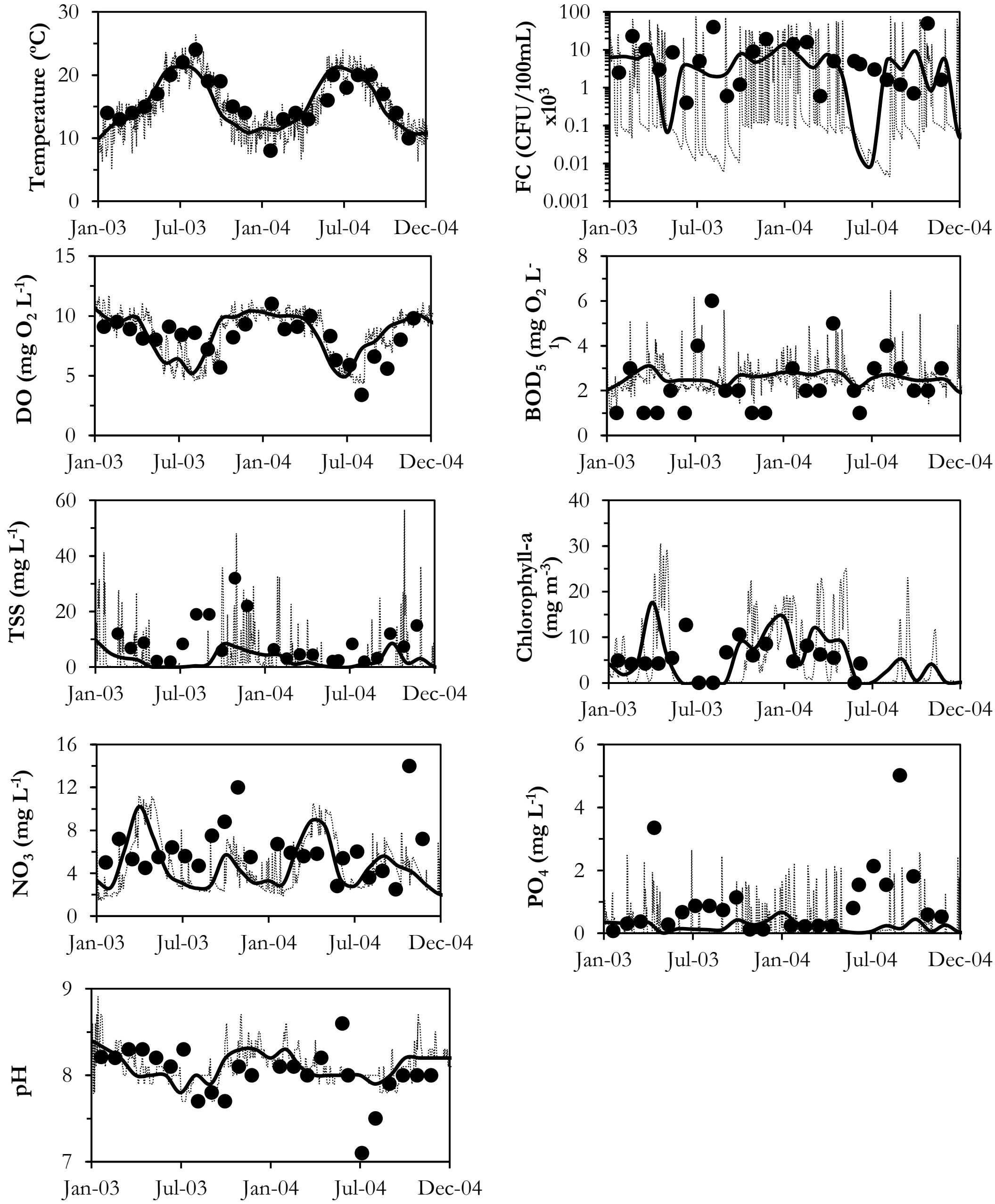

Figure 6.3 Calibration results for 15E07 station; – monthly average; -- daily simulation; • observed values.

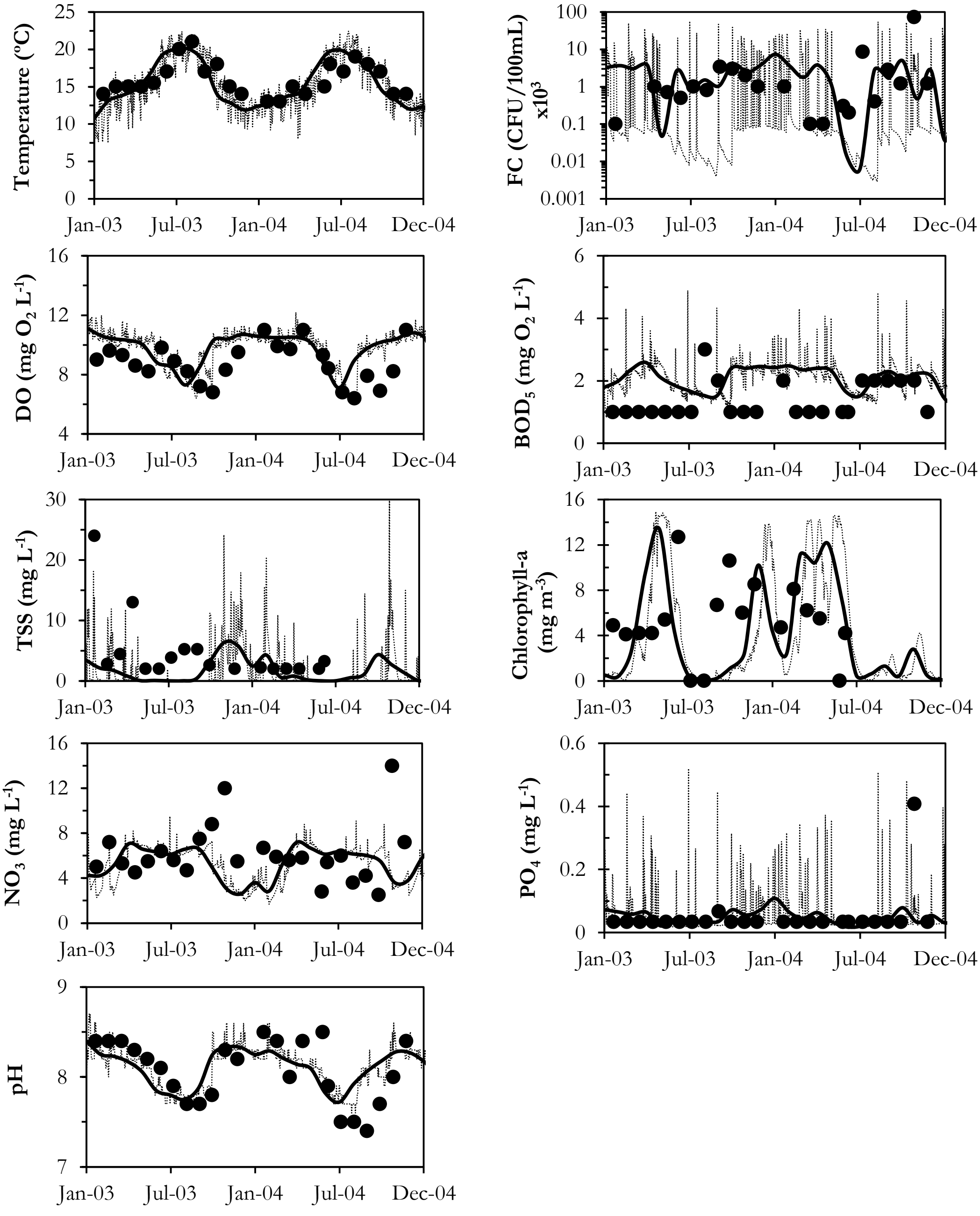

Figure 6.4 Calibration results for 16E01 station; – monthly average; -- daily simulation; • observed values.

The purpose of validation in the present study was to demonstrate the applicability of the HSPF model to different conditions in the river basin, by comparing model predictions with observed data (Figure 6.5 through Figure 6.7).

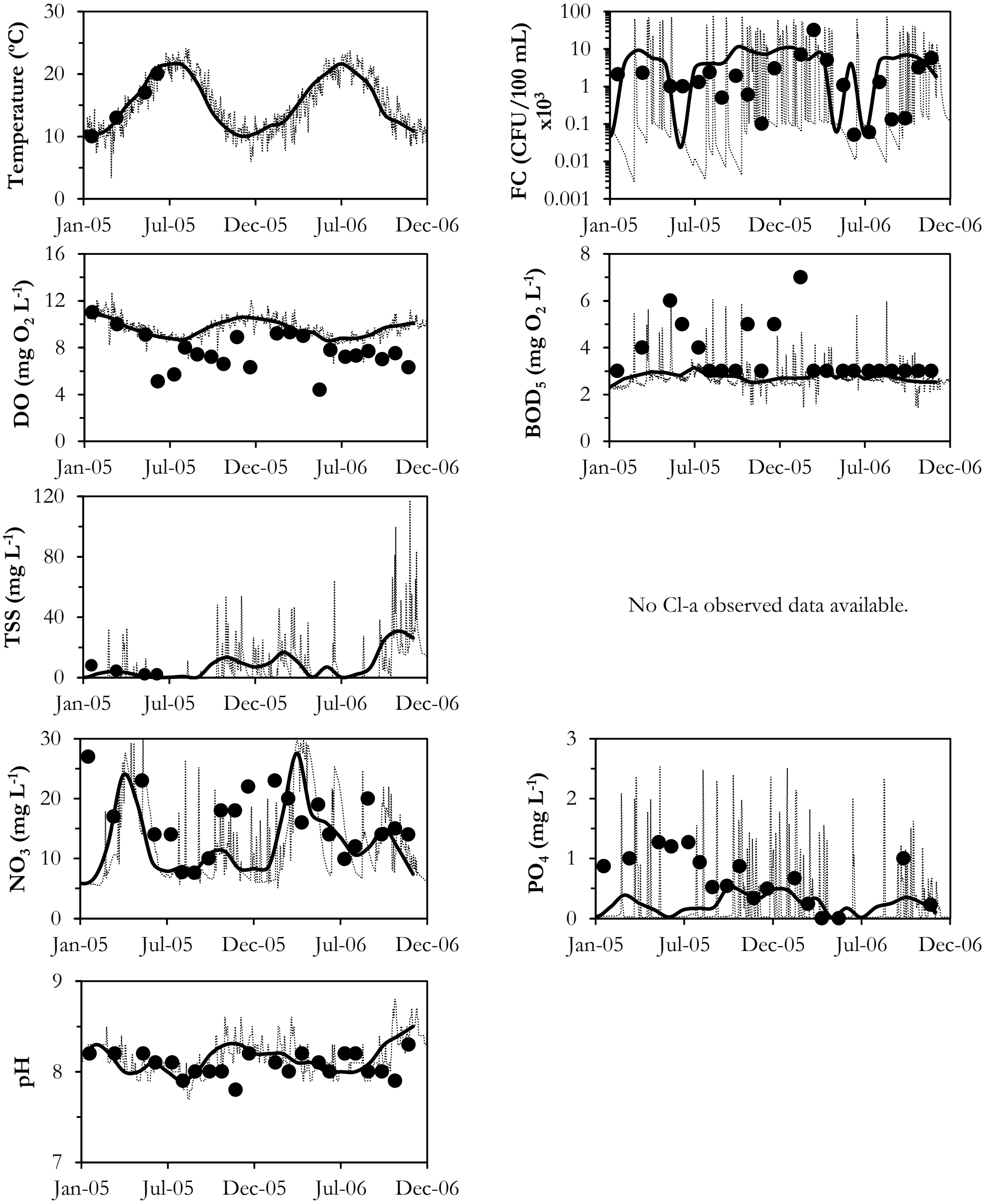

Figure 6.5 Validation results for 15E03 station; – monthly average; -- daily simulation; • observed values.

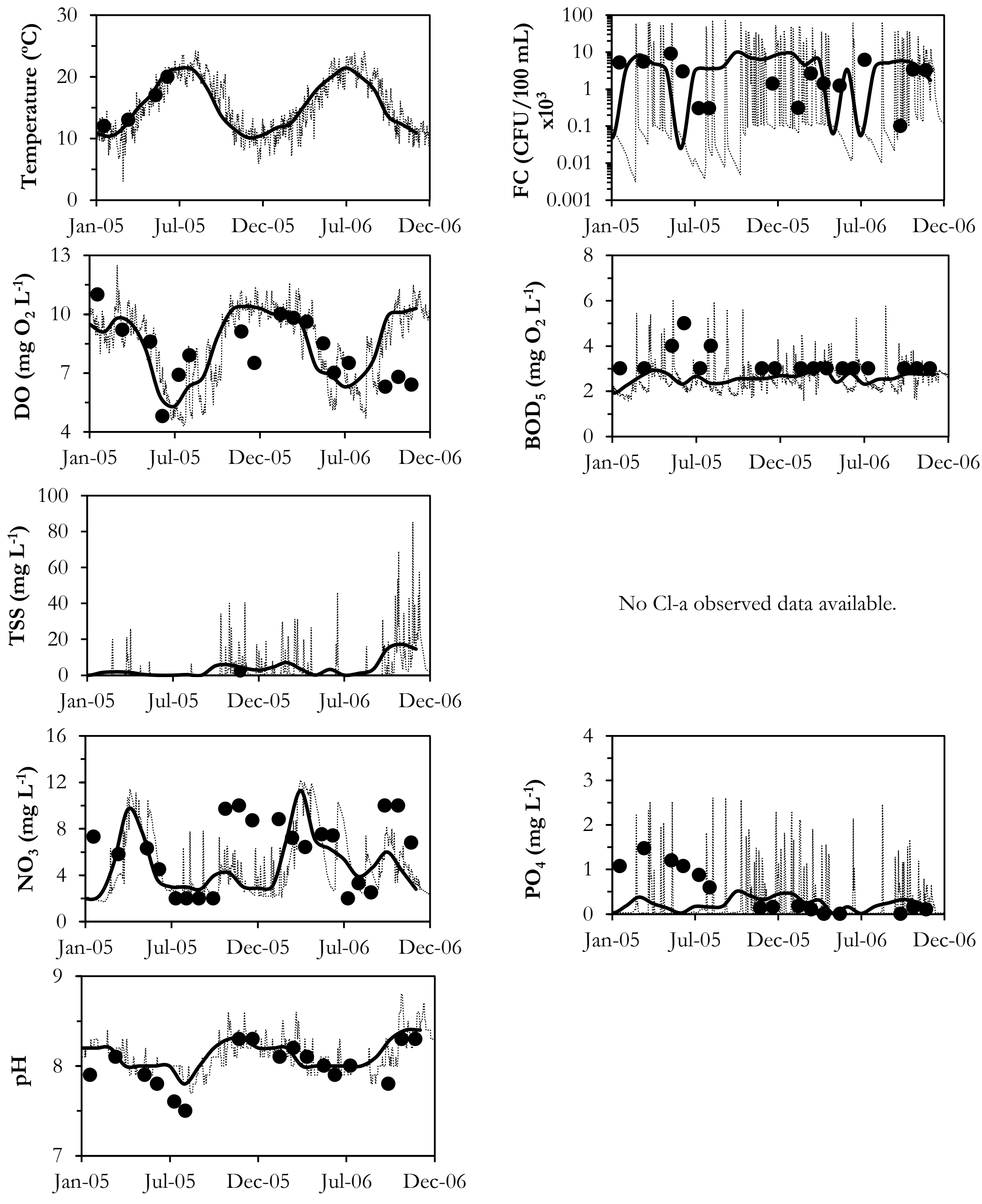

Figure 6.6 Validation results for 15E07 station; – monthly average; -- daily simulation; • observed values.

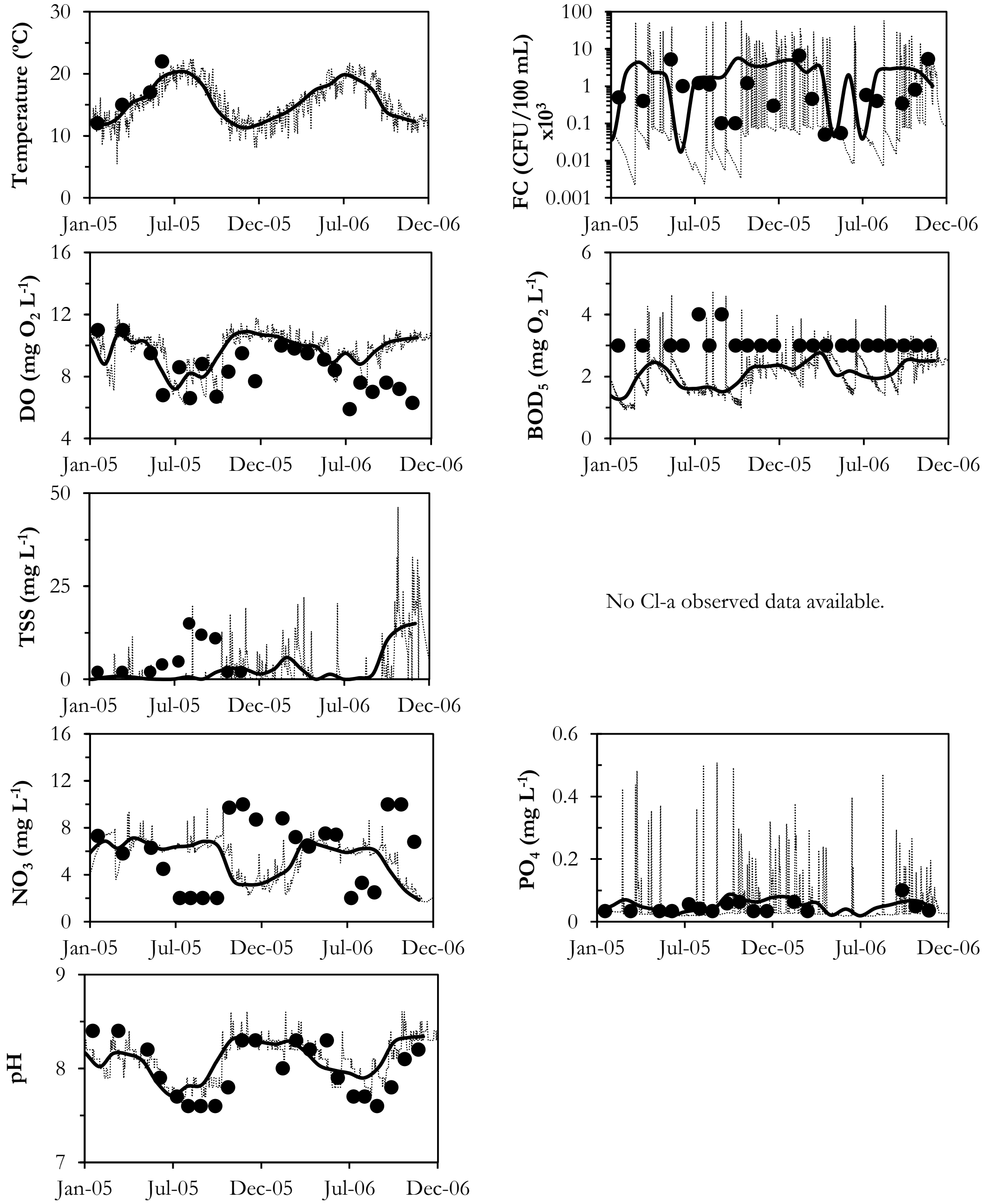

Figure 6.7 Validation results for 16E01 station; – monthly average; -- daily simulation; • observed values.

The average annual balance (Table 6.3) shows that the model is well suited for all constituents except for fecal coliforms where validation didn't reproduce good results. This could be associated to the criteria used in the Bacterial Indicator Tool regarding the distribution of the number of animals or simply due to monitoring samplings since these are random campaigns without any kind of control measures and are subjected to different hydrologic and meteorological conditions. For the year 2004 the results are good overall since it is the year in our simulation period during which the annual rainfall was closest to the average annual rainfall of the basin.

Table 6.3 Annual average balance on quality constituents.

	NO_3 (mg L^{-1})		PO_4 (mg L^{-1})		BOD_5 (mg L^{-1})		TSS (mg L^{-1})		Faecal Coliforms (CFU/100 mL)	
	Obs	**Sim**	**Obs**	**Sim**	**Obs**	**Sim**	**Obs**	**Sim**	**Obs**	**Sim**
15E03										
2003	20.5	17.7	0.4	0.6	2.5	3.3	22.1	25.7	18825	9400
2004	17.2	16.9	0.7	0.6	3.8	3.3	7.1	6.1	10208	10100
2005	16.2	16.9	0.8	0.6	4.0	3.2	4.1	0.3	1473	9430
2006	16.1	15.8	0.4	0.5	3.4	3.3	---	---	5069	8180
15E07										
2003	16.2	18.0	0.7	0.6	2.1	3.4	17.9	20.9	9410	10150
2004	19.6	20.0	1.2	0.7	2.7	3.4	5.9	5.0	10200	8508
2005	16.6	18.7	0.8	0.6	3.5	3.3	---	---	9650	3088
2006	13.3	19.5	0.1	0.5	3.0	3.3	---	---	8090	2033
16E01										
2003	6.5	6.3	0.04	0.1	1.3	2.1	11.9	12.5	1800	1125
2004	5.8	5.7	0.1	0.08	1.5	2.2	2.2	7.8	1077	1932
2005	5.5	8.1	0.04	0.1	3.2	1.9	5.7	2.2	677	1009
2006	6.5	4.6	0.1	0.1	3.0	2.3	---	---	1211	1334

Obs- Observed; Sim – Simulated

Comparing the results obtained (Table 6.3) with the water quality standards established by the Council Directive 75/440/EEC (1975) (Table 6.4), the main concern lies in faecal coliform concentration values observed for the entire simulation period. The faecal coliform mai pollution sources are the input from bacteria indicator tool, which is directly related to diffuse pollution (accumulation and storage in soils) from the existing piggeries and livestock in the basin. Inadequate wastewater treatment systems, considering the number of domestic animals, and animal feedlot runoff or bad agriculture practices, such as fertilizer application techniques, can be responsible by the increase of faecal coliforms in the stream as well. Regarding faecal coliforms concentration (100 CFU/100 mL, 2000 CFU/100 mL and 20000 CFU/100 mL), the treatment standard methods for drinking water production from surface water are, respectively, simple physical treatment and disinfection (A1), normal physical treatment, chemical treatment and disinfection (A2) and, intensive physical and chemical treatment, extended treatment and disinfection (A3). This indicates that both station 15E03 and 15E07 will require a type A2 treatment while 16E01 a type A1 treatment.

Table 6.4 Characteristics of surface water intended for the abstraction of drinking water.

Parameter	Value
pH	5.5-9.0
Temperature (ºC)	22-25
Nitrates (mg L^{-1})	25-50
Orthophosphates (mg L^{-1})	0.4
BOD_5 (mg L^{-1})	3
Faecal Coliforms (CFU/100mL)	100
TSS (mg L^{-1})	25

Table 6.5 Monthly *PBIAS,* R^2 and E values for the constituents model output.

	15E03	16E01	15E07
NO_3			
PBIAS	-0.03	-0.07	0.14
R^2	0.56	0.54	0.56
E	0.43	0.38	0.36
PO_4			
PBIAS	-0.02	-0.16	-0.26
R^2	0.51	0.42	0.97
E	0.58	0.31	0.64
BOD_5			
PBIAS	0.05	-0.06	0.16
R^2	0.98	0.01	0.74
E	0.71	0.16	0.52
Faecal Coliforms			
PBIAS	-0.03	0.23	0.20
R^2	0.53	0.40	0.62
E	0.55	0.28	0.47

For stations 15E03 and 15E07 the phosphates concentration for both simulation and observed records were above the maximum recommend value for abstraction of surface water to produce water for human consumption. Animal feedlot runoff, human sewage and excessive use of fertilizers for crops are the main factors responsible by the phosphates load into the river basin. Annual average total suspended solids were found to be below the guide value for a class *A1* treatment (25 mg L^{-1}), but it should be noted that values higher than 25 mg L^{-1} were observed several times, which indicates that more control is needed on this quality parameter, especially if water is used for irrigation. Dissolved oxygen levels show that the simulation mirrored well the field measurements, with exception for a low observed DO value at station 15E03.

The calibrated model was also evaluated by comparison of the *PBIAS,* R^2 and E criteria mentioned in Chapter 2. These results (Table 6.5) show good to very good correlation for the *PBIAS* coefficient for all stations. Regarding R^2 only station 16E01 showed a value inferior to 0.5 for orthophosphates and faecal coliforms. Seasonal simulation trends (Winter – December through February; Summer – June through August) were examined for each year for the water quality constituents addressed in this study (Table 6.6). High levels of fecal coliforms were also observed for both scenarios and all stations. BOD results show a high deterioration of water quality in summer months for 15E03 and 15E07 stations and for station 16E01 the results show to be below the quality standards of surface water intended for drinking water production. Apart from station 16E01, PO_4 exceeds the water quality standards, showing in most cases to have values two times higher than the minimum allowed values. Although nitrates do not exceed water quality standards for the entire simulation period, they still show high concentration for summer months.

In order to compare the impact of point and nonpoint sources in Lena River, two isolated scenarios were modeled: 1) only point sources were considered and 2) only nonpoint sources were used as input in the model. The results for both scenarios are shown in Figure 6.8, Figure 6.9 and Figure 6.10 for stations 15E03, 15E07 and 16E01. As stated previously, high fecal coliform concentration in Lena River is mainly attributed to nonpoint sources (diffuse sources), and septic systems discharges to the stream are almost negligible when compare with the normal case scenario. Still, considering only the contribution of septic's loads (point sources only); the fecal coliform concentration also exceeds the water quality standards allowed.

Table 6.6 Seasonal water quality analysis.

	FC (CFU/100 mL)		NO_3 (mg L^{-1})		PO_4 (mg L^{-1})		BOD_5 (mg L^{-1})		SST (mg L^{-1})		FLOW (m^3 s^{-1})	
	Winter	Summer	Winter	Summer	Winter	Summer	Winter	Summer	Winter	Summer	Winter	Summer
15E03												
2003	10015	5583	7.5	21.4	0.8	0.9	3	5.9	13.6	0.4	2.3	0.2
2004	13543	6217	5.1	20.5	0.9	0.9	3.4	5.8	12.2	0.8	2.4	0.3
2005	7890	5649	13.4	21.8	0.9	0.9	3.5	5.9	3	0.3	0.8	0.2
2006	13700	6414	5.9	14.9	1	0.7	3.4	5.6	8.9	3	1.9	0.7
15E07												
2003	9753	5886	7.3	16.6	0.8	0.7	3.2	7.2	7.9	0.2	1.9	0.1
2004	13100	6516	10.6	18.2	1	0.7	3.5	7	4.8	0.4	2	0.2
2005	8048	6060	10.6	16.8	0.9	0.7	3.8	7.2	1.5	0.1	0.6	0.1
2006	13433	6609	10.7	21	1.1	0.6	3.4	6.4	3.8	1.4	1.6	0.6
16E01												
2003	6350	2947	4	6.3	0.1	0.1	1.9	2	2.9	0.1	0.7	0.05
2004	8002	1467	3	6.2	0.1	0.1	2.5	2	4.2	0.2	0.8	0.07
2005	2511	2125	5.5	6.3	0.1	0.1	1.6	2	0.6	0.2	0.2	0.04
2006	7019	1994	3.42	6.1	0.1	0.1	2.3	2.2	2.3	0.6	0.6	0.2

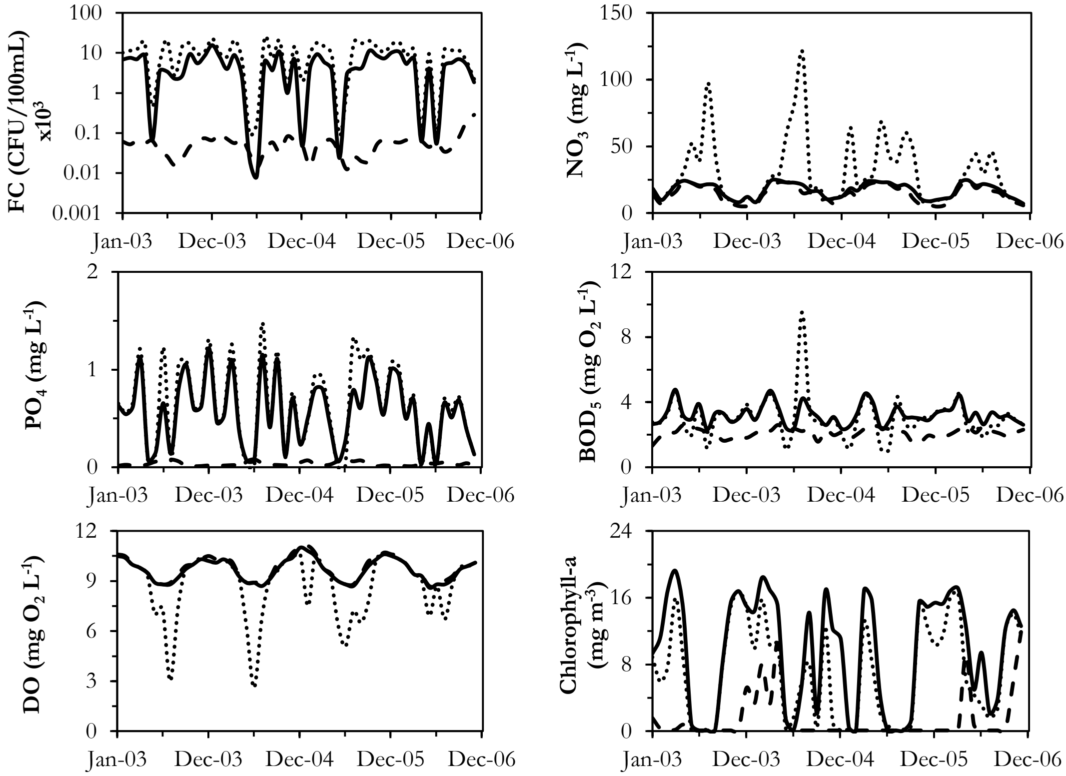

Figure 6.8 Point source and diffuse scenarios comparison at station 15E03; - Normal scenario; -- Point sources only; … Diffuse source only.

The overall water quality in Lena River is a result of diffuse source pollution for all parameters addressed in this study, except for nitrates at station 16E01. This is related to the low nitrogen loads (diffuse source) for that sub basin (Figure 3). Looking at nitrogen loads for station 16E01 presented in Tables 3 and 5 (12132 and 10132 kg yr^{-1} respectively), even though point source loads are inferior they have greater impact since they are discharged directly into the stream. For the second scenario, only diffuse sources considered, there is an increase of nutrients concentration, especially in summer months. This occurs since point sources show a low nutrient load, which originates a dilution of the diffuse load contribution.

The maximum daily load can be determined by identifying the day on which the maximum value of the constituents concentration lies below the maximum recommend values and then determining the corresponding daily load (Bicknell et al., 2005). Generally, maximum daily load calculations are more accurate the larger the simulation period, including a wider variation of flow and climate conditions, resulting in a more realistic calculation.

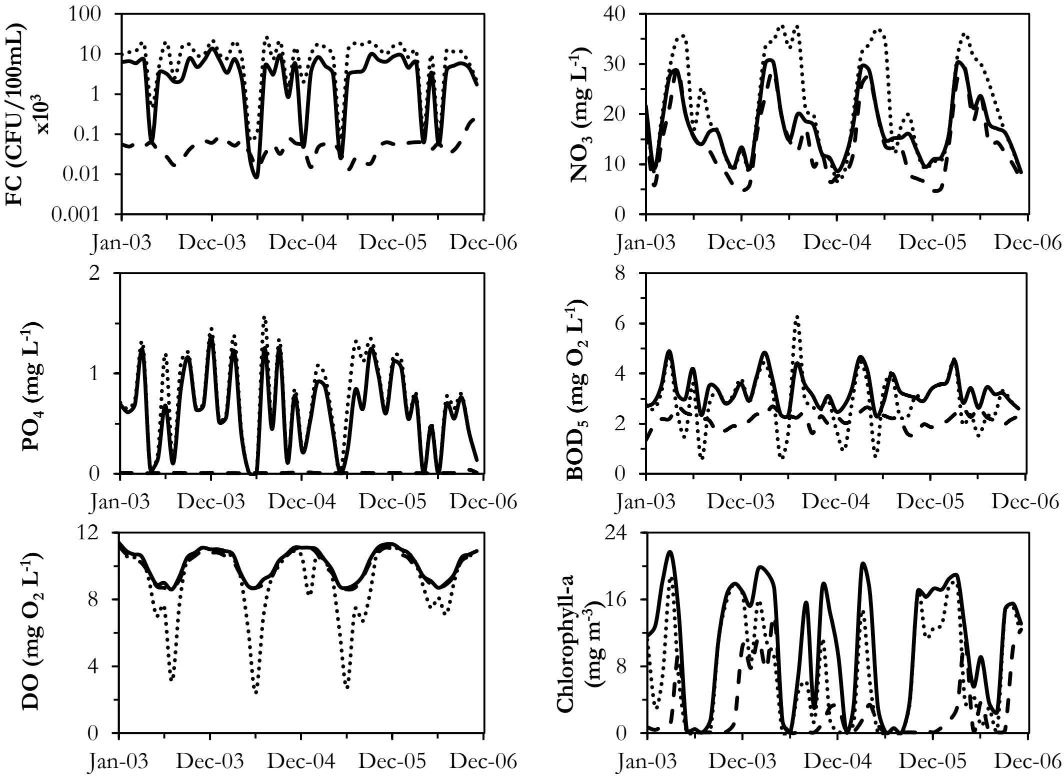

Figure 6.9 Point source and diffuse scenarios comparison at station 15E07; - Normal scenario; -- Point sources only; ··· Diffuse source only.

The results obtained here correspond to the entire simulation period (4 year). The maximum daily load value is determined when the maximum concentration of nitrates, orthophosphates and fecal coliforms is below the above mentioned surface water quality standards including margin of safety (10%) for daily simulations. An average reduction of 46%, 82% and 99% of nitrates, orthophosphates and fecal coliforms loads in Lena basin are necessary to comply with the guide value for a class *A3* treatment. Table 6.7 compares the load values obtained against those in normal conditions (existing scenario).

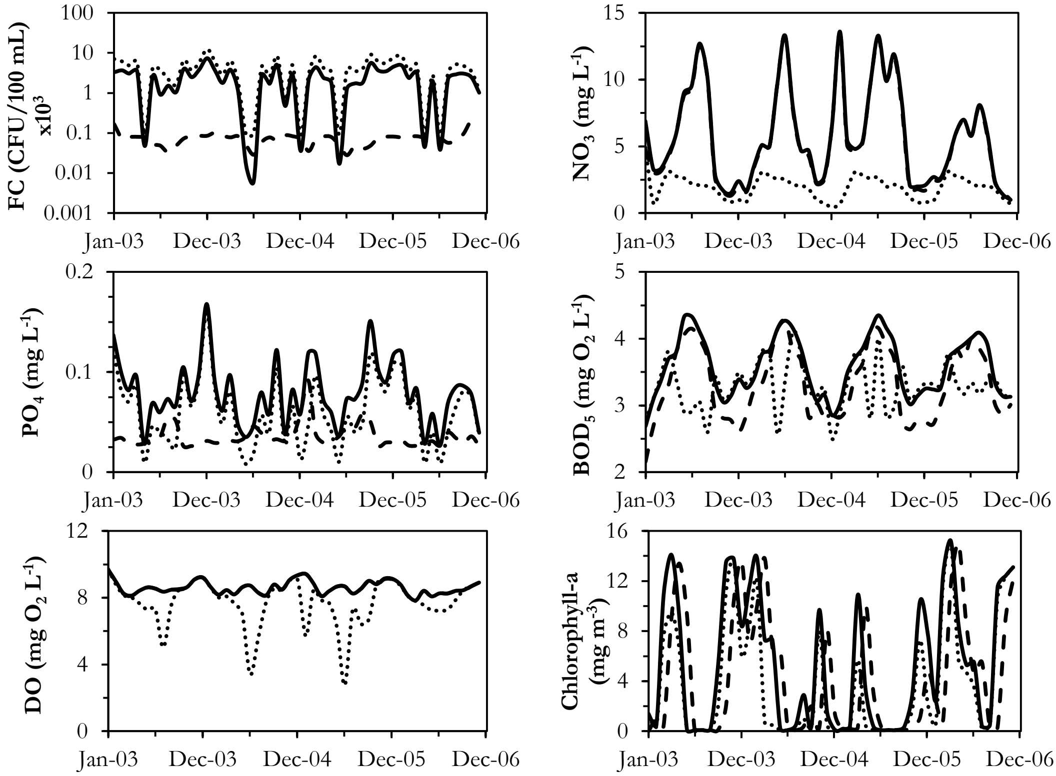

Figure 6.10 Point source and diffuse scenarios comparison at station 16E01; - Normal scenario; -- Point sources only; ··· Diffuse source only.

Table 6.7 Maximum daily load for nutrients and faecal coliforms for Lena sub basins.

	15E03	**15E07**	**16E01**
NO_3 (kg day^{-1})			
Existing Conditions	20.0	253.8	6.8
Maximum Daily Load	10.8	132.0	3.7
Reduction	46%	48%	45%
PO_4 (kg day^{-1})			
Existing Conditions	5.1	72.5	6.9
Maximum Daily Load	0.3	4.2	2.9
Reduction	94%	94%	58%
FC (CFU day^{-1})			
Existing Conditions	$4.1x10^{11}$	$1.2x10^{12}$	$5.8x10^{11}$
Maximum Daily Load	$3.3x10^{8}$	$9.4x10^{8}$	$5.8x10^{8}$
Reduction	>99%	>99%	>99%

The source loading reduction applied throughout the year will comply with the surface water quality standards.

6.2.3 Restoration Measures

The results show that there is a serious pollution problem in Lena tributary which is mainly due to the high presence of piggeries and livestock associated with a poor wastewater treatment system. These discharges are subject to regulation and licensing and their enforcement is a key factor to protect receiving waters. A stricter land use program, and an inspection and monitoring plan to the main pollution sources, must be implemented in order to achieve a proper basin management. The implementation of dry/wet retention basins or filter strips can be interesting solutions for the restoration of the basin, principally for fecal coliforms reduction. Regarding nitrates, a possible solution could lie in seasonal discharge programs improving summer water quality, although a complete revamp of the wastewater treatment systems is necessary since fecal coliforms, biochemical oxygen demand and orthophosphates are above the surface water quality standards for both scenarios.

6.3 Conclusions

HSPF model was successfully calibrated and validated using water quality data collected for a period of four years each, from Lena River watershed in Leiria region. The model demonstrated its ability to reproduce observed watershed temperatures and concentrations of various water constituents in the river. Contrary to hydrological data that are often available in the form of continuous daily records, water quality data are typically limited or scarce, therefore model validation is important especially for evaluating compliance of water quality guidelines.

The model revealed that pollution in Lena River is due mainly to diffuse sources, indicating fecal coliforms as the worst quality indicator. Both BOD_5 and PO_4 were found to be above the maximum recommend values throughout the entire simulation period. Seasonal analysis shows that nitrates are a concern in summer months. An average reduction of 46%, 82% and 99% of nitrates, orthophosphates and fecal coliforms loadings are necessary to comply with surface water quality standards. The study showed that Lena River is fairly polluted calling for awareness at behavioral change of waste management in order to prevent the escalation of these effects with especially attention to fecal coliforms. The results also indicate that HSPF could provide decision support actions for water quality restoration and protection, particularly to fecal coliform loadings where values are above the allowable limits. The implementation of a water quality sampling plan is fundamental for decision makers and proper river basin management.

6.4 References

75/440/EEC, 1975. Council Directive 75/440/EEC of 16 June 1975 concerning the quality required of surface water intended for the abstraction of drinking water in the Member States. Volume 1.

2000/60/EC, 2000. Directive 2000/60/EC of the European Parliament and of the Council of 23 October 2000 establishing a framework of Community action in the field of water policy.

Alameddine, I., Qian, S.S., Reckhow, K.H., 2011. A Bayesian changepoint–threshold model to examine the effect of TMDL implementation on the flow–nitrogen concentration relationship in the Neuse River basin. Water Research 45, 51-62.

Bicknell, B., Imhoff, J., Kittle, J., Jobes, T., Donigian, A., 2005. Hydrological Simulation Program - FORTRAN: HSPF Version 12.2 User's Manual, Athens, GA.

Bouraoui, F., Grizzetti, B., 2014. Modelling mitigation options to reduce diffuse nitrogen water pollution from agriculture. Science of The Total Environment 468–469, 1267-1277.

Chen, D., Dahlgren, R.A., Shen, Y., Lu, J., 2012. A Bayesian approach for calculating variable total maximum daily loads and uncertainty assessment. Science of The Total Environment 430, 59-67.

Donigian Jr., A.S., 2002. Watershed Model Calibration and Validation: The HSPF Experience. AquaTerra Consultants, Mountain View, California.

Freni, G., Mannina, G., Viviani, G., 2011. Assessment of the integrated urban water quality model complexity through identifiability analysis. Water Research 45, 37-50.

Godos, I.d., Vargas, V.A., Blanco, S., González, M.C.G., Soto, R., García-Encina, P.A., Becares, E., Muñoz, R., 2010. A comparative evaluation of microalgae for the degradation of piggery wastewater under photosynthetic oxygenation. Bioresource Technology 101, 5150-5158.

He, L.-M., Lu, J., Shi, W., 2007. Variability of fecal indicator bacteria in flowing and ponded waters in southern California: Implications for bacterial TMDL development and implementation. Water Research 41, 3132-3140.

Imhoff, J.C., Kittle, J.L., Dinigian Jr., A.S., Johanson, R.C., 1981. User's Manual for Hydrological Simulation Program - Fortran (HSPF). U.S. Environmental Protection Agency, Athens, Georgia.

Lee, C.-S., Chang, C.-H., Wen, C.-G., Chang, S.-P., 2010. Comprehensive nonpoint source pollution models for a free-range chicken farm in a rural watershed in Taiwan. Agriculture, Ecosystems & Environment 139, 23-32.

León, L.F., Soulis, E.D., Kouwen, N., Farquhar, G.J., 2001. Nonpoint source pollution: a distributed water quality modeling approach. Water Research 35, 997-1007.

Liu, Y., Wang, Y., Sheng, H., Dong, F., Zou, R., Zhao, L., Guo, H., Zhu, X., He, B., 2014. Quantitative evaluation of lake eutrophication responses under alternative water diversion scenarios: A water quality modeling based statistical analysis approach. Science of The Total Environment 468–469, 219-227.

Loehr, R.C., Ryding, S.O., Sonzogni, W.C., 1989. Estimating Nutrient Loading to a Waterbody. In: The control of Eutrophication of Lakes and Reservoirs. United Nations Educational Scientific and Cultural Organization, The Parthenon Publishing Group, New Jersey.

Mannina, G., Viviani, G., 2010. Water quality modelling for ephemeral rivers: Model development and parameter assessment. Journal of Hydrology 393, 186-196.

McElroy, A.D., Chiu, S.Y., Nebgen, J.W., Aleti, A., Vandegrift, A.E., 1975. Water pollution from nonpoint sources. Water Research 9, 675-681.

Rauch, W., Bertrand-Krajewski, J., krebs, P., Mark, O., Schilling, W., Schutze, M., Vanrolleghem, P., 2002. Deterministic Modelling of Integrated Urban Drainage Systems. Water Science and Technology 45, 81-94.

Refsgaard, J.C., van der Sluijs, J.P., Højberg, A.L., Vanrolleghem, P.A., 2007. Uncertainty in the environmental modelling process – A framework and guidance. Environmental Modelling & Software 22, 1543-1556.

ReuBner, F., Muschalla, D., Alex, J., Bach, M., Schutze, M., 2008. OpenMI Based Basin Wide Integrated Modelling Considering Multiple Urban Areas, 11th International Conference on Urban Drainage, Edinburgh, Scotland, UK.

Vieira, J., Fonseca, A., Vilar, V., Boaventura, R., Botelho, C., 2013. Water Quality Modelling of Lis River, Portugal. Environ Sci Pollut Res 20, 508-524.

Voyslavov, T., Tsakovski, S., Simeonov, V., 2013. Hasse diagram technique as a tool for water quality assessment. Analytica Chimica Acta 770, 29-35.

Wang, X., Wang, Q., Wu, C., Liang, T., Zheng, D., Wei, X., 2012. A method coupled with remote sensing data to evaluate non-point source pollution in the Xin'anjiang catchment of China. Science of The Total Environment 430, 132-143.

Zhang, B., Song, X., Zhang, Y., Han, D., Tang, C., Yu, Y., Ma, Y., 2012. Hydrochemical characteristics and water quality assessment of surface water and groundwater in Songnen plain, Northeast China. Water Research 46, 2737-2748.

7 Impact of Land Use on Lis and Ave River Basins Water Quality

Changes in climate and land use have a significant impact on water resources worldwide. The main challenge of this work was to assess the impact of land use on nutrient nonpoint source pollution in the Lis River basin, an 853 km^2 watershed in center Portugal and Ave River basin a 1388 km^2 watershed in northern Portugal. The Hydrological Simulation Program – FORTRAN was used to assess the impact of land use on water quality of both river basins. Hypothetical land use scenarios were created for Lis River basin. Deforestation due to urbanization reduces nitrogen and phosphorous loads by 5 and 19%, respectively. On the other hand, deforestation for agricultural land use increases the nitrogen load by 3% and reduces the phosphorous load by 12%. The conversion of agricultural areas into urban areas originated 6 and 8% reduction in nitrogen and phosphorus loads, respectively. Scenarios for Ave River basin land use consisted in projected land use development for the years 2050, 2100 and 2150 based on the existing land uses in 1990, 2000 and 2006. Additionally three scenarios were designed considering an increase of the impervious coefficient of urban areas. Best management practices (BMPs) such as dry and wet detention basins applied to agricultural land (for 3, 6, 9, 12 and 15% area) were addressed in Ave River basin with removal efficiencies of 50% for faecal coliforms; 30% for nitrogen; 30% for phosphorus and 30% for biochemical oxygen demand. The inflow of water quality constituents was reduced in all scenarios, with faecal coliforms achieving the highest reduction between 5.8 and 28.9% and nutrients and biochemical oxygen demand between 2 and 13%. The BMPs scenarios showed a significant improvement in the water quality of Este River (Ave River tributary). Biochemical oxygen demand and orthophosphates concentrations correspond to good water quality status according to the European Directive (Directive, 1991) for scenarios BMP3 (BMP applied to 3% agricultural area) and BMP12 (BMP applied to 12% agricultural area), with the correct water treatment. Faecal coliforms levels in both Ave and Este River require further treatment to fall below the established value in the above mentioned directive. This study shows that agricultural watersheds such as Lis and Ave basins demand special attention as regards nonpoint source pollution effects on water quality and nutrient loads.

7.1 Introduction

Since the implementation of the Water Framework Directive (WFD) (2000/60/EC, 2000), river basin management plans have been adopted in order to achieve the protection, improvement and sustainable use of the water, aiming at reaching a good status until 2015. Despite considerable progress, the WFD recognizes that the achievement of good status might take more time in some water bodies, and for this reason, it allows Member States to rely on an exemption on the basis of the natural conditions of the water body, and to extend the deadline up to 2027 or beyond (European-Comission, 2012).

The most significant human impact on the hydrologic system, whether at local, regional or global scale is associated to the land-use change. Use of land for agricultural, industrial or residential purposes critically alters the hydrologic characteristics of a watershed. Watershed scale modelling has arisen as an important scientific research and management tool, particularly when trying to understand and control water pollution (Liu et al., 2005; Yurekli and Kurunç, 2005). Understanding and assessing the natural processes in a watershed leading to water quality deterioration is a continuing challenge for modellers and decision makers (Kourakos et al., 2012; Shen and Zhao, 2010; Yang et al., 2013). Development of watershed protection plans must ensure water quality for production of water intended for human consumption, recreational use and flooding control by restoring riparian and wetland areas (NIRPC, 2012). Robust monitoring and methods for a comprehensive assessment of the status of water bodies, conjugated with robust watershed models are essential elements for sound water management, allowing the prediction of different scenarios before their implementation. The cost of monitoring/modelling is much lower than the cost of inappropriate decisions.

Nonpoint pollution sources (NPS), resulting from agricultural activities and urban development, have been identified as a significant cause of water-quality pollution worldwide (Borah and Bera, 2003; Chen et al., 2009; León et al., 2001). Treatment and control options for nonpoint pollution sources are more difficult to identify than for point sources. A comprehensive understanding of the problem requires several watershed factors to be considered, including climatic conditions, hydrologic parameters and site-specific physical parameters (Sadeghi and Arnold, 2002), which are broadly categorized according to its origin:

agricultural, silvicultural or urban (Bouraoui and Dillaha, 1996). The management of nonpoint pollution sources in watersheds has become a hot research topic, resulting in the development of numerous studies and models (Fonseca et al., 2014; Gao et al., 2014; León et al., 2001; McFarland and Hauck, 2001; Mostaghimi et al., 1997; Schaffner et al., 2009; Shen et al., 2008). The majority of those models simulate hydrologic, chemical and physical processes involved in the catchment and transport of nutrients and bacteria but the problem lies on identifying the sources and quantifying the loads to model NPS. Contrary to a point source where a known amount of a contaminant is discharged from an identifiable source, diffuse pollution is an aggregate of contaminant inputs (i.e. fertilizers, manure, irrigation water, etc.) distributed through a watershed (CS/AR-17, 2000).

Total Maximum Daily Loads (TMDLs) correspond to values of the maximum amount of a pollutant that a water body can receive while still meeting water quality standards, and consist in an essential tool for the development of a watershed plan in order to achieve water quality standards and restore impaired water bodies. TMDLs are developed using a wide range of techniques, from simple mass balance calculations to complex water quality modelling approaches, where different factors must be considered, such as, the water body type, flow conditions complexity, and pollutants causing the impairment.

Watershed models provide easy water quality assessment by simulating the hydrologic process affected by different climate conditions, land use change and best management practices (BMPs). While a comprehensive monitoring system may not be cost effective to implement, modelling of alternative scenarios will reduce costs associated with developing and implementation of water quality management plans.

A watershed model can be used to better understand the relationship between land use activities and water quality processes occurring within a watershed (Im et al., 2003; Novotny and Olem, 1994). Depending on the conditions and characteristics of the land use within the watershed and the dilution capacity of the receiving river, the impacts on river water quality can be significant. Parameterizing water quantity and quality models is particularly challenging because of the significant data requirements, which vary both spatially and temporally (Broekhuizen et al., 2012; Cotter et al., 2003; Thorndahl and Willems, 2008).

The main goal of this study was to evaluate the impact of land use changes on nutrient nonpoint source pollution for the Lis and Ave River basins. The strategy adopted in this work included the following activities: i) calibration and validation of the hydrological behaviour of the entire Lis and Ave River basins; ii) calibration and validation of the water quality for the existing monitoring stations, taking into account different type of information, such as, water quality data (faecal coliforms, dissolved oxygen, nitrates, orthophosphates, biochemical oxygen demand and chlorophyll-a), point sources, non-point sources and land use; iii) Maximum Daily Loads calculation, considering the quality required of surface water intended for the abstraction of drinking water, as established by the European Council Directive 75/440/EEC; iv) prediction of the effect of land use changes on nutrient loads.

7.2 Results and Discussion-Lis River

7.2.1 Nonpoint Source Loads

Nitrogen and phosphorus nonpoint loadings inputs to HSPF were simulated by changing monthly values of accumulation rate, maximum limiting storage, concentration in interflow, outflow and groundwater, for each constituent at the start of each month. The simulation of nonpoint loads were considered satisfactory when the difference between observed and simulated loads were inferior to 10%. The highest nutrient loads for both total nitrogen and total phosphorous were observed in stations 15E08 and 15E07, located in the area of the highest concentration of piggeries. The lowest contribution was observed at station 15E06. Every coefficient falls within the interval found in the literature except for forest land use coefficients and total phosphorus for barren land. This may be due to the consideration reported previously where the loadings were considered evenly distributed in the sub basin according to the land use composition. This reflected in an overestimation of the coefficients when populating the accumulation rates and storage tables in HSPF. Figure 7.1 shows the distribution loads of total nitrogen and total phosphorus in the basin. The highest loads in the basin were found to be associated with agricultural areas and the location of the piggeries.

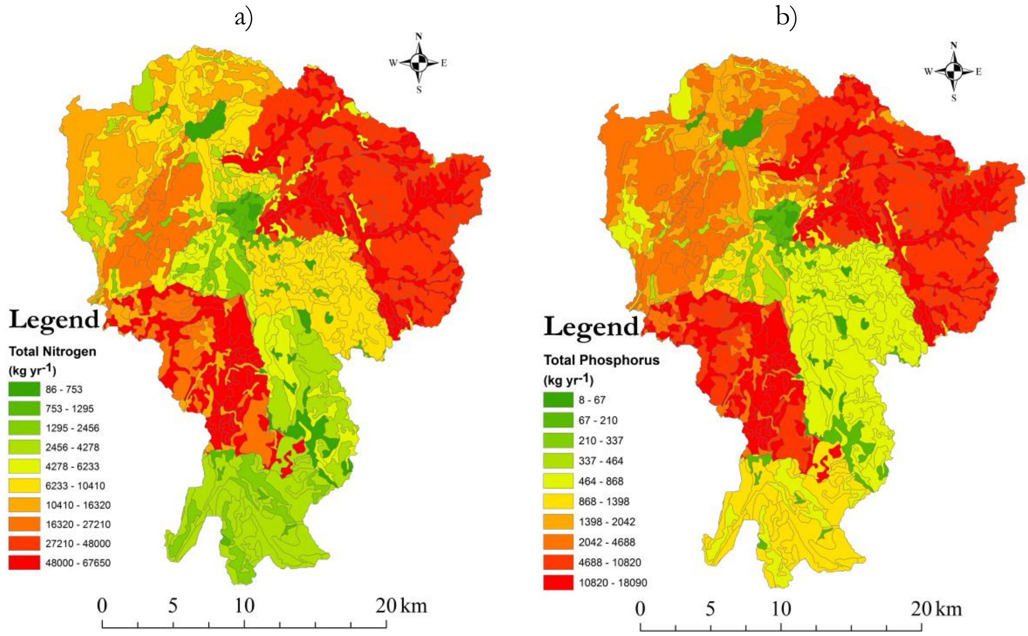

Figure 7.1 Nutrients distribution in Lis Basin: a) Nitrogen loads; b) Phosphorus loads.

7.2.2 In stream Water Quality Calibration and Validation

Water quality data was available at 8 stations for a period of 4 years from 2003 to 2006 at monthly time step interval. Hence, it was decided that the data from 2003 to 2004 would be used for water quality calibration and the remaining 2 years for water quality validation. Simulated in stream concentrations of nitrates for stations 15E06, 15E08 and 16E01 reproduced low output values when compared to the observed data. To perform the calibration, new nonpoint parameter loads adjustments were performed for these sub basins. The average nutrient load coefficients obtained for each land use are within or close to the range reported in the literature (Table 7.1), obtained in other studies using HSPF as a tool to predict nonpoint pollution sources.

Table 7.1 Average land use nutrient load coefficient (Loehr et al., 1989).

($kg\ ha^{-1}yr^{-1}$)	Simulated		Literature*	
	TN	**TP**	**TN**	**TP**
Agricultural	10.6	2.1	4.0-13.0	0.80-2.90
Barren	2.0	0.5	0.5-6.0	0.05-0.25
Forest	9.9	2.4	1.0-8.3	0.01-1.88
Urban	8.0	1.9	4.7-25.0	0.30-3.70

* (Loehr et al., 1989)

To achieve the calibration targets for water constituents, in stream parameter adjustments were performed based on statistical criteria results (*PBIAS*, R^2 and *E*). The calibration and validation model output plots for DO, NO_3, PO_4, BOD_5 and chlorophyll-a are shown in Figure 7.2 through Figure 7.10.

All parameters show good visual fitting of both daily and monthly values against the observed ones. The model was not validated for chlorophyll-a since there was no observed data available at any monitoring station. Biochemical oxygen demand (BOD_5) was particularly hard to calibrate since observed data shows only values of 1 mg L^{-1} or 3 mg L^{-1} for many data samples. The calibration was achieved by simulating BOD_5 between those values.

The lowest concentration of PO_4 was observed during winter and coincided with chlorophyll-*a* maximum. Both PO_4 and NO_3 concentrations vary interannually, but with no specific seasonal pattern for most of the stations. Their behaviour is not clear and might reflect a potential storage or transfer of dissolved phosphorus or nitrogen between different phases that were not studied (i.e., dissolved organic, adsorbed, particulate phosphorus or nitrogen).

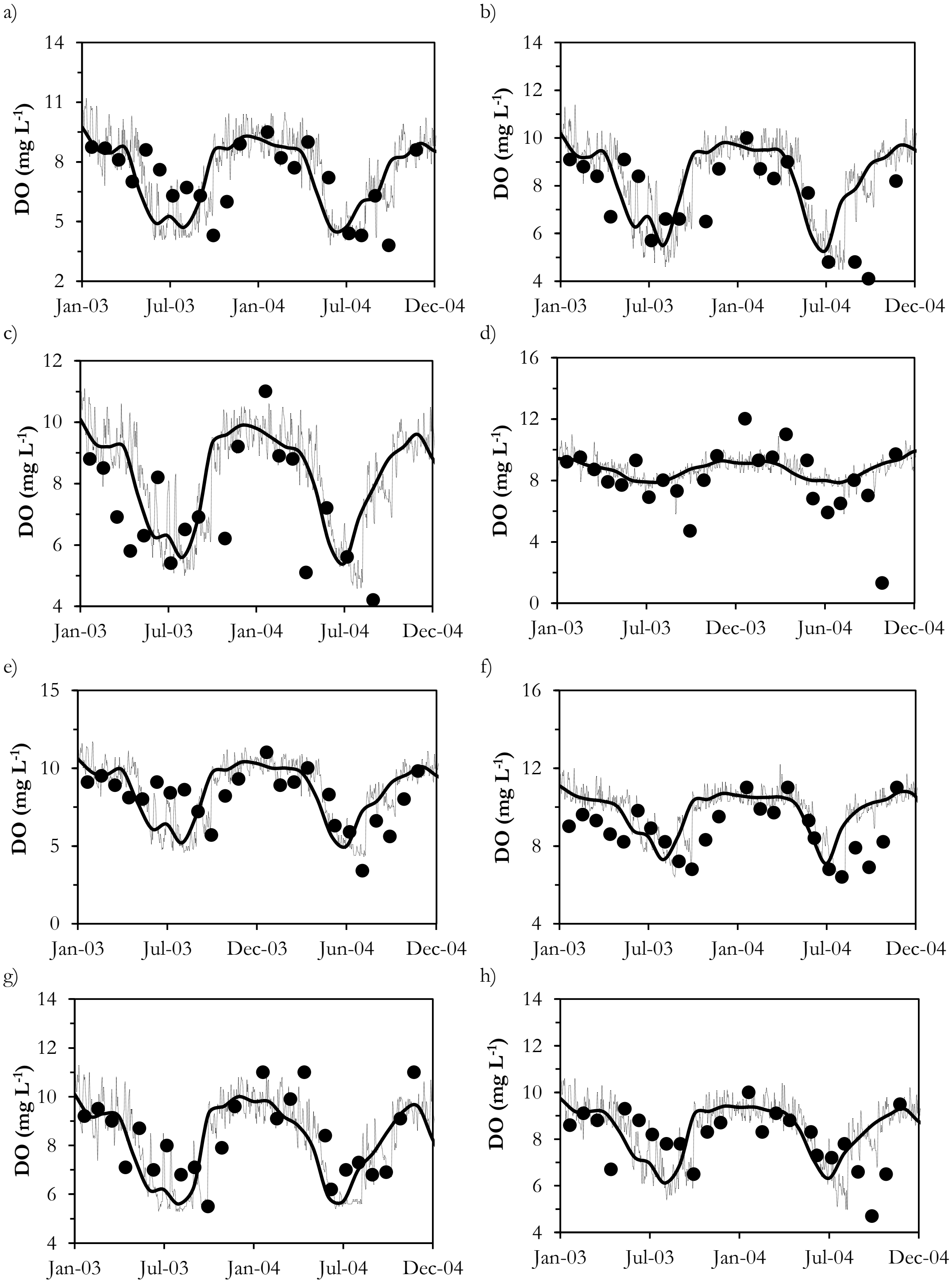

Figure 7.2 Calibration results of dissolved oxygen in Lis basin: a) 14D03 station; b) 15D01 station; c) 15E08 station; d) 15E03 station; e) 15E07 station; f) 16E01 station; g) 15E05 station; h) 15E06 station; – monthly average; -- daily simulation; • observed values.

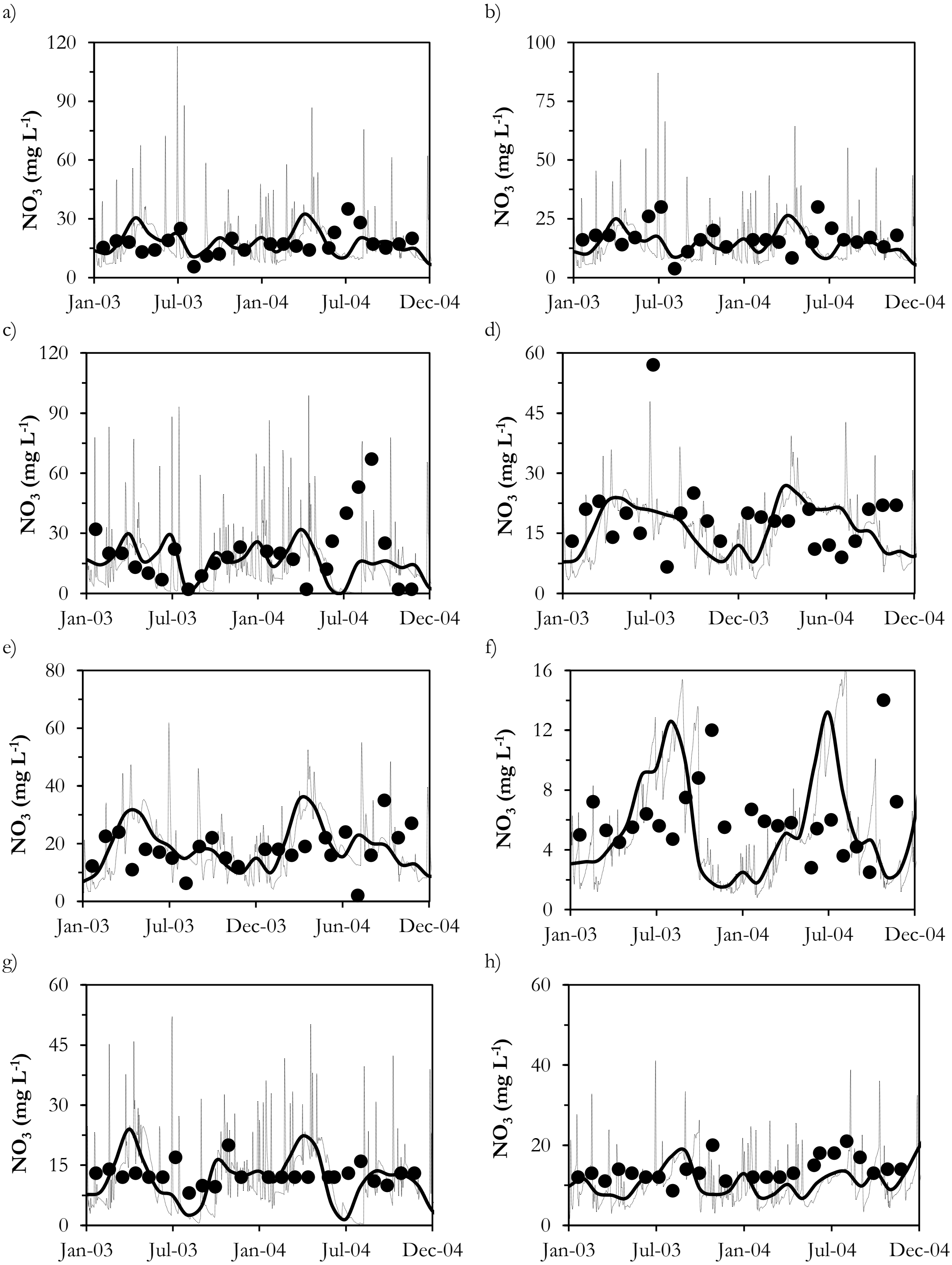

Figure 7.3 Calibration results of nitrates in Lis basin: a) 14D03 station; b) 15D01 station; c) 15E08 station; d) 15E03 station; e) 15E07 station; f) 16E01 station; g) 15E05 station; h) 15E06 station; – monthly average; -- daily simulation; • observed values.

a)

b)

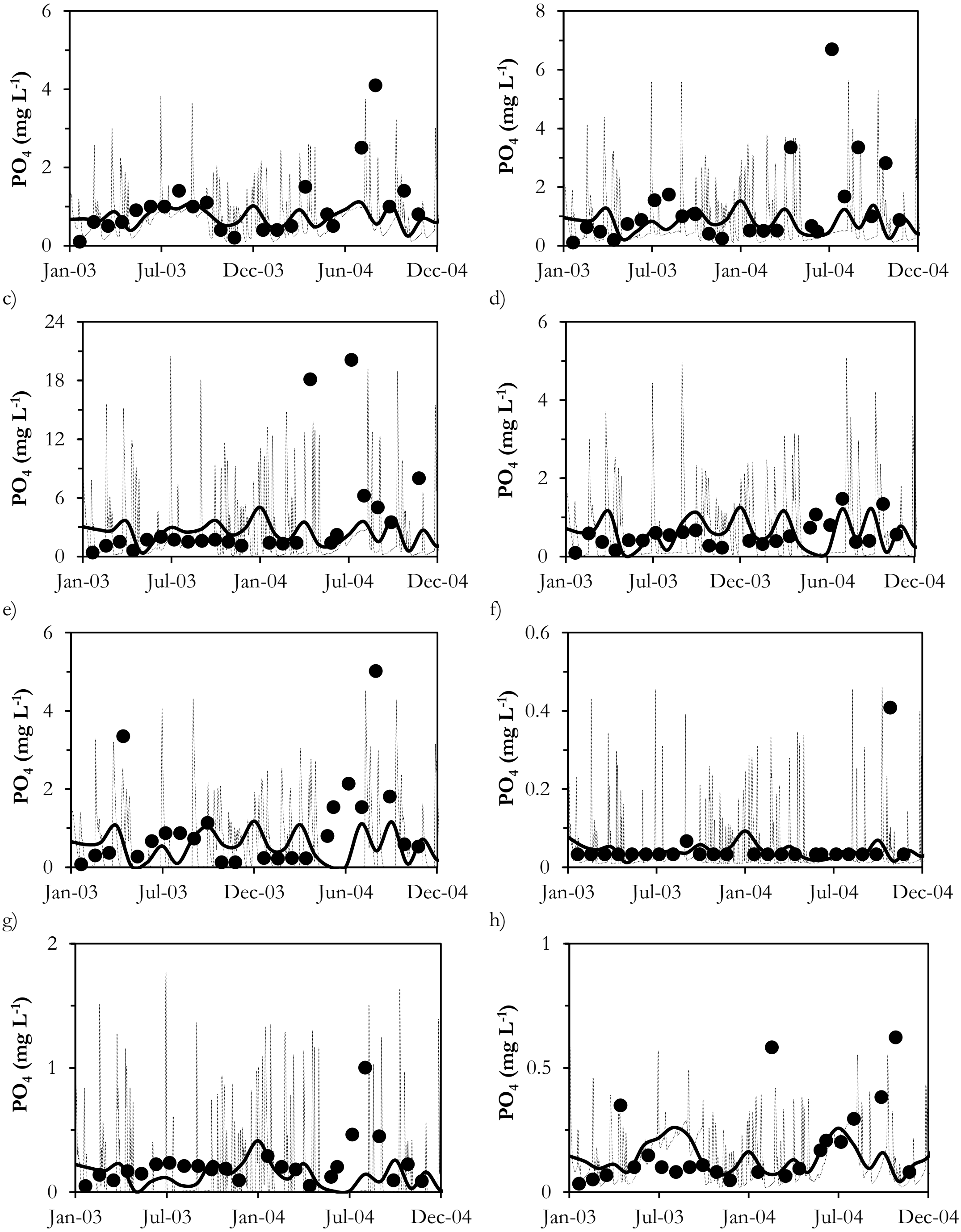

Figure 7.4 Calibration results of orthophosphate in Lis basin: a) 14D03 station; b) 15D01 station; c) 15E08 station; d) 15E03 station; e) 15E07 station; f) 16E01 station; g) 15E05 station; h) 15E06 station; – monthly average; -- daily simulation; • observed values.

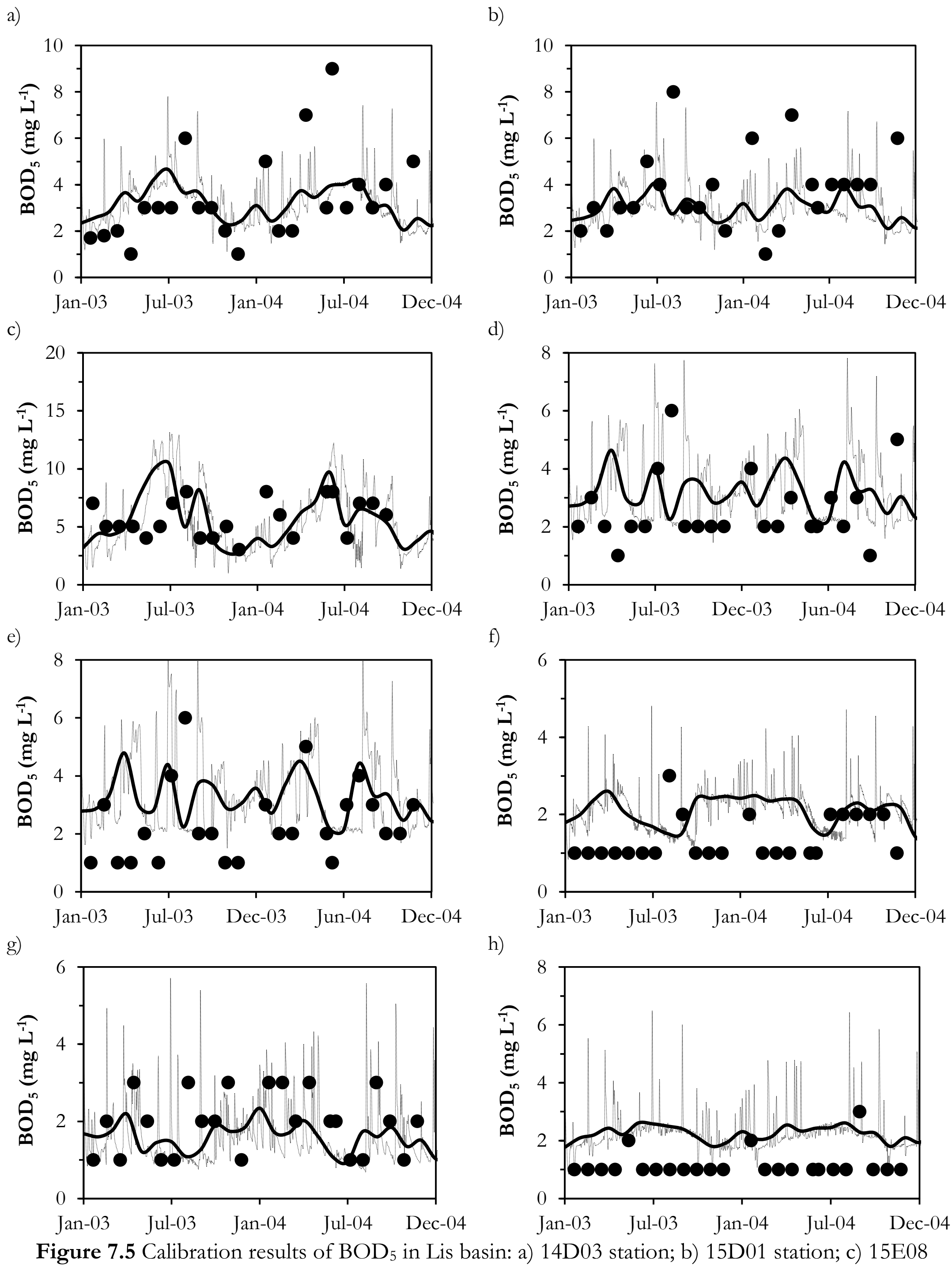

Figure 7.5 Calibration results of BOD_5 in Lis basin: a) 14D03 station; b) 15D01 station; c) 15E08 station; d) 15E03 station; e) 15E07 station; f) 16E01 station; g) 15E05 station; h) 15E06 station; – monthly average; -- daily simulation; • observed values.

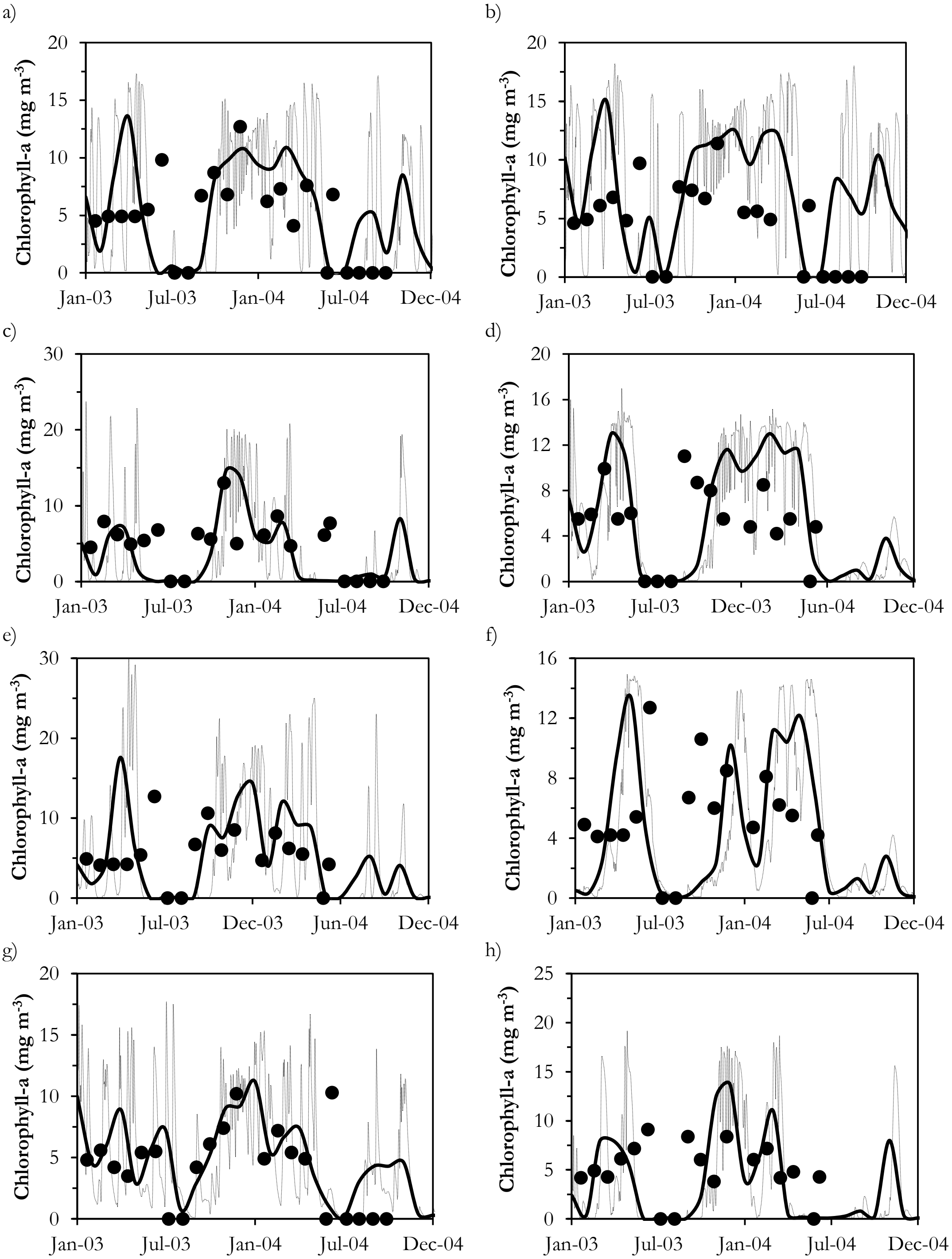

Figure 7.6 Calibration results of chlorophyll-a in Lis basin: a) 14D03 station; b) 15D01 station; c) 15E08 station; d) 15E03 station; e) 15E07 station; f) 16E01 station; g) 15E05 station; h) 15E06 station; – monthly average; -- daily simulation; • observed values.

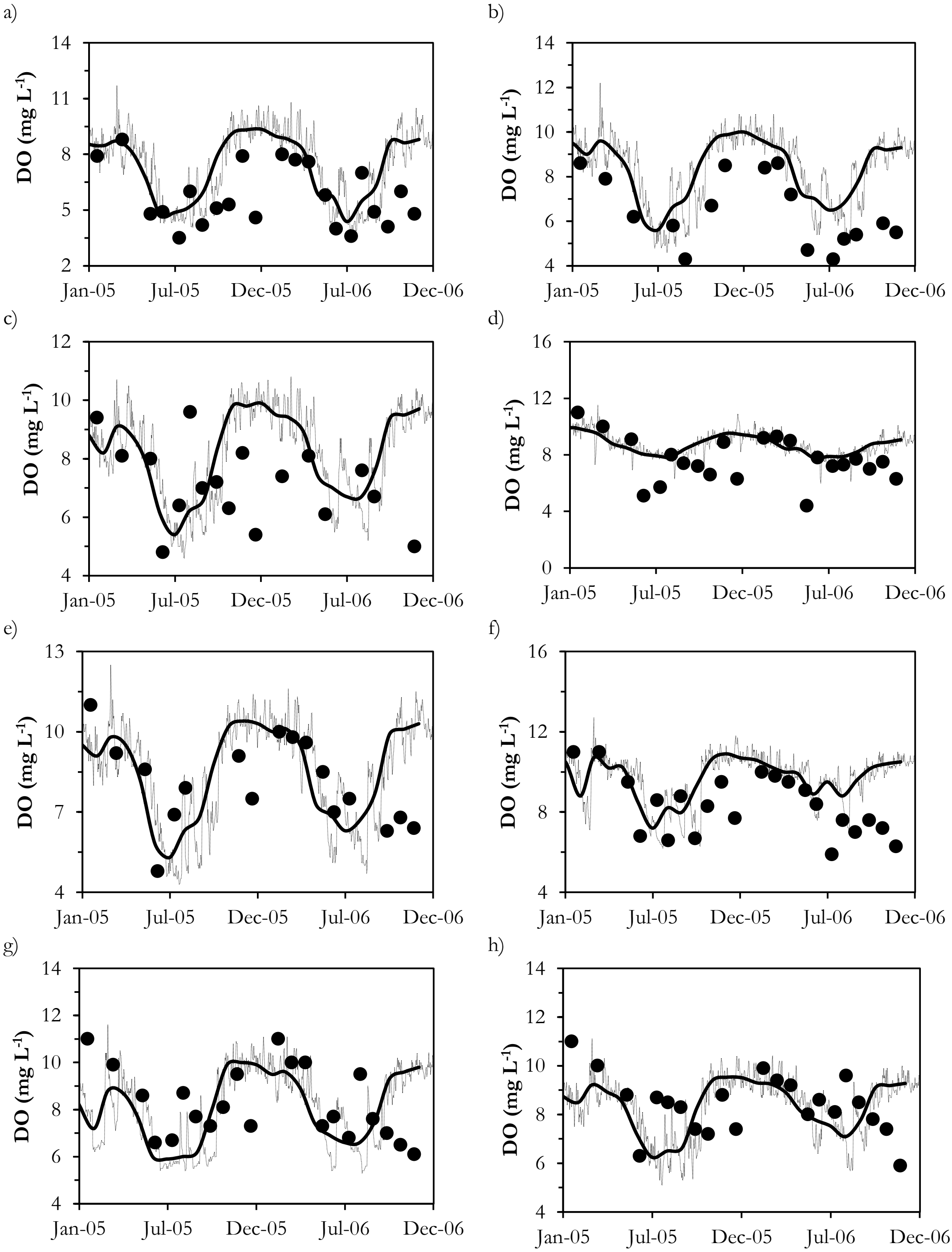

Figure 7.7 Validation results of dissolved oxygen in Lis basin: a) 14D03 station; b) 15D01 station; c) 15E08 station; d) 15E03 station; e) 15E07 station; f) 16E01 station; g) 15E05 station; h) 15E06 station; – monthly average; -- daily simulation; • observed values.

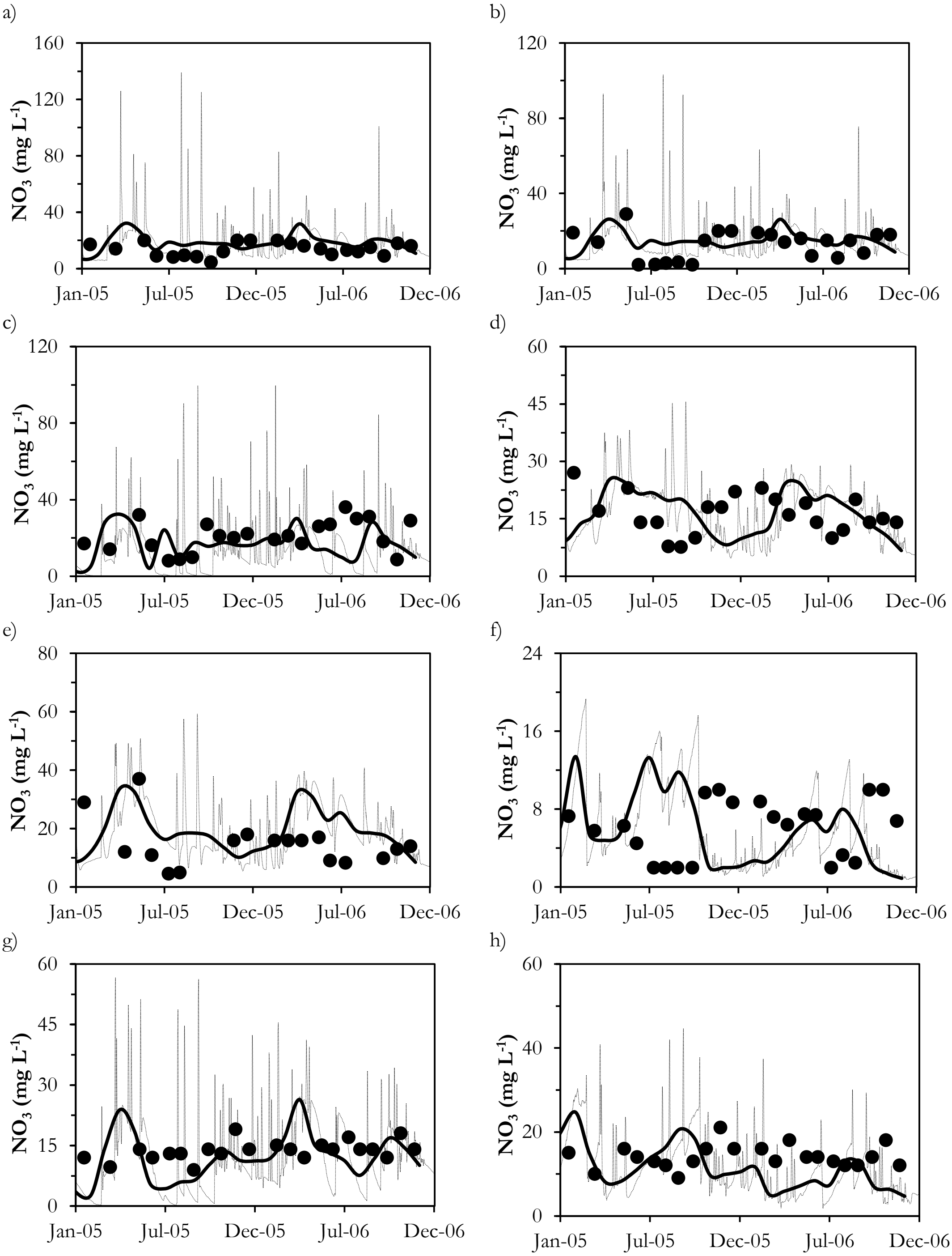

Figure 7.8 Validation results of nitrates in Lis basin: a) 14D03 station; b) 15D01 station; c) 15E08 station; d) 15E03 station; e) 15E07 station; f) 16E01 station; g) 15E05 station; h) 15E06 station; – monthly average; -- daily simulation; • observed values.

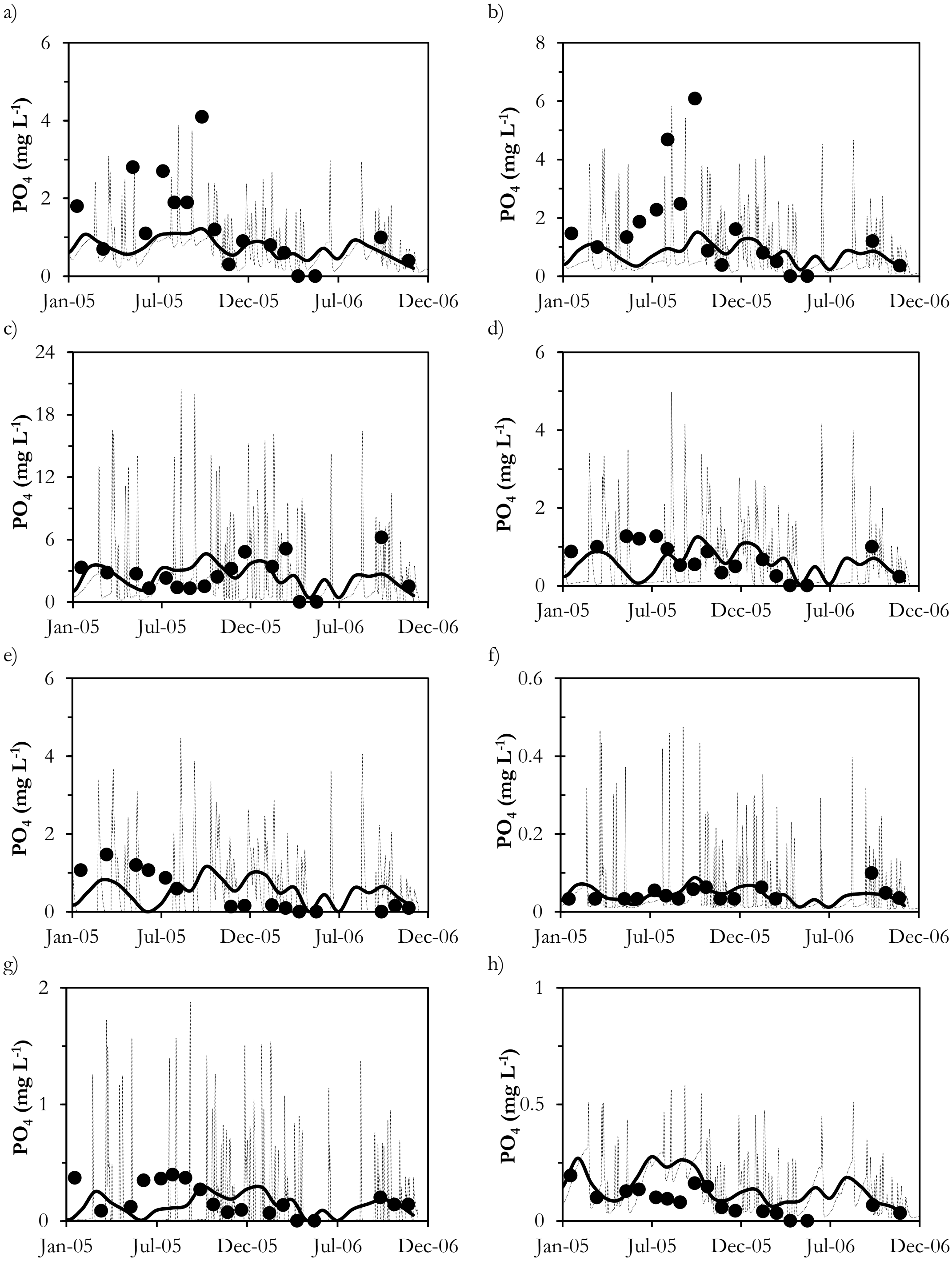

Figure 7.9 Validation results of orthophosphate in Lis basin: a) 14D03 station; b) 15D01 station; c) 15E08 station; d) 15E03 station; e) 15E07 station; f) 16E01 station; g) 15E05 station; h) 15E06 station; – monthly average; -- daily simulation; • observed values.

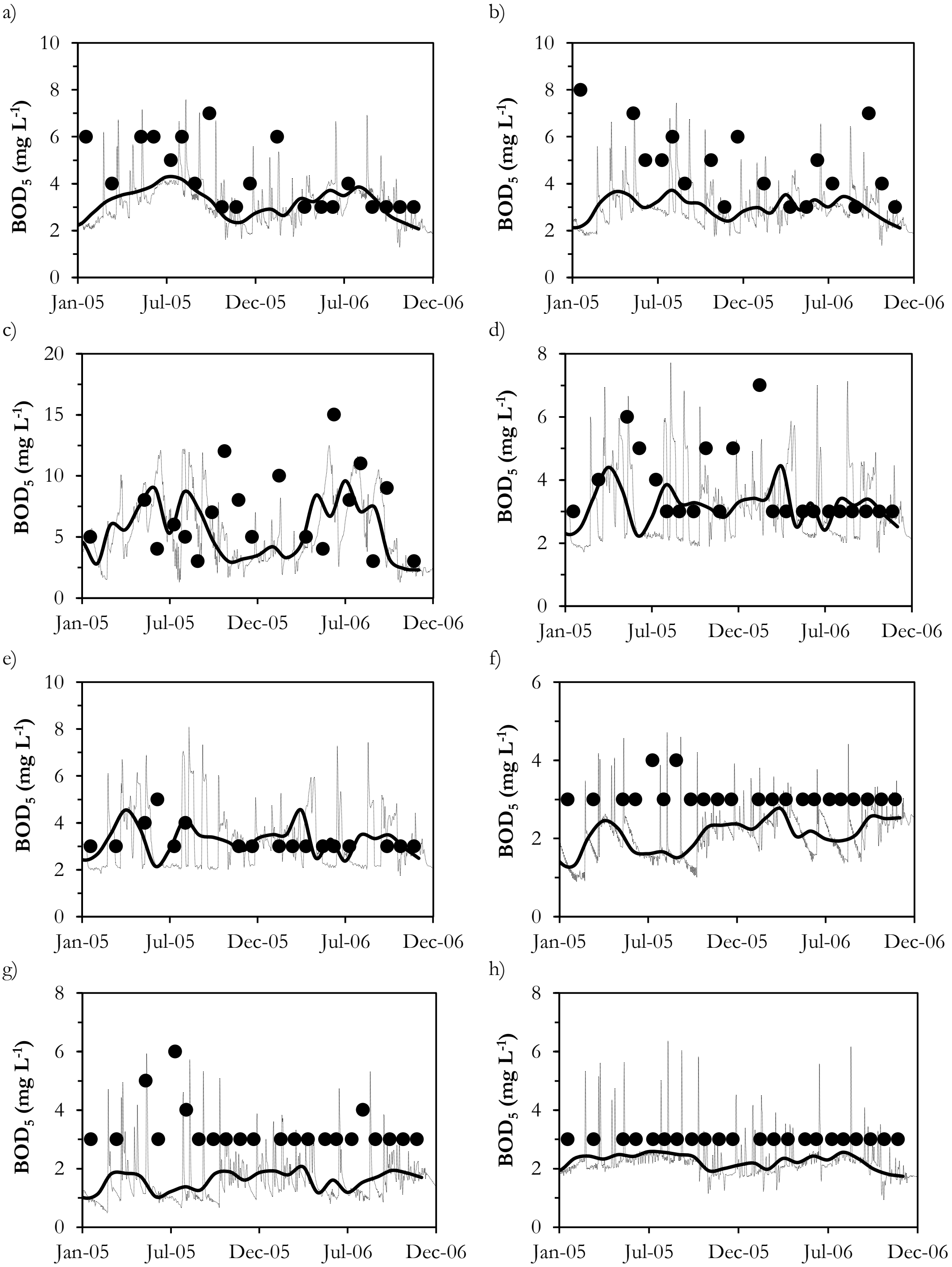

Figure 7.10 Validation results of BOD_5 in Lis basin: a) 14D03 station; b) 15D01 station; c) 15E08 station; d) 15E03 station; e) 15E07 station; f) 16E01 station; g) 15E05 station; h) 15E06 station; – monthly average; -- daily simulation; • observed values.

7.2.3 Statistical criteria evaluation

Simulated and observed daily and monthly concentrations of nitrates, orthophosphates and biochemical oxygen demand for calibration and validation were visually compared and evaluated by statistical criteria (Table 7.2).

Table 7.2 Monthly *PBIAS*, R^2 and E values for the constituents model output.

	15E06	15E03	14D03	15D01	15E08	15E05	16E01	15E07
Calibration								
NO_3								
PBIAS	-0.21	-0.03	0.37	0.14	-0.08	-0.09	-0.07	0.14
R^2	0.10	0.56	0.54	0.61	0.72	0.42	0.54	0.56
E	0.22	0.43	0.32	0.53	0.61	0.33	0.38	0.36
PO_4								
PBIAS	-0.19	-0.02	-0.23	-0.14	-0.12	-0.33	-0.16	-0.26
R^2	0.13	0.51	0.65	0.57	0.61	0.05	0.42	0.97
E	0.24	0.58	0.60	0.38	0.51	0.18	0.31	0.64
BOD_5								
PBIAS	0.28	0.05	-0.28	-0.26	-0.08	-0.40	-0.06	0.16
R^2	0.51	0.98	0.50	0.02	0.86	0.10	0.01	0.74
E	0.33	0.71	0.28	0.17	0.69	0.20	0.16	0.52
Validation								
NO_3								
PBIAS	-0.16	0.03	0.09	0.08	-0.11	-0.12	-0.01	0.21
R^2	0.44	0.58	0.69	0.54	0.68	0.54	0.57	0.56
E	0.36	0.44	0.31	0.40	0.51	0.42	0.54	0.38
PO_4								
PBIAS	0.16	0.12	-0.16	-0.23	0.06	-0.27	0.02	-0.08
R^2	0.33	0.53	0.55	0.38	0.56	0.35	0.66	0.67
E	0.26	0.46	0.61	0.26	0.48	0.24	0.48	0.51
BOD_5								
PBIAS	-0.24	-0.09	0.13	-0.31	-0.12	-0.35	-0.28	0.06
R^2	0.72	0.58	0.51	0.48	0.56	0.61	0.51	0.65
E	0.40	0.57	0.31	0.24	0.53	0.32	0.29	0.51

The statistical criteria were used as a guide in estimating satisfactory model performance. The *PBIAS* was estimated within acceptable range, where nitrates concentration is in agreement with the very good status criteria at all stations except at station 14D03, where a satisfactory result was obtained (*PBIAS* > 0.30). Regarding orthophosphates, stations 15E05 and 15E07 achieved satisfactory results whereas the remaining stations showed good and very good status. The R^2 results demonstrate an acceptable simulation with all values above 0.5 at stations 15E03, 15E08 and 15E07 for all parameters. Stations 15E06 and 15E05 originated unsatisfactory results according to the coefficient of correlation. To perform a more accurate calibration and validation of the model regarding BOD_5 more data is needed. The entire period simulation for NO_3, PO_4 and BOD_5 in Lis River shows percent bias of 3%, -10% and -8% respectively.

7.2.4 Maximum Daily Loads Calculation

The maximum daily loads were determined based on the entire simulation period of 4 years. The values shown in Table 7.3 represent the daily loads for each sub basin where the simulated daily concentration for each constituent was always below the quality standards for a *A3* treatment for water quality according to the European Directive (Directive, 1991) including the margin of safety. The results show that an overall reduction of 76% loads in total nitrogen and 87% in total phosphorus is necessary to achieve a good status of water quality, with the highest observed load reduction occurring at the station 14D03.

Table 7.3 Maximum Daily Loads of nutrients for Lis River sub basins

	14D03	15E03	15E07	16E01	15D01	15E08	15E05	15E06
NO_3 (kg day^{-1})								
Existing Conditions	54.3	20.0	253.8	6.8	1.7	256.7	1.8	3.3
TMDL	2.7	10.8	132.0	3.7	0.1	12.8	0.1	0.4
Reduction	95%	46%	48%	45%	95%	95%	95%	89%
PO_4 (kg day^{-1})								
Existing Conditions	10.7	5.1	72.5	6.9	0.2	78.0	0.3	4.1
TMDL	0.1	0.3	4.2	2.9	0.01	2.2	0.005	1.7
Reduction	99%	94%	94%	58%	96%	97%	99%	59%

7.2.5 Land Use Scenarios and Precipitation Effect on Water Quality

The modelling results for the land use scenarios associated to precipitation events indicated that the amount of total nitrogen and total phosphorus (Figure 7.11) markedly varies with the land use type. The percent difference allows the comparison of the respective scenario with the base scenario according to precipitation, this means that when looking at the percent difference for a normal precipitation event, where forest is converted to urban area, the difference is in respect to the normal precipitation event where no land use change occurs, i.e. is the same for low and high precipitation.

As expected, increasing precipitation in the basin for scenarios 1 (forest to urban), 2 (forest to agriculture) and 3 (agriculture to urban), caused higher nitrogen loads to the recipient water (73.7, 90.3 and 55.7%, respectively) than phosphorus loads (12.3, 19, 16% respectively). On the other hand, considering low precipitation events, reductions of nitrogen loads of 91.3, 91.7 and 90% and phosphorus loads of 54, 51 and 51% are observed for scenarios 1, 2 and 3. Scenarios 1 and 2 show nitrogen loads reduction but long term predictions will result in an increase of nitrogen loads, whereas reduction loads with increasing conversion areas are observed in scenario 3. Phosphorus loads for all scenarios decrease with increasing conversion areas. For the average precipitation scenario phosphorus loads decrease independently of the land use changes at an average of 12.3, 6.3 and 7.1% load reductions for scenarios 1, 2 and 3 respectively. The type of land use that originated the highest amount of nutrient loads was agricultural land followed by forest land and urban areas. Sub basins corresponding to stations 15E08 and 15E07, which account for only 22% of the total watershed area, were identified as the main responsible for nutrient load into Lis River Basin, representing 85% of the total watershed loads. These two sub basins contribute with 27% agricultural area, 24% forest area and 27% urban area for the total land use area of Lis basin.

For the land use scenarios considered, scenario 2 yields the highest total nitrogen loads for high precipitation events. On the other hand, for low precipitation events scenarios 1 and 2 show the highest reduction in total nitrogen loadings (12.7 and 14.7% respectively). All 3 scenarios results show an increase of nitrogen loads with area conversion for high precipitation events. Even though the nutrient coefficient loads decrease when changing agricultural to urban areas, urban areas have a high impervious coefficient. Thus, surface water instead of infiltrating will runoff to rivers more quickly dragging polluting substances on its way.

The land use scenarios presented here, even though hypothetical, show nutrient load reductions in Lis basin, indicating that further pollution prevention is necessary to comply with the maximum daily loads presented earlier.

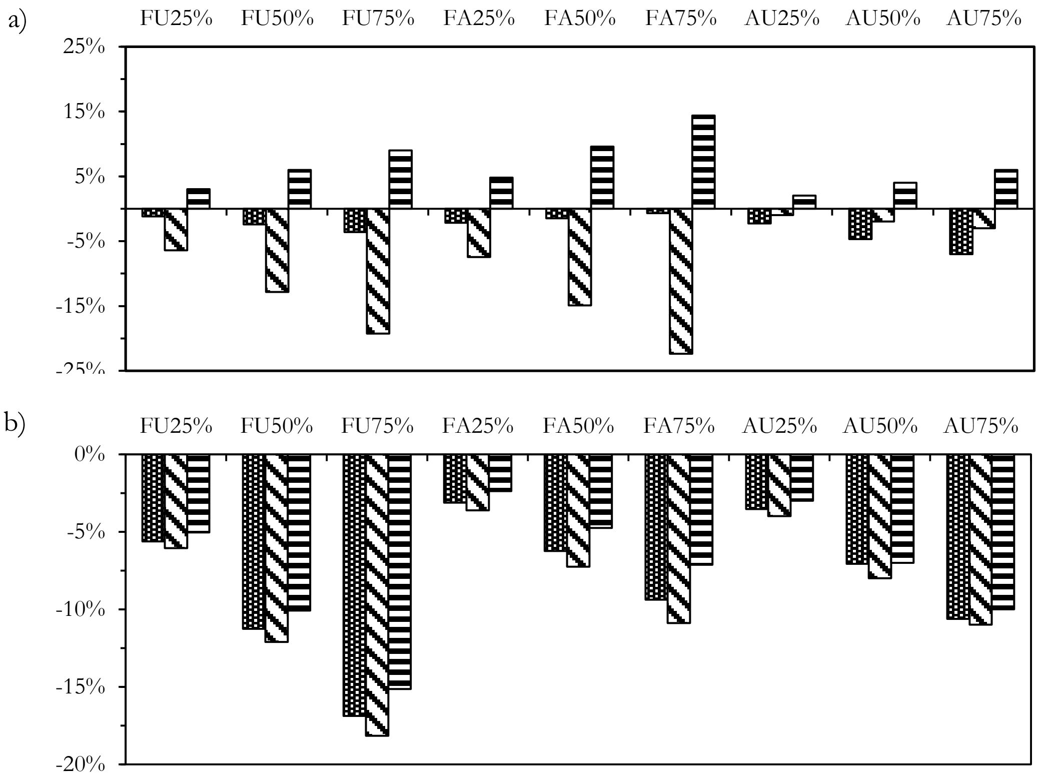

Figure 7.11 Percent difference of nutrient loadings to Lis River Basin for different precipitation events; a) Total Nitrogen; b) Total Phosphorus. FU – Forest land to Urban area; FA – Forest land to Agricultural land; AU – Agricultural land to Urban area. Average precipitation; Low precipitation; High precipitation.

7.3 Results and Discussion-Ave River

To perform the calibration, new nonpoint parameter loads adjustments were performed for urban areas, since they resulted in very low nutrient load coefficients and the knowledge of nonpoint sources in this type of land use was uncertain. On the other hand, nutrient load coefficient was already high in forest and agricultural areas. The average nutrient load coefficients obtained for each land use are specified in Table 7.4.

The scenarios of land use evolution (-0.21% Agricultural land; -0.15% Forest land and +0.36% Urban areas; per year for the years 2050; 2100 and 2150, including the increase of impervious land) and the Best Management Practices (applied to 3; 6; 9; 12 and 15% of the agricultural land with removal efficiencies of 50% for faecal coliforms; 30% for nitrogen;

30% for phosphorus and 30% for biochemical oxygen demand), as discussed in chapter 3 (section 3.4.2), were assessed to reflect their impact on water quality of the Ave River.

Table 7.4 Average land use nutrient load coefficient.

(kg ha^{-1}yr^{-1})	**Simulated**	
	TN	**TP**
Agricultural Land	16.9	5.3
Barren Land	1.8	0.3
Forest Land	11.3	4.3
Urban or Build-up Land	6.2	1.8

Figure 7.12 shows the inflow reduction from the land to the water stream for all the scenarios considered. BMP scenarios have greater impact on faecal coliforms inflow reduction from 5.78 up to 28.9%, while all other quality constituents remain below 10% reduction. Land use evolution scenarios show an improvement in the inflow of nutrients. This is a result of the difference between the nutrient load coefficients, since predicted scenarios show decrease of agricultural and forest land. On the other hand, land use scenarios with increased impervious coefficient have a lower reduction since the increase of runoff volume will also reflect in increased receiving stream degradation.

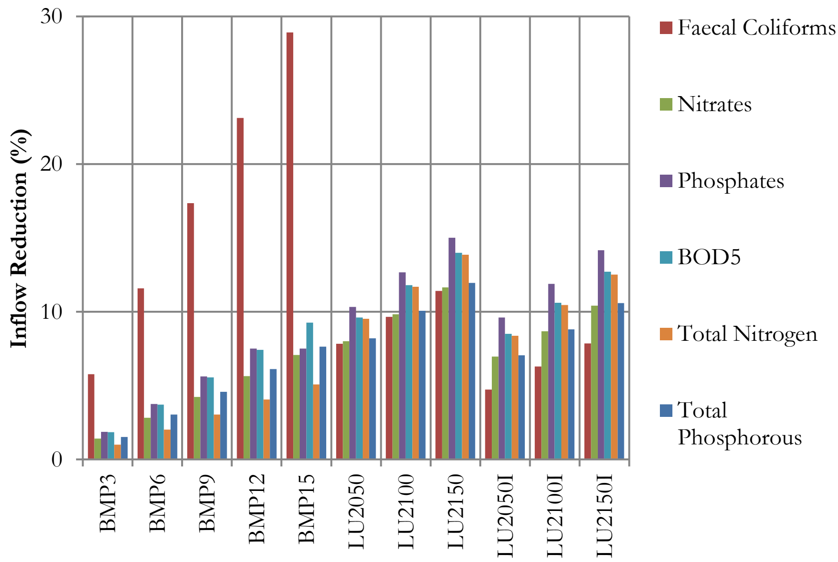

Figure 7.12 Inflow load reduction of quality constituents.

The reflex of the scenarios considered on water quality constituents concentration is illustrated in Figure 7.13 and Figure 7.14 for Este and Ave River, respectively. Land use scenarios with increased impervious coefficient show the highest reduction of concentration for all water quality constituents at both Este and Ave monitoring stations. As explained earlier the higher the impervious coefficient, the higher the runoff and consequently the higher the dilution.

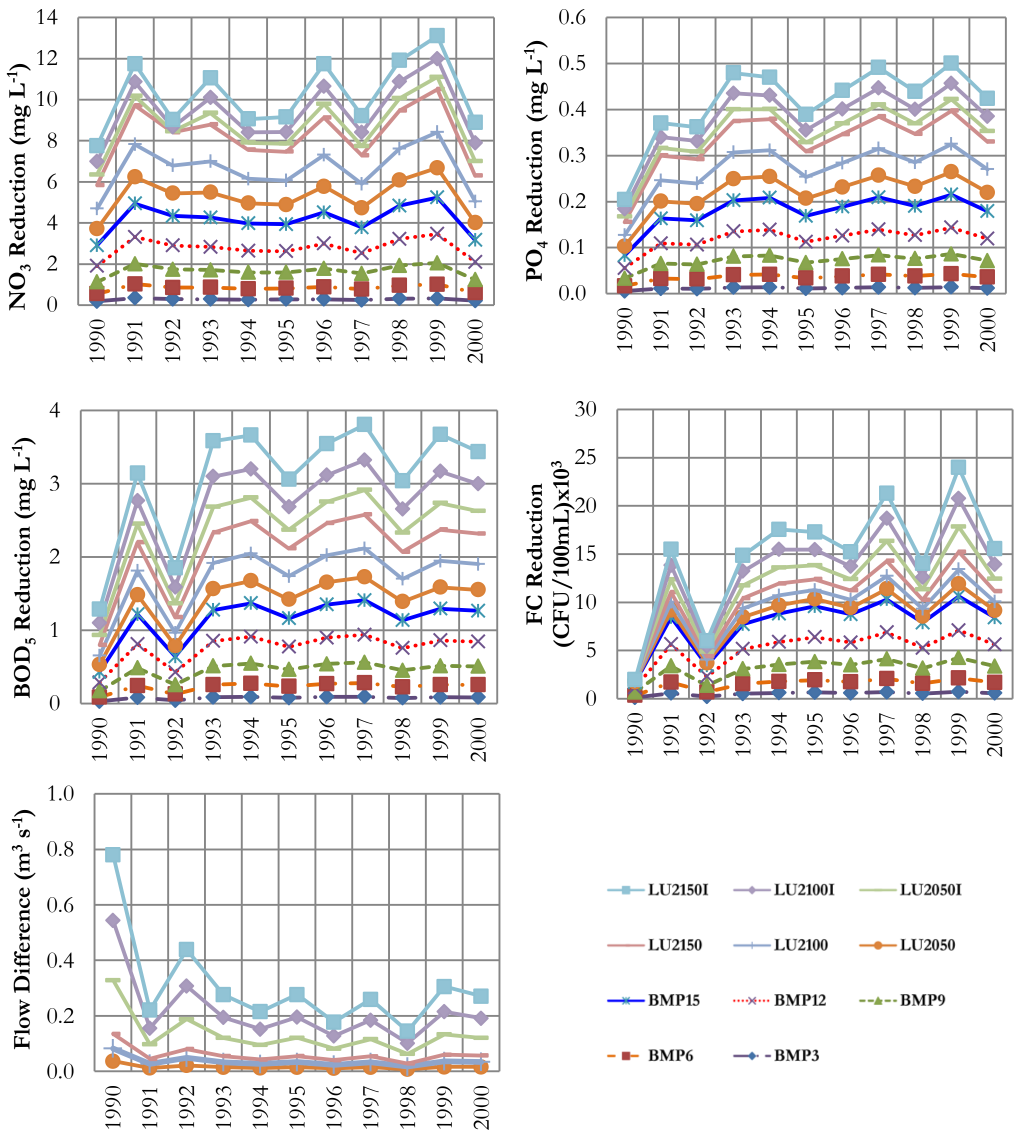

Figure 7.13 Concentration reduction of quality constituents in Este River.

Without considering any of the scenarios, nitrates, orthophosphates and biochemical oxygen demand are below the maximum allowed (mandatory values for a class *A3* treatment) according to (Directive, 1991) at Ave River monitoring station. Even though all scenarios show concentration reduction for all constituents, faecal coliforms still remain above the maximum value allowed (guide value for class *A3* treatment, 20000 CFU/100mL) at both monitoring stations. At Este River segment good water quality status is achieved for biochemical oxygen demand at scenario *BMP3* (<7 mg L^{-1}); for orthophosphates at scenario *BMP12* (<0.7 mg L^{-1}); nitrates lowest value is achieved at scenarios *BMP15* (54.4 mg L^{-1}) and *LU2150* (53.2 mg L^{-1}) which is above the mandatory value for a class A3 treatment (50 mg L^{-1}) and more than twice the guide value for a class A1 treatment (25 mgL^{-1}).

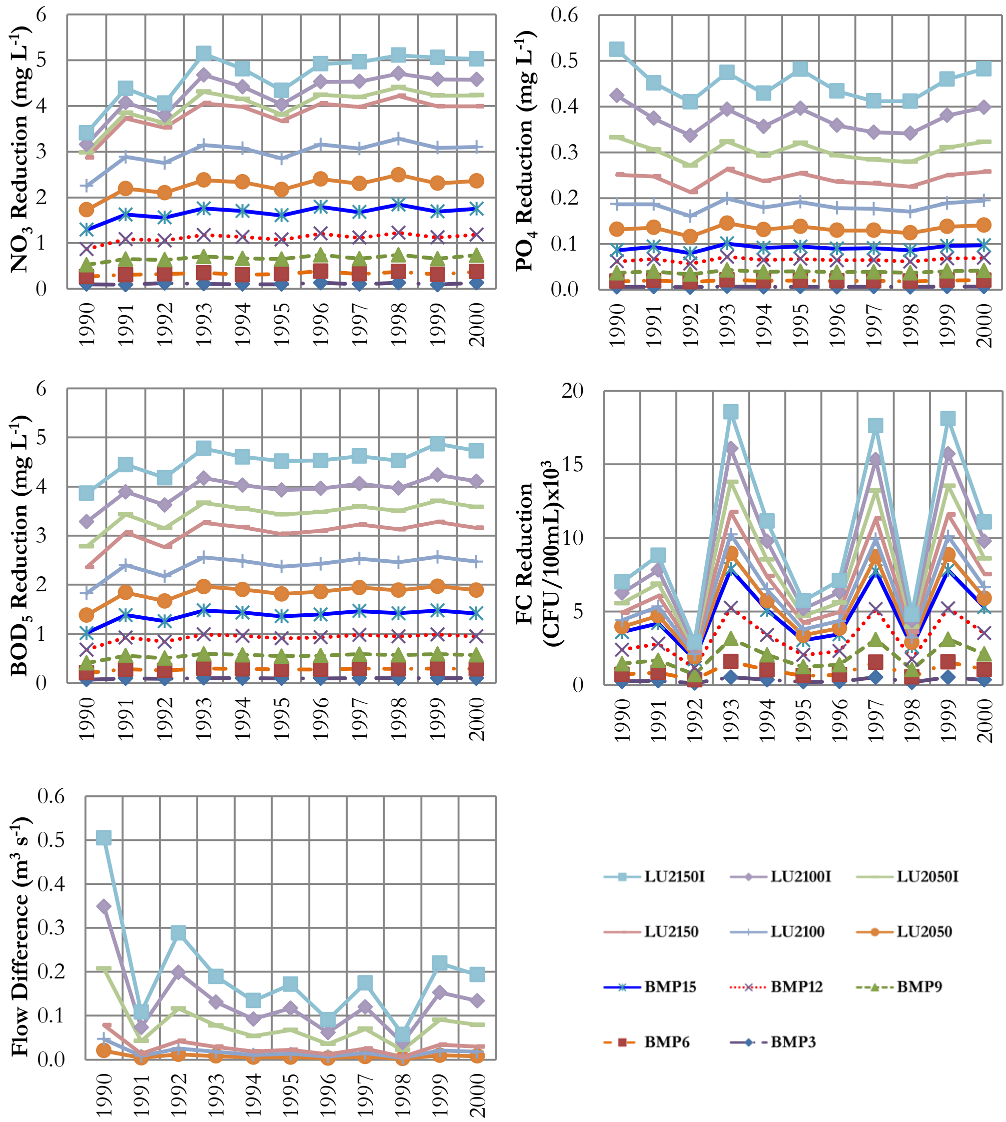

Figure 7.14 Concentration reduction of quality constituents in Ave River.

7.4 Conclusions

HSPF model was successfully applied to assess land use development impacts on water quality, thus making it an essential tool to support management decisions when considering best management practices. Hydrology and water quality modelling of the Lis river watershed was achieved with satisfactory results, considering the monitoring data available, making it possible to characterize water quality in Lis River watershed and to predict its behaviour regarding land use development or climate changes as well as mass discharges loads (TMDLs).

Agriculture area was identified as the dominant source of nutrients loads in Lis River watershed. Beyond that, two sub basins, covering 22% of the total watershed area, contribute to more than 85% of the estimated nutrient pollution load for the entire watershed. Thus, effective nonpoint source pollution control in these sensitive areas can significantly contribute to long term pollution management in Lis River watershed. The maximum daily loads projections show that nitrogen and phosphorus loads reductions of 76 and 87%, respectively, are required to fall below the mandatory values for a class *A3* treatment. Changes in land use, in agreement with possible evolution scenarios of the watershed, showed to have a high impact on nutrients load. Deforestation due to urbanization will reduce nitrogen and phosphorous loads. On the other hand, deforestation for agriculture will increase nitrogen. Urbanization of agricultural areas will also result in nutrient reduction. In general, the effects of climate change due to precipitation in water quality were more pronounced than land use changes, since higher pollutant loads are generated at higher precipitation events, especially from agricultural areas. Overall, deforestation resulted in an increment in the annual average loads for high precipitation events in the watershed.

Ave River basin pollution is dominated by the presence of high faecal coliform concentrations. Nutrients and biochemical oxygen demand are below the limits for a class *A3* treatment at Ave River segment. In Este River additional measures are necessary to reduce orthophosphates and biochemical oxygen demand below or to values that would require a class *A3* treatment for the best management practices scenarios presented.

Just like Lis River, Este River basin will require addressing the problem concerning the pollution sources (i.e. better fertilizer control, improved treatment of wastewater; control of animal feedlots runoff; etc.) in order to reduce the high concentrations of nitrates and faecal coliforms in the water.

7.5 References

2000/60/EC, 2000. Directive 2000/60/EC of the European Parliament and of the Council of 23 October 2000 establishing a framework of Community action in the field of water policy.

Borah, D.K., Bera, M., 2003. Watershed-Scale hydrologic and Nonpoint-Source Pollution Models: Review of Mathematical Bases. American Society of Agricultural Engineers.

Bouraoui, F., Dillaha, T.A., 1996. ANSWERS-2000: Runoff and sediment transport model. Journal of Environmental Engineering 122, 493-502.

Broekhuizen, N., Park, J.B.K., McBride, G.B., Craggs, R.J., 2012. Modification, calibration and verification of the IWA River Water Quality Model to simulate a pilot-scale high rate algal pond. Water Research 46, 2911-2926.

Chen, D., Lu, J., Shen, Y., Dahlgren, R.A., Jin, S., 2009. Estimation of critical nutrient amounts based on input–output analysis in an agriculture watershed of eastern China. Agriculture, Ecosystems & Environment 134, 159-167.

Cotter, A.S., Chaubey, I., Costello, T.A., Soerens, T.S., Nelson, M.A., 2003. Water Quality Model Output Uncertainty as Affected by Spatial Resolution of Input Data. JAWRA Journal of the American Water Resources Association 39, 977-986.

CS/AR-17, 2000. Surface Water Quality Assessment of River Kali, U.P., with Special Emphasis to Non-Point Source Pollution. National Institute of Hydrology Jalvigyan Bgawan.

Directive, C., 1991. 75/440/EEC of 16 June 1975 concerning the quality required of surface water intended for the abstraction of drinking water in the Member States as amended by Council Directive 79/869/EEC (further amended by Council Directive 81/855/EEC and Council Regulation 807/2003/EC) and both amended by Council Directive 91/692/EEC (further amended by Regulation 1882/2003/EC).

European-Comission, 2012. River Basin Management Plans. Report from the Comission to the European Parliament and the Council on the Implementation of the Water Framework Directive (2000/60/EC), Brussels.

Fonseca, A., Ames, D.P., Yang, P., Botelho, C., Boaventura, R., Vilar, V., 2014. Watershed Model Parameter Estimation and Uncertainty in Data-Limited Envrionments. Environmental Modelling & Software 51, 84-93.

Gao, M., Qiu, J., Li, C., Wang, L., Li, H., Gao, C., 2014. Modeling nitrogen loading from a watershed consisting of cropland and livestock farms in China using Manure-DNDC. Agriculture, Ecosystems & Environment 185, 88-98.

Im, S., Brannan, K., Mostaghimi, S., Cho, J.P., 2003. A Comparison of SWAT and HSPF Models for Simulating Hydrologic and Water Quality Responses from an Urbanizing Watershed. American Society of Agricultural Engineers (ASAE), Riviera Hotel and Convention Center, Las Vegas, Nevada, USA.

Kourakos, G., Klein, F., Cortis, A., Harter, T., 2012. A groundwater nonpoint source pollution modeling framework to evaluate long-term dynamics of pollutant exceedance probabilities in wells and other discharge locations. Water Resources Research 48, W00L13.

León, L.F., Soulis, E.D., Kouwen, N., Farquhar, G.J., 2001. Nonpoint source pollution: a distributed water quality modeling approach. Water Research 35, 997-1007.

Liu, G.D., Wu, W.L., Zhang, J., 2005. Regional differentiation of non-point source pollution of agriculture-derived nitrate nitrogen in groundwater in northern China. Agriculture, Ecosystems & Environment 107, 211-220.

Loehr, R.C., Ryding, S.O., Sonzogni, W.C., 1989. Estimating Nutrient Loading to a Waterbody. In: The control of Eutrophication of Lakes and Reservoirs. United Nations Educational Scientific and Cultural Organization, The Parthenon Publishing Group, New Jersey.

McFarland, A.M.S., Hauck, L.M., 2001. Determining Nutrient Export Coefficients and Source Loading Uncertainty Using In-Stream Monitoring Data. JAWRA Journal of the American Water Resources Association 37, 223-236.

Mostaghimi, S., Park, S.W., Cooke, R.A., Wang, S.Y., 1997. Assessment of management alternatives on a small agricultural watershed. Water Research 31, 1867-1878.

NIRPC, 2012. The Water Resource Protection and Conservation Toolkit. 6100 Southport Road, Portage, IN 46368.

Novotny, V., Olem, H., 1994. Water Quality; Prevention. Identification, and Management of Diffuse Pollution, New York, NY.

Sadeghi, A., Arnold, J., 2002. A SWAT/Microbial sub-model for predicting pathogen loadings in surface and groundwater at watershed and basin scales. In: Proceedings of the March 11–13, 2002 Conference, Total Maximum Daily Load (TMDL) Environmental Regulations. In: Proceedings of the March 11–13, 2002 Conference, Total Maximum Daily Load (TMDL) Environmental Regulations, Fort Worth, Texas, 56-63.

Schaffner, M., Bader, H.-P., Scheidegger, R., 2009. Modeling the contribution of point sources and non-point sources to Thachin River water pollution. Science of The Total Environment 407, 4902-4915.

Shen, J., Zhao, Y., 2010. Combined Bayesian statistics and load duration curve method for bacteria nonpoint source loading estimation. Water Research 44, 77-84.

Shen, Z., Hong, Q., Yu, H., Liu, R., 2008. Parameter uncertainty analysis of the non-point source pollution in the Daning River watershed of the Three Gorges Reservoir Region, China. Science of The Total Environment 405, 195-205.

Thorndahl, S., Willems, P., 2008. Probabilistic modelling of overflow, surcharge and flooding in urban drainage using the first-order reliability method and parameterization of local rain series. Water Research 42, 455-466.

Yang, F., Xu, Z., Zhu, Y., He, C., Wu, G., Qiu, J.R., Fu, Q., Liu, Q., 2013. Evaluation of agricultural nonpoint source pollution potential risk over China with a Transformed-Agricultural Nonpoint Pollution Potential Index method. Environmental Technology, 1-13.

Yurekli, K., Kurunç, A., 2005. Testing the Residuals of an ARIMA Model on the Çekerek Stream Watershed in Turkey. Turkish J Eng Environ Sci 29, 61-74.

8 Climate Change Effects on Faecal Coliform Bacterium Watershed Impairments[4]

Impairment of surface waters quality by faecal coliform bacteria is an issue of great importance across the globe. A water quality model, Hydrological Simulation Program FORTRAN (HSPF) was used to predict the impacts of farming and climate change on faecal coliform loads and concentrations in streams of Lis River watershed, in Leiria region, Portugal. The calibrated faecal coliform model simulated well the patterns and range of observed faecal coliform concentrations. The accuracy of the model was evaluated by the percent bias coefficient and the coefficient of determination. The results indicate a general deterioration of the water quality regarding faecal contamination in Lis River. Maximum daily loads were calculated for each of the impaired streams; an average of 77% reduction in the current faecal coliform load from the watershed is necessary to achieve the established water quality goals by the Council Directive 75/440/EEC (1975). Climate change scenarios (increments on temperature and precipitation) were assumed to predict the behaviour of faecal coliform bacteria in the watershed. The simulated results showed that an increase of 1ºC in air daily temperature results in an increase of water temperature of 1.1ºC and 1.5% decrease on faecal coliform bacteria in stream concentration. The combined effect of air temperature (+1ºC) and precipitation (+7%) increment lead to an increase of approximately 2% in bacteria inflow to the basin.

[4] Fonseca, A., Botelho, C., Boaventura, R.A.R., Vilar, V.J.P., 2014. "Global Warming Effects on Faecal Coliform Bacterium Watershed Impairments in Portugal" River Research and Applications. DOI: 10.1002/rra.2821

8.1 Introduction

The Water Framework Directive (WFD) introduces a system of coordinated objectives to be met through integrated River Basin Management Plans. It takes into consideration water quality, water resources and natural habitats (2000/60/EC, 2000). However, the WFD does not acknowledge risks posed by climate change towards the achievement of its objectives (Wilby et al., 2006) but they should also be considered of great importance as all other risks pertaining water quantity and quality as shown in recent studies (Jiang et al., 2013; Park et al., 2010; Prathumratana et al., 2008).

Besides extreme hydrological events and land use evolution (deforestation, urban spreading, etc.), surface water quality is also affected by climate change. Commonly, water pollution is attributed to human activities of urban, industrial and agricultural origin and, climate change could lead to water quality degradation as an indirect repercussion of these activities (Delpla et al., 2009). According to Wentz et al. (2007) precipitation is increasing at a rate of 7% per degree Celsius of surface temperature as a response to global warming. Global average temperatures are expected to raise at least 4º C by 2100 and twice that by 2200 due to carbon oxide emissions (Sherwood et al., 2014). In addition to greenhouse gas emissions, changes in the hydrologic cycle will likely occur (Allen and Ingram, 2002; Held and Soden, 2006; Lu et al., 2013).

Faecal coliforms is commonly designated as an indicator of pathogen contamination when evaluating water quality in freshwater systems (Kim et al., 2005; Liu and Huang, 2012; Tate et al., 2006; Tate et al., 2000). Climate factors are one of the drivers of water contamination due to their influence on the transport of contaminants by precipitation induced runoff (Bonte and Zwolsman, 2010; Cha et al., 2010; Interlandi and Crockett, 2003; Kistemann et al., 2002). Since faecal coliforms concentration tends to be positively related to precipitation (Cha et al., 2010), due to the corresponding increase of runoff that will most likely heighten the transport potential of faecal contaminants, it will likely elevate contamination levels in the coming years. Quantifying the influence of climate variability on surface water faecal contamination is one way to ensure water quality and maintain public health (St Laurent and Mazumder, 2014). The identification and quantification of sources of contamination allows establishing water protection efforts and increases the capacity to forecast variability in water contamination, which can result in water treatment process improvements (Avery et al., 2004; Brookes et al., 2004; Charron et al., 2004; Ferguson et al., 2003).

The main climate change factors affecting water quality are air temperature and the increase of extreme hydrological events. Temperature influences all physico-chemical constants, i.e. several transformations in water will be favoured as a result of temperature increase, such as dissolution, solubilisation, evaporation, etc. Other direct effects on water quality, dilution or concentration of dissolved substances, are affected by floods and droughts. While high precipitation events incur higher runoff and increased material transportation, droughts may impact water quality by increasing residence times and concentration of nutrients and reducing the dilution capacity of point source effluents.

Therefore, this study aims at assessing the long-term trends given the pressure provided by observations and physical understanding of climate change (temperature and precipitation) on surface water quality impairment by the presence of faecal coliform bacteria. The scenarios studied comprise the expected temperature projections across the globe as explained by Sherwood et al. (2014) and precipitation effects resulting from the projected temperature increase specified by (Wentz et al., 2007). The Hydrological Simulation Program FORTRAN was used to calibrate and validate in stream faecal coliform concentrations and to develop four scenarios: 1) 2ºC increment in air temperature; 2) 4ºC increment in air temperature; 3) 2ºC increment in air temperature and 14% precipitation increase and 4) 4ºC increment in air temperature and 28% precipitation increase. The study consist in four tasks: 1) evaluate water quality status on faecal coliform at 8 cross sections along Lis River; 2) identify and quantify point and nonpoint sources of faecal coliform in Lis basin; 3) determine maximum daily loads to achieve the desired water quality status established in 75/440/EEC (1975) for surface waters intended for the abstraction of drinking water; 4) evaluate faecal coliform loadings and in stream concentrations with different temperature and precipitation patterns.

8.2 Results and Discussion

8.2.1 In stream Water Quality Calibration and Validation

8.2.1.1 Temperature

For a successful calibration of faecal coliforms, prior calibration of water temperature is required. Elevation data of each reach and the mean difference between the reach and the temperature gage station were obtained through the digital elevation model and inserted in the HSPF model. The correction factor for solar radiation (CFSAEX) is a key parameter in water temperature modeling, as it represents the amount of solar radiation reaching the stream. CFSAEX was adjusted accordingly to calibrate water temperature in Lis River watershed. Other less important factors that influence water temperature are bed heat conduction and stream heat transport by conduction-convection (contributions from interflow and groundwater). The calibration and validation results plot for in-stream temperature are presented Figure 8.1 and Figure 8.2 respectively.

Although little observed data was available for validation, the water temperature predicted by the model fitted really well with more than 96% of observed data falling between the maximum and minimum daily simulations. Uncertainty lies with observed water temperature for station 15E06 which varies only between 15 and 17ºC for all samples, implying only a difference of 2ºC from winter and summer seasons.

a)

b)

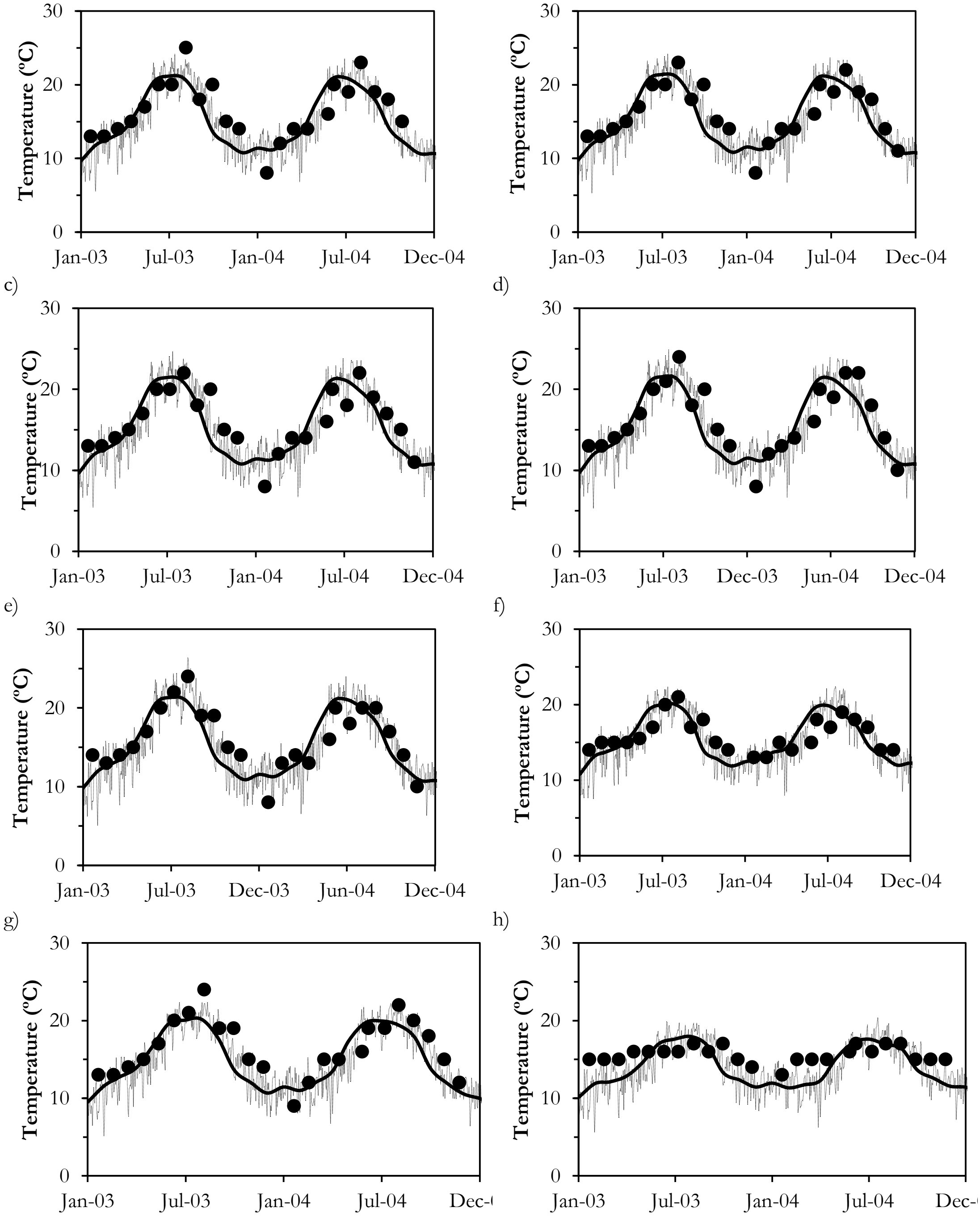

Figure 8.1 Calibration results of water temperature in Lis basin: a) 14D03 station; b) 15D01 station; c) 15E08 station; d) 15E03 station; e) 15E07 station; f) 16E01 station; g) 15E05 station; h) 15E06 station; – monthly average; -- daily simulation; • observed values.

a) b)

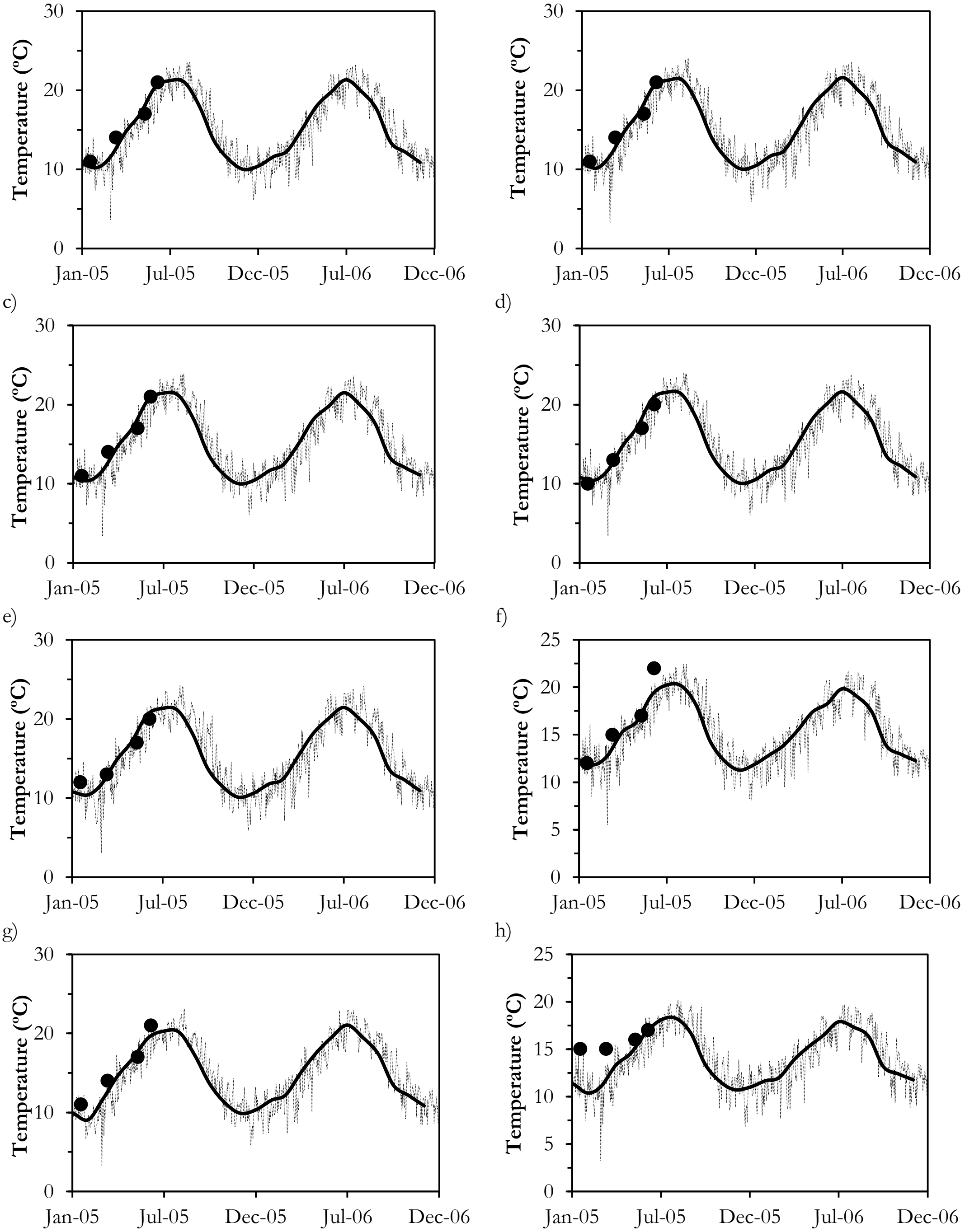

Figure 8.2 Validation results of water temperature in Lis basin: a) 14D03 station; b) 15D01 station; c) 15E08 station; d) 15E03 station; e) 15E07 station; f) 16E01 station; g) 15E05 station; h) 15E06 station; – monthly average; -- daily simulation; • observed values.

8.2.1.2 Faecal Coliforms

The calibration and validation results plot for faecal coliform in-stream concentration are presented in Figure 8.3 and Figure 8.4 respectively.

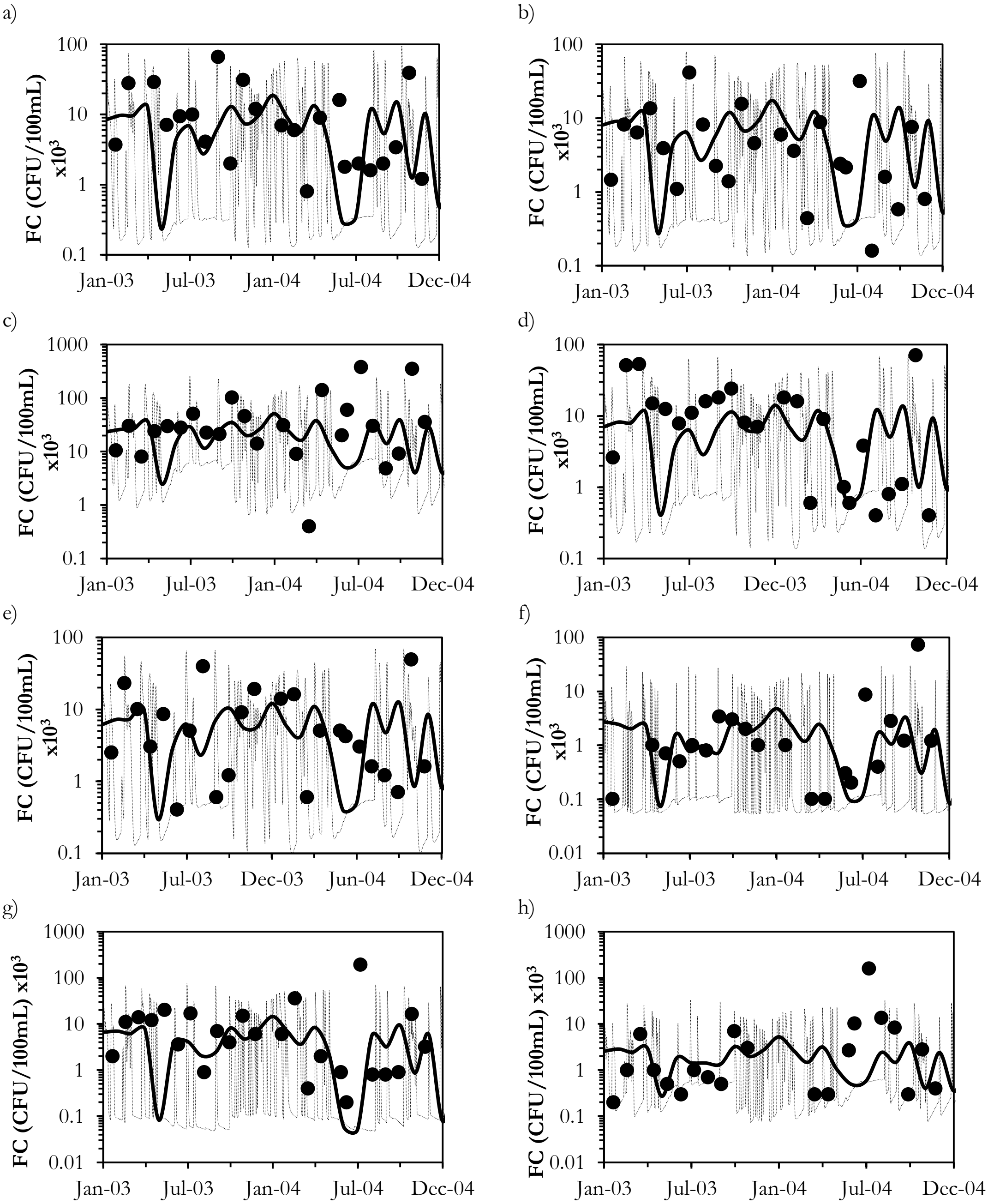

Figure 8.3 Calibration results of faecal coliforms in Lis basin: a) 14D03 station; b) 15D01 station; c) 15E08 station; d) 15E03 station; e) 15E07 station; f) 16E01 station; g) 15E05 station; h) 15E06 station; – monthly average; -- daily simulation; • observed values.

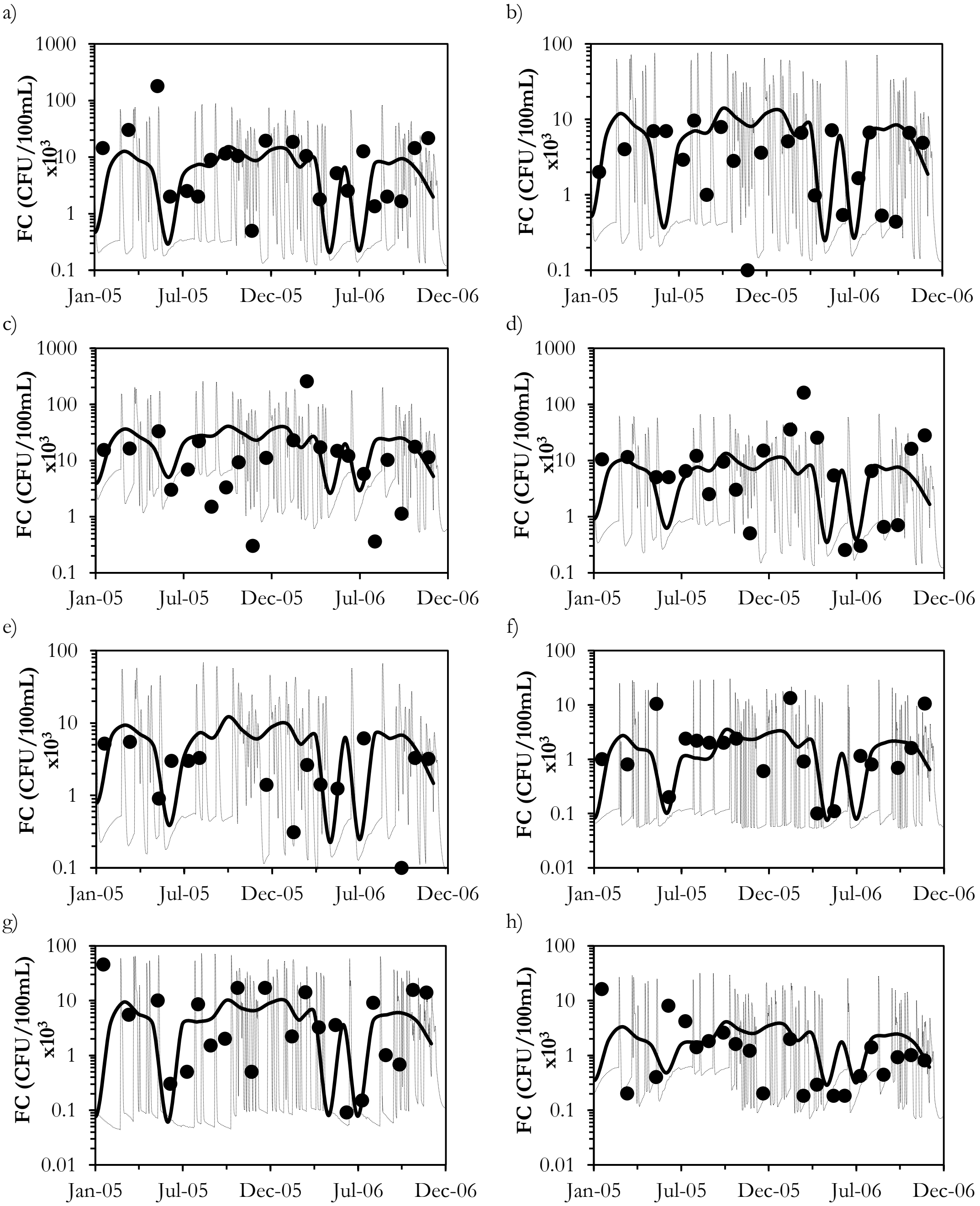

Figure 8.4 Validation results of faecal coliforms in Lis basin: a) 14D03 station; b) 15D01 station; c) 15E08 station; d) 15E03 station; e) 15E07 station; f) 16E01 station; g) 15E05 station; h) 15E06 station; – monthly average; -- daily simulation; • observed values.

Faecal coliforms was modelled as dissolved constituent using separate build-up / wash off relationship for impervious and pervious areas, along with a first order decay relationship within stream reaches. Three HSPF parameters control the fate of faecal coliforms within stream reaches: first order decay rate coefficient, FSTDEC; temperature correction coefficient, THFST and; mean monthly water temperature, TWAT. The recommended default value for THFST was used for all sub basins, 1.07. Direct comparisons were made between simulated and observed faecal coliform bacteria concentrations and evaluated by the statistical parameters.

Figure 8.5a shows the spatial distribution of faecal coliform in-stream concentration per sub basin. When comparing this map with Figure 8.5b there is a clear relationship between loads and in-stream concentration. Downstream sub basins show high faecal coliform in-stream concentration when compared to faecal coliform loads as a result of upstream contamination. There is a clear association between the piggeries location and the simulated faecal coliform loads in the basin. This provides the insight that piggeries are the main faecal coliform load contributors in Lis River basin.

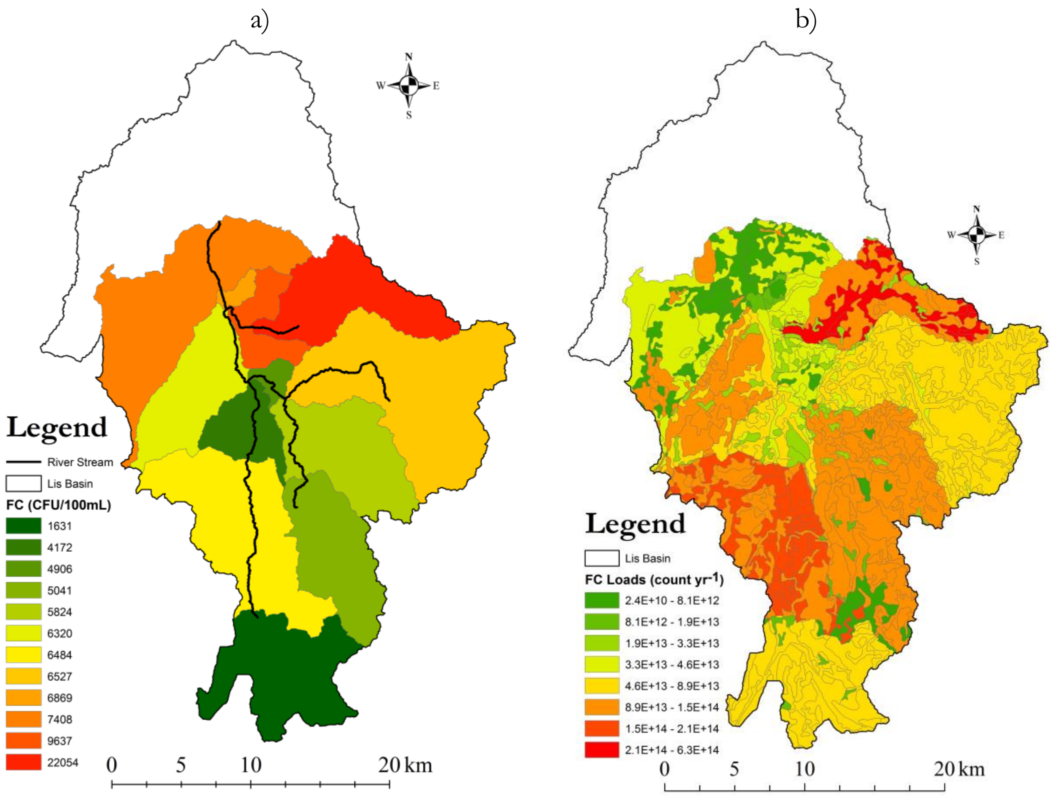

Figure 8.5 Spatial distribution of average faecal coliform in-stream concentration

Increases in simulated faecal coliform load inflow are a result of rainfall events where bacteria are washed off the land surface as observed in Figure 8.6. When for the same precipitation pattern faecal coliforms inflow increases this is due to direct input of contamination into surface water from grazing or septic systems failure.

The calibrated faecal coliforms model was also evaluated by comparison of the *PBIAS* and R^2 criteria mentioned in chapter 3. These results (Table 8.1) show good to very good model calibration for the *PBIAS* coefficient for all stations except for station 15D01 and 15E05. Regarding R^2 only station 16E01 showed a value inferior to 0.5, for calibration. Validation statistical results confirm the results from calibration with only the R^2 for stations 15E03, 15D01 and 16E01 reproducing unsatisfactory results.

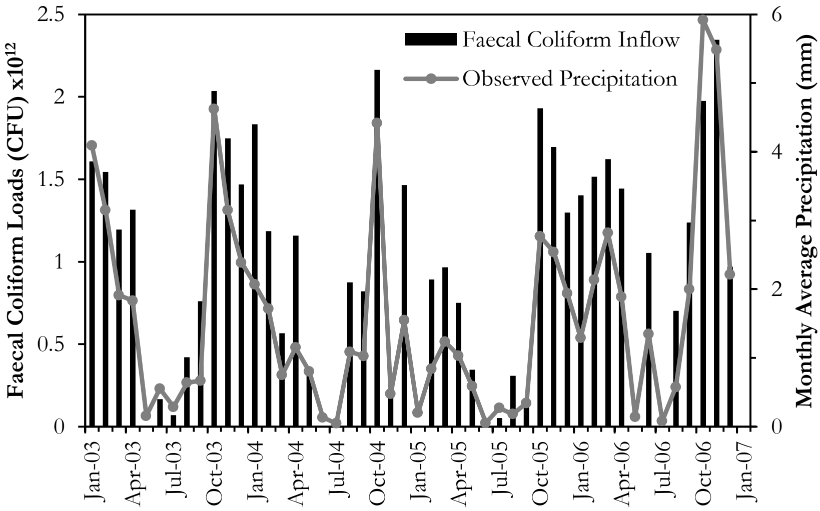

Figure 8.6 Simulated faecal coliforms load inflow versus monthly observed precipitation.

Table 8.1 Simulated faecal coliforms statistical criteria results.

	15E06	15E03	14D03	15D01	15E08	15E05	16E01	15E07
Calibration								
PBIAS	-0.03	-0.02	-0.35	-0.45	-0.02	-0.45	0.23	0.20
R^2	0.84	0.50	0.89	0.66	0.56	0.69	0.40	0.62
E	0.67	0.58	0.42	0.33	0.57	0.33	0.42	0.49
Validation								
PBIAS	0.06	0.05	0.20	-0.23	0.05	-0.27	0.31	0.29
R^2	0.71	0.47	0.80	0.44	0.52	0.58	0.38	0.68
E	0.61	0.53	0.49	0.27	0.56	0.31	0.40	0.27

In general the model represents reasonably the observed faecal coliforms concentration.

8.2.2 Maximum Daily Loads calculation

The maximum daily loads were determined based on the entire simulation period of 4 years. Faecal coliforms loads (point and nonpoint sources) were reduced iteratively until the target water quality conditions were met (20000 CFU/100 mL). The values shown in Table 8.2 represent the daily loads for each sub basin where the simulated daily concentration for each constituent was always below the quality standards for water quality according to the European Directive 75/440/EEC (1975) including the margin of safety. The necessary load reduction of faecal coliforms loads in the study area is approximately 77% in order to achieve the requirements established in the European Directive.

Table 8.2 Faecal coliforms maximum daily loads for Lis River sub basins.

	15E06	15E03	14D03	15D01	15E08	15E05	16E01	15E07
FC (CFU day^{-1})								
Normal	$3x10^{14}$	$2x10^{14}$	$5x10^{14}$	$2x10^{13}$	$3x10^{14}$	$5x10^{13}$	$2x10^{14}$	$4x10^{14}$
Maximum Daily Loads	$2x10^{14}$	$4x10^{13}$	$5x10^{13}$	$1x10^{13}$	$2x10^{13}$	$8x10^{5}$	$1x10^{14}$	$9x10^{13}$
Percent Reduction	40%	72%	90%	30%	93%	99%	40%	80%

8.2.3 Climate change effects on faecal coliform bacteria watershed contamination

The impact of climate change on faecal coliform bacteria contamination was analysed by comparing the model outputs of faecal coliform concentration and inflow to stream for the following scenarios: (Scenario 1) + 2ºC air temperature increase; (Scenario 2) + 4ºC air temperature increase; (Scenario 3) + 2ºC air temperature increase with 14% precipitation increase and (Scenario 4) + 4ºC air temperature increase with 28% precipitation increase. As shown in Figure 8.7 an increment in daily air temperature will result in a decrease of faecal coliform bacteria concentration. The model predicts a decrease of approximately 1.5% (810 CFU/100 mL) of average monthly faecal coliform per 1ºC increase in air temperature.

The integrated effect of the increased air temperature and precipitation (scenarios *3* and *4*) on faecal coliform concentration is also show in Figure 8.7. The increment on the precipitation may result in an increase of surface runoff, which will result in a decrease of faecal coliform bacteria concentration in the water, but on the other hand washoff increases the inflow of faecal coliform. The results show an overall decrease of bacteria concentration versus the base scenario except for May through July months. An average increase of 77 and 134% faecal coliforms inflow is observed in July (Table 8.3) for scenarios *3* and *4*, increasing faecal coliform concentration.

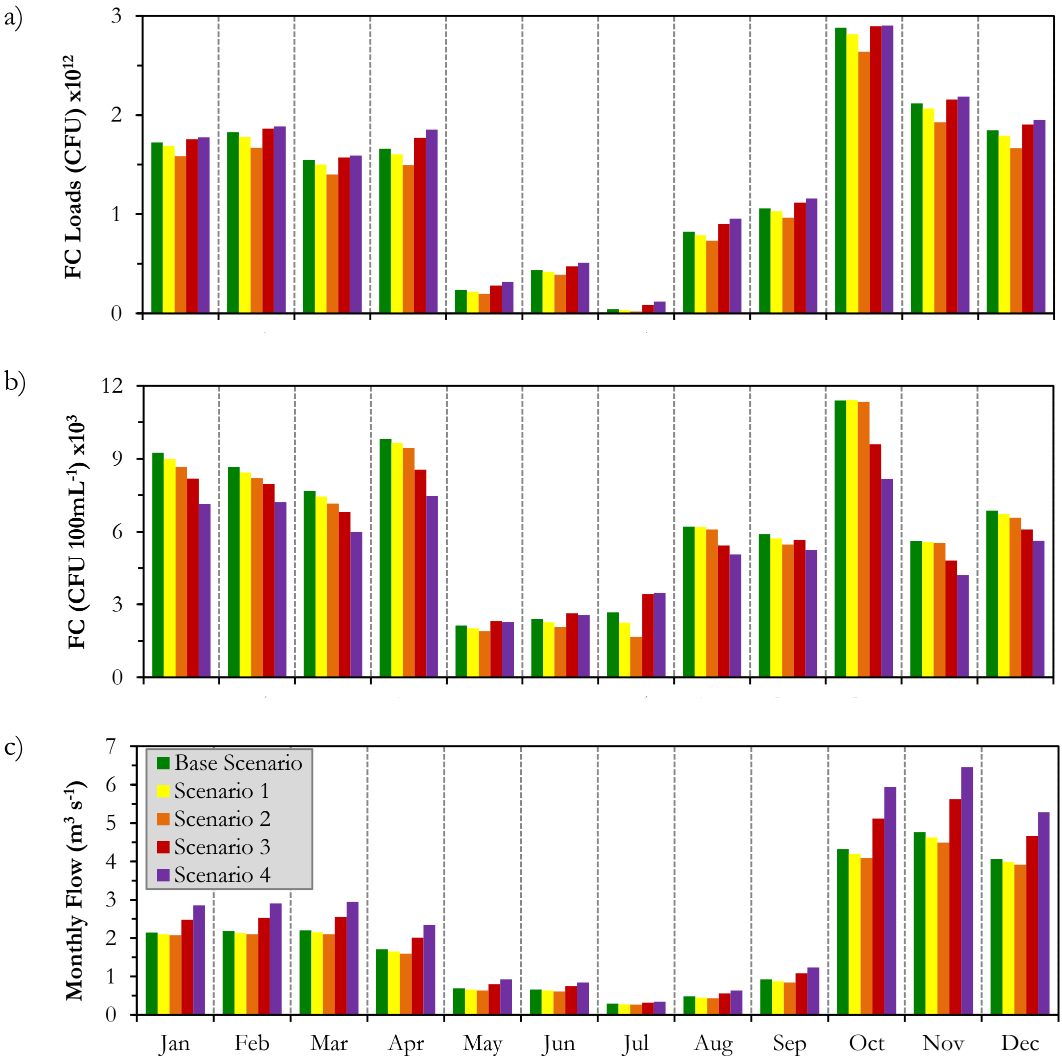

Figure 8.7 Scenarios comparison of monthly average of: a) faecal coliforms load inflow, b) faecal coliforms concentration and c) flow.

Table 8.3 Monthly average change of studied parameters versus the base scenario.

Monthly Average Change	Scenario	Jan	Feb	Mar	Apr	May	Jun	Jul	Aug	Sep	Oct	Nov	Dec	Annual Average
Water Temperature (°C)	1	0.5	0.5	0.6	0.6	0.7	0.8	0.8	0.8	0.8	0.7	0.5	0.5	0.6
	2	1	1.1	1.2	1.2	1.3	1.5	1.5	1.6	1.5	1.4	1	0.9	1.3
	3	0.5	0.5	0.6	0.6	0.6	0.7	0.7	0.8	0.7	0.7	0.5	0.5	0.6
	4	1	1	1.2	1.2	1.2	1.4	1.5	1.5	1.4	1.3	1.1	0.9	1.2
FC Concentration	1	-7%	-6%	-7%	-7%	-9%	-8%	-23%	-7%	-9%	-4%	-5%	-6%	-8%
	2	-14%	-12%	-15%	-14%	-19%	-16%	-48%	-14%	-18%	-9%	-10%	-13%	-17%
	3	-15%	-12%	-14%	-16%	3%	5%	31%	-14%	-7%	-18%	-17%	-13%	-8%
	4	-30%	-23%	-27%	-29%	2%	2%	32%	-24%	-17%	-32%	-30%	-24%	-18%
FC Inflow	1	-6%	-6%	-7%	-7%	-11%	-6%	-28%	-8%	-7%	-6%	-6%	-6%	-9%
	2	-11%	-13%	-13%	-14%	-22%	-12%	-53%	-15%	-14%	-12%	-11%	-12%	-17%
	3	1%	1%	1%	4%	16%	3%	77%	5%	6%	1%	1%	2%	9%
	4	-%	2%	2%	7%	24%	5%	134%	8%	10%	3%	2%	3%	15%
Flow	1	-2%	-2%	-3%	-4%	-5%	-4%	-6%	-8%	-6%	-3%	-3%	-2%	-4%
	2	-4%	-4%	-5%	-7%	-9%	-8%	-11%	-13%	-10%	-6%	-6%	-4%	-7%
	3	17%	17%	16%	17%	18%	14%	11%	16%	18%	19%	18%	15%	16%
	4	35%	35%	34%	37%	37%	28%	20%	31%	36%	40%	36%	30%	33%

Although precipitation patterns are very similar for summer months, the increase of observed flow in July for these scenarios is not enough to mitigate the effect on faecal coliform concentration in the water. This happens because the increase of flow in July is only 11% (scenario *3*) and 20% (scenario *4*) of the base scenario. The results of the scenarios show an annual average increase on water temperature of 0.6, 1.3, 0.6, and 1.3 ºC for scenario *1*, *2*, *3* and *4* respectively. The water volume difference for the entire simulated period is almost negligible for scenarios *1* and *2* (-4 and -7%, respectively), but for scenarios *3* and *4* an increase of 16 and 33% is observed.

Even though the annual average of faecal coliform bacteria decreases for all scenarios, the inflow quantity increases for scenarios *3* and *4* due to increase of runoff. Therefore the accumulative faecal coliform bacteria inflow was also studied to predict its behaviour for all scenarios. Figure 8.8 shows that the increment of air temperature alone will reduce bacteria inflow but when considering the increase of precipitation, scenarios *3* and *4*, an increase of 3.5 and 6.1% of bacteria reaching the stream is observed for a 4 year period, which could lead to impaired waters in long term scenarios, especially in summer months as stated previously.

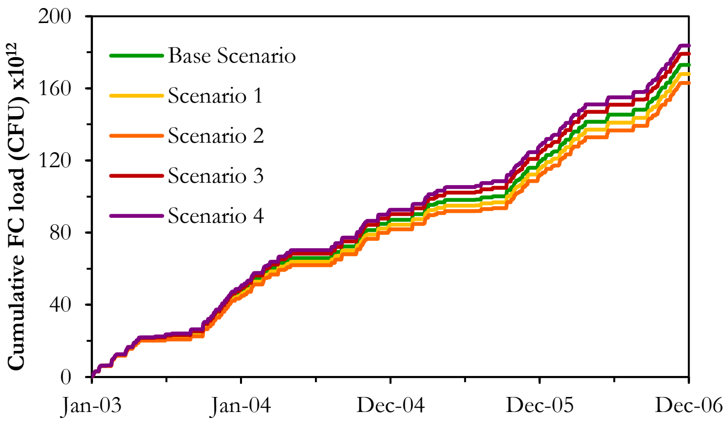

Figure 8.8 Impact of climate change on cumulative faecal coliforms loads inflow.

8.3 Conclusions

The Hydrological Simulation Program FORTRAN model was used successfully to simulate faecal coliform bacteria on Lis River under different climate change scenarios. Although there are many areas of uncertainty in modelling faecal coliforms, like the evaluation of parameters used to simulate fate and transport of faecal coliform bacteria, the model was able to predict the observed values with confidence. The results show that faecal coliform bacteria in Lis River do not meet the criteria established by the European Directive 75/440/EEC (1975). Faecal coliform maximum daily loads were developed for Lis watershed. In the light of the results, an implementation of a 77% faecal coliform load reduction in the basin should be adequate to reduce faecal coliform bacteria concentration to achieve the goals established for surface water quality. Four climate change scenarios were developed to study faecal coliform bacteria variability. Faecal coliforms concentration decreased with the increase of air temperature at an average of 810 UFC/100 mL per 1ºC. The combined increment of precipitation and daily air temperature will result in an average increase of faecal coliform inflow to the water stream of 1.6% and runoff of 1.2% per 1ºC air temperature and 7% precipitation increase. This Chapter shows that climate change should be taken into consideration to effectively achieve the Water Framework Directive objectives, especially in summer months where the increased bacteria loads, for scenarios 3 and 4, derived from potential increased precipitation are not mitigated by the increase of temperature. In this study it seems that water quality could improve with future climate change projections in winter months but long term effects of increased faecal coliform loads are still unknown.

8.4 References

75/440/EEC, 1975. Council Directive 75/440/EEC of 16 June 1975 concerning the quality required of surface water intended for the abstraction of drinking water in the Member States. Volume 1.

2000/60/EC, 2000. Directive 2000/60/EC of the European Parliament and of the Council of 23 October 2000 establishing a framework of Community action in the field of water policy.

Allen, M.R., Ingram, W.J., 2002. Constraints on future changes in climate and the hydrologic cycle. Nature 419, 224-232.

Avery, S., Moore, A., Hutchison, M., 2004. Fate of Escherichia coli originating from livestock faeces deposited directly onto pasture. Letters in Applied Microbiology 38, 355-359.

Bonte, M., Zwolsman, J.J.G., 2010. Climate change induced salinisation of artificial lakes in the Netherlands and consequences for drinking water production. Water Research 44, 4411-4424.

Brookes, J.D., Antenucci, J., Hipsey, M., Burch, M.D., Ashbolt, N.J., Ferguson, C., 2004. Fate and transport of pathogens in lakes and reservoirs. Environment International 30, 741-759.

Cha, S.M., Lee, S.W., Park, Y.E., Cho, K.H., Lee, S., Kim, J.H., 2010. Spatial and temporal variability of faecal indicator bacteria in an urban stream under different meteorological regimes. Water Science and Technology 61, 3102-3108.

Charron, D.F., Thomas, M.K., Waltner-Toews, D., Aramini, J.J., Edge, T., Kent, R.A., Maarouf, A.R., Wilson, J., 2004. Vulnerability of waterborne diseases to climate change in Canada: A review. Journal of Toxicology and Environmental Health - Part A 67, 1667-1677.

Delpla, I., Jung, A.V., Baures, E., Clement, M., Thomas, O., 2009. Impacts of climate change on surface water quality in relation to drinking water production. Environment International 35, 1225-1233.

Ferguson, C., Husman, A.M.d.R., Altavilla, N., Deere, D., Ashbolt, N., 2003. Fate and transport of surface water pathogens in watersheds.

Held, I.M., Soden, B.J., 2006. Robust responses of the hydrological cycle to global warming. Journal of Climate 19, 5686-5699.

Interlandi, S.J., Crockett, C.S., 2003. Recent water quality trends in the Schuylkill River, Pennsylvania, USA: a preliminary assessment of the relative influences of climate, river discharge and suburban development. Water Research 37, 1737-1748.

Jiang, T., Fischer, T., Lu, X.X., 2013. Larger Asian rivers: Changes in hydro-climate and water environments. Quaternary International 304, 1-4.

Kim, G., Choi, E., Lee, D., 2005. Diffuse and point pollution impacts on the pathogen indicator organism level in the Geum River, Korea. Science of The Total Environment 350, 94-105.

Kistemann, T., Claßen, T., Koch, C., Dangendorf, F., Fischeder, R., Gebel, J., Vacata, V., Exner, M., 2002. Microbial load of drinking water reservoir tributaries during extreme rainfall and runoff. Applied and environmental microbiology 68, 2188-2197.

Liu, W.-C., Huang, W.-C., 2012. Modeling the transport and distribution of faecal coliform in a tidal estuary. Science of The Total Environment 431, 1-8.

Lu, X., Kicklighter, D.W., Melillo, J.M., Yang, P., Rosenzweig, B., Vörösmarty, C.J., Gross, B., Stewart, R.J., 2013. A contemporary carbon balance for the northeast region of the United States. Environmental science & technology 47, 13230-13238.

Park, J.-H., Duan, L., Kim, B., Mitchell, M.J., Shibata, H., 2010. Potential effects of climate change and variability on watershed biogeochemical processes and water quality in Northeast Asia. Environment International 36, 212-225.

Prathumratana, L., Sthiannopkao, S., Kim, K.W., 2008. The relationship of climatic and hydrological parameters to surface water quality in the lower Mekong River. Environment International 34, 860-866.

Sherwood, S.C., Bony, S., Dufresne, J.-L., 2014. Spread in model climate sensitivity traced to atmospheric convective mixing. Nature 505, 37-42.

St Laurent, J., Mazumder, A., 2014. Influence of seasonal and inter-annual hydro-meteorological variability on surface water faecal coliform concentration under varying land-use composition. Water Research 48, 170-178.

Tate, K.W., Atwill, E.R., Bartolome, J.W., Nader, G., 2006. Significant Attenuation by Vegetative Buffers on Annual Grasslands. Journal of Environmental Quality 35, 795-805.

Tate, K.W., Atwill, E.R., McDougald, N.K., George, M.R., Witt, D., 2000. A method for estimating cattle faecal loading on rangeland watersheds. Journal of Range Management, 506-510.

Wentz, F.J., Ricciardulli, L., Hilburn, K., Mears, C., 2007. How much more rain will global warming bring? Science 317, 233-235.

Wilby, R.L., Orr, H.G., Hedger, M., Forrow, D., Blackmore, M., 2006. Risks posed by climate change to the delivery of Water Framework Directive objectives in the UK. Environment International 32, 1043-1055.

9 Final Remarks

9.1 Conclusions

The integrated modelling of hydrology and water quality with a Geographical Information System (GIS) interface was applied successfully to the Lis and Ave Rivers basins as a tool for river basin management. The Better Science Integrating point and Nonpoint Sources (BASINS) is a multipurpose environmental analysis system, based in an open source GIS (Map Window) with an extensible plugin architecture. Plugins such as the delineation tool, segmentation tool, climate assessment tool (CAT), weather data management utility (WDMUtil) and the Hydrological Simulation Program – FORTAN (HSPF) were applied to model watershed hydrology and in stream processes for both watersheds.

A large number of modelling parameters have been defined based upon the best available data, standard modelling assumptions, and comparison with relevant literature. In the process, a calibrated HSPF water quantity and quality model for Lis and Ave Rivers basins have been developed. The simulated flow has been calibrated and validated based on monthly flows for a 2 and 5 year period, respectively. Model validation was also performed for 2 and 5 year periods. Simulated temperature, faecal coliforms, dissolved oxygen, nitrates and, orthophosphorus were calibrated and validated graphically and statistically comparing with the observed values. The model prediction demonstrated a good agreement with the historical data for both watersheds. Despite the accuracy of the model be limited by the quantity and quality of data available, HPSF proved to be a reliable tool even for data limited environments. Current water quality does not meet the targets for a good water status for Lena, Lis and Este Rivers segments. Ave River segment shows a good water quality for all water quality constituents studied except for faecal coliforms.

Predictive scenarios of land use development, climate change effects and point and nonpoint pollution sources were presented, facilitating the understanding of the impact in water quality. Model results indicate that nonpoint source pollution is dominant in both watersheds and pollutant loading from agriculture areas is the highest of any other land use type.

The modelling included Monte Carlo simulations as well as sensitivity and uncertainty analysis. The Monte Carlo simulation was used to assess model uncertainty for streamflow in Lena River segment and water quality in Ave River. The hydrology parameters of HSPF were generated by uniform and triangular distributions.

9.1.1 Lis River Basin

Lis River basin hydrology and water quality model was used to calculate the loading of nitrogen and phosphorus as a result of various land uses. The model can be edited to reflect land use projections and give total loading results on a sub basin area basis. Nutrient content in the river can be reduced by controlling mainly nonpoint nutrient inputs from the catchment area. However, a substantial reduction is required (up to 76% for nitrogen and 87% for phosphorus) to comply with water quality standards for drinking water production. Lis River will require significant changes in agriculture practices to reduce the amount of nutrient loads in the basin.

Hypothetical scenarios were created taking into attention that the total area contributing to each sub basin was not changed. An analysis was performed to determine the loading coming from each land use; loading rates of nitrogen and phosphorus were calculated for all land use scenarios. The basin loading rates of nitrogen from agricultural land are higher than forest land which in turn is higher than urban land. Phosphorus loading rates in forest land are higher than agricultural land followed by urban land. Hypothetical scenarios resulted in an increase in total nitrogen and total phosphorus loads for high precipitation events since, high precipitation can generate significant loadings of pollutants from the soil into the water stream.

Climate change scenarios showed an improvement in water quality for faecal coliforms concentrations in water mainly due to the following factors: i) the increment of inflow of faecal coliform loads is mitigated by the increase of stream flow promoting dilution; ii) the increment of water temperature increases the faecal coliform decay rate. For the scenarios considering an increment of both precipitation and temperature, the increase of streamflow in summer months is not enough to mitigate the effect of faecal coliforms inflow resulting in an increase of concentration in water.

The application of Generalized Likelihood Uncertainty Estimation (GLUE) based on the Nash-Sutcliffe coefficient of efficiency led to a good prediction uncertainty regarding the coverage of measurements by the uncertainty bands. The sensitivity analysis on hydraulic parameters showed that monitoring climate conditions and stream flow are important in model performance, but special attention should be devoted to soil and land use data collection.

9.1.2 Ave River Basin

Better modelling results were obtained for Ave River basin than for Lis River basin, according to statistical criteria used, due to the increase of data availability to run the model. Model segmentation proved to be a valuable asset describing the watershed, by assigning spatial variability of meteorological conditions.

The water quality on Ave River segment showed a good status for all constituents addressed, except for faecal coliforms. On the other hand Este River water quality can achieve a good status for biochemical oxygen demand and orthophosphates with the implementation of best management practices applied to agricultural land. Best management practices (BMPs) were evaluated in this study with the objective of reduce pollutant loads to the water stream. It was found that BMPs are promising and recommendable measures to ensure and improve water quality in Este River segment. Regardless of the limitations in the available data, the study provides insights into a process based analysis of BMPs effectiveness for a watershed that shows representative topographic and soil characteristics of northern Portugal region. It may therefore be concluded that the effectiveness of BMPs evaluated in this study is similar for other intensively agriculture areas of the region.

The sensitivity model parameters, the first order decay rate (*FSTDEC*) and the rate of surface runoff that removes 90% of the stored faecal coliforms (*WSQOP*) showed to be the most important parameters when assessing faecal coliforms concentration.

To evaluate the sensitivity of water quality parameters implies looking at all parameter interactions involved in a specific water quality constituent balance. This study refers to parameters associated with oxygen interactions: dissolved oxygen, biochemical oxygen demand and orthophosphates. Cumulative frequency distributions were created to visually assess the parameter sensitivity in model results. Since the study was inconclusive, showing similar frequencies for almost all parameters, a statistical significance test (*p*-value) was determined for each parameter. The overall *p*-value results showed that none of the parameters is considered statistically significant for a 95% confidence interval. Though, the biochemical oxygen demand decay rate at 20ºC (*KBOD20*) and settling rate (*KODSET*) showed the lowest *p*-value, thus being considered parameters to look for in model calibration.

9.2 Future Work

It was the overall objective to promote good modelling practices and to provide in a systematic way methods that help the water manager to minimize uncertainty on model results. Several suggestions for further investigations are proposed:

- The same methodology can be followed to predict the water quantity and quality in other watersheds where water issues are identified or needed to be addressed;

- Further delineation with different Digital Elevation Models (DEMs): determine the impact of cell size on the outcome of the simulation. In this study a 25 m and 80 m

DEM resolution was used, but DEM resolutions from 1 m, 5 m and, 10 m should be considered for further studies;

- Conduct field experiments to obtain correct measurements of the river channel profile to further improve the outcome of stream flow calibration and enable the creation of flood maps;

- Investigation of local agricultural; agricultural nonpoint pollution (pesticides, inorganic fertilizers and their excess applications) is commonly considered the main element of contamination of water bodies, although the lack of efficient monitoring programs to provide systematic analytical data (temporal and spatial), difficult the support decision on mitigation techniques;

- Address the climate change effects scenarios presented in this thesis, on other water quality constituents such as: nitrates, orthophosphates, etc.;

- On-going continuous monitoring programs; as more water quality data is available additional refinement of HSPF model setup can be achieve;

- Extend the HSPF model with dynamic modelling tools affecting the fate of micro pollutants (i.e. physical, chemical and biological) in the receiving waters.

Appendix

A HSPF rates, constants and kinetics formulations

A.1 Kinematic Wave Equation

The kinematic wave equations are the simplest form of the dynamic wave equations, and it can be expressed as:

$$\frac{\partial h}{\partial t}+u\frac{dh}{dx}+v\frac{\partial h}{\partial y}+h\frac{\partial u}{\partial x}+h\frac{\partial v}{\partial y}=S,\ \ u=\frac{\sqrt{|S_{0_x}|}}{n}h^{2/3},\ \ v=\frac{\sqrt{|S_{0_y}|}}{n}h^{2/3}$$

Where:

u, v = water velocity (m s^{-1});

S = bed slope (m m^{-1});

So_x = bed slope in x direction (m m^{-1});

So_y = bed slope in y direction (m m^{-1})

n = Manning's roughness coefficient;

h = flow depth (m);

t = time (s).

Ignoring the acceleration and pressure gradient (Borah and Bera 2003) and being HSPF a one dimensional model the governing equation can be expressed as:

$$\frac{\partial h}{\partial t}+\frac{\partial Q}{\partial x}=q$$

$$Q=\alpha h^{m}$$

$$\text{Manning's Formula} \qquad Q=\frac{1}{n}\,AR^{2/3}\,S_f^{1/2}$$

Where:

q = lateral inflow per unit width and per unit length ($m^3\ s^{-1}\ m^{-1}\ m^{-1}$);

Q = flow per unit width ($m^3\ s^{-1}\ m^{-1}$);

a = kinematic wave parameter;

m = kinematic wave exponent;

h = flow depth (m);

t = time (s);

x = longitudinal distance (m)

n = Manning's roughness coefficient;

A = flow cross-sectional area per unit depth ($m^2\ m^{-1}$);

R = hydraulic radius (m);

S_f = energy gradient ($m\ m^{-1}$).

A.2 Dissolved Oxygen

A.2.1 Saturation

Dissolved oxygen saturation, C_{DOS}, is a basic parameter used in many water quality models. In HSPF the effects of pressure on saturation values are expressed as a ratio of site pressure to sea level, where C_{DOS} is expressed as (Imhoff, Kittle et al. 1981):

$$C_{DOS}=\left(14.652-0.41022T+0.007910T^{2}-7.7774\times10^{-5}T^{3}\right)\times\left(\frac{P}{29.92}\right)$$

Where:

C_{DOS} = dissolved oxygen saturation (mg L^{-1});
T = temperature (ºC);
P = barometric pressure (inHg).

A.2.2 Reaeration

Reaeration is the process of oxygen exchange between the atmosphere and a water body in contact with the atmosphere.

The reaeration process is modelled as the product of a mass-transfer coefficient multiplied by the difference between dissolved oxygen saturation and the actual dissolved oxygen concentration:

$$F_{C_{DO}} = k_L(C_{DOS} - C_{DO})$$

Where:
F_{CDO} = flux of dissolved oxygen across the water surface (mass per area and time);
C_{DO} = dissolved oxygen concentration (mass per volume);
C_{DOS} = saturation dissolved oxygen concentration (mass per volume);
k_L = surface transfer coefficient (length per time).

For river modelling application and for vertically mixed estuaries a depth average flux (F'_C), is used:

$$F'_{CDO} = \frac{F_{CDO}}{d} = \frac{k_L}{d}(C_{DOS} - C_{DO})$$

Where:
d = water depth (length).

The reaeration rate coefficient commonly found in literature as k_2 or k_a, or in HSPF as *KOREA* is expressed as:

$$REAK = k_2 = \frac{k_L}{d}$$

A.2.3 Carbonaceous Deoxygenation

Biochemical oxygen demand (BOD) is the utilization of dissolved oxygen by aquatic microbes to metabolize organic matter, oxidize reduced nitrogen and mineral species. BOD is commonly divided in two fractions: carbonaceous (CBOD) and nitrogenous matter (NBOD).

Carbonaceous oxygen demand

HSPF characterize CBOD decay with first order kinetics represented by:

$$\frac{\partial C_{CBOD}}{\partial t} = -k_0 CBOD$$

Where:

C_{CBOD} = carbonaceous BOD concentration (mg L^{-1});

k_0 = first order oxidation rate (day^{-1});

t = time (day).

Nitrogenous biochemical oxygen demand

The transformation of reduced forms of nitrogen to more oxidized forms consumes oxygen. Nitrification is a two stage process, the oxidation of ammonia to nitrite and nitrite to nitrate. First order kinetics is used by HSPF:

$$\frac{\partial C_{DO}}{\partial t} = -\alpha_1 k_{n_1} N_1 - \alpha_2 k_{n_2} N_2$$

Where:

k_{n1} = ammonia to nitrite oxidation rate (KTAM in HSPF) (day^{-1});

k_{n2} = nitrite to nitrate oxidation rate (KNO2 in HSPF) (day^{-1});

a_1 = 3.43, typically;

a_2 = 1.14, typically;

N_1= ammonia-nitrogen concentration (mg L^{-1})

N_2= nitrite-nitrogen concentration (mg L^{-1});

A.3 pH and Alkalinity

The value of pH is controlled by the carbonate system. There are three species of importance to the system: $[H_2CO_3^*]$, $[HCO_3^-]$ and $[CO_3^{2-}]$. $[H_2CO_3^*]$ is defined as the sum of $[H_2CO_3]$ and $[CO_2]$. For modelling purposes $[H_2CO_3]$ is negligible relative to $[CO_2]$. The carbonate system can be described by the following equations:

$$\text{K1EQU} = \frac{[HCO_3^-][H^+]}{[H_2CO_3]}$$

$$\text{K2EQU} = \frac{[CO_3^{2-}][H^+]}{[HCO_3^-]}$$

$$\text{KWEQU} = [H^+][OH^-]$$

$$TIC = [H_2CO_3^*] + [HCO_3^-] + [CO_3^{2-}]$$

$$ALK = [HCO_3^-] + 2[CO_3^{2-}] + [OH^-] - [H^+]$$

Where:

TIC = total inorganic carbon (mol L^{-1});

$[H^+]$ = hydrogen ion concentration (mol L^{-1});

$[OH^-]$ = hydroxide ion concentration (mol L^{-1});

$[CO_3^{2-}]$ = carbonate ion concentration (mol L^{-1});

$[HCO_3^-]$ = bicarbonate ion concentration (mol L^{-1})

$[H_2CO_3^*]$ = carbonic acid/carbon dioxide concentration (mol L^{-1});

K1EQU= first dissociation constant for carbonic acid, (mol L^{-1});

K2EQU= second dissociation constant for carbonic acid (mol L^{-1});

KWEQU = ionization product of water, (mol L^{-1});

ALK = alkalinity (mol L^{-1}).

The equilibrium constants K1EQU, K2EQU and KWEQU vary with temperature according to the following relationships (Tetra Tech 1979):

$$\text{K1EQU}=10^{\left[14.8435-0.032786\mathrm{T_k}-\left(\frac{3404.71}{\mathrm{T_k}}\right)\right]}$$

$$\mathrm{K2EQU} = 10^{\left[6.498 - 0.02379 T_k - \left(\frac{2902.39}{T_k}\right)\right]}$$

$$\mathrm{KWEQU} = 10^{\left[35.3944 - 0.00835 T_k - \left(\frac{5242.4}{T_k} - 11.826 \log(T_k)\right)\right]}$$

Where, T_k is the absolute temperature of water (Kelvin).

Once TIC, ALK and the equilibrium constants values have been determined an hydrogen ion equilibrium concentration can be reduced to a fourth order polynomial expression:

$$[H^+]^4 + A\times[H^+]^3 + B\times[H^+]^2 + C\times[H^+] + D = 0$$

Where:
A = ALK+K1EQU;
B = $-K_W$ + ALK × K1EQU + K1EQU × K2EQU – TIC × K1EQU;
C = –2 × K1EQU × K2EQU × TIC – K1EQU × KWEQU + ALK × K1EQU × K2EQU;
D = –K1EQU × K2EQU × KWEQU

A.4 Nutrients

Nutrients are modelled by using a system of coupled mass balance equations describing each nutrient compartment and each of the following process: dissolved inorganic and organic nutrients, particulate organic nutrients and sediment nutrients. HSPF does not simulate dissolved organic nutrient forms. The equations for each nutrient are expressed as follow:

Dissolved inorganic nutrients

$$\frac{\partial S_i}{\partial t} = -V_S + k_i S' - k_{ii} S_i + f_1 k_{det} S_{det} + f_2 k_{sed} S_{sed}$$

Particulate organic nutrients

$$\frac{\partial S_{det}}{\partial t} = e_p + M_p - k_{det} S_{det} - k_s S_{det} - G_z$$

Sediment nutrients

$$\frac{\partial S_{sed}}{\partial t} = k_s S_{det} + A_S - k_{sed} S_{sed}$$

Where:

S_i = dissolved inorganic nutrient concentration, (mass volume^{-1});

S' = another inorganic form of the nutrient which decays to the form S (e.g., NH_3, NO_3), (mass volume^{-1});

S_{org} = dissolved organic nutrient concentration, (mass volume^{-1});

S_{det} = suspended particulate organic nutrient concentration, (mass volume^{-1});

S_{sed} = organic sediment nutrient concentration, (mass volume^{-1});

k_i = transformation rate of S' into S, (time^{-1});

k_{ii} = transformation rate of S into some other dissolved inorganic form of the nutrient, (time^{-1});

k_{org} = hydrolysis rate of dissolved organic nutrient (time^{-1})

k_{det} = decomposition rate of particulate organic nutrient, (time^{-1});

k_{sed} = decomposition rate of organic sediment nutrient, (time^{-1});

k_S = settling rate of particulate organic nutrient, (time^{-1});

V_S = photosynthetic uptake rate for nutrient S, (mass volume^{-1} time^{-1});

e_S = soluble excretion rate of nutrient by all organisms, (mass volume^{-1} time^{-1});

f_1 = fraction of soluble excretions which are inorganic;

f_2 = fraction of detritus decomposition products which are immediately available for algal uptake;

f_3 = fraction of sediment decomposition products which are immediately available for algal uptake;

e_p = particulate excretion rate of nutrient by all animals, (mass volume^{-1} time^{-1});

M_p = total rate of plankton mortality, (mass volume^{-1} time^{-1});

G_z = detritus grazing rate by zooplankton, (mass volume^{-1} time^{-1});

A_S = algal settling rate to sediment, (mass volume^{-1} time^{-1}).

A.5 Phytoplankton

Phytoplankton dynamics are governed by the following processes: growth, respiration and excretion, settling, grazing losses and decomposition. The general equation is expressed as:

$$\frac{\partial A}{\partial t} = (\mu - r - e_x - s - m)A - G$$

Where:

A = phytoplankton biomass or concentration (dry weight biomass, cholophyll-a, or equivalent mass of carbon, nitrogen, or phosphorus, (mass or mass volume^{-1});

μ = gross grow rate, (time^{-1}), MALGR in HSPF;

r = respiration rate, (time^{-1}), ALR20 in HSPF;

e_x = excretion rate, (time^{-1});

s = settling rate, (time^{-1}), PHYSET in HSPF;

m = nonpredatory mortality (or decomposition) rate, (time^{-1});

G = loss rate due to grazing, (mass time^{-1} or mass volume^{-1} time^{-1}).

This equation is based when phytoplankton are modelled in terms of either biomass or nutrient equivalents (carbon, nitrogen, phosphorus, etc.) which is the case of HSPF.

A.6 Fecal coliforms

A simple first order kinetics approach is used for coliform modelling, taken into account the decay rate:

$$\frac{dC_{FC}}{dt} = -k_{FC}C_{FC}$$

$$C_{FCt} = C_{FC0}e^{-k_{FC}t_e}$$

Where:

C_{FC} = coliform concentration (count 100 mL^{-1});

C_{FC0} = initial coliform concentration (count 100 mL^{-1});

C_{FCt} = coliform concentration at time t (count 100 mL^{-1});

k_{FC} = disappearance rate constant (time^{-1});

t_e = exposure time (time^{-1}).

A.7 Simulation of hydrologic/hydraulic processes

A.7.1 PWATER section in PERLND module

The hydrologic process modelled by PWATER is expressed by the following water budget equation:

$$P + SWI + GWI = ET + SWO + GWO + \Delta S$$

Where:

P = precipitation;

SWI / SWO = surface water inflow / surface water outflow;

GWI / GWO = groundwater inflow / groundwater outflow;

ET = evapotranspiration;

S = change in storage.

Water enters the surface detention storage and make up infiltration and runoff. Infiltrated water moves to the lower zone and groundwater storage, and other water retained in the upper zone storage may be routed as runoff for surface detention or interflow storage, or may stay on the overland flow plane, from which it runs off or infiltrates at a later time. Surface conditions such as heavy turf on mild slopes restrict the velocity of overland flow and reduce the total quantity of runoff by allowing more time for infiltration.

A.7.1.1 Infiltration and surface runoff

Simulations of infiltration and surface runoff are based on the work of Philips (1957). The infiltration/interflow/surface runoff distribution function of section PWATER is described in **Figure A.1**.

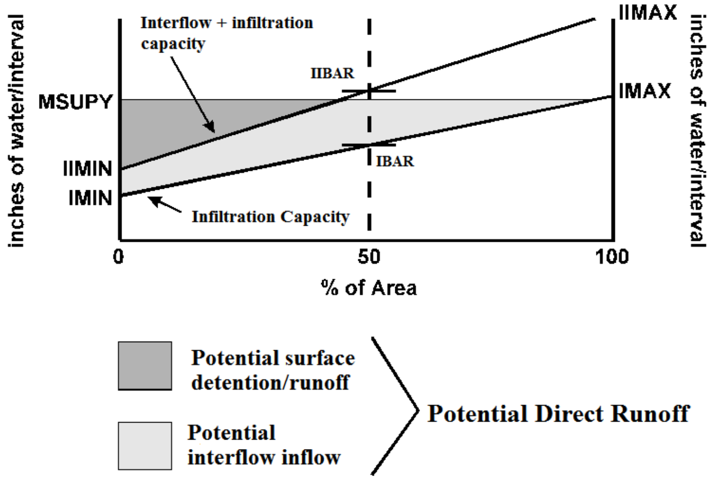

Figure A.1 Determination of infiltration and interflow inflow (Imhoff, Kittle et al. 1981) .

$$IBAR=\frac{INFILT}{\left(\frac{LZS}{LZSN}\right)^{INFEXP}}\times INFFAC$$

$$IMAX=INFILD\times IBAR$$

$$IMIN=IBAR-(IMAX-IBAR)$$

$$RATIO=INTFW\times 2^{\left(\frac{LZS}{LZSN}\right)}$$

Where:

IBAR = mean infiltration capacity over the land segment (in interval^{-1});

INFILT = infiltration parameter (in interval^{-1});

LZS = lower zone storage (in);

LZSN = parameter for lower zone nominal storage (in);

INFEXP = exponent parameter greater than one;

INFFAC = factor to account for frozen ground effects, if applicable;

IMAX = maximum infiltration capacity (in interval^{-1});

INFILD = parameter giving the ratio of maximum to mean infiltration capacity over the land segment;

IMIN = minimum infiltration capacity (in interval^{-1});

RATIO = ratio of the ordinates of line II to line I;
INTFW = interflow inflow parameter.

A.7.1.2 Upper Zone Behaviour

Percolating water from the upper zone moves to low zone storage and remaining water in upper zone storage is available for evapotranspiration. Percolation only occurs when the difference between *UZRAT* and *LZRAT* is greater than 0.01, and is calculated by following empirical expression:

$$\text{PERC}=0.1\times\text{INFILT}\times\text{INFFAC}\times\text{UZSN}\times(\text{UZRAT-LZRAT})^3$$

Where:
PERC = percolation from the upper zone (in interval^{-1});
INFILT = infiltration parameter (in interval^{-1});
INFFAC = factor to account for frozen ground, if any;
UZSN = parameter for upper zone nominal storage (in);
UZRAT = ratio of upper zone storage to UZSN;
LZRAT = ratio of lower zone storage to lower zone nominal storage (LZSN).

A.7.1.3 Lower Zone Behaviour

The fraction of the lower zone inflow, which is the sum of direct infiltration, percolation, lower zone lateral inflow, and irrigation application, that enters the lower zone storage (LZS) is based on the lower zone storage ratio of LZS/LZSN where LZSN is the lower zone nominal capacity. The inflowing fraction is determined empirically by:

$$\text{LZFRAC}=1.0\text{-LZRAT}\times\left(\frac{1.0}{(1.0+\text{INDX})}\right)^{\text{INDX}}$$

And when LZRAT is less than 1.0 by:

$$\text{LZFRAC}=\left(\frac{1.0}{(1.0+\text{INDX})}\right)^{\text{INDX}}$$

When LZRAT is greater than 1.0. INDX is defined by:

$$INDX=1.5 \times ABS(LZRAT-1.0)+1.0$$

Where:

LZFRAC = fraction of infiltration plus percolation plus lower zone lateral inflow that enters *LZS*.

$$LZRAT=\frac{LZS}{LZSN}$$

ABS = function for determining absolute value.

A.7.1.4 Groundwater Behaviour

The groundwater outflow is estimated by:

$$AGWO=KGW\times(1.0+KVARY\times GWVS)\times AGWS$$

Where:

AGWO = active groundwater outflow (in $interval^{-1}$);

KGW = groundwater outflow recession parameter ($interval^{-1}$);

KVARY = parameter which can make active groundwater storage to outflow relation nonlinear (in^{-1});

GWVS = index to groundwater slope (in^{-1});

AGWS = active groundwater storage at the start of the interval (in).

A.7.2 HYDR section in RCHRES module

The basic equation of water budget in a reach is as follow:

$$VOL-VOLS=IVOL+PRSUPY-VOLEV-ROVOL$$

Where:

VOL = volume at the end of time step;

VOLS = volume at the start of time step;

ROVOL = outflow volume;

IVOL = inflow volume;

PREC = volume of precipitation;

EVAP = volume of evaporation.

This can be written as:

$$VOL=VOLT-ROVOL$$

Where:

$$VOLT=IVOL+PRSUPY-VOLEV+VOLS$$

$$ROVOL=(KS\times ROS+COKS\times ROD)\times DELTS$$

Where:

KS = weighting factor (0 <= *KS* <= 0.99)

COKS = 1.0 - *KS* (complement of *KS*);

ROS = total rate of outflow from the RCHRES at the start of the interval;

ROD = total rate of demanded outflow for the end of the interval;

DELTS = simulation interval in seconds.

A.8 Heat Exchange and Water Temperature

Mechanisms which can increase the heat content of the water are absorption of solar radiation, absorption of longwave radiation, and conduction-convection. Mechanisms which decrease the heat content are emission of longwave radiation, conduction-convection, and evaporation.

A.8.1 Shortwave solar radiation

$$QSR=0.97\times CFSAEX\times SOLRAD\times 10.0$$

Where:

QSR = shortwave radiation (kcal m^{-2} $interval^{-1}$);

0.97 = fraction of incident radiation which is assumed absorbed (3 percent is assumed reflected);

CFSAEX = ratio of radiation incident to water surface to radiation incident to gage where data were collected. This factor also accounts for shading of the water body, e.g., by trees;

SOLRAD = solar radiation (langleys interval^{-1});

10.0 = conversion factor from langleys to kcal m^{-2}.

A.8.2 Longwave Radiation

$$\mathrm{QB}=\mathrm{SIGMA}\times\left(\left(\mathrm{TWKELV}^{4}\right)-\mathrm{KATRAD}\times\left(10^{-6}\right)\times\mathrm{CLDFAC}\times\left(\mathrm{TAKELV}^{6}\right)\right)\times\mathrm{DELT60}$$

Where:

QB = net transport of longwave radiation (kcal m^{-2} interval^{-1});

SIGMA = Stephan-Boltzman constant multiplied by 0.97 to account for emissivity of water;

TWKELV = water temperature (degrees Kelvin);

KATRAD = atmospheric longwave radiation coefficient with a typical value of 9.0;

TAKELV = air temperature corrected for elevation difference (degrees Kelvin);

DELT60 = *DELT* (minutes) divided by 60.

$\mathrm{CLDFAC}=1.0+\left(0.0017\times\mathrm{C}^{2}\right)$;

C = cloud cover, expressed as tenths (range = 0 - 10).

A.8.3 Conduction convection

$$\mathrm{QH}=\mathrm{CFPRES}\times\left(\mathrm{KCOND}\times10^{-4}\right)\times\mathrm{WIND}\times(\mathrm{TW}-\mathrm{AIRTMP})$$

Where:

QH = conductive-convective heat transport (kcal m^{-2} interval^{-1});

CFPRES = pressure correction factor (dependent on elevation);

KCOND = conductive-convective heat transport coefficient (typically in the range 1 - 20);

WIND = wind speed (m interval^{-1});

TW = water temperature (degrees Celsius);

AIRTMP = air temperature (degrees Celsius).

QH is positive for heat transfer from the water to the air.

A.8.4 Evaporative heat loss

$$EVAP = \left(KEVAP \times 10^{-9}\right) \times WIND \times (VPRESW - VPRESA)$$

Where:

EVAP = quantity of water evaporated (m interval^{-1});

KEVAP = evaporation coefficient with typical values of 1 – 5;

WIND = wind movement 2 m above the water surface (m interval^{-1});

VPRESW = saturation vapour pressure at the water surface (mbar);

VPRESA = vapour pressure of air above water surface (mbar).

The heat removed by evaporation is then calculated:

$$QE = HFACT \times EVAP$$

Where:

QE = heat loss due to evaporation (kcal m^{-2} interval^{-1});

HFACT = heat loss conversion factor (latent heat of vaporization multiplied by density of water).

A.8.5 Bed conduction

$$QBED = KMUD \times (TGRND - TW)$$

Where:

QBED = heat flux from ground to water (kcal m^{-2} interval^{-1});

TGRND = equilibrium ground temperature (degrees Celsius);

TW = water temperature (degrees Celsius);

KMUD = water-ground heat conduction coefficient (kcal m^{-2} interval^{-1}).

A.8.6 Net heat exchange

The net heat exchange at the water surface is represented as:

$$QT = QSR - QB - QH - QE + QP + QBED$$

Where:

QT = net heat exchange (kJ m^{-2} hr^{-1});

QSR = net heat transport from incident shortwave radiation (kJ m^{-2} hr^{-1});

QB = net heat transport from longwave radiation (kJ m^{-2} hr^{-1});

QH = heat transport from conduction-convection (kJ m^{-2} hr^{-1});

QE = heat transport from evaporation (kJ m^{-2} hr^{-1});

QP = heat content of precipitation (optional) (kJ m^{-2} hr^{-1});

QBED = net heat exchange with bed (kJ m^{-2} hr^{-1}).

A.8.7 . Calculation of water temperature

$$\mathrm{DELTTW} = \frac{\mathrm{CVQT} \times \mathrm{QT}}{(1.0 + \mathrm{SPD} \times \mathrm{CVQT})}$$

Where:

DELTTW = change in water temperature (degrees Celsius);

CVQT = conversion factor to convert total heat exchange expressed in kcal m^{-2} $interval^{-1}$ to degrees Celsius $interval^{-1}$ (volume dependent);

QT = net heat exchange in kcal m^{-2} $interval^{-1}$(with terms evaluated at starting temperature);

SPD = sum of partial derivatives of *QB*, *QH*, and *QE* with respect to water temperature.

A.9 Simulation of quality constituent (faecal coliforms)

A.9.1 Accumulation rate

If *QSOFG*=1, then the storage is updated once a day to account for accumulation and removal which occurs independent of runoff by the equation:

$$\mathrm{SQO} = \mathrm{ACQOP} + \mathrm{SQOS} \times (1.0 - \mathrm{REMQOP})$$

Where:

ACQOP = accumulation rate of the constituent (quantity ac^{-1} day^{-1});

SQOS = *SQO* at the start of the interval;

REMQOP = unit removal rate of the stored constituent (day^{-1}).

A.9.2 Removal rate

The removal rate is recomputed every interval as:

$$\text{REMQOP}=\frac{\text{ACQOP}}{\text{SQOLIM}}$$

Where:

SQOLIM = asymptotic limit for SQO as time approaches infinity (quantity ac^{-1}), if no washoff occurs:

$$\text{WSFAC}=\frac{2.30}{\text{WSQOP}}$$

Where:

WSQOP = rate of surface runoff that results in 90 percent washoff in one hour (in hr^{-1}).

A.10 Simulation of sediment processes

A.10.1 SEDMNT section in PERLND module

SEDMNT in PERLND module simulate the detachment, attachment, and removal of sediment from a pervious land segment.

A.10.1.1 Detach Soil by Rainfall

Kinetic energy from rain falling on the soil detaches particles which are then available to be transported by overland flow. The equation that simulates detachment is:

$$\text{DET}=\text{DELT60}\times(1.0\text{-CR})\times\text{SMPF}\times\text{KRER}\times\left(\frac{\text{RAIN}}{\text{DELT60}}\right)^{\text{JRER}}$$

Where:

DET = sediment detached from the soil matrix by rainfall (tons ac^{-1} $interval^{-1}$);

DELT60 = number of hours per interval;

CR = fraction of the land covered by snow and other cover;

SMPF = supporting management practice factor;

KRER = detachment coefficient dependent on soil properties;

RAIN = rainfall (in interval^{-1});

JRER = detachment exponent dependent on soil properties.

A.10.1.2 Transport Soil by Surface Flow

$$\mathrm{STCAP} = \mathrm{DELT60} \times \mathrm{KSER} \times \left(\frac{(\mathrm{SURS} + \mathrm{SURO})}{\mathrm{DELT60}} \right)^{\mathrm{JSER}}$$

Where:

STCAP = capacity for removing detached sediment (tons ac^{-1} interval^{-1});

DELT60 = hours per interval;

KSER = coefficient for transport of detached sediment;

SURS = surface water storage (in);

SURO = surface outflow of water (in interval^{-1});

JSER = exponent for transport of detached sediment.

A.10.1.3 Re-attachment of Detached Sediment

$$\mathrm{DETS}_{(t)} = \mathrm{DET}_{(t-1)} \times (1.0\text{-}\mathrm{AFFIX}) + \mathrm{NVSI}$$

Where:

DETS = Storage of detached sediment (tons ac^{-1});

AFFIX = Fraction by which DETS decrease each day as a result of soil compaction (day^{-1});

NVSI = vertical sediment input;

t = temporal (day).

A.10.2 SEDTRN section in RCHRES module

SEDTRN section in RCHRES module simulate inorganic sediment load into three components which is sand, silt, and clay. Sand transport is simulated by Toffaleti method, Colby method, and Power function method.

A.10.2.1 Sand transport simulation – Power function

$$PSAND = KSAND \times AVVELE^{EXPSND}$$

Where:

PSAND = Potential sand concentration;

AVVELE = Average velocity;

KSAND = Coefficient (input parameter);

EXPSND = Exponent (input parameter).

A.10.2.2 Scour/Deposition for cohesive sediments (silt and clay)

$$S = M \times \left(\frac{TAU}{TAU} - 1.0 \right)$$

$$D = W \times CONC \times \left(1.0 - \frac{TAU}{TAUCD} \right)$$

$$TAU = SLOPE \times GAM \times HRAD$$

Where:

S = Scour Rate

D = Deposit Rate

TAU = Shear Stress

M = Erodibility coefficient (lb ft^{-2} hr^{-1});

TAUSC = Critical shear stress for scour (lb ft^{-2});

TAUCD = Critical shear stress for deposition (lb ft^{-2});

CONC = Suspended sediment (lb ft^{-3});

GAM = Density of water (lb ft^{-3});

HRAD = Hydraulic radius.

A.11 Simulation of quality constituents processes

A.11.1 PQUAL section in PERLND module

The PQUAL module simulates water quality constituents using simple relationships;

A.11.1.1 Association with sediment removal

$$\mathrm{WASHQS=WSSD\times POTFW}$$

Where:

WASHQS = flux of quality constituent associated with detached sediment washoff (quantity ac^{-1} per interval);

WSSD = washoff of detached sediment (tons ac^{-1} per interval);

POTFW = washoff potency factor (quantity ton^{-1}).

A.11.1.2 Accumulation/depletion rate (buildup-washoff)

$$\mathrm{SQO=ACQOP+SQOS\times(1.0\text{-}REMQOP)}$$

Where:

$$\mathrm{REMQOP}=\left(\frac{\mathrm{ACQOP}}{\mathrm{SQOLIM}}\right)$$

SQO = Storage of available quality constituent on the surface;

ACQOP = Accumulation rate of the constituent;

SQOS = SQO at the start of the interval;

SQOLIM = limit for SQO, if no washoff occurs;

$$\mathrm{SOQO=SQO\times\left(1.0\text{-}e^{(-SURO\times WSFAC)}\right)}$$

$$\mathrm{WSFAC}=\frac{2.3}{\mathrm{WSQOP}}$$

Where:

SOQO = washoff of the quality constituent from the land surface;

SURO = surface out flow of water;

WSQOP = rate of surface runoff that result in 90% washoff in one hour.

A.11.1.3 Association with interflow or groundwater flow

$$OCONC=LIFAC\times LICONC+(1.0-LIFAC)\times CONC$$

Where:

OCONC = effective outflow concentration;

LIFAC = lateral inflow weighting factor for soil layer;

LICONC = lateral inflow concentration;

CONC = outflow concentration computed from other algorithms and parameters.

A.11.2 RQUAL section in RCHRES module

RQUAL simulate the following constituents involved in biochemical transformations: dissolved oxygen, biochemical oxygen demand, ammonia, nitrite, nitrate, orthophosphorus, phytoplankton, benthic algae, zooplankton, dead refractory organic nitrogen, dead refractory organic phosphorus, dead refractory organic carbon, total inorganic carbon, pH and carbon dioxide.

A.11.2.1 DO and BOD Balances - OXRX

Subroutine OXRX considers the following processes in determining oxygen balance: longitudinal advection of DOX and BOD, sinking of BOD material, benthal oxygen demand, benthal release of BOD material, reaeration, oxygen depletion due to decay of BOD materials.

Oxygen reaeration and saturation

The general equation for reaeration is:

$$DOX=DOXS+KOREA\times(SATDO-DOXS)$$

Where:

DOX = dissolved oxygen concentration after reaeration (mg L^{-1});

KOREA = reaeration coefficient (greater than zero and less than one);

SATDO = oxygen saturation level for given water temperature (mg L^{-1});

DOXS = dissolved oxygen concentration at start of interval (mg L^{-1}).

The power function of hydraulic depth and velocity is (Covar 1976):

$$\mathrm{KOREA}=\mathrm{REAK}\times\left(\mathrm{AVVELE}^{\mathrm{EXPREV}}\right)\times\left(\mathrm{AVDEPE}^{\mathrm{EXPRED}}\right)\times\left(\mathrm{TCGINV}^{(\mathrm{TW}-20)}\right)\times\mathrm{DELT60}$$

Where:

REAK = empirical constant for reaeration equation (hr^{-1});

AVVELE = average velocity of water (ft s^{-1});

EXPREV = exponent of velocity function;

AVDEPE = average of water depth (ft);

EXPRED = exponent to depth function

TCGINV = temperature correction coefficient for reaeration;

DELT60 = conversion factor from units per hour to units per interval.

The general equation for saturation is:

$$\mathrm{SATDO}=14.65+\mathrm{TW}\times\mathrm{f}\times\left(-0.4102+\mathrm{TW}\times\left(0.007991-7777\times10^{-5}\times\mathrm{TW}\right)\right)$$

Tw = Water temperature (ºC);

f = Correction factor based on reach elevation.

A.11.2.2 BOD Decay

The BOD decay process is assumed to follow first-order kinetics and is represented by:

$$\mathrm{BODOX}=\left(\mathrm{KBOD20}\times\mathrm{TCBOD}^{(\mathrm{TW}-20)}\right)\times\mathrm{BOD}$$

Where:

BODOX = quantity of oxygen required to satisfy BOD decay (mg L^{-1} per interval);

KBOD20 = BOD decay rate at 20 oC ($interval^{-1}$);

TCBOD = temperature correction coefficient, defaulted to 1.075;

TW = water temperature (ºC);

BOD = BOD concentration (mg L^{-1}).

Benthal oxygen demand

The effects of temperature and dissolved oxygen concentration on realized benthal demand are determined by the following equation:

$$BENOX=BENOD\times\left(TCBEN^{TW20}\right)\times\left(1.0\text{-}e^{(-EXPOD\times DOX)}\right)$$

Where:

BENOX = amount of oxygen demand exerted by benthal muds (mg m^{-2} per interval);

BENOD = reach dependent benthal oxygen demand at 20 degrees Celsius (mg m^{-2} per interval);

TCBEN = temperature correction factor for benthal oxygen demand;

TW20 = water temperature, 20.0 (degrees Celsius);

EXPOD = exponential factor to benthal oxygen demand function (default value = 1.22);

DOX = dissolved oxygen concentration (mg L^{-1}).

A.11.2.3 Inorganic Nitrogen and Phosphorus Balances

<u>Benthal Release</u>

$$RELEAS=BRCON(I)\times SCRFRAC\times DEPCOR$$

Where:

RELEAS = amount of constituent released (mg L^{-1} per interval);

BRCON(I) = benthal release rate (*BRNIT* or *BRPO4*) for constituent (mg m^{-2} per interval);

SCRFAC = scouring factor, dependent on average velocity of the water (SCRFAC is computed in *RQUAL*);

DEPCOR = conversion factor from mg m^{-2} to mg L^{-1}.

<u>Nitrification</u>

$$TAMNIT=KTAM20\times TCNIT^{(TW\text{-}20)}\times TAM$$

Where:

TAMNIT = amount of NH_3 oxidation (mg N L^{-1} per interval);

KTAM20 = ammonia oxidation rate coefficient at 20 ºC ($interval^{-1}$);

TCNIT = temperature correction coefficient, defaulted to 1.07;

TW = water temperature (ºC);

TAM = total ammonia concentration (mg N L^{-1});

Adsorption/Desorption of Ammonia and Orthophosphorus

$$SNUT(J)=DNUT\times ADPM(J)$$

Where:

SNUT(J) = equilibrium concentration of adsorbed nutrient on sediment fraction *J* (mg kg^{-1});

DNUT = the equilibrium concentration of dissolved nutrient (mg L^{-1});

ADPM (J) = adsorption parameter (or *Kd*) for sediment fraction *J* (L kg^{-1}).

Plankton Population and Associated Reactions

- Unit Growth and Respiration Rates for Algae

$$MALGRT=MALGR\times TCMALG$$

Where:

MALGRT = temperature corrected maximum algal growth rate;

MALGR = maximum unit growth rate for algae;

TCMALG = temperature correction to growth;

- Algal Respiration

$$RES=ALR20\times\left(\frac{TW}{20}\right)$$

Where:

RES = unit algal respiration rate ($interval^{-1}$);

ALR20 = unit respiration rate at 20 ºC;

TW = water temperature (ºC).

A.12 References

Borah, D. K. and M. Bera (2003). "Watershed-Scale hydrologic and Nonpoint-Source Pollution Models: Review of Mathematical Bases." American Society of Agricultural Engineers(ISSN 0001-2351).

Covar, A. P. (1976). "Selecting the Proper Reaeration Coefficient for Use in WaterQuality Models." Proceedings of the Conference on Environmental Modeling and Simulation EPA 600/9-76-016: 861.

Imhoff, J. C., et al. (1981). "User's Manual for Hydrological Simulation Program - Fortran (HSPF)." U.S. Environmental Protection Agency, Athens, Georgia.

Philips, J. R. (1957). "The Theory of Infiltration: The Infiltration Equation and Its Solution, Soil Science. 83:345-375."

Tetra Tech, I. (1979). "Methodology for Evalutation of Multiple Power Plant Cooling System Effects, Volume II: Techincal Basis for Computations." Electric Power Research Institute, Report EPRI EA-1111.

B HSPF parameter values for Lis River water calibration

B.1 Hydraulic parameters

Table B.1 Second group of PWATER parameters.

Description	LZSN	INFILT	LSUR	SLSUR	KVARY	AGWRC
15E03	5	0.25	250	0.0977	0	0.93
15E07	5	0.25	250	0.0977	0	0.93
16E01	5	0.25	250	0.0977	0	0.93
14D03	5	0.25	250	0.0977	0	0.93
15D01	5	0.25	250	0.0977	0	0.93
15E08	5	0.25	250	0.0977	0	0.93
15E05	5	0.25	250	0.0977	0	0.93
15E06	5	0.25	250	0.0977	0	0.93

Table B.2 Third group of PWATER parameters.

Description	PETMAX	PETMIN	INFEXP	INFILD	DEEPFR	BASETP	AGWETP
15E03	40	35	2	2	0.1	0.02	0
15E07	40	35	2	2	0.1	0.02	0
16E01	40	35	2	2	0.1	0.02	0
14D03	40	35	2	2	0.1	0.02	0
15D01	40	35	2	2	0.1	0.02	0
15E08	40	35	2	2	0.1	0.02	0
15E05	40	35	2	2	0.1	0.02	0
15E06	40	35	2	2	0.1	0.02	0

Table B.3 Fourth group of PWATER parameters.

Description	NSUR
15E03	0.2
15E07	0.2
16E01	0.2
14D03	0.2
15D01	0.2
15E08	0.2
15E05	0.2
15E06	0.2

Table B.4 Monthly values of interception storage capacity (CEPSC).

Description	Jan	Feb	Mar	Apr	May	Jun	Jul	Aug	Sep	Oct	Nov	Dec
15E03	0.1	0.11	0.12	0.2	0	0.005	0	0	0.01	0	0.13	0.12
15E07	0.1	0.11	0.12	0.2	0	0.005	0	0	0.01	0	0.13	0.12
16E01	0.1	0.11	0.12	0.2	0	0.005	0	0	0.01	0	0.13	0.12
14D03	0.1	0.11	0.12	0.2	0	0.005	0	0	0.01	0	0.13	0.12
15D01	0.1	0.11	0.12	0.2	0	0.005	0	0	0.01	0	0.13	0.12
15E08	0.1	0.11	0.12	0.2	0	0.005	0	0	0.01	0	0.13	0.12
15E05	0.1	0.11	0.12	0.2	0	0.005	0	0	0.01	0	0.13	0.12
15E06	0.1	0.11	0.12	0.2	0	0.005	0	0	0.01	0	0.13	0.12

Table B.5 Monthly values of interflow inflow parameter (INTFW).

Description	Jan	Feb	Mar	Apr	May	Jun	Jul	Aug	Sep	Oct	Nov	Dec
15E03	0.8	0.8	0.4	0.1	0.4	0.4	0.8	0.8	0.5	0.6	0.5	0.5
15E07	0.8	0.8	0.4	0.1	0.4	0.4	0.8	0.8	0.5	0.6	0.5	0.5
16E01	0.8	0.8	0.4	0.1	0.4	0.4	0.8	0.8	0.5	0.6	0.5	0.5
14D03	0.8	0.8	0.4	0.1	0.4	0.4	0.8	0.8	0.5	0.6	0.5	0.5
15D01	0.8	0.8	0.4	0.1	0.4	0.4	0.8	0.8	0.5	0.6	0.5	0.5
15E08	0.8	0.8	0.4	0.1	0.4	0.4	0.8	0.8	0.5	0.6	0.5	0.5
15E05	0.8	0.8	0.4	0.1	0.4	0.4	0.8	0.8	0.5	0.6	0.5	0.5
15E06	0.8	0.8	0.4	0.1	0.4	0.4	0.8	0.8	0.5	0.6	0.5	0.5

Table B.6 Monthly values of upper zone nominal storage (UZSN).

Description	Jan	Feb	Mar	Apr	May	Jun	Jul	Aug	Sep	Oct	Nov	Dec
15E03	1	1.4	1.4	1.4	0.9	1.2	0.8	0.7	0.5	0.5	1.2	1.3
15E07	1	1.4	1.4	1.4	0.9	1.2	0.8	0.7	0.5	0.5	1.2	1.3
16E01	1	1.4	1.4	1.4	0.9	1.2	0.8	0.7	0.5	0.5	1.2	1.3
14D03	1	1.4	1.4	1.4	0.9	1.2	0.8	0.7	0.5	0.5	1.2	1.3
15D01	1	1.4	1.4	1.4	0.9	1.2	0.8	0.7	0.5	0.5	1.2	1.3
15E08	1	1.4	1.4	1.4	0.9	1.2	0.8	0.7	0.5	0.5	1.2	1.3
15E05	1	1.4	1.4	1.4	0.9	1.2	0.8	0.7	0.5	0.5	1.2	1.3
15E06	1	1.4	1.4	1.4	0.9	1.2	0.8	0.7	0.5	0.5	1.2	1.3

Table B.7 Monthly values of interflow recession constant (IRC).

Description	Jan	Feb	Mar	Apr	May	Jun	Jul	Aug	Sep	Oct	Nov	Dec
15E03	0.7	0.7	0.6	0.4	0.35	0.3	0.2	0.2	0.5	0.5	0.7	0.7
15E07	0.7	0.7	0.6	0.4	0.35	0.3	0.2	0.2	0.5	0.5	0.7	0.7
16E01	0.7	0.7	0.6	0.4	0.35	0.3	0.2	0.2	0.5	0.5	0.7	0.7
14D03	0.7	0.7	0.6	0.4	0.35	0.3	0.2	0.2	0.5	0.5	0.7	0.7
15D01	0.7	0.7	0.6	0.4	0.35	0.3	0.2	0.2	0.5	0.5	0.7	0.7
15E08	0.7	0.7	0.6	0.4	0.35	0.3	0.2	0.2	0.5	0.5	0.7	0.7
15E05	0.7	0.7	0.6	0.4	0.35	0.3	0.2	0.2	0.5	0.5	0.7	0.7
15E06	0.7	0.7	0.6	0.4	0.35	0.3	0.2	0.2	0.5	0.5	0.7	0.7

Table B.8 Monthly values of lower zone E-T parameters (LZETP).

Description	Jan	Feb	Mar	Apr	May	Jun	Jul	Aug	Sep	Oct	Nov	Dec
15E03	0.2	0.3	0.3	0.2	0.2	0.4	0.1	0.1	0.1	0.3	0.1	0.1
15E07	0.2	0.3	0.3	0.2	0.2	0.4	0.1	0.1	0.1	0.3	0.1	0.1
16E01	0.2	0.3	0.3	0.2	0.2	0.4	0.1	0.1	0.1	0.3	0.1	0.1
14D03	0.2	0.3	0.3	0.2	0.2	0.4	0.1	0.1	0.1	0.3	0.1	0.1
15D01	0.2	0.3	0.3	0.2	0.2	0.4	0.1	0.1	0.1	0.3	0.1	0.1
15E08	0.2	0.3	0.3	0.2	0.2	0.4	0.1	0.1	0.1	0.3	0.1	0.1
15E05	0.2	0.3	0.3	0.2	0.2	0.4	0.1	0.1	0.1	0.3	0.1	0.1
15E06	0.2	0.3	0.3	0.2	0.2	0.4	0.1	0.1	0.1	0.3	0.1	0.1

Table B.9 Monthly distribution of surface layer temperature (ºC).

	Surface Layer Temperature											
	Jan	Feb	Mar	Apr	May	Jun	Jul	Aug	Sep	Oct	Nov	Dec
Agriculture	13	16	18	21	23	24	25	25	23	20	16	13
Barren	13	16	18	21	23	24	25	25	23	20	16	13
Forest	13	16	18	21	23	24	25	25	23	20	16	13
Urban	13	16	18	21	23	24	25	25	23	20	16	13

Table B.10 Heat exchange parameters.

Reach	ELEV	CFSAEX	KATRAD	KCOND	KEVAP	MUDDEP	TGRND	KMUD	KGRND
16E01	126	1	9.5	6.12	2.24	0.33	59	50	1.4
15E07	35	1	9.5	6.12	2.24	0.33	59	50	1.4
15E03	45	1	9.5	6.12	2.24	0.33	59	50	1.4
14D03	26	1	9.5	6.12	2.24	0.33	59	50	1.4
15D01	10	1	9.5	6.12	2.24	0.33	59	50	1.4
15E08	114	1	9.5	6.12	2.24	0.33	59	50	1.4
15E05	35	1	9.5	6.12	2.24	0.33	59	50	1.4
15E06	102	1	9.5	6.12	2.24	0.33	59	50	1.4

B.2 Water quality parameters

Table B.11 Rate of surface runoff.

	WSQOP
Agriculture	0.5
Barren	0.2
Forest	0.2
Urban	0.5

Table B.12. Fecal coliform monthly accumulation.

	ACQOP - Monthly Accumulation											
	Jan	**Feb**	**Mar**	**Apr**	**May**	**Jun**	**Jul**	**Aug**	**Sep**	**Oct**	**Nov**	**Dec**
Agriculture												
15E03	7.9×10^{9}	8.2×10^{9}	7.9×10^{9}	2.7×10^{10}	2.7×10^{10}	2.2×10^{10}	2.2×10^{10}	2.2×10^{10}	2.6×10^{10}	4.4×10^{10}	5.0×10^{10}	7.9×10^{9}
15E07	4.9×10^{9}	5.1×10^{9}	4.9×10^{9}	1.6×10^{10}	1.6×10^{10}	1.3×10^{10}	1.3×10^{10}	1.3×10^{10}	1.6×10^{10}	2.7×10^{10}	3.0×10^{10}	4.9×10^{9}
16E01	3.0×10^{9}	3.2×10^{9}	3.0×10^{9}	1.0×10^{10}	1.0×10^{10}	8.1×10^{9}	8.0×10^{9}	8.0×10^{9}	9.7×10^{9}	1.6×10^{10}	1.8×10^{10}	3.0×10^{9}
Barren	1200000	1200000	1200000	1200000	1200000	1200000	1200000	1200000	1200000	1200000	1200000	1200000
Forest	8.4×10^{8}	8.4×10^{8}	8.4×10^{8}	8.4×10^{8}	8.4×10^{8}	8.4×10^{8}	8.4×10^{8}	8.4×10^{8}	8.4×10^{8}	8.4×10^{8}	8.4x108	8.4×10^{8}
Urban	8.6×10^{6}	8.6×10^{6}	8.6×10^{6}	8.6×10^{6}	8.6×10^{6}	8.6×10^{6}	8.6×10^{6}	8.6×10^{6}	8.6×10^{6}	8.6×10^{6}	8.6×10^{6}	8.6×10^{6}

Table B. 13 Fecal coliform monthly limit storage.

	SQOLIM – Maximum Limit Storage											
	Jan	**Feb**	**Mar**	**Apr**	**May**	**Jun**	**Jul**	**Aug**	**Sep**	**Oct**	**Nov**	**Dec**
Agriculture												
15E03	$1.4x10^{10}$	$1.4x10^{10}$	$1.4x10^{10}$	$4.1x10^{10}$	$4.1x10^{10}$	$3.3x10^{10}$	$3.3x10^{10}$	$3.3x10^{10}$	$4.0x10^{10}$	$8.0x10^{10}$	$9.0x10^{10}$	$1.4x10^{10}$
15E07	$8.8x10^{9}$	$9.1x10^{9}$	$8.8x10^{9}$	$2.5x10^{10}$	$2.5x10^{10}$	$2.0x10^{10}$	$2.0x10^{10}$	$2.0x10^{10}$	$2.4x10^{10}$	$4.8x10^{10}$	$5.4x10^{10}$	$8.8x10^{9}$
16E01	$5.5x10^{9}$	$5.7x10^{9}$	$5.5x10^{9}$	$1.5x10^{10}$	$1.5x10^{10}$	$1.2x10^{10}$	$1.2x10^{10}$	$1.2x10^{10}$	$1.4x10^{10}$	$2.9x10^{10}$	$3.2x10^{10}$	$5.5x10^{9}$
Barren	$1.2x10^{7}$	$1.2x10^{7}$	$1.2x10^{7}$	$1.2x10^{7}$	$1.2x10^{7}$	$1.2x10^{7}$	$1.2x10^{7}$	$1.2x10^{7}$	$1.2x10^{7}$	$1.2x10^{7}$	$1.2x10^{7}$	$1.2x10^{7}$
Forest	$1.5x10^{9}$	$1.5x10^{9}$	$1.5x10^{9}$	$1.5x10^{9}$	$1.5x10^{9}$	$1.5x10^{9}$	$1.5x10^{9}$	$1.5x10^{9}$	$1.5x10^{9}$	$1.5x10^{9}$	$1.5x10^{9}$	$1.5x10^{9}$
Urban	$1.5x10^{7}$	$1.5x10^{7}$	$1.5x10^{7}$	$1.5x10^{7}$	$1.5x10^{7}$	$1.5x10^{7}$	$1.5x10^{7}$	$1.5x10^{7}$	$1.5x10^{7}$	$1.5x10^{7}$	$1.5x10^{7}$	$1.5x10^{7}$

Table B.14 Sediment parameters.

Reach	KSAND	EXPSND	$TAUCD_{(silt)}$	$TAUCS_{(silt)}$	$TAUCD_{(clay)}$	$TAUCS_{(clay)}$	M
16E01	0.1	3	0.15	0.18	0.15	0.18	0.01
15E07	0.1	3	0.18	0.2	0.18	0.2	0.01
15E03	0.1	3	0.08	0.11	0.1	0.13	0.01
14D03	0.1	3	0.08	0.11	0.1	0.13	0.01
15D01	0.1	3	0.08	0.11	0.1	0.13	0.01
15E08	0.1	3	0.08	0.11	0.1	0.13	0.01
15E05	0.1	3	0.08	0.11	0.1	0.13	0.01
15E06	0.1	3	0.08	0.11	0.1	0.13	0.01

Table B. 15 General oxygen parameters.

Reach	KBOD20	TCBOD	KODSET	SUPSAT
16E01	0.064	1.047	0.1	1.15
15E07	0.004	1.047	0.027	1.15
15E03	0.004	1.047	0.0004	1.15
14D03	0.004	1.047	0.1	1.15
15D01	0.004	1.047	0.1	1.15
15E08	0.004	1.047	0.1	1.15
15E05	0.004	1.047	0.1	1.15
15E06	0.004	1.047	0.1	1.15

Table B. 16 Oxygen benthic parameters.

Reach	BENOD	TCBEN	EXPOD	BRBOD1	BRBOD2
16E01	500	1.074	1.22	0.001	0.001
15E07	500	1.074	1.22	0.001	0.001
15E03	50	1.074	1.22	0.001	0.001
14D03	50	1.074	1.22	0.001	0.001
15D01	50	1.074	1.22	0.001	0.001
15E08	50	1.074	1.22	0.001	0.001
15E05	50	1.074	1.22	0.001	0.001
15E06	50	1.074	1.22	0.001	0.001

Table B. 17 Reaeration parameters.

Reach	EXPREL	TCGINV	REAK	EXPRED	EXPREV
16E01	2.82	1.024	2	-1.673	0.969
15E07	2.82	1.024	2	-1.673	0.969
15E03	2.82	1.024	0.8	-1.673	0.969
14D03	2.82	1.024	0.8	-1.673	0.969
15D01	2.82	1.024	1	-1.673	0.969
15E08	2.82	1.024	0.9	-1.673	0.969
15E05	2.82	1.024	2	-1.673	0.969
15E06	2.82	1.024	1.8	-1.673	0.969

Table B. 18 Nutrient benthic parameters.

Reach	BRNIT1	BRNIT2	BRPO41	BRPO42	ANAER
16E01	100	100	0	0	0.001
15E07	30	30	2	2	0.001
15E03	80	80	3	3	0.001
14D03	80	80	3	3	0.001
15D01	80	80	3	3	0.001
15E08	80	80	3	3	0.001
15E05	80	80	3	3	0.001
15E06	80	80	3	3	0.001

Table B. 19 Nitrification and denitrification parameters.

Reach	KTAM20	KNO220	TCNIT	KNO320	TCDEN	DENOXT
16E01	0.015	0.002	1.07	0.4	1.04	1
15E07	0.015	0.002	1.07	0.4	1.04	1
15E03	0.015	0.002	1.07	0.4	1.04	1
14D03	0.015	0.002	1.07	0.4	1.04	1
15D01	0.015	0.002	1.07	0.4	1.04	1
15E08	0.015	0.002	1.07	0.4	1.04	1
15E05	0.015	0.002	1.07	0.4	1.04	1
15E06	0.015	0.002	1.07	0.4	1.04	1

Table B. 20 Phytoplankton parameters.

Reach	MALGR	PHYSET	ALR20
16E01	0.085	0.02	0.005
15E07	0.12	0.05	0.005
15E03	0.008	0.001	0.005
14D03	0.008	0.001	0.005
15D01	0.008	0.001	0.005
15E08	0.008	0.001	0.005
15E05	0.008	0.001	0.005
15E06	0.008	0.001	0.005

C HSPF parameter values for Ave River water calibration

C.1 Hydraulic parameters

Table C.21 Second group of PWATER parameters.

Description	LZSN	INFILT	LSUR	SLSUR	KVARY	AGWRC
Ave	3	0.25	250	0.196	0	0.98
Este	3	0.25	250	0.196	0	0.98

Table C.22 Third group of PWATER parameters.

Description	PETMAX	PETMIN	INFEXP	INFILD	DEEPFR	BASETP	AGWETP
Ave	40	35	2	2	0.1	0.02	0
Este	40	35	2	2	0.1	0.02	0

Table C.23 Fourth group of PWATER parameters.

Description	NSUR
Ave	0.2
Este	0.2

Table C.24 Monthly values of interception storage capacity (CEPSC).

Description	Jan	Feb	Mar	Apr	May	Jun	Jul	Aug	Sep	Oct	Nov	Dec
Ave	0.3	0.1	0.1	0.1	0.1	0.1	0.1	0.1	0.1	0.2	0.3	0.3
Este	0.3	0.1	0.1	0.1	0.1	0.1	0.1	0.1	0.1	0.2	0.3	0.3

Table C.25 Monthly values of interflow inflow parameter (INTFW).

Description	Jan	Feb	Mar	Apr	May	Jun	Jul	Aug	Sep	Oct	Nov	Dec
Ave	0.6	0.5	0.4	0.3	0.3	0.3	0.3	0.3	0.3	0.4	0.5	0.6
Este	0.6	0.5	0.4	0.3	0.3	0.3	0.3	0.3	0.3	0.4	0.5	0.6

Table C.26 Monthly values of upper zone nominal storage (UZSN).

Description	Jan	Feb	Mar	Apr	May	Jun	Jul	Aug	Sep	Oct	Nov	Dec
Ave	0.8	0.8	0.8	0.8	0.8	0.8	0.8	0.8	0.8	0.8	0.8	0.8
Este	0.8	0.8	0.8	0.8	0.8	0.8	0.8	0.8	0.8	0.8	0.8	0.8

Table C.27 Monthly values of interflow recession constant (IRC).

Description	Jan	Feb	Mar	Apr	May	Jun	Jul	Aug	Sep	Oct	Nov	Dec
Ave	0.85	0.85	0.85	0.85	0.85	0.85	0.85	0.85	0.85	0.85	0.85	0.85
Este	0.85	0.85	0.85	0.85	0.85	0.85	0.85	0.85	0.85	0.85	0.85	0.85

Table C.28 Monthly values of lower zone E-T parameters (LZETP).

Description	Jan	Feb	Mar	Apr	May	Jun	Jul	Aug	Sep	Oct	Nov	Dec
Ave	0.1	0.1	0.1	0.1	0.2	0.2	0.2	0.2	0.1	0.1	0.1	0.1
Este	0.1	0.1	0.1	0.1	0.2	0.2	0.2	0.2	0.1	0.1	0.1	0.1

Table C.29 Monthly distribution of surface layer temperature (ºC).

	Surface Layer Temperature											
	Jan	**Feb**	**Mar**	**Apr**	**May**	**Jun**	**Jul**	**Aug**	**Sep**	**Oct**	**Nov**	**Dec**
Agriculture	8	8	11	14	16	21	22	22	21	16	10	8
Barren	8	8	11	14	16	21	22	22	21	16	10	8
Forest	8	8	11	14	16	21	22	22	21	16	10	8
Urban	8	8	11	14	16	21	22	22	21	16	10	8

Table C.30 Heat exchange parameters.

Reach	**ELEV**	**CFSAEX**	**KATRAD**	**KCOND**	**KEVAP**	**MUDDEP**	**TGRND**	**KMUD**	**KGRND**
Ave	46	1	9.5	6.12	2.24	0.33	59	50	1.4
Este	27	1	9.5	6.12	2.24	0.33	59	50	1.4

C.2 Water quality parameters

Table C.31 Rate of surface runoff.

	WSQOP
Agriculture	0.5
Barren	0.2
Forest	0.2
Urban	0.5

Table C.32. Fecal coliform monthly accumulation.

	ACQOP - Monthly Accumulation											
	Jan	**Feb**	**Mar**	**Apr**	**May**	**Jun**	**Jul**	**Aug**	**Sep**	**Oct**	**Nov**	**Dec**
Agriculture												
Ave	$3x10^{10}$	$4x10^{10}$	$5x10^{10}$	$5x10^{10}$	$6x10^{10}$	$3x10^{10}$	$3x10^{10}$	$3x10^{10}$	$3x10^{10}$	$3x10^{11}$	$3x10^{11}$	$3x10^{10}$
Este	$2x10^{11}$	$2x10^{11}$	$3x10^{11}$	$3x10^{11}$	$3x10^{11}$	$2x10^{11}$	$2x10^{11}$	$2x10^{11}$	$2x10^{11}$	$2x10^{12}$	$2x10^{12}$	$2x10^{11}$
Barren	200000	200000	200000	200000	200000	200000	200000	200000	200000	200000	200000	200000
Forest	$8.4x10^8$	$8.4x10^8$	$8.4x10^8$	$8.4x10^8$	$8.4x10^8$	$8.4x10^8$	$8.4x10^8$	$8.4x10^8$	$8.4x10^8$	$8.4x10^8$	8.4x108	$8.4x10^8$
Urban	$9x10^6$	$9x10^6$	$9x10^6$	$9x10^6$	$9x10^6$	$9x10^6$	$9x10^6$	$9x10^6$	$9x10^6$	$9x10^6$	$9x10^6$	$9x10^6$

Table C. 33 Fecal coliform monthly limit storage.

	SQOLIM – Maximum Limit Storage											
	Jan	**Feb**	**Mar**	**Apr**	**May**	**Jun**	**Jul**	**Aug**	**Sep**	**Oct**	**Nov**	**Dec**
Agriculture												
Ave	$6x10^{10}$	$7x10^{10}$	$8x10^{10}$	$8x10^{10}$	$8x10^{10}$	$5x10^{10}$	$5x10^{10}$	$5x10^{10}$	$5x10^{10}$	$5x10^{11}$	$5x10^{11}$	$6x10^{10}$
Este	$4x10^{11}$	$4x10^{11}$	$5x10^{11}$	$5x10^{11}$	$5x10^{11}$	$3x10^{11}$	$3x10^{11}$	$3x10^{11}$	$3x10^{11}$	$3x10^{12}$	$3x10^{12}$	$4x10^{11}$
Barren	$2x10^{7}$	$2x10^{7}$	$2x10^{7}$	$2x10^{7}$	$2x10^{7}$	$2x10^{7}$	$2x10^{7}$	$2x10^{7}$	$2x10^{7}$	$2x10^{7}$	$2x10^{7}$	$2x10^{7}$
Forest	$2x10^{9}$	$2x10^{9}$	$2x10^{9}$	$2x10^{9}$	$2x10^{9}$	$2x10^{9}$	$2x10^{9}$	$2x10^{9}$	$2x10^{9}$	$2x10^{9}$	$2x10^{9}$	$2x10^{9}$
Urban	$2x10^{7}$	$2x10^{7}$	$2x10^{7}$	$2x10^{7}$	$2x10^{7}$	$2x10^{7}$	$2x10^{7}$	$2x10^{7}$	$2x10^{7}$	$2x10^{7}$	$2x10^{7}$	$2x10^{7}$

Table C.34 Sediment parameters.

Reach	KSAND	EXPSND	$TAUCD_{(silt)}$	$TAUCS_{(silt)}$	$TAUCD_{(clay)}$	$TAUCS_{(clay)}$	M
Ave	0.1	3	0.15	0.18	0.16	0.18	0.01
Este	0.1	3	0.08	0.11	0.11	0.13	0.01

Table C. 35 General oxygen parameters.

Reach	KBOD20	TCBOD	KODSET	SUPSAT
Ave	0.001	1	0.1	1.15
Este	0.0001	1	0.1	1.15

Table C. 36 Oxygen benthic parameters.

Reach	BENOD	TCBEN	EXPOD	BRBOD1	BRBOD2
Ave	280	1.074	1.22	0.001	0.001
Este	100	1.074	1.22	0.001	0.001

Table C. 37 Reaeration parameters.

Reach	EXPREL	TCGINV	REAK	EXPRED	EXPREV
Ave	2.82	1.024	0.1	-1.673	0.969
Este	2.82	1.024	0.04	-1.673	0.969

Table C. 38 Nutrient benthic parameters.

Reach	BRNIT1	BRNIT2	BRPO41	BRPO42	ANAER
Ave	0	0	0	0	0.001
Este	0	0	0	0	0.001

Table C. 39 Nitrification and denitrification parameters.

Reach	KTAM20	KNO220	TCNIT	KNO320	TCDEN	DENOXT
Ave	0.25	0.45	1.5	0.02	1.04	3
Este	0.25	0.45	1.5	0.5	1.04	3

Table C. 40 Phytoplankton parameters.

Reach	MALGR	PHYSET	ALR20
Ave	0.085	0.02	0.005
Este	0.1	0.02	0.005